

THE EFFECT OF DENTICITY ON THE ELECTROCHEMISTRY AND OXYGENATION KINETICS  
OF POLYDENTATE SCHIFF BASE COMPLEXES OF MANGANESE

by

Fred Charles Frederick

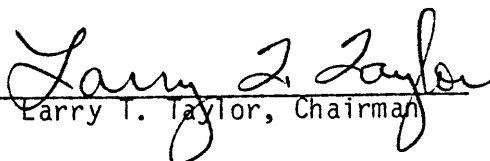
Dissertation submitted to the Graduate Faculty of the  
Virginia Polytechnic Institute and State University  
in partial fulfillment of the requirements for the degree of

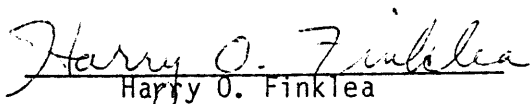
Doctor of Philosophy

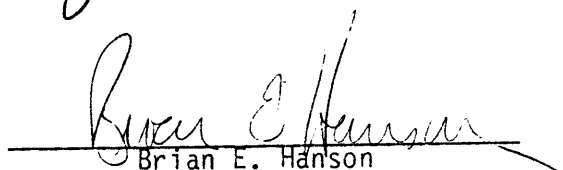
in

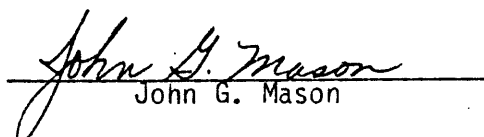
Chemistry

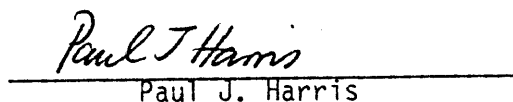
APPROVED:

  
Larry T. Taylor, Chairman

  
Harry O. Finklea

  
Brian E. Hanson

  
John G. Mason

  
Paul J. Harris

December, 1983  
Blacksburg, Virginia 24060

THE EFFECT OF DENTICITY ON THE ELECTROCHEMISTRY AND OXYGENATION KINETICS  
OF POLYDENTATE SCHIFF BASE COMPLEXES OF MANGANESE

by

Fred Charles Frederick

(ABSTRACT)

Manganese(II) and (III) complexes of potentially bidentate and tridentate Schiff base ligands have been prepared. The ligands were prepared from substituted salicylaldehyde or pyridine-2-carboxaldehyde and amines with hydrocarbon or alkylpyridyl substituents. The electrochemistry and the oxygenation kinetics of these and similar tetradentate, pentadentate, and hexadentate complexes have been studied.

The electrochemistry of the majority of the complexes involves the Mn(III)/Mn(II) couple. However, varying the solvent shows that electron transfer is often accompanied by slow changes in the number of solvent molecules coordinated to the metal or changes in the actual denticity of the ligand.

Activation energies and entropies for the reactions with  $O_2$  show that a large number of parameters influence the rate of reaction. Primary among these is competition between  $O_2$ , solvent molecules, and donor atoms from the ligands for coordination sites on the metal. However, the reactions were all (with one exception) found to be first order in both complex and  $O_2$ , implying that the slow step is formation of a Mn(III)-superoxo complex. The exception was with complexes of the tetradentate Mn(SALC<sub>n</sub>) type, where a simple rate law could not be fitted. This was explained by either steric hindrance or polymerization of the complex due to the flexibility imparted by the long polymethylene

chain in the tetradentate ligand.

## ACKNOWLEDGMENTS

First and foremost, I would like to thank Dr. Larry Taylor for his continuing support through both the good and bad times. His deep concern for his students and employees is something that should be more common in academia.

I would also like to thank my parents for their support both up to and during my time in Blacksburg. Any endeavor is made easier by knowing that you have a warm and loving home to retreat to when needed.

A sincere "Thanks" must be extended to a group of people who made my first years away from home an enjoyable time: Eugene, Bob, John C., John H., Chuck and Sandi, Gene, Steve and Jan, Donna and Mike, Tom Furtsch, and last, but definitely not least, J.S.

A more professional "Thank you" goes to J. Hughes, T. Fritz, B. Boggess, T. Henderson, C. Anderson, and the members of my committee, to W. Coleman and S. Coleman for synthesizing some of the complexes, and S. Morelen for performing some of the oxygen uptakes.

Research funding from the National Institute of Health is also acknowledged.

## TABLE OF CONTENTS

	<u>PAGE</u>
ACKNOWLEDGMENTS.....	iv
LIST OF TABLES.....	vii
LIST OF FIGURES.....	viii
CHAPTER I. INTRODUCTION.....	1
CHAPTER II. HISTORICAL.....	4
Reaction Products of <u>M</u> and O <sub>2</sub> .....	5
Oxygen Sensitive Manganese Complexes.....	9
Manganese Schiff Base Complexes.....	19
1. Oxygenation Properties.....	19
a) Solid State Oxygenation.....	21
b) Solution Oxygenation.....	26
2. Electrochemistry.....	34
CHAPTER III. EXPERIMENTAL .....	40
Materials.....	40
Preparation of New Complexes.....	40
Previously Reported Complexes.....	44
Physical Measurements.....	44
Kinetic Studies.....	45
Electrochemical Studies.....	46
CHAPTER IV. RESULTS AND DISCUSSION.....	47
Composition of Newly Synthesized Complexes.....	47
Physical Properties of New Complexes.....	54
Oxygen Reactivity.....	61

	<u>PAGE</u>
1. Solid State.....	61
a) Bidentate Complexes.....	61
b) Tridentate Complexes.....	62
2. Solution Oxygenation.....	64
a) Bidentate Complexes.....	64
b) Tridentate Complexes.....	69
Electrochemistry.....	76
1. Bidentate Complexes.....	77
2. Tridentate Complexes.....	90
3. Tetradentate Complexes.....	107
4. Summary.....	124
Oxygenation Kinetics.....	124
1. General Comments.....	124
2. Bidentate Complexes.....	128
3. Tridentate Complexes.....	146
4. Tetradentate Complexes.....	146
a) Mn(XSALEN).....	146
b) Mn(SALC <sub>n</sub> ).....	157
5. Pentadentate Complexes.....	167
6. Hexadentate Complexes.....	179
Oxygenation Mechanisms Review.....	184
1. Bidentate Complexes.....	184
2. Tridentate Complexes.....	184
3. Tetradentate Complexes.....	185
4. Pentadentate Complexes.....	186
5. Hexadentate Complexes.....	188
CHAPTER V. SUMMARY AND CONCLUSIONS.....	189
APPENDIX I.....	195
REFERENCES.....	198
VITA.....	205
ABSTRACT.....	

## LIST OF TABLES

	<u>PAGE</u>
I. Elemental Analyses for New Complexes.....	49
II. Infrared Data for New Complexes.....	50
III. UV-Visible Absorbance Maxima of New Complexes.....	55
IV. Physical Properties of New Complexes.....	60
V. Peak Potentials for Bidentate Complexes.....	79
VI. Peak Potentials for Tridentate Complexes.....	93
VII. Peak Potentials for XSALEN Complexes.....	108
VIII. Peak Current Ratios for XSALEN Complexes.....	111
IX. Peak Separations(V) and $E^{\circ}$ (V vs. SCE) for XSALEN Complexes.....	114
X. Kinetic Parameters for Oxygenation of Bidentate Complexes.....	136
XI. Kinetic Parameters for Oxygenation of Tridentate Complexes.....	143
XII. Kinetic Parameters for Tetradentate Oxgenations.....	156
XIII. Kinetic Parameters for Oxygenation of Pentadentate Complex.....	174

## LIST OF FIGURES

	<u>PAGE</u>
1. Products of $M + O_2$ Reaction.....	6
2. Metal d Orbital Stabilization of $M^+-O^-$ .....	8
3. Proposed Mechanism for Reversible Oxygenation of Manganese Phosphine Complexes.....	10
4. Structure of $TPMnO_2$ .....	17
5. Structure of ([14]-ane $N_4$ ).....	18
6. Synthesis of Schiff Base Ligands.....	20
7. Solid State Oxygen Uptake of $Mn(SALHXDA)$ .....	23
8. Early Reported Structures for Oxygenated Tetradentate Complexes.....	24
9. Heptadentate Ligands for Manganese.....	27
10. Structure of Polymeric Bidentate $Mn(III)$ Complex.....	29
11. Oxygen Uptakes of Pentadentate Complexes in Toluene.....	31
12. $N_3S_2$ Ligand.....	32
13. Oxygen Uptakes of Hexadentate Complexes in Pyridine.....	35
14. Cyclic Voltammogram of $Mn(SALDPT)$ in DMSO.....	37
15. Structural Formulae of New Complexes.....	48
16. Proposed Structures of New Complexes.....	53
17. Ligand and Complex Spectra in DMSO.....	56
18. Oxygen Uptake of $Mn(SALPMA)_2$ in DMSO.....	65
19. Oxygen Uptake of $Mn(SAL-4-BrANL)_2$ in Pyridine.....	66
20. Oxygen Uptake of $Mn(SALAEP)_2$ in DMSO.....	71
21. Oxygen Uptake of $Mn(SALAEP)_2$ in Pyridine.....	72
22. $MnL_2^+$ and Oxygenated $MnL_2$ Spectra in DMSO.....	73

	<u>PAGE</u>
23. Oxygen Uptake of Deprotonated HSALAEP in DMSO.....	75
24. Cyclic Voltammograms of Bidentate Complexes in Pyridine...	78
25. Cyclic Voltammogram of Bidentate Complexes in DMSO.....	82
26. Cyclic Voltammograms of Mn(SAL-4-BrANL) <sub>2</sub> in DMSO.....	84
27. CFSE Stabilization of Bidentate Complexes.....	85
28. Effect of Substituent on Voltammetric Peak Heights.....	87
29. Cyclic Voltammograms of Mn(SAL-4-BrANL) <sub>2</sub> in DMSO and 1/4 DMSO/Pyridine.....	89
30. Cyclic Voltammograms of Tridentate Complexes in Pyridine..	91
31. Comparison of HSALPMA and HSALAMP.....	95
32. Cyclic Voltammograms of Tridentate Complexes in DMSO.....	97
33. Solvation Model for Tridentate Complexes.....	98
34. Effect of Scan Rate on Voltammetric Peak Heights.....	99
35. Tautomerism of N <sub>7</sub> Ligand.....	101
36. Cyclic Voltammograms of Mn(5-ClSALAEP) <sub>2</sub> (NCS) and Mn(5-MeOSALAEP) <sub>2</sub> (NCS).....	104
37. Effect of Solvent on Cyclic Voltammograms of Tridentate Complexes.....	105
38. Cyclic Voltammogram of Mn(5-ClSALEN) in DMSO.....	109
39. Cyclic Voltammogram of Mn(3-MeOSALEN) in Pyridine.....	110
40. Anodic Peak Current vs. Square Root of Scan Rate for Mn(XSALEN) in DMSO.....	112
41. Anodic Peak Current vs. Square Root of Scan Rate for Mn(XSALEN) in Pyridine.....	113
42. Coordinated Solvent Effect on Macrocyclic Complex Redox Potentials.....	116
43. Cyclic Voltammogram of Mn(SALOTDA) in Pyridine.....	119

	<u>Page</u>
44. Possible Polymeric Structure of Mn(SALC <sub>n</sub> ) Complexes.....	120
45. Cyclic Voltammogram of Mn(SALDCDA) in Pyridine.....	122
46. Second Oxidation Peak for Mn(SALDCDA).....	123
47. Clark Plot for Oxygenation of Mn(SALPMA) <sub>2</sub> in DMSO.....	129
48. First Order Clark Plot for Oxygenation of Mn(SALPMA) <sub>2</sub> in DMSO.....	130
49. Repetitive Scan of Oxygenation of Mn(SALPMA) <sub>2</sub> in Pyridine.	131
50. First Order Plot for Oxygenation of Mn(SALPMA) <sub>2</sub> in Pyridine.....	133
51. Arrhenius Plot for Oxygenation of Mn(SALPMA) <sub>2</sub> in Pyridine.	135
52. First Order Clark Plot for Oxygenation of Mn(SALAEP) <sub>2</sub> in DMSO.....	139
53. Repetitive Scan of Oxygenation of Mn(SALAMP) <sub>2</sub> in Pyridine.....	140
54. First Order Plot for Oxygenation of Mn(SALAMP) <sub>2</sub> in DMSO.....	141
55. Repetitive Scan of Oxygenation of Mn(SALEN) in DMSO.....	147
56. High Temperature Repetitive Scan of Oxygenation of Mn(SALEN) in DMSO.....	149
57. Repetitive Scan of Oxygenation of Mn(SALEN) in Pyridine.....	150
58. Slow Repetitive Scan of Oxygenation of Mn(3-MeOSALEN) in Pyridine.....	152
59. First Order Clark Plot for Oxygenation of Mn(SALEN) in DMSO.....	153
60. First Order Plot for Oxygenation of Mn(3-MeOSALEN) in Pyridine.....	154
61. Repetitive Scan of Oxygenation of Mn(SALHXDA) in Pyridine.....	158

	<u>PAGE</u>
62. Repetitive Scan of Oxygenation of Mn(SALOTDA) in DMSO..	159
63. First Order Clark Plot for Oxygenation of Mn(SALHTDA) in Pyridine.....	161
64. First Order Plot for Oxygenation of Mn(SALOTDA) in Pyridine.....	162
65. Second Order Plot for Oxygenation of Mn(SALOTDA) in Pyridine.....	163
66. Potential Dimeric Structure of Mn(SALC <sub>n</sub> ) Complexes.....	165
67. Repetitive Scan of Mn(5-NO <sub>2</sub> SALDPT) in Toluene.....	168
68. Repetitive Scan of Oxygenation of Mn(5-NO <sub>2</sub> SALDPT) in Pyridine.....	169
69. First Order Clark Plot for Oxygenation of Mn(5-NO <sub>2</sub> SALDPT) in Toluene.....	172
70. First Order Plot for Oxygenation of Mn(5-NO <sub>2</sub> SALDPT) in Toluene.....	173
71. O <sub>2</sub> Attack on Pentadentate Complexes.....	178
72. Repetitive Scan of Oxygenation of Mn(SAL 1,5,8,12) in Pyridine.....	180
73. Initial Rate Plot for Oxygenation of Mn(SAL 1,5,8,12) in DMSO.....	182
74. First Order Clark Plot for Oxygenation of Mn(SAL 1,5,8,12) in DMSO.....	183
75. Possible Intermediates in Reaction of (LMn) <sub>2</sub> O with O <sub>2</sub> (L=Tetradentate Ligand).....	187
76. Reaction Scheme for Electrochemistry of Mn(SALC <sub>n</sub> ) Complexes.....	191

## CHAPTER I

### INTRODUCTION

The importance of transition metal complexes in our present civilization is something that most non-chemists and chemists alike underestimate to a great extent. How many of us taking out the garbage in a polyethylene bag remember that the 1963 Nobel Prize in chemistry was awarded for development of the Ziegler-Natta catalyst, an alkyltitanium complex? Or, when entering an automobile showroom, do we look at the shiny chrome on a new car and think of the ongoing research into why the plating bath must contain Cr(VI) and not Cr(III)? Research into areas such as these have undoubtedly made our lives much more comfortable.

However, other transition metal complexes which have been around for much longer than the science of chemistry, or even civilization, are much more fundamental to our existence. These are, of course, biologically active molecules upon whose workings life itself is dependent. The most well known of these is hemoglobin, the oxygen transporting component of blood in vertebrates. This contains four iron ions each complexed by a porphyrin ring, attached to a large protein. Many other fundamental processes are controlled by metal containing proteins. Nitrogen fixation is performed in legumes by an Fe-Mo center. A Cu ion is the O<sub>2</sub>-carrying center in hemocyanin, found in some molluscs. Mn and Mg are the metals involved in photosynthesis in green plants. Elucidating the exact mechanisms at work in these reactions, especially in vivo, is at least of as much importance, or at least interest, to many scientists as commercially applicable reactions.

Unfortunately, chemistry has not yet reached the stage where a reaction can easily be studied in a living organism. Even studies of isolated enzyme systems are sometimes rendered difficult by the large size of the molecules involved. In an attempt to overcome these difficulties, many groups have resorted to model systems, small inorganic complexes which are expected to mimic the behavior of the active centers of the larger molecules. These have sometimes worked out quite well, reproducing the biological activity of the enzymes. Often, however, the behavior of the models is quite different, implying a substantial effect on the reaction by the proteinaceous part of the enzyme. Studies using these models have primarily focused on those reactions involving small molecules and ions, eg.  $\text{H}_2\text{O}$ ,  $\text{O}_2$ ,  $\text{CO}$ ,  $\text{N}_2$ ,  $\text{CO}_3^{2-}$ ,  $\text{NO}_2^-$ , and small organic molecules. These were chosen for two reasons; first, a large number of enzymes act directly on such species, therefore, a study would be directly applicable to the biological system being modeled; second, because a number of enzymes act on much larger molecules, information gained on small substrates is easier to gather and extrapolate to the larger systems, exactly as with the enzymes.

The most studied of all these systems are the oxygen carriers, probably because of the intimate involvement we have with our own hemoglobin. Fe, Cu, Co, and Mn model systems with a wide range of ligands have been employed in an attempt to further our understanding of the outwardly simple function of hemoglobin. A number of important facts have been garnered from those studies, but some questions are still unanswered, especially those concerning exactly what conditions

(metal/ligand combinations) are best for mimicking the natural system, i.e. producing reversible coordination of O<sub>2</sub>.

The purpose of this research was to study the kinetics of the reactions of oxygen with a series of polydentate Schiff base complexes of manganese. Since very few complexes of Mn react reversibly with O<sub>2</sub>, it was felt that a study of the effect of varying denticity (the number of donor atoms in the chelate) would be beneficial to the understanding of other irreversibly and reversibly reacting complexes. The electrochemistry of the selected complexes was also studied, in an attempt to correlate redox potentials of the complexes with the ease of oxygenation. Attack of O<sub>2</sub> on the Mn center involves oxidation of the metal ion, therefore factors that affect the oxygenation should also affect electrooxidation.

## CHAPTER II

### HISTORICAL

Since Werner and Mylius<sup>1</sup> first reported that an ammoniacal solution of Co(II) will absorb oxygen from the atmosphere, numerous studies have been performed on oxygen-sensitive transition metal complexes. The aim of many of these studies was the development of a reversibly oxygenating system that would mimic biological O<sub>2</sub>-carrying molecules. In many cases the complexes were found to undergo irreversible oxygenation/oxidation, but, fortunately, a great deal of the information gathered on the reactions of those complexes helped lead to a better understanding of the operation of the reversible systems. Also, these results were applicable to the natural systems since even they undergo irreversible reactions after a period of time (eg. auto-oxidation of hemoglobin to methemoglobin), and a reversible model system could not explain this.

Although quite a few transition metals have been found to react with O<sub>2</sub>, the majority of the studies have been on complexes of iron and cobalt. The iron work has been largely on complexes containing planar macrocyclic N<sub>4</sub> ligands such as porphyrins and phthalocyanines, i.e. models for the heme group. Cobalt complexes have come under much scrutiny simply because of the large number of O<sub>2</sub>-sensitive ones which can be prepared, often with very simple ligands. Strangely, Co is not known to participate in any biological role as an O<sub>2</sub>-carrier. A third metal which has only relatively recently drawn much attention in this area is manganese. It is similar to Fe and Co in having relatively

stable II and III states, and forms a number of O<sub>2</sub>-sensitive compounds with ligands that produce the same effect with the other two metals. However, because of the chemical differences between the three metals, few simply reversible Mn systems have been prepared.

The following section will attempt to provide the reader with: first, a short discussion of the products of reactions of transition metal complexes with O<sub>2</sub>; second, an overview of non-Schiff base Mn complexes which react with O<sub>2</sub>; and third, a presentation of previous work on polydentate Schiff base complexes of manganese.

#### Reaction Products of M + O<sub>2</sub>

Figure 1 shows the more common products of oxygenation of transition metal complexes. Beginning at the upper left corner of the flow chart, the simplest type of reaction is one which, overall, involves simple oxidation of the metal. This may occur either by simple outer sphere electron transfer or by decomposition of an unstable intermediate containing coordinated oxygen. When oxygen remains coordinated to the metal, there are a number of possible products. The attack of one or two metals on the O<sub>2</sub> molecule and attendant internal electron transfer leads to one of the various superoxo- or peroxo-species. If the O-O bond is cleaved during the reaction, then an oxo- or hydroxo-compound forms, depending on whether or not the cleavage is initiated by a proton source. There are a number of other known products but these are usually singular compounds.

The final product of the reaction is controlled by a number of variables, including, of course, metal and ligand, but also solvent,



temperature,  $O_2$  pressure, and time of reaction. A number of the compounds can be interconverted, although this is quite often an irreversible process.

Although many of these reactions produce only one final product, stable intermediates can often be isolated when reaction conditions are properly adjusted. For example, a number of complexes pass through consecutive superoxo- and  $\mu$ -peroxo-complex steps in their oxygenations. A number of researchers have found that high  $O_2$  concentrations and low M concentrations facilitate formation of the superoxo-product since virtually all of M will be quickly trapped in this form, and none will be available for reaction to produce the  $\mu$ -peroxo-species. Steric hindrance induced by bulky ligands on M will also have this effect, but by preventing the approach of an M molecule to a superoxo-complex. Other factors which have the same effect are use of polar solvents-(the superoxo-complex is more polar than the  $\mu$ -peroxo-complex, and is stabilized by such) and low temperatures (to slow down the second step kinetically).

In some cases, if the reaction proceeds to the  $\mu$ -peroxo-stage, immediate autoxidation occurs with cleavage of the O-O bond. This seems to be primarily dependent on the metal in the complex. Ochiai<sup>2</sup> has interpreted this as being due to different degrees of stabilization of the  $M^+-O^-$  cleavage product by interaction of metal d electrons with the odd electron on  $O^-$  (Figure 2). Only metals with five or fewer d electrons can stabilize the  $M^+-O^-$  species, and thus facilitate the autoxidation. Metals with six or more d electrons will have at least

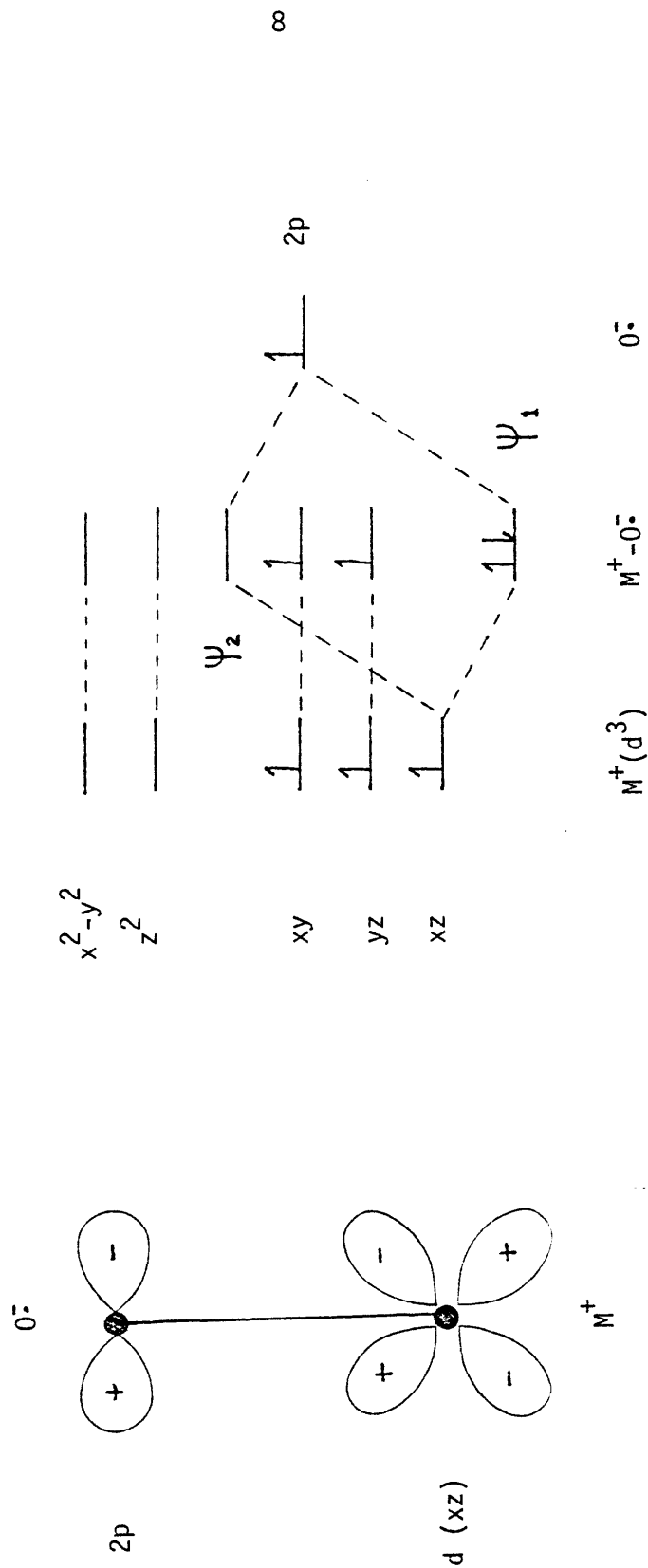
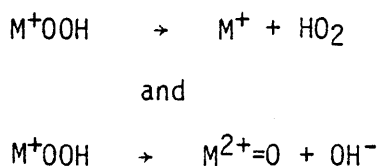


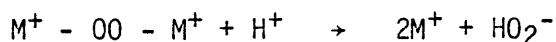
Figure 2: Metal d Orbital Stabilization of  $M^+0$ .

one electron in  $\psi_2$ , and form a relatively stable  $\mu$ -peroxo-compound.

Another factor which can be controlled is the presence or absence of proton sources, which are necessary for formation of the various hydroxy-species. Protons will also react with virtually any of the products in Figure 1 to produce the  $M^+$  species. The most common reaction is simple hydrolysis of the various oxo- and hydroxo-species. However, protons can also interfere with isolation of superoxo- and  $\mu$ -peroxo-species. Superoxo-complexes will react almost immediately with protons because protons are not sterically hindered, nor are their reactions slowed much by low temperature. The product,  $M^+-OOH$ , may undergo a number of reactions including:



$\mu$ -Peroxo complexes will also react with protons via:



### Oxygenation Sensitive Manganese Complexes

Manganese complexes which react with  $O_2$  include many with ligands which produce  $O_2$ -sensitive complexes with other metals, but also a few unique to itself. McAuliffe et al. have reported a remarkable, simple system which mimics hemoglobin to the extent of showing cooperative effects.<sup>3</sup> The complexes, of the general formula  $MnLX_2$  (L = tertiary phosphine, but not  $PPh_3$ , X = anion), formed a final product believed to

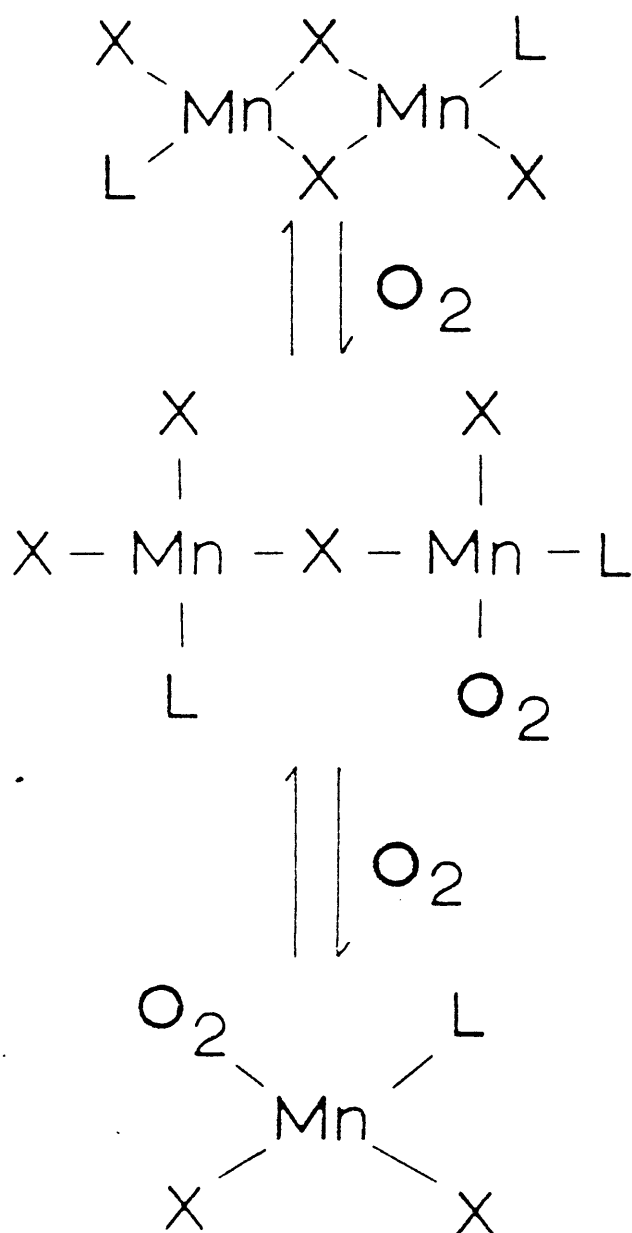
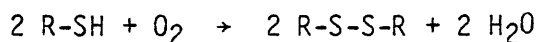


Figure 3: Proposed Mechanism for Reversible Oxygenation of Manganese Phosphine Complexes.

be  $MnLX_2 \cdot O_2$  with a 1:1 ratio of coordinated triplet and singlet oxygen, and Mn still in the II state. The reaction was facile in both the solid state and in solution.  $Mn(PPhEt_2)Br_2$  in particular exhibited a sigmoidal  $O_2$  uptake curve in THF, similar to hemoglobin as a function of  $O_2$  pressure. Oxygenation was reported to be totally reversible even after thousands of cycles. The starting complex was believed to be dimeric and the uptake is thought to be a two step process (Figure 3). The fact that a Mn complex was the first to mimic both the cooperativity and quick reversibility of hemoglobin was quite interesting in view of the non-oxygen-carrying nature of Mn hemoglobin.<sup>4</sup>

Certain amino acid complexes of Mn(II) were  $O_2$  sensitive when dissolved in water or ethanol/water mixtures.<sup>5</sup> When cysteine and penicillamine or some of their derivatives were the ligands, a number of color changes occurred during the reaction, dependent on the ligand, the ligand-to-metal ratio, and the solution pH. Variable products were also obtained, but  $MnO_2$  and oxidized forms of the acids were the final products. The acids were believed to oxidize to the coupled products, cystine and the penicillamine disulfide via:



The free ligands were also susceptible to oxidation under strongly basic conditions.

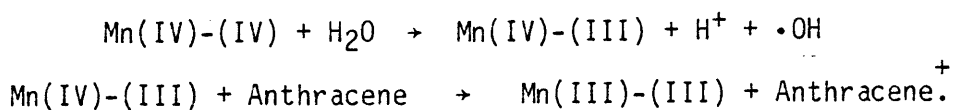
Sawyer's group has extensively examined a number of Mn(II) and (III) systems containing polyhydroxy ligands such as sorbitol, glucaric acid, and inositol.<sup>6,7</sup> The complexes reacted with  $O_2$  in basic solution

to produce Mn(III) and Mn(IV) complexes, respectively, and biperoxide anion in stoichiometric amounts. The Mn(II) complexes would also react with  $\text{HO}_2^-$  to produce the Mn(III) complex, but the reaction stoichiometry indicated some complexity in the reaction because the Mn(II) oxidized/ $\text{HO}_2^-$  reduced ratio depended on the ligand concentration. A Fenton type reaction<sup>8</sup> producing Mn(III)(OH) and  $\cdot\text{OH}$  was postulated to occur. The reactions were first order in both complex and  $\text{O}_2$ , and the Mn(II) and (III) reactants and products were binuclear. Interestingly, the reactions were all equilibria, and could be reversed by lowering the pH to produce the lower oxidation states and the original oxidant.

Sawyer's group had also reported that Mn (and V) complexes of 3,5-di-tert-butylcatechol reversibly absorbed  $\text{O}_2$ .<sup>9-11</sup> They based their report on spectral and electrochemical changes on introduction of  $\text{O}_2$  to solutions of the complexes and apparent reversibility of these changes on subsequent purging with Ar. However, later papers by Cooper et al. demonstrated that the results were actually due to formation of unstable semiquinone and quinone complexes which decomposed to produce apparent reversible oxygenation.<sup>12,13</sup> Similar spurious results were earlier reported (and corrected) by Allcock et al.<sup>14</sup> and Boyer and Holzbach<sup>15</sup> who were studying polymer-supported Fe systems. Both used dithionite in situ to prepare the Fe(II) precursors, and apparent reversal was actually due to reduction by excess dithionite.

Cryogenic sublimation of  $\text{Mn}_2(\text{CO})_{10}$  in the presence of  $\text{O}_2$  produced a species identified as  $\cdot\text{O}_2\text{Mn}(\text{CO})_5$  from its ESR spectrum.<sup>16</sup> No mention was made of any reversibility of the reaction on heating.

An interesting group of compounds containing di- $\mu$ -oxo-bridges were the bipyridyl and phenanthroline complexes whose ions had the general formula  $(L_2MnO_2MnL_2)^{x+}$  ( $x = 2,3,4$ ).<sup>17-20</sup> Although they were structurally similar to the oxygenation products of certain tetradentate Schiff base complexes of Mn(II) (vide infra), they could not be prepared by reaction of Mn(II) phen or bipy complexes with  $O_2$ . This was due to the high oxidation potential of the Mn(II) complexes ( $\sim +1.3V$  vs. SCE in  $CH_3CN/0.1M$  tetrapropylammonium perchlorate). Unlike the rather inert Schiff base di- $\mu$ -oxo-complexes, the phen and bipy di- $\mu$ -oxo-complexes were soluble in aqueous and organic solvent systems, and underwent interesting redox reactions to form III-III, III-IV, and IV-IV dimers which were proposed as models for manganese species involved in photosynthesis. Particularly interesting were photo-induced electron transfers between the Mn species and substrates such as water (producing  $\cdot OH$ ) and anthracene (producing anthraquinone). The electron transfer reactions were:



Anthracene reacted with  $H_2O$  to produce anthroquinone.

Manganese phthalocyanine was shown in 1959 to reversibly bind  $O_2$  when dissolved in pyridine.<sup>21</sup> Since then, a number of other solvents were found to facilitate the reaction (N-methylimidazole, 3-picoline, and piperidine)<sup>22</sup>, and the products of the reactions have been identified as  $(SMnPc)_2O$  ( $S = \text{solvent}$ ).<sup>23</sup> The mechanism was first

believed to involve a  $\text{PcMn(III)(OH)}$  intermediate,<sup>24</sup> however later evidence showed that this assignment was incorrect<sup>25</sup>. A more interesting  $\text{PcMn}^{\text{III}}\text{O}_2^-$  product could be isolated from *N,N*-dimethylacetamide (DMA).<sup>26</sup> This could be converted to the  $\mu$ -oxo-complex ( $\text{S}=\text{DMA}$ ) by addition of imidazole to an aerated DMS solution (proton-catalyzed?). It could also revert to  $\text{Mn(II)}$  under vacuum when photolyzed. In the absence of  $\text{O}_2$ , this addition (or that of  $\text{Me}_2\text{NH}$  or  $\text{Et}_3\text{N}$ ) converted the adduct back to  $\text{MnPc}$ . More importantly, the  $\mu$ -oxo-complex could be changed back to the superoxo-complex under high  $\text{O}_2$  pressure in the absence of protons, and back to the  $\text{Mn(II)}$  complex by treatment with triethylamine in vacuo. The assignment as a superoxo-complex was in contrast to the  $\text{TPPMn}^{\text{IV}}\text{O}_2^{2-}$  product of oxygenation of  $\text{Mn}^{\text{II}}\text{TPP}$  (TPP = tetraphenylporphyrin<sup>2-</sup>), which was formulated as a side-on peroxo-complex.<sup>27</sup> Similar results were found for the complex with a 4, 4', 4'', 4'''-tetrasulfonated ligand,<sup>28</sup> but this complex was further investigated in aqueous solution. The degree of electron transfer from  $\text{Mn}$  to  $\text{O}_2$  was found to be pH dependent, as determined by ESR. Below pH 12,  $\text{TsPcMn}^{\text{I}}\text{O}_2$  was the preferred arrangement, while  $\text{TsPcMn}^{\text{III}}\text{O}_2^-$  was more favored above pH 12. At still higher pH's, the system became "oxidase-like", producing an unidentified  $\text{Mn}$  complex, which could also be produced by over-reduction of  $\text{TsPcMnO}_2$ , and  $\text{H}_2\text{O}_2$ . These researchers also reported spectroscopic evidence of a  $\mu$ -peroxo-complex, similar to that postulated for the  $\text{Mn(TPP)}$  system.<sup>29</sup>

Recently Lever et al.,<sup>25</sup> in an intensive study of the reaction, demonstrated that  $\text{MnPc}$  would not react with  $\text{O}_2$  in dry pyridine. Dry

DMA, however, would facilitate the reaction. They also reported a number of other anomalies. For example, N-methylimidazole catalyzed the reaction of  $\text{PcMnO}_2$  to the  $\mu$ -oxo-product, as was found earlier for imidazole, therefore this was not a proton-catalyzed reaction in DMA. Lever's new interpretation was that electron transfer from the 2-position on the ring kept some  $\text{PcMn}$  present to react with the immediately formed  $\text{PcMnO}_2$ . However, an equimolar mixture of  $\text{PcMn}$  and  $\text{PcMnO}_2$  did not react. Also, the  $\mu$ -oxo-complex disproportionated to  $\text{PcMnO}_2$  in wet pyridine or pure DMA, presumably by the reverse of the formation reaction. However, no explanation could be advanced for variation in the relative proportions of the products. Further, when  $\text{PcMnO}_2$  was photolyzed to  $\text{PcMn}$  in the presence of imidazole or  $\text{Et}_3\text{N}$  in DMA or wet pyridine, no  $\text{O}_2$  was detected. However, this observation could be rationalized as a catalase reaction, producing  $\text{O}_2$ .

Oxygenation of porphyrin complexes of Mn has not received as much mechanistic study as phthalocyanine complexes, but more interest has been paid to their use as model systems or catalytic agents. An X-ray study of the oxo-bridged dimer was first performed in 1969.<sup>30</sup> Work since then has shown that the various substituted systems show a wider range of oxidation states than similar Co and Fe complexes.  $\text{MnTPP}$  in various donor solvents could be reduced by one or two electrons, but these apparently went into the ring system, producing  $\text{Mn}^{\text{I}}\text{TPP}^-$  and  $\text{Mn}^{\text{II}}\text{TPP}^{2-}$ , respectively.<sup>31</sup> Water soluble Mn(III) porphyrins could be oxidized to  $\mu$ -oxo-Mn(IV) dimers, and further to a Mn(V)=O compound.<sup>32</sup> The Mn(IV) complex was believed to be formed from an initial  $[\text{Mn}^{\text{II}}\text{P}^+]^{2+}$

oxidation product.

Mn porphyrins underwent an interesting oxygen transfer with iodosylbenzene.<sup>33</sup> The Mn(III) porphyrin reacted to produce a Mn(IV)  $\mu$ -oxo-dimer, which was originally believed to be a Mn<sup>V</sup>=O compound.<sup>34</sup> A Mn(II) porphyrin, however, would react to produce a Mn<sup>IV</sup>=O complex, which would transfer O to PPh<sub>3</sub> to produce OPPh<sub>3</sub> and Mn(III).<sup>35</sup>

More interesting was the formation of reversible complexes of the type TPPMnO<sub>2</sub>. As previously mentioned both experimental evidence<sup>36</sup> and Huckel<sup>37</sup> calculations indicated that the complexes had the general formula TPPMn<sup>IV</sup>O<sub>2</sub><sup>2-</sup>, with the peroxide bound side-on (Figure 4) and Mn above the plane of the ligand. This was the first good example of Griffith type bonding for porphyrin complexes. An equilibrium study of the reactions with various metal, porphyrin, and axial ligand substitutions<sup>27</sup> has shown that ground state electronic and steric effects are responsible for the difference between Mn and other metal porphyrins.

Besides the oxidation of PPh<sub>3</sub> discussed above, a number of other catalytic reactions involving Mn porphyrins have been reported. Perée-Fauvet and Gaudemer showed that olefins could be oxidized to ketones (and then reduced to aldehydes) by the system TPPMnCl/O<sub>2</sub>/NBu<sub>4</sub>BH<sub>4</sub>.<sup>38</sup> Further study of the reaction<sup>39</sup> demonstrated that similar results could be obtained by using TPPMn/O<sub>2</sub> or TPPMn(III)/O<sub>2</sub><sup>-</sup> as the starting reagents. A very novel system involving (N<sub>3</sub>TPPMn)<sub>2</sub>O could oxidize hydrocarbons by cleaving aromatic and aliphatic C-H bonds.<sup>40</sup>

One interesting Mn(II) complex, Mn([14]-ane N<sub>4</sub>)X<sub>2</sub> (Figure 5), is

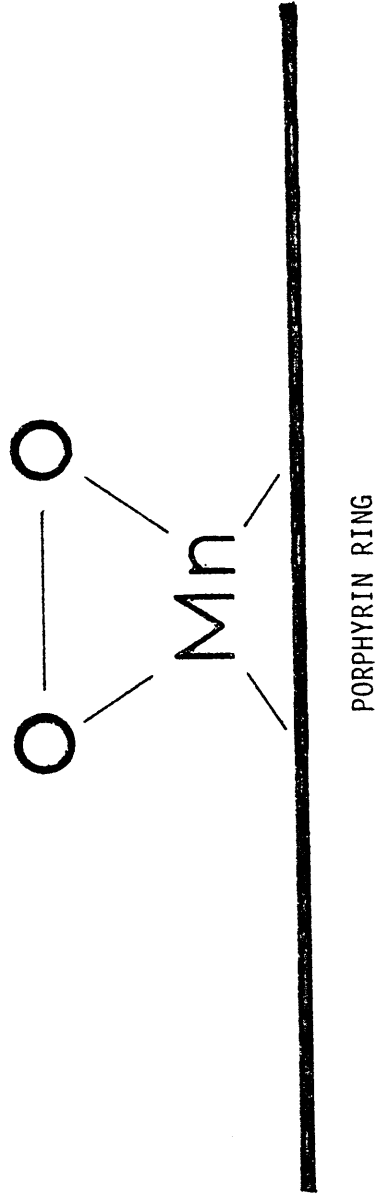


Figure 4: Structure of TPPMnO<sub>2</sub> (TPP=Tetraphenylporphyrin<sup>2-</sup>).

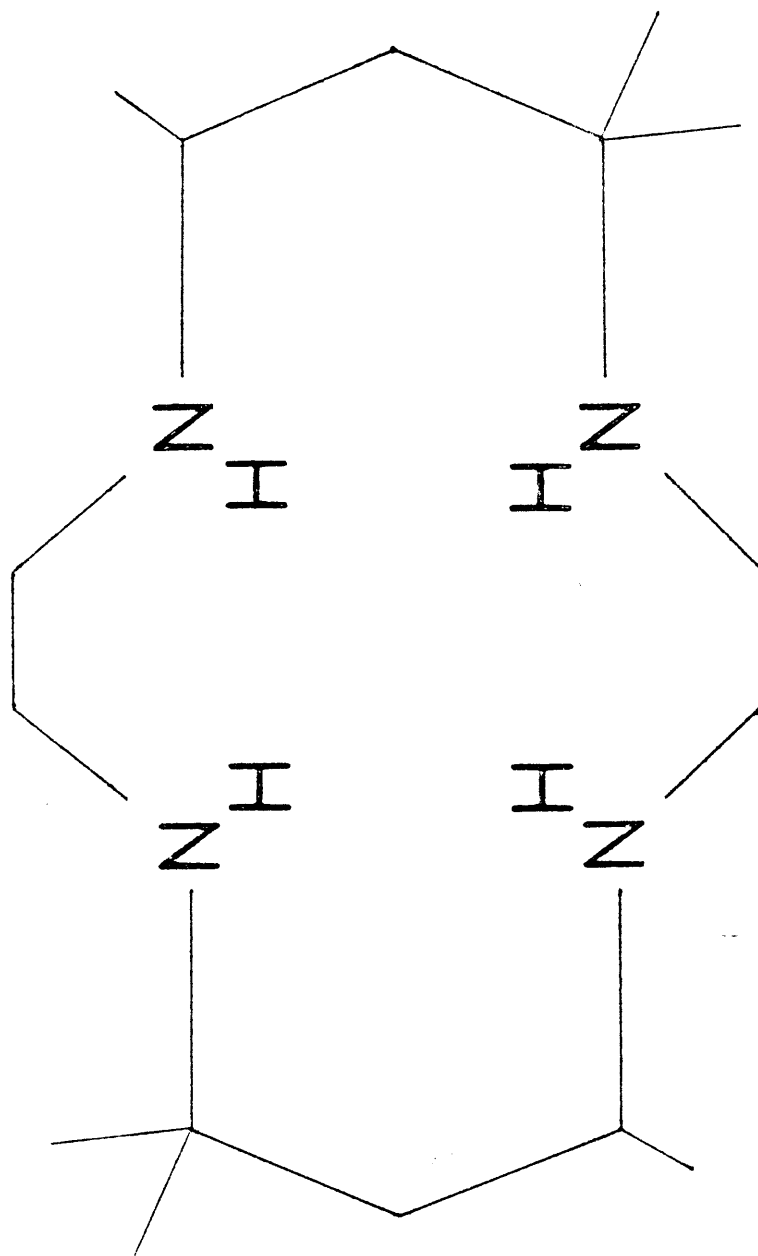


Figure 5: Structure of ([14]-ane N<sub>4</sub>).

the only solution  $O_2$ -sensitive complex with an uncharged polydentate ligand.<sup>41</sup> Solutions of the complex in aromatic solvents gave a dark precipitate with no organic component ( $Mn_xO_y \cdot zH_2O$ ) on exposure to dry  $O_2$ .

The above discussion has demonstrated that manganese complexes react with  $O_2$  in a variety of ways. Also, these complexes have been shown to be useful in a number of cases as models for biological systems such as oxygen carriers and oxygenases. Another common property that has not been specifically discussed is the high reactivity of these systems with other compounds besides  $O_2$  (and  $O_2^-$  and  $H_2O_2$ ), especially other oxidizing agents such as  $I_2$ .<sup>42</sup>

### Schiff Base Complexes of Manganese

Schiff bases, or imines, are compounds containing the C=N bond. These may be conveniently produced by condensation of a primary amine with an aldehyde or a ketone (Figure 6).<sup>43</sup> Depending on the R groups, ligands containing various numbers of other donor atoms besides the imine nitrogen may be prepared. Complexes of many transition metals have been prepared with these ligands, but this section will only present a discussion of those with Mn.

#### 1. Oxygenation Properties

Studies of  $O_2$ -sensitive manganese Schiff base complexes have lagged behind those of cobalt complexes. The first such reported Mn complex was Mn(SALEN)<sup>44</sup> in 1933, five years before Co(SALEN) was found to be  $O_2$ -sensitive. The Mn complexes, however, were irreversibly oxidized so

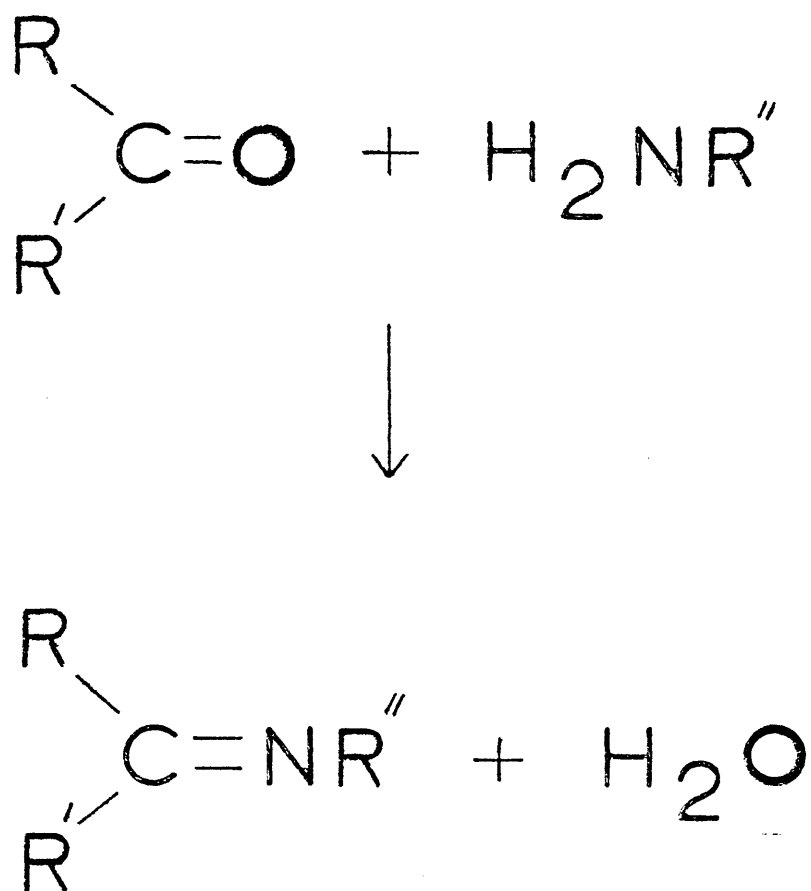


Figure 6: Synthesis of Schiff Base Ligands.

interest focused on the reversibly oxygenating Co complexes. However, with more hindsight, Mn has more known stable oxidation states than any other transition metal, and should have been a good candidate for these studies. Regardless, a large number of Mn complexes have now been investigated and many of these have been found to be oxygen sensitive. In recent years especially, now that some theories have been advanced to explain which types of complexes should react, tailoring of ligands and environments has led to a dramatic growth in the number of publications on this subject. A recent review of the oxygen sensitivity of Mn(II) complexes of various Schiff bases and other ligands should be referred to for a more comprehensive discussion.<sup>45</sup>

a) Solid State Oxygenation

Lewis et al.<sup>46</sup> reported on magnetic properties of some bidentate Mn(II) complexes with ligands formed from salicylaldehyde and a primary amine, but neglected to report if the samples reacted with air in the solid state. Matsushita et al. have reported a series of similar Mn(III)<sup>47</sup> and (IV)<sup>48</sup> bis(bidentate) complexes with coordinated Cl<sup>-</sup> anions that were air stable. Van den Bergen et al.<sup>49</sup> reported tris(bidentate) (MnL<sub>3</sub>) and bis(bidentate) (ML<sub>2</sub>X) Mn(III) species that were also air stable.

Butler et al.<sup>50</sup> studied magnetic properties of tridentate Mn(II) complexes of formula MnL prepared from salicylaldehyde and hydroxyaniline or anthranilic acid, but specifically stated that their complexes were NOT air sensitive when dry. This was also true for the Mn(II) complexes prepared by Chiswell and Lee with a ligand containing the N<sub>2</sub>As donor

set.<sup>51</sup> A Mn(III) tridentate complex, as reported by Dey and Ray,<sup>52</sup> was also O<sub>2</sub>-insensitive. They prepared their ligand from salicylaldehyde and o-aminophenol, and the complex had the formula Mn(L)(OAc)·H<sub>2</sub>O, with a coordinated acetate ion.

Tetradentate Mn(II) complexes were solid state sensitive, depending on the precise ligand.<sup>53</sup> Mn(SALEN), probably the best studied complex of this type, was not reactive, nor were complexes of the Mn(SALC<sub>n</sub>) type with three to five methylene groups between the imine nitrogens. Complexes with six to ten carbons, however, were reactive. No explanation was advanced at the time for the difference, but a clue may have been lurking in the ESR spectra of the complexes, which exhibited a postulated change from square-planar to tetrahedral geometry as the chain was lengthened. Mn(SALEN) was postulated to be dimeric square planar in the solid state<sup>54</sup>, and it is not difficult to envision how stacking of these units could preclude O<sub>2</sub> from the matrix. Tetrahedral molecules, however, would allow gaps for O<sub>2</sub> to enter in the solid state. Apparently the crossover point for appearance of an available site for O<sub>2</sub> attack was between n = 5 and 6. Figure 7 shows a typical O<sub>2</sub> uptake curve for one of these SALC<sub>n</sub> species. The product of the first step has a 0.25 ratio of O<sub>2</sub>/Mn, and was believed to be a μ-oxo-Mn(III) dimer, based on experimental evidence from ESR, IR, and magnetic moment studies. The second step of the uptake resulted in a di-μ-oxo-Mn(IV) dimer, formerly postulated to be either a μ-peroxo- or di-μ-hydroxo-Mn(III) dimer, an oxo-Mn(IV) monomer, or a catena-oxo-Mn(IV) chain (Figure 8).<sup>55,56</sup> Addition of chloro-substituents to the SAL rings

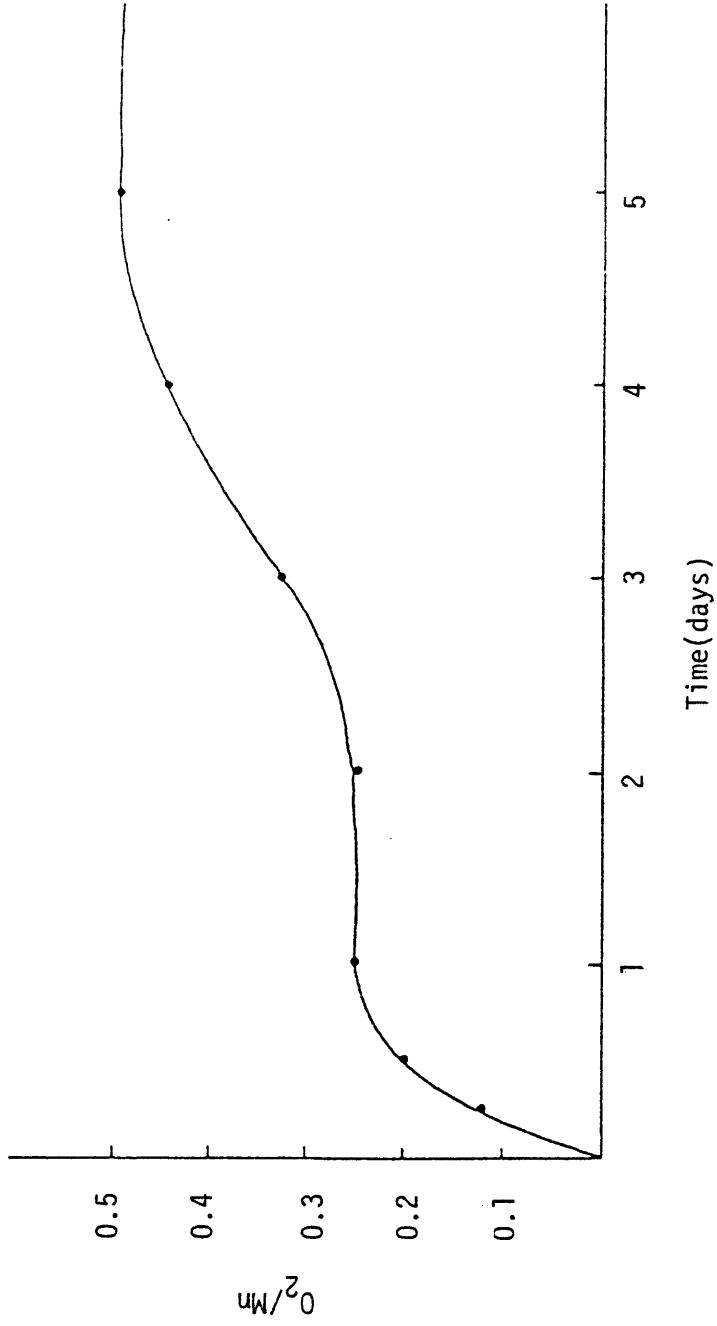
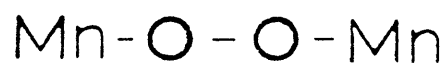
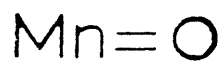


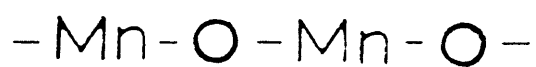
Figure 7: Solid State Oxygen Uptake of Mn(SALHXDA) .



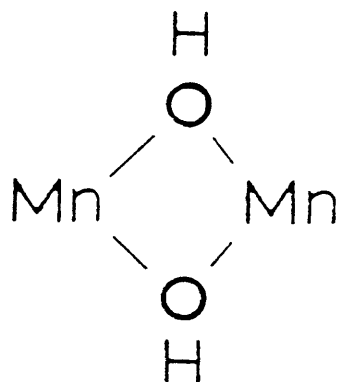
$\mu$ -Peroxo



Oxo



Catena-Oxo



Di- $\mu$ -Hydroxo

Figure 8: Early Reported Structures for Oxygenated Tetradentate Complexes.

produced unreactive complexes, but whether this was due to the electron-withdrawing ability of the chloro-group destabilizing Mn(III), or a different crystal structure, was not known. Compounds containing pyridine-2-carboxaldehyde rather than salicylaldehyde condensed with a linear diamine were O<sub>2</sub>-insensitive, both in the solid state and in solution.<sup>57</sup> The same is true for Mn(III) complexes of either the SALOPHEN<sup>58</sup> or the SALC<sub>n</sub><sup>59</sup> type.

A large number of pentadentate complexes have also been studied. PY-based ligands once again totally inhibited O<sub>2</sub> reactivity regardless of the bridging group.<sup>60</sup> With replacement by the activating SAL ring, solid state reactivity was found for the complex Mn(3-MeOSALDPT) and a set of complexes with the O<sub>2</sub>N<sub>2</sub>P donor set, Mn(ZSALPhDAPP) (Z=H, 5-NO<sub>2</sub>, 5-MeO).<sup>61</sup> Mn(3-MeOSALDPT) reacted with ~0.5 mol of O<sub>2</sub> to produce a Mn(III)-hydroxy-species.<sup>62</sup> Mn(SALDAPE) and Mn(SALBPT)<sup>63</sup> were also O<sub>2</sub>-sensitive as solids, but their products were not characterized. Pentadentate Mn(III) species formed with the same ligands, as well as other O<sub>2</sub>N<sub>3</sub> and O<sub>3</sub>N<sub>2</sub> ligands, are also O<sub>2</sub>-insensitive.<sup>64</sup>

Hexadentate PY-based complexes were O<sub>2</sub>-insensitive, as expected, but surprisingly, all of the unsubstituted SAL-complexes of this type were sensitive in the solid state, although with different rates of reaction. In general, the longer the chains between adjacent nitrogens the less reactive the complex was towards O<sub>2</sub>. This was the reverse of the tetradentate case, where the long chain complexes were the most sensitive. Another property unique to the hexadentates was that their

uptake curves continued past stoichiometric ratios of  $O_2/Mn$  of 0.25 or 0.5, indicative of initial oxidation to Mn(III) followed by ligand oxidation. Mn catalyzed oxidation of organic compounds has been reported for the tetradentate complex Mn(SALEN).<sup>65</sup> Oxygenated complexes contained a peak near  $630\text{ cm}^{-1}$  in their IR spectra, indicative of formation of an Mn-O bond. The isolated Mn(III) complexes, however, were not solid state sensitive.

Heptadentate Mn(II) complexes<sup>66,67</sup> have been reported to be insensitive in both solid state and solution studies. Both macrocyclic and chelating types (Figure 9) have been reported. Interestingly, the electrochemically reduced form of the chelated complex was  $O_2$ -sensitive,<sup>68</sup> although it was believed that the electron entered a ligand-centered orbital, and Mn(I) was not formed.

#### b) Solution Oxygenation

Studies of solution reactions with  $O_2$  are more numerous than those performed in the solid state, since, as previously stated, there are many more complexes which are  $O_2$ -sensitive in solution. Lewis et al.<sup>46</sup> prepared bidentate Mn(II) complexes under  $N_2$ , therefore it is presumed that they are  $O_2$ -sensitive in solution. The Mn(III) and (IV) bidentate complexes of Matsushita et al. reacted with  $O_2^-$  and  $H_2O$ , respectively, to produce the Mn(II) complex and  $O_2$  in certain cases. For some ligands, however, the Mn(III) complexes reacted with  $O_2^-$  to produce "Mn<sup>III</sup>-superoxo" complexes. Since this also occurred with some Mn(III) tetradentate complexes whose Mn(II) counterparts react with  $O_2$ , it may be assumed that bidentate complexes with the same ligands would also

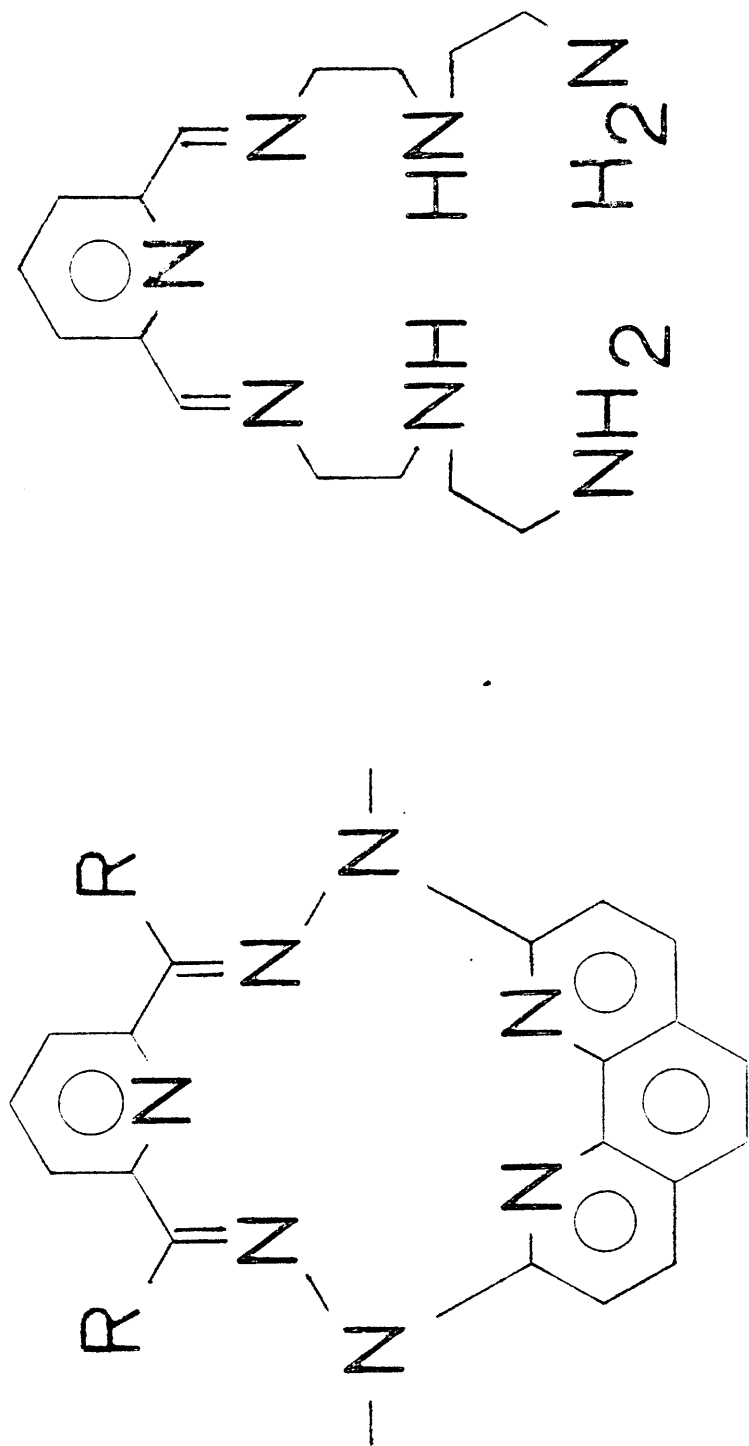


Figure 9: Heptadentate Ligands for Manganese.

have been  $O_2$ -sensitive. The same group has also studied  $O_2^-$  reactions of Mn(III) complexes containing similar polymeric ligands<sup>69</sup> (Figure 10). In this study, they found that all of the polymeric complexes produced Mn(III)- $O_2^-$  complexes identical to oxygenated Mn(II) complexes. They attributed this to steric hindrance of the polymer preventing the solvent (DMSO) from displacing the " $O_2$ " moiety. This must be contrasted, however, with the report by Coleman and Taylor<sup>70</sup> that Mn(SALEN)Cl (and Mn(SALOPHEN)(NCS)) are unreactive with  $O_2^-$ .

Tridentate complexes of Mn(II) made by Butler et al.<sup>49</sup> were "extremely susceptible to aerial oxidation when wet with solvent." Again, Mn(III) complexes with tridentate ligands were  $O_2$ -insensitive.

Tetradentate Mn(II) complexes with XSALC<sub>n</sub> type ligands were solution sensitive; this was true for all chain lengths, i.e., n=2 to 10, and for all types of substituents on either the SAL ring or the imine nitrogen. The uptake curves for the XSALC<sub>n</sub> complexes in solution were the same as those in the solid state, but the time for oxygenation was generally less, i.e. the reaction was faster. Products of the two steps were the same as in the solid state, i.e. a  $\mu$ -oxo-Mn(III) dimer, and a di- $\mu$ -oxo-Mn(IV) dimer. In another study, Mn(III)(XSALC<sub>n</sub>)(ClO<sub>4</sub>) (n=2,3) complexes with X = 5-sec-butyl were soluble enough to be subjected to mild base hydrolysis in air.<sup>71</sup> The resulting products were believed to be the di- $\mu$ -oxo-Mn(IV) dimers, which seemed to be the final fate of all of these XSALC<sub>n</sub> complexes. A similar complex could also be prepared from the 5-sec-butylSALEN complex of Mn(III) by reaction with H<sub>2</sub>O<sub>2</sub>, but the product of this reaction was better

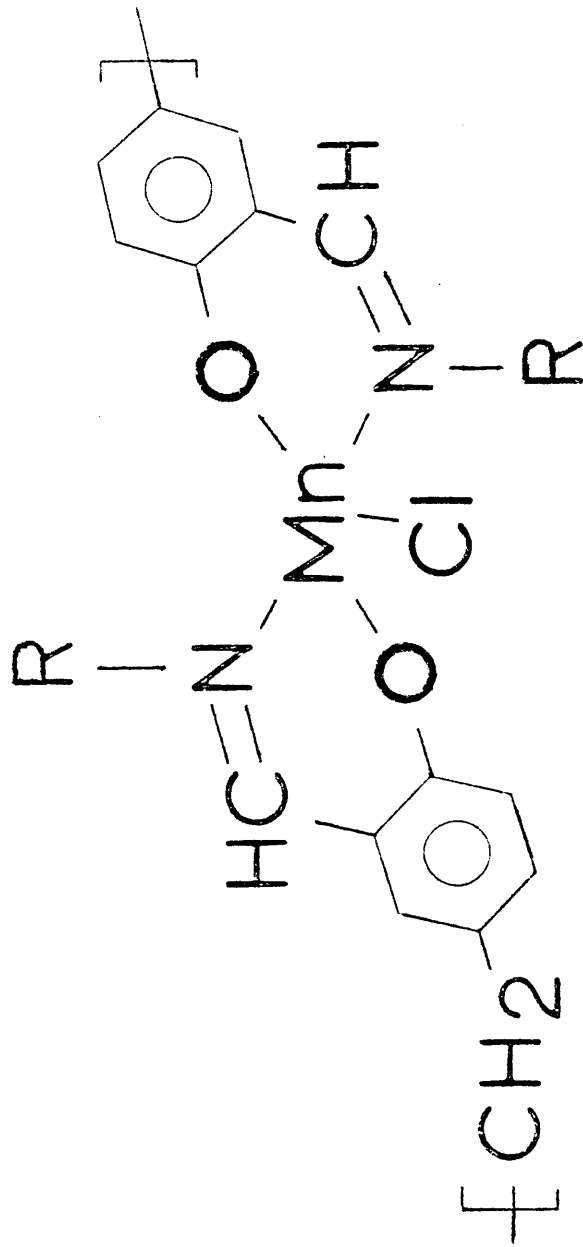


Figure 10: Structure of Polymeric Bidentate Mn(III) Complex .

formulated as a  $\mu$ -oxo- $\mu$ -hydroxy-Mn(III,IV) dimer, according to circular dichroism studies.<sup>72</sup> Oxygenations of simple  $\text{Mn}^{\text{III}}\text{LX}$  in other solvents, i.e. where hydrolysis does not occur, did not go past the Mn(III) state.

A similar tetradentate complex,  $\text{Mn}(\text{XSALROPHEN})$ , was presumed to be  $\text{O}_2$ -sensitive in solution since Mn(III) products were prepared from a  $\text{Mn}(\text{OAc})_2$  precursor in situ.<sup>58</sup> The products were formulated as  $\text{Mn}^{\text{III}}\text{L}(\text{OAc})$  or  $\text{Mn}^{\text{III}}\text{L}(\text{OH})$ , depending on the reaction conditions, but it was possible that the hydroxide was actually a di- $\mu$ -oxo-Mn(IV) compound.

Pentadentate complexes containing XSALRDPT type ligands underwent a number of types of oxygenation, depending on the nature of X and R.<sup>62</sup> When R=H, all complexes except those with X= $\text{NO}_2$  underwent an uptake similar to that in Figure 11. For X= $\text{NO}_2$ , the uptake leveled off at a ratio of 0.5  $\text{O}_2/\text{Mn}$ . This was believed to be, as was the case with some solid studies, due to Mn(III) formation followed by ligand oxidation. With the  $\text{NO}_2$ -substituent, the ligand was rendered inactive due to the electron-withdrawing nature of the group. If R = alkyl or aryl, the uptake initially resembled that of  $\text{Mn}(5\text{-NO}_2\text{SALDPT})$  (i.e. it leveled off at 0.5), but uptake continued after an incubation period). The length of the incubation period was relatively solvent independent; therefore, this was also believed to lead to ligand oxidation. It should be noted that cationic PYDPT complexes were not sensitive, nor were those of a similar ligand (Figure 12), where thiols replaced the phenols of SALDPT (and the HC=N bond was reversed).<sup>73</sup> The reason for the stability of this complex was believed to be a soft acid/soft base interaction

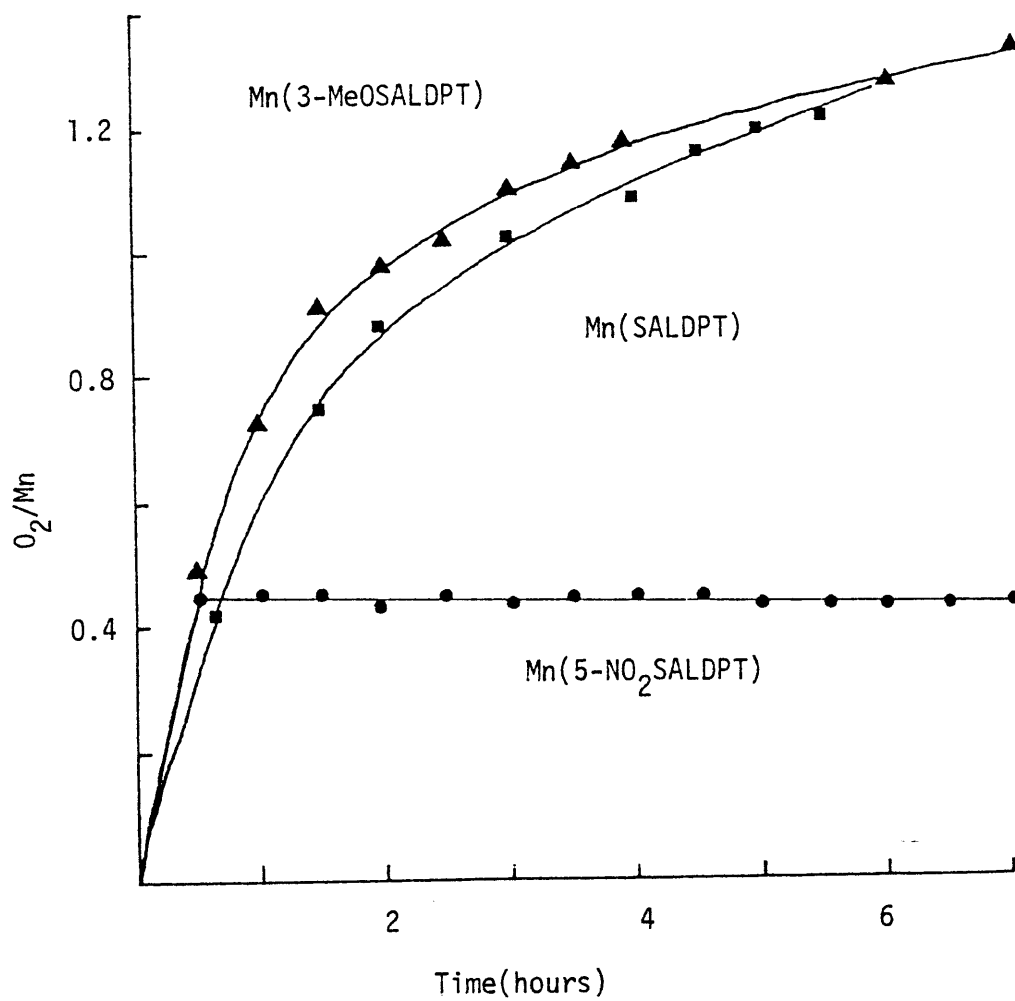
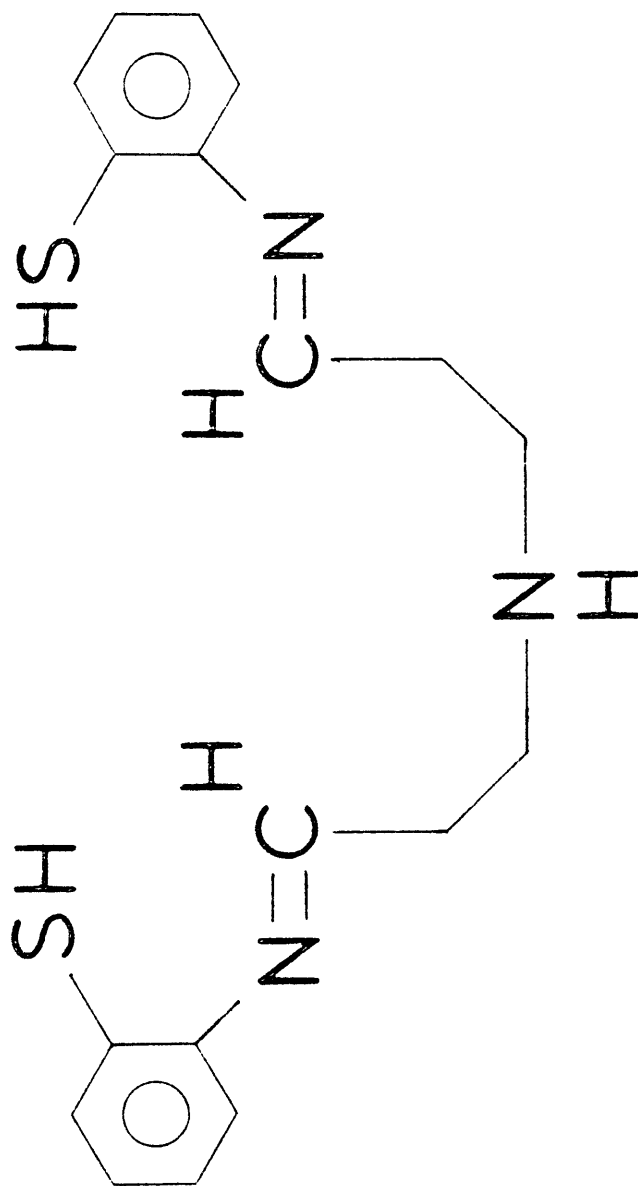


Figure 11: Oxygen Uptakes of Pentadentate Complexes in Toluene.

Figure 12: N<sub>3</sub>S<sub>2</sub> Ligand.

between Mn(II) and S stabilizing the lower oxidation state. The previously mentioned complexes containing the  $O_2N_2P$  donor set, Mn(ZSALPhDAPP), were solution sensitive but a complex containing PYPPhDAPP was not.

Attempts to isolate simple oxygenation products of Mn(XSALRDPT) were fruitless except for the  $NO_2$ -substituted complexes. If the reaction was performed under anhydrous conditions, the product was a  $\mu$ -peroxo-Mn(III) dimer, but failure to exclude water led to a hydroxy-Mn(III) complex. Modifications of the dialkylamino chain produced little change in the properties of the complexes; therefore Mn(SALDAPE), Mn(SALEPT), and Mn(SALBPT) all behave like Mn(SALDPT). The same was true for modifications on the SAL ring (Mn(NAPDPT)) or the imine nitrogen (Mn(HBPDPT)). The effect of a nitro-SAL substituent was also the same for most complexes, i.e., the uptake stopped at  $0.5 O_2/Mn$ . If the oxygenation reactions were performed in alcoholic solution in the presence of an anion<sup>74</sup>, salts of the simple  $MnL^+$  cation could be isolated. The oxygen sensitivity of these Mn(III) complexes was not investigated, but the continuous  $O_2$  uptake of the Mn(II) complexes suggested that the ligand in the Mn(III) complex was oxidizable. A number of pentadentate Mn(III) complexes reacted with  $O_2^-$  to produce postulated  $Mn^{II}-O_2^0$  complexes<sup>70</sup>. This was in contrast to the already mentioned bi- and tetradentate Mn(III) complexes of Matsuhita et al., which produced either a  $Mn^{III}-O_2^-$  species or Mn(II) and  $O_2$  on reaction with  $O_2^-$ . The particular pentadentate ligands chosen apparently made the reduction potentials of the complexes sufficiently positive to allow

full electron transfer from  $O_2^-$  to Mn(III) to occur.  $HO_2^-$  produced the Mn(II) complexes.

Hexadentate complexes of Mn(II) with ligands derived from SAL or PY with linear tetraamines exhibited extreme  $O_2$ -sensitivity (SAL-based) or no sensitivity (PY-based) in solution. A typical uptake curve for SAL-derived ligands is shown in Figure 13. The curve resembled that of the pentadentate SALDPT complexes in that there were two sections to the curve, but the break between the two parts was less marked. Other properties were also similar to those of the pentadentates, i.e. no isolable products were produced on oxygenation if the complex alone was present, and oxygenation in an alcoholic solvent with a counterion present produced the  $Mn^{III}LX$  compound. One major difference, however, is that introduction of a nitro-substituent onto the SAL ring generally rendered the Mn(II) complex inert to  $O_2$ . In the pentadentate study, the same change decreased the sensitivity, but not to such a marked degree. The Mn(III) complexes themselves were not examined for  $O_2$ -sensitivity, but, as with the pentadentates, the oxygen uptakes of the Mn(II) complexes suggested ligand oxidation may have occurred in the Mn(III) complexes. Hexadentate Mn(III) complexes react with  $O_2^-$  to produce a  $Mn^{II}-O_2^0$  species, and with  $HO_2^-$  to give the Mn(II) complex.

## 2. Electrochemistry

Previous studies of the electrochemistry of manganese Schiff base complexes were performed with bi-, tetra-, penta-, hexa-, and heptadentate ligands in DMSO and acetonitrile. The ligands used contained a number of different donor atom sets, ON,  $O_2N_2$ ,  $O_2N_3$ ,  $O_3N_2$ ,

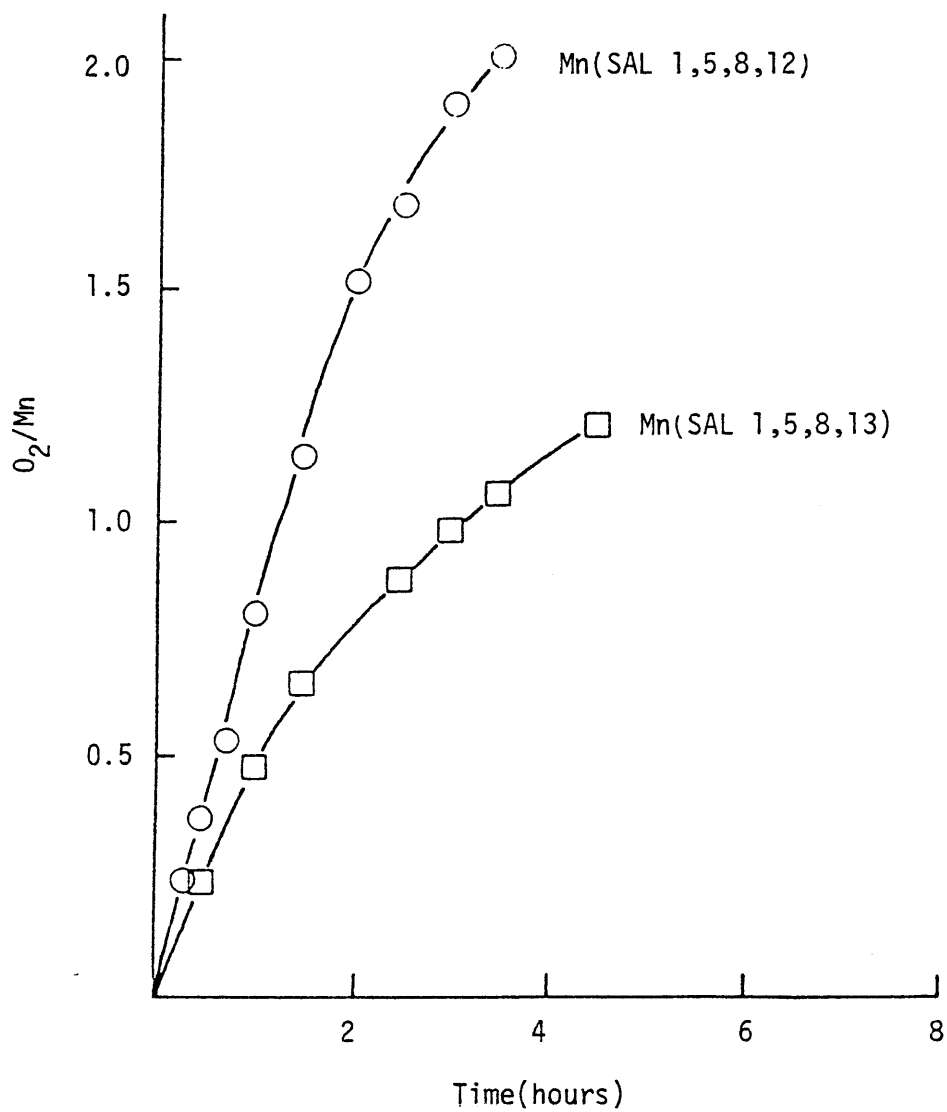


Figure 13: Oxygen Uptakes of Hexadentate Complexes in Pyridine.

$O_2SN_2$ ,  $O_2N_4$ , and  $O_2N_5$ . Mn(II), (III), and (IV) complexes were used. The majority of the Mn(II) and Mn(III) complexes studied produced voltammograms with a single quasireversible pair of peaks which were assigned to Mn(III)/Mn(II) (Figure 14). The Mn(III) and (IV) complexes of Matsushita et al. were studied by polarography, but showed reduction waves assignable to Mn(IV) $\rightarrow$ Mn(III) and Mn(III) $\rightarrow$ Mn(II).

A number of anomalous voltammograms did appear, however. The tetradentate species Mn(SALHTDA)(NCS)(SALHTDA<sup>2-</sup> = SALC<sub>n</sub><sup>2-</sup>, n = 7) produced an irreversible reduction peak, explained by a monomeric Mn(III) complex being reduced to a polymeric Mn(II) complex.<sup>59</sup> The pentadentate complexes Mn(SALEPT), Mn(SALDIEN), and Mn(SALDAES), and the hexadentate complex, Mn(SAL 1,4,7,10)(NCS) exhibited a second redox couple on or near the solvent oxidation wave in DMSO. A number of explanations for this feature were advanced, including a Mn(IV)/Mn(III) couple, oxidation of a secondary amine, two-step oxidation of a dimeric species (II,II $\rightarrow$ II,III $\rightarrow$  III,III), and differences in coordination between ligands with the same potential donors, but no strong argument could be made for any of these. The Mn(IV) complexes of Matsushita et al.<sup>75</sup> did produce both (IV)/(III) and (III)/(II) peaks but the E°'s for the (IV)/(III) couple were at about +0.9V in acetonitrile, outside the range normally accessible in DMSO.

Mn(SALDAES), as well as Mn(5-NO<sub>2</sub>SALDIEN), exhibited a further aberration. The single oxidation peak assigned to Mn(II) $\rightarrow$ Mn(III) produced two reduction peaks on the reverse scan. The sweep rate dependence of the relative reduction peak heights led to two possible

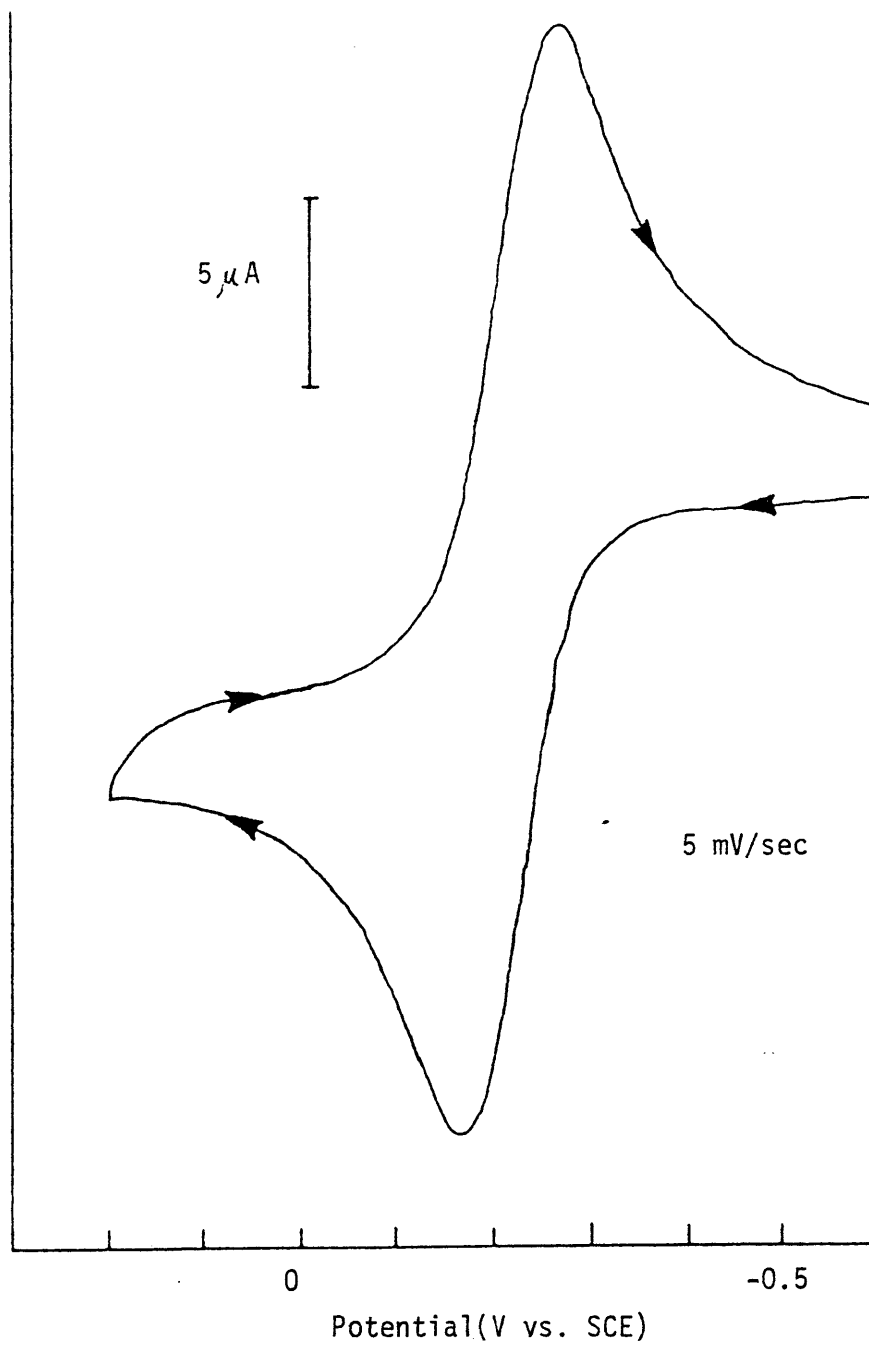


Figure 14: Cyclic Voltammogram of Mn(SALDPT) in DMSO.

explanations. The first involved two forms of Mn(III) in solution, an immediate oxidation product and a slowly formed coordination rearrangement product where a donor atom not coordinated by Mn(II) would be pulled in by the more acidic Mn(III). Less likely was a similar combination of an initial Mn(III)-Mn(II) dimer and a slowly formed decomposition mixture of the monomers. This would imply that a dimeric Mn(II) species was the stable form for these particular complexes.

The heptadentate species,  $\text{Mn(L)}^{2+}$  (L is on the right in Figure 9) underwent an irreversible reduction to  $\text{Mn(L)}^+$ , but the extra electron was postulated to go into a ligand orbital, so the reduction product was actually  $[\text{Mn}^{2+}(\text{L}^-)]^+$ . Mn(III) complexes with ZSALPhDAPP<sup>2-</sup> ligands produced irreversible reductions, as opposed to the quasireversible reductions for the Mn(III)ZSALRDPT complexes.

These individual peculiarities aside, a number of trends were seen when changes were made in the ligands. The change with the greatest effect was replacement of the salicylaldehyde ring with that of pyridine-2-carboxaldehyde. This produced electrochemical inactivity in the range normally associated with the Mn(III)/Mn(II) couple (+0.3 to -0.3V). Oxidation of the SCN<sup>-</sup> counterion was seen on the solvent limit, and a ligand reduction produced a peak at -1.30V. A second trend was found when substitutions were made on the salicylaldehyde ring. Adding an electron-donating group such as MeO<sup>-</sup> moved the peaks to more negative potentials, while an anodic shift occurred with electron-withdrawing groups such as -NO<sub>2</sub>.<sup>64</sup> The electron density apparently transferred to the metal center, and a higher electron density

stabilized the relatively electron-poor Mn(III) state, i.e. facilitated oxidation. Substitution on the imine carbon had a similar effect, with a phenyl group causing a cathodic shift relative to a hydrogen, as did addition of an alkyl group to one of the secondary nitrogens in the chain. Replacement of one of these nitrogens with a less basic oxygen or sulfur atom had the expected effect of moving the potential anodically.

## CHAPTER III

### EXPERIMENTAL

#### Materials

The following chemicals were obtained commercially and used without further purification: Manganous acetate tetrahydrate (Fisher Certified): Salicylaldehyde (Fisher Reagent): 5-Chlorosalicylaldehyde (Eastman): 5-Nitrosalicylaldehyde (Eastman): Pyridine-2-carboxaldehyde (Aldrich): 4-Bromoaniline (Eastman): Benzylamine (Eastman): 2-Aminomethylpyridine (Aldrich): 2-(2-Aminoethyl)pyridine (Aldrich).

6-Methylpyridine-2-carboxaldehyde was obtained from Aldrich and purified by vacuum distillation prior to use.

#### Preparation of New Complexes

Mn(SAL-4-BrANL)<sub>2</sub>: This complex was prepared via a two-step procedure. The ligand was first prepared by refluxing 0.06 mol (7.33 g) salicylaldehyde and 0.06 mol (10.32 g) 4-bromoaniline in 50 mL of benzene. A Dean and Stark trap was attached to the flask containing the refluxing yellow solution in order to remove water formed during the reaction. Upon completion of the reaction, i.e. when no further water was carried over, the solution was cooled to room temperature and vacuum filtered. The resulting yellow crystals were recrystallized from benzene and air dried.

The complex itself was prepared by initially dissolving 0.01 mol (2.76 g) SAL-4-BrANL in 60 mL of methanol. NaOH (0.01 mol, 0.40 g) dissolved in 10 mL of methanol was added, and the orange solution refluxed under N<sub>2</sub> for 30 minutes. After cooling to room temperature, 50

mL of previously deaerated methanol containing 0.005 mol (1.23 g)  $\text{Mn}(\text{OAc})_2 \cdot 4\text{H}_2\text{O}$  was added dropwise, with stirring. The solution became red-orange on addition of one drop, and a precipitate began to form after ~10 mL of the manganese solution was added. Stirring was continued for 90 minutes after addition, then the flask was capped and transferred to an inert atmosphere box. The suspension was stirred for a further 2 hours in the box, and then vacuum filtered. The resulting red-orange microcrystalline material was washed with methanol and dried over silica gel under vacuum for 12 hours.

$\text{Mn}(\text{SALPMA})_2$ : Salicylaldehyde (0.01 mol, 1.22 g), benzylamine (0.01 mol, 1.07 g), and NaOH (0.01 mol, 0.40 g) were dissolved in 60 mL isopropanol. The suspension of the yellow Na-Schiff base salt was refluxed under  $\text{N}_2$  for 30 minutes, then cooled to room temperature. Fifty (50) mL of deaerated  $\text{H}_2\text{O}$  containing  $\text{Mn}(\text{OAc})_2 \cdot 4\text{H}_2\text{O}$  (0.005 mol, 1.23 g) were added dropwise with stirring. The suspension dissolved after ~3 mL of solution was added, and reprecipitation of a second solid occurred after ~40 mL were added. Stirring was continued for 1 hour after addition. The flask was then capped and transferred to the glove box. The yellow-orange product was filtered, washed with 95% ethanol and hexane, and dried under vacuum over silica gel for 12 hours.

$\text{Mn}(\text{SALAEPP})_2 \cdot 2\text{H}_2\text{O}$ : Ten(10) mL of methanol containing preformed salicylideneiminato-2-(2-ethyl)pyridine (0.01 mol) was diluted with 50 mL of methanol. A further 10 mL of methanol was added containing only NaOH (0.01 mol, 0.40 g), and the entire solution was refluxed under  $\text{N}_2$  for 15 minutes. After cooling to room temperature, 20 mL of deaerated  $\text{H}_2\text{O}$  containing  $\text{Mn}(\text{OAc})_2 \cdot 4\text{H}_2\text{O}$  (0.005 mol, 1.23 g) were added dropwise,

with stirring continuing for a further 90 minutes after addition. The flask was then capped and transferred to the glove box. The yellow-brown precipitate was filtered, washed with methanol, and dried under vacuum over silica gel for 12 hours.

Mn(SALAMP)<sub>2</sub>·C<sub>3</sub>H<sub>7</sub>OH: Salicylaldehyde (0.01 mol, 1.22 g) and 2-aminomethylpyridine (0.01 mol, 1.08 g) were dissolved in 60 mL isopropanol. The solution was refluxed under N<sub>2</sub> for 30 minutes. KOH (0.01 mol, 0.56 g) was then added, and the solution allowed to cool to room temperature. Mn(OAc)<sub>2</sub>·4H<sub>2</sub>O (0.005 mol, 1.23 g) dissolved in 25 mL deaerated water was added dropwise, with stirring continued for 1 hour after the addition. The flask was capped and transferred to the glove box, and the light brown precipitate filtered, washed with 95% ethanol and heptane, and dried under vacuum over silica gel for 12 hours.

Mn(5-ClSALAMP)<sub>2</sub>·H<sub>2</sub>O: 5-Chlorosalicylaldehyde (0.01 mol, 1.56 g) and 2-aminomethylpyridine (0.01 mol, 1.08 g) were dissolved in 60 mL isopropanol. The solution was refluxed under N<sub>2</sub> for 30 minutes, KOH (0.01 mol, 0.56 g) was added, and the solution cooled to room temperature. Deaerated H<sub>2</sub>O (30 mL) containing Mn(OAc)<sub>2</sub>·4H<sub>2</sub>O (0.005 mol, 1.23 g) was added dropwise, with stirring continuing for 1 hour after addition. The flask was then capped and transferred to the glove box. The bright yellow precipitate was filtered, washed with 95% ethanol and heptane, and dried under vacuum over silica gel for 12 hours.

Mn(5-NO<sub>2</sub>SALAEPP)<sub>2</sub>: The synthetic procedure for this complex was designed to produce a Mn(III) complex; however, the presence of the nitro-group seems to inhibit oxidation of the metal. Therefore, a Mn(II) species was isolated instead.

2-(2-Aminoethyl)pyridine (0.005 mol) dissolved in 20 mL isopropanol was added to 5-nitrosalicylaldehyde (0.005 mol), also in 20 mL isopropanol.  $N_2$  was continuously bubbled through the yellow-orange solution. KOH (0.01 mol) in 10 mL deaerated  $H_2O$  was added, followed by dropwise addition of  $Mn(OAc)_2 \cdot 4H_2O$  (0.0025 mol) in another 10 mL of deaerated  $H_2O$ . Solid  $NH_4NCS$  (0.03 mol) was then added, and bubbling continued until complete dissolution had occurred. The  $N_2$  flow was stopped and replaced by a stream of air. Aeration was continued for 30 minutes, after which the orange precipitate was filtered, washed with 95% ethanol and water, and dried at  $100^\circ C$  in vacuum.

$Mn(5-C1SALAMP)_2(NCS)$ ,  $Mn(5-C1SALAEP)_2(NCS)$  and  $Mn(5-MeOSALAEP)_2(NCS)$ : These compounds were prepared via the same procedure as  $Mn(5-NO_2SALAEP)_2$  except for starting reagents, 5-chlorosalicylaldehyde and 2-aminomethylpyridine for  $Mn(5-C1SALAMP)_2(NCS)$ , 5-chlorosalicylaldehyde and 2-(2-aminoethyl)pyridine for  $Mn(5-C1SALAEP)_2(NCS)$ , and 5-methoxysalicylaldehyde and 2-(2-aminoethyl)pyridine for  $Mn(5-MeOSALAEP)_2(NCS)$ . Unlike the nitro-complex, however, oxidation did occur in these compounds, and the aerated solutions and products were a green-brown color.

$Mn(6-MePYAMP)_2(NCS)_2$ ,  $Mn(PYAEP)(NCS)_2$ , and  $Mn(6-MePYAEP)(NCS)_2$ : The synthetic procedures for these three compounds are identical except for starting materials, 6-methylpyridine-2-carboxaldehyde and 2-aminomethylpyridine for  $Mn(6-MePYAMP)_2(NCS)_2$ , pyridine-2-carboxaldehyde and 2-(2-aminoethyl)pyridine for  $Mn(PYAEP)(NCS)_2$ , and 6-methylpyridine-2-carboxaldehyde and 2-(2-aminoethyl)pyridine for  $Mn(6-MePYAEP)(NCS)_2$ .

The appropriate amine (0.005 mol) dissolved in 12 mL isopropanol was added to a stirring solution of the aldehyde (0.005 mol), also in 12 mL isopropanol, with continuous N<sub>2</sub> bubbling into the yellow solution. Mn(OAc)<sub>2</sub>·4H<sub>2</sub>O (0.0025 mol) in 10 mL deaerated H<sub>2</sub>O was then added, followed by a further 10 mL H<sub>2</sub>O containing NH<sub>4</sub>NCS (0.03 mol). Bubbling continued for another 30 minutes. The resulting yellow-orange precipitate was washed with isopropanol and water and dried at 100°C in vacuum.

#### Previously Reported Complexes

The following complexes were synthesized according to repetitions or modifications of previously reported literature procedures<sup>53,62,76</sup>: Mn(SALEN), Mn(3-MeOSALEN), Mn(5-C1SALEN), Mn(SALBTDA), Mn(SALHXDA), Mn(SALHTDA), Mn(SALOTDA), Mn(SALDCDA), Mn(SALDPT), Mn(3-MeOSALDPT), Mn(5-C1SALDPT), Mn(5-NO<sub>2</sub>SALDPT), and Mn(SAL 1,5,8,12).

#### Physical Measurements

Carbon, hydrogen, and nitrogen analyses were performed by Atlantic Microlab, Inc., Atlanta, GA, and by the Microchemical Analysis Laboratory, Department of Chemistry, University of California, Berkeley, CA. Mass spectral analyses were performed in the Department of Biochemistry at VPI & SU on a Varian MAT 112 Electron Impact Mass Spectrometer, with a probe temperature of 200°C and an electron energy of 70 eV.

Infrared spectra were obtained on Nujol mulls or neat liquids from 4000 to 400 cm<sup>-1</sup> between KBr discs using a Perkin-Elmer 283 Infrared Spectrophotometer. Routine UV-visible spectra were obtained on a

Perkin-Elmer 552 Spectrophotometer.

Magnetic susceptibility data were obtained at room temperature via the Faraday method.  $\text{Hg}[\text{Co}(\text{SCN})_4]$  and  $\text{Ni}(\text{en})_3\text{S}_2\text{O}_3$  were used as calibrants. A Cahn RG electrobalance was used in combination with a Varian V-4005 electromagnet and V-2900 power supply. Conductivity measurements in solution were performed using a Beckman conductivity bridge. Oxygen uptake measurements were performed using a modified Warburg apparatus.<sup>77</sup>

### Kinetic Studies

UV-visible spectra for kinetic studies were run on an Aminco DW-2 Spectrophotometer in the repetitive scan mode. The reactions were initiated as follows: 20 mL of solvent was saturated with  $\text{O}_2$  by bubbling for 30 minutes. The temperature of the solvent was maintained at  $25 \pm 1^\circ\text{C}$  by immersion in a large volume of water preheated to  $25^\circ\text{C}$ . A small amount of complex was added, the solution was stirred vigorously for a few seconds, and an aliquot removed by syringe. This aliquot was injected into a 1 cm quartz spectrophotometer cell through a Swinny filter containing a Millipore teflon filter to remove any undissolved particulate matter. The cell was then placed in the thermostated sample compartment of the spectrophotometer, along with a blank containing oxygenated solvent. The amount of solid added was sufficiently small to insure at least a 10:1 ratio of  $\text{O}_2$  to complex.

Kinetic studies following the change in  $\text{O}_2$  concentrations were performed using a 731 Clark-type oxygen electrode from Transidyne General Corp., Ann Arbor, MI, with potential control and current

measuring circuitry donated by Dr. P. Hall of the Department of Chemistry at VPI & SU. To initiate the reaction, a small aliquot of oxygenated solvent was added to a deaerated, relatively concentrated solution (at least 10:1 complex to  $O_2$ ) of complex in a sealed cell containing the electrode tip, with magnetic stirring to insure quick mixing. Data were examined by standard kinetic methods.<sup>78-80</sup> Cells for both studies were cleaned between runs using a concentrated solution of acidic  $H_2O_2$  to insure removal of oxidized species, especially  $MnO_2$ .

### Electrochemical Studies

Voltammetric studies were performed using a Bioanalytical Systems CV-1A cyclic voltammetry instrument, or, more frequently, a combination 551 Potentiostat-Galvanostat, 567 Function Generator, and 731 Digital Integrator from ECO Instruments, Cambridge, MA. The electrodes used were a Beckman platinum disc working electrode, Fisher saturated calomel reference electrode, and platinum coil counter electrode. The solvents used were DMSO and pyridine, with a 0.1M tetraethylammonium perchlorate electrolyte. Solutions were degassed with  $N_2$  before use and a flow of gas was maintained over them during recording of the voltammograms. Scan rates were routinely varied from 1 to 100 mV/sec. The concentrations of the complexes were  $\sim 1 \times 10^{-3}M$ . Coulometric studies were performed using the ECO control instrumentation, but a cell with a mercury pool working electrode and frit-isolated compartments for calomel and counter electrodes was employed.

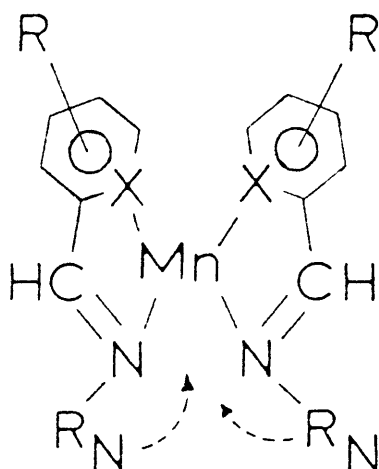
## CHAPTER IV

### RESULTS AND DISCUSSION

#### Composition of Newly Synthesized Complexes

Attempts at isolating new complexes containing bi- and tridentate ligands were rather frustrating. Most of the higher denticity complexes, first prepared by previous researchers, sometimes seemed to just fall out of solution, making the difficulty in preparing the new complexes quite puzzling. Of ~100 attempted syntheses of ~40 different complexes, only the 12 presented in Table I were produced at a purity level deemed suitable for further work. As seen in Figure 15, these have the general formulae  $MnL_2$ ,  $MnL_2(NCS)$ ,  $MnL_2(NCS)_2$ , and  $MnL(NCS)_2$ . The analytical results (Table I) show that even these complexes sometimes have borderline purity, but after numerous synthetic attempts, it was hoped that any impurities would not significantly affect the results of the oxygenation and electrochemical studies. Attempts to recrystallize the impure complexes, both these and unreported ones, were failures. As with previous complexes of this type, any solvent in which they dissolved seems to cause decomposition of the complex on recrystallization, usually with great loss of N as found by subsequent CHN analysis.

The composition of the compounds is in all cases compatible with IR spectra (Table II).<sup>81,82</sup> Because of the means of synthesis of the complexes, the first diagnostic tools are examination of the C=O ( $1700\text{ cm}^{-1}$ ) and N-H ( $3500$  and  $3400\text{ cm}^{-1}$ ) stretching regions to see if there is any unreacted amine or aldehyde. The absence of such peaks implies that



<u>Complex</u>	<u>X</u>	<u>R<sub>N</sub></u>	<u>R</u>
<u>Mn(II)</u>			
Mn(SALPMA) <sub>2</sub>	CO <sup>-</sup>	CH <sub>2</sub> φ	H
Mn(SAL-4-BrANL) <sub>2</sub>	CO <sup>-</sup>	φBr	H
Mn(SALAEPA) <sub>2</sub>	CO <sup>-</sup>	C <sub>2</sub> H <sub>4</sub> PY	H
Mn(SALAMP) <sub>2</sub>	CO <sup>-</sup>	CH <sub>2</sub> PY	H
Mn(5-ClSALAMP) <sub>2</sub>	CO <sup>-</sup>	CH <sub>2</sub> PY	5-Cl
Mn(5-NO <sub>2</sub> SALAEPA) <sub>2</sub>	CO <sup>-</sup>	C <sub>2</sub> H <sub>4</sub> PY	5-NO <sub>2</sub>
Mn(6-MePYAMP) <sub>2</sub> (NCS) <sub>2</sub>	N	CH <sub>2</sub> PY	6-Me
Mn(PYAEPA)(NCS) <sub>2</sub>	N	C <sub>2</sub> H <sub>4</sub> PY	H
Mn(6-MePYAEPA)(NCS) <sub>2</sub>	N	C <sub>2</sub> H <sub>4</sub> PY	6-Me
<u>Mn(III)</u>			
Mn(5-ClSALAMP) <sub>2</sub> (NCS)	CO <sup>-</sup>	CH <sub>2</sub> PY	5-Cl
Mn(5-MeOSALAEPA) <sub>2</sub> (NCS)	CO <sup>-</sup>	C <sub>2</sub> H <sub>4</sub> PY	5-MeO
Mn(5-ClSALAEPA) <sub>2</sub> (NCS)	CO <sup>-</sup>	C <sub>2</sub> H <sub>4</sub> PY	5-Cl

The dotted arrows represent potential coordination by the pyridine group in the AMP/AEP ligands.

Figure 15: Structural Formulae of New Complexes.

Table I. Elemental Analyses for New Complexes

Complex	$\%C/\text{Calcd.}$	$\%C/\text{Fnd.}$	$\%H/\text{Calcd.}$	$\%H/\text{Fnd.}$	$\%N/\text{Calcd.}$	$\%N/\text{Fnd.}$
<u>Mn(II)</u>						
Mn(SALPMA) <sub>2</sub>	70.74	70.61	5.09	5.12	5.89	5.86
Mn(SAL-4-BrANL) <sub>2</sub>	51.60	51.36	3.00	3.09	4.63	4.57
Mn(SALAEF) <sub>2</sub> ·2H <sub>2</sub> O	62.11	61.12	5.60	5.60	10.34	10.20
Mn(SALAMP) <sub>2</sub> ·C <sub>3</sub> H <sub>7</sub> OH	64.80	63.37	5.64	5.18	10.42	10.55
Mn(6-MePYAMP) <sub>2</sub> (NCS) <sub>2</sub>	55.80	56.01	4.53	4.33	18.60	18.23
Mn(PYAEF)(NCS) <sub>2</sub>	47.12	47.87	3.43	3.63	18.31	18.07
Mn(6-MePYAEF)(NCS) <sub>2</sub>	48.49	48.90	3.81	3.92	17.66	17.62
Mn(5-ClSALAMP) <sub>2</sub> ·H <sub>2</sub> O	55.35	55.34	3.93	3.95	9.93	9.90
Mn(5-NO <sub>2</sub> SALAEF) <sub>2</sub>	56.47	56.59	4.06	4.25	14.12	13.95
<u>Mn(III)</u>						
Mn(5-ClSALAMP) <sub>2</sub> (NCS)	53.65	53.32	3.34	3.03	11.59	11.74
Mn(5-MeOSALAEF) <sub>2</sub> (NCS)	58.85	58.90	4.94	4.80	11.07	11.17
Mn(5-ClSALAEF) <sub>2</sub> (NCS)	55.08	54.80	3.83	3.90	11.07	10.97

Table II. Infrared Data for New Complexes ( $\text{cm}^{-1}$ )(a)

<u>Complex</u>	<u>C-N(imine)</u>	<u>C-O</u>	<u>C-N(pyridine)</u>	<u>SCN<sup>-</sup></u>
<u>Mn(II)</u>				
Mn(SALPMA) <sub>2</sub>	1618	1229	-	-
Mn(SAL-4-BrANL) <sub>2</sub>	1607(1621)	1225(1230)	-	-
Mn(SALAEF) <sub>2</sub>	1620(1631)	1220(1220)	1568(1590)	-
Mn(SALAMP) <sub>2</sub>	1620(1633)	1220(1210)	1571(1591)	-
Mn(5-C1SALAMP) <sub>2</sub>	1621	1219	1575	-
Mn(5-NO <sub>2</sub> SALAEF) <sub>2</sub>	1618	1209	1538	-
Mn(6-MePYAMP) <sub>2</sub> (NCS) <sub>2</sub>	1595	-	1567	2041
Mn(PYAEF)(NCS) <sub>2</sub>	1590	-	1562	2041
Mn(6-MePYAEF)(NCS) <sub>2</sub>	1590	-	1560	2041
<u>Mn(III)</u>				
Mn(5-C1SALAMP) <sub>2</sub> (NCS)	1620	1228	1573	2029
Mn(5-MeOSALAEF) <sub>2</sub> (NCS)	1590	1228	1536	2037
Mn(5-C1SALAEF) <sub>2</sub> (NCS)	1618	1205	1572	2030

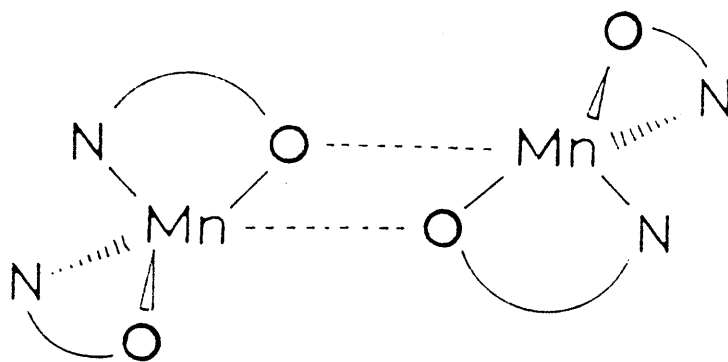
(a) Numbers in brackets are values for the free ligands.

formation of the Schiff base was quantitative, or at least no unreacted precursors were incorporated into the complex. The ligands should contain two other bands, C=N ( $1620\text{ cm}^{-1}$ ) and C-O ( $1225\text{ cm}^{-1}$ ) (except for the PY-based complexes) stretches. These are present in all cases. Not only should the peaks be there, but if the free ligand's spectrum is available for comparison, these vibrational frequencies should be shifted to a lower value in the complex, as donation of charge from the heteroatom decreases the bond order. In the three cases where comparisons could be made, a decrease in the C=N frequency of  $\sim 10\text{ cm}^{-1}$  was observed, but not that for C-O. Reexamination of the free ligand spectra shows a strong indication of intramolecular chelate H-bonding (a large broad peak from  $3300$  to  $2600\text{ cm}^{-1}$ ), which may have decreased the C-O frequency before coordination.

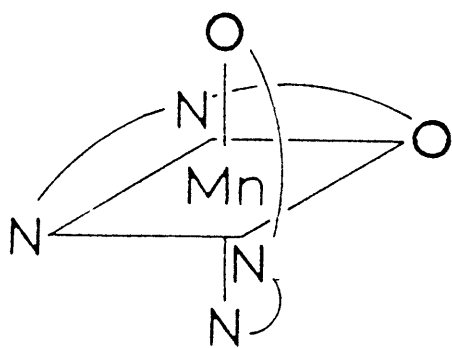
Other features in the IR spectra include the C=N pyridine ring stretch at  $1550\text{ cm}^{-1}$  for the tridentate ligands. A decrease in this frequency of  $\sim 20\text{ cm}^{-1}$  can be seen on coordination due to the same effect as for the imine C=N. The absorbance of the  $\text{SCN}^-$  ion in the Mn(III) and PY-based complexes is also quite marked ( $2040\text{ cm}^{-1}$ ). An attempt was made to use the peak position to determine if the ion was coordinated or not, but the peak position is ambiguous. Free  $\text{SCN}^-$  (KSCN) absorbs at  $2050\text{ cm}^{-1}$ , while the complexed ion (N-bonded) absorbs at  $\sim 2000\text{ cm}^{-1}$ . Bridging and/or S-bonded thiocyanate forms can be ruled out entirely because each absorbs near or above  $2100\text{ cm}^{-1}$ . Compounds formulated as solvates show a broad band assignable to the O-H stretch of hydrogen-bonded lattice solvent from  $3300$  down to  $2700\text{ cm}^{-1}$ . The hydrated

species should show an H-O-H bending peak at  $1620\text{ cm}^{-1}$  but this region is obscured by the C=N(imine) stretch. Nujol vibrations interfere with the detection of any bands due to the isopropyl group in  $\text{Mn}(\text{SALAMP})_2 \cdot \text{C}_3\text{H}_7\text{OH}$ . The non-donor substituent groups such as  $-\text{NO}_2$ , C-Cl, and C-Br should also exhibit characteristic absorbances in their IR spectra, but only the very strong  $-\text{NO}_2$  symmetric and asymmetric stretches ( $1500$  and  $1320\text{ cm}^{-1}$ ) could be definitely assigned.<sup>83</sup> A number of spectra contained peaks in the Mn-O stretching region ( $600\text{--}700\text{ cm}^{-1}$ ), but these did not interfere with observation of actual Mn-O stretches.

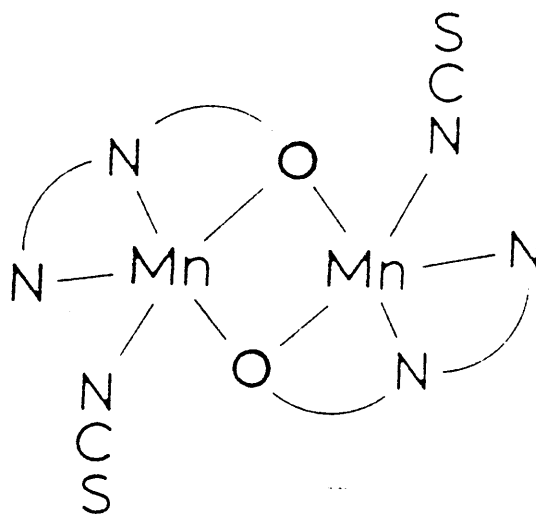
One thing that is unfortunately lacking here is a useful piece of experimental evidence as to the coordination geometry of the complexes. Co and Ni, two other transition metals whose Schiff base complexes have been studied, often have their complex geometries assigned from d-d bands in their visible spectra.<sup>84,85</sup> Unfortunately, Mn complex spectra are remarkably bland, containing either one broad peak (Mn(III)) or no d-d peaks (Mn(II)) (vide infra). However, studies with molecular models indicate that the ligands used here are flexible enough to allow full coordination, and the postulated solid state coordination geometries (Figure 16) are octahedral, with meridional coordination (for most tridentate ligands), or pseudo-tetrahedral with possible dimerization, producing a distorted trigonal bipyramidal structure, for the bidentate ligands<sup>86</sup>. For the Mn(III) compounds and the 6-MePYAMP compound, this implies that the  $\text{SCN}^-$  ion is not coordinated. The PYAEP complexes present an anomalous case in that the Mn:ligand ratio is 1:1. For these compounds, there may be a dimeric trigonal bipyramidal structure



BIDENTATES



TRIDENTATES



MN(ZSALAEP)(NCS)

Figure 16: Proposed Structures of New Complexes.

involving both ligand and  $\text{SCN}^-$  coordination similar to that reported for  $\text{Cu}(\text{SALAEP})\text{Cl}$ .<sup>87</sup>

### Physical Properties of New Complexes

The properties of the new complexes which were studied were their UV-visible spectra, solution conductivities, and magnetic moments. The UV-visible spectra were almost featureless in the visible region (Table III). This of course is due to the electronic configuration of Mn(II) and (III) compounds in fields of cubic symmetry (presupposed).<sup>88</sup> High spin Mn(II)( $d^5$ ) in near-tetrahedral or octahedral coordination has no spin-allowed d-d transitions. The yellow/orange color of these complexes is therefore entirely due to either intraligand or charge-transfer transitions extending into the visible. Mn(III)( $d^4$ ) in near-tetrahedral or octahedral coordination has one allowed d-d transition. This is a broad peak at  $\sim 600$  nm ( $\Delta\lambda_{1/2} \approx 125$  nm). The width of the peak is undoubtedly due to Jahn-Teller distortion of the complex into tetragonal symmetry. This visible absorbance causes the characteristic dark brown/green color observed for these complexes.

Comparison of ligand UV spectra with complex UV spectra (Figure 17) shows that the Mn(II) complexes have one peak or shoulder that is not found for the free ligand at around 370 nm, as well as minor perturbations in other peaks. This new peak is probably a charge-transfer transition. The direction of transfer can be determined only by examining spectral changes accompanying oxidation of Mn(II) to Mn(III). When this happens the peak disappears, and it must be assumed that it shifts to lower wavelength and is hidden under the intraligand

Table III. UV-Visible Absorbance Maxima for New Complexes(a)

Complex	DMSO			Pyridine		
	$\pi \rightarrow \pi^*$	M+L	d+d	$\pi \rightarrow \pi^*$	M+L	d+d
<u>Mn(III)</u>						
Mn(SALPMA) <sub>2</sub>	295(sh)	358			372	
Mn(SAL-4-BRANL) <sub>2</sub>	270,	341			340	
Mn(SALAMP) <sub>2</sub>	314(262, 313)	358			372	
Mn(SALAE) <sub>2</sub>	315(272, 315)	348			370	
Mn(5-C1SALAMP) <sub>2</sub>		390			378	
Mn(5-NO <sub>2</sub> SALAE) <sub>2</sub>	370(sh), 400, 440(sh)				386	
Mn(6-MePYAMP) <sub>2</sub> (NCS) <sub>2</sub>		360(sh)			360(sh)	
Mn(PYAE) <sub>2</sub> (NCS) <sub>2</sub>	265			$\pi \rightarrow \pi^*$ tail only		
Mn(6-MePYAE) <sub>2</sub> (NCS) <sub>2</sub>	268, 276(sh)			$\pi \rightarrow \pi^*$ tail only		
<u>Mn(III)</u>						
Mn(5-C1SALAMP) <sub>2</sub> (NCS)		380	590(sh)	326	380(sh)	590(sh)
Mn(5-MeOSALAE) <sub>2</sub> (NCS)	325(sh)		660(sh)	340(sh)		650(sh)
Mn(5-C1SALAE) <sub>2</sub> (NCS)	325(sh)	386	590(sh)	320	388	600(sh)

(a) Values for free ligands in brackets

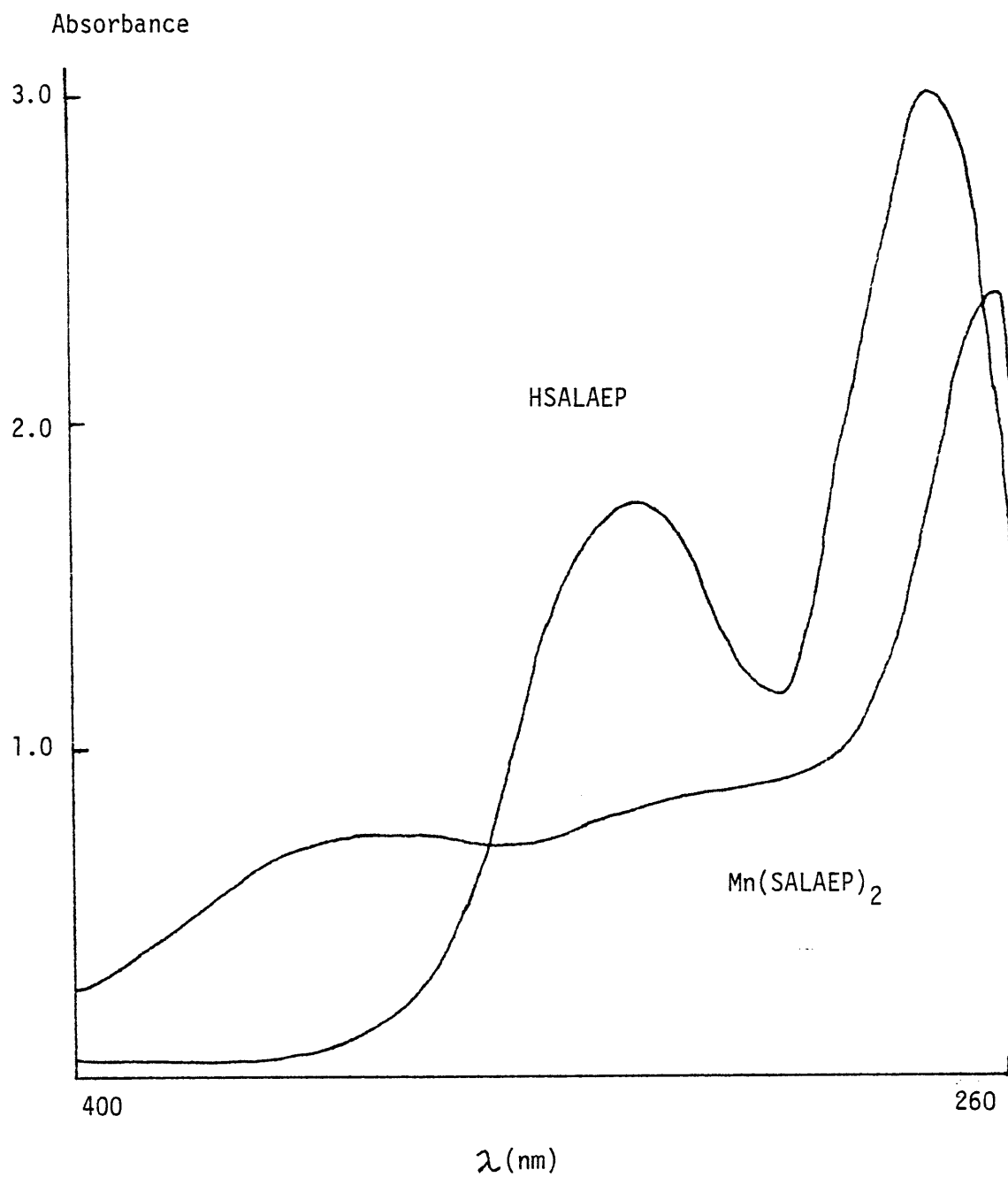


Figure 17: Ligand and Complex Spectra in DMSO.

bands. Since the transition becomes more difficult as the charge on Mn increases, this implies a metal-to-ligand charge-transfer assignment for the 370 nm band. As the charge on Mn increases, the electrostatic pull on electrons in metal-centered molecular orbitals increases and more energy is required to shift them to ligand-centered orbitals. Increased photon energy means shorter wavelengths, therefore the blue (towards the UV) shift. Ligand-to-metal charge-transfer would be facilitated by the oxidation, and the peak would move into the visible if it were due to such.

Ligand substituents also can be seen to affect the spectra. For the bidentates, a more electron-withdrawing substituent on the imine nitrogen (p-bromophenyl) causes a blue shift of spectral peaks, presumably by stabilization of the ground electronic states with respect to the excited states, and increasing the energy required for the transition. For example, the peaks at 358 and 295 nm in DMSO for Mn(SALPMA)<sub>2</sub> correspond to those at 341 and 270 nm for Mn(SAL-4-BrANL)<sub>2</sub> in the same solvent. For the tridentates, substitutions on the SAL ring have the opposite effect on all peaks but the d-d peaks, i.e. blue shifts for electron-donating substituents. For example, the charge-transfer peak at 358 nm for Mn(SALAMP)<sub>2</sub> in DMSO moves to 390 nm on introduction of a 5-NO<sub>2</sub>-group. This may be interpreted by relative stabilization of the ground state by the electron-donating substituents. The d-d transitions for the Mn(III) complexes are shifted to the red by electron donation, eg. 650 nm for Mn(5-MeOSALAEP)<sub>2</sub>(NCS) and 600 nm for Mn(5-ClSALAEP)<sub>2</sub>(NCS), in pyridine. This is the reverse of the expected

shift, since a better ligand (electron-donating) should increase  $\Delta$ , the ligand field splitting parameter, and cause a blue shift. There are two reasons, however, why this may be occurring. First, the error in the values for the peak positions is large, plus or minus 25 or 30 nm, and there may actually be no shift. Second, it has been shown for other Schiff base ligands that changes in the binding ability of one part of ligands the ligand may be counterbalanced by changes in other parts. For example, adding a NO<sub>2</sub>-substituent to the SAL ring of certain potentially pentadentate ligands may cause the central nitrogen to move from a non-coordinated to a coordinated position to balance the effect of the electron withdrawal by the nitro-group. If the contributions to  $\Delta$  are changed by such movements, then a reversal in the expected shift may occur.

Solvent effects on the spectra are not as predictable. For the Mn(II) tridentate complexes, where two solvent molecules are believed to be coordinated, the effect should be quite marked. However, the changes, although quite substantial, are not in the same directions for different complexes. For example, the M $\rightarrow$ L charge-transfer peaks for Mn(SALAEP)<sub>2</sub> and Mn(5-NO<sub>2</sub>SALAEP)<sub>2</sub>, at 348 and 400 nm, respectively, in DMSO, move to 370 and 386 nm in pyridine. Interactions of the solvent with both ligand and metal may have variable offsetting effects, causing this unpredictable behavior. The M $\rightarrow$ L peaks in bidentate complexes are also unpredictable, eg. shift from 358 to 372 nm for Mn(SALPMA)<sub>2</sub> and 341 to 340 nm for Mn(SAL-4-BrANL)<sub>2</sub> on going from DMSO to pyridine. A nephelauxetic effect, due to stabilization of the excited state by

uncoordinated solvent dipoles, can explain the 341 to 340 nm shift but not that from 358 to 372 nm. Finally, solvent change has virtually no effect on the Mn(III) spectra.

Solution conductivities of the complexes in DMSO are those expected from the formulated compositions (Table IV).<sup>89</sup> In the Mn(II) SAL-based complexes, the charge on the metal ion is neutralized by the anionic ligands, therefore no counterion is required, and the complexes are non-electrolytes. The Mn(III) SAL complexes require the presence of one anion because of the higher charge on the Mn. The anion is not associated in solution, however, and these complexes are 1:1 electrolytes ( $\Lambda_m \sim 33$ ). The Mn(II) PY-based complexes have neutral ligands, require two anions for charge balance, and are 1:2 electrolytes in DMSO ( $\Lambda_m \sim 74$ ).

Magnetic moments of the complexes (Table IV) are near those of similar Mn(II) and Mn(III) complexes.<sup>90</sup> The values expected for the magnetic moments may be calculated from the formula,  $\mu = \sqrt{n(n+2)}$ , where  $n$  is the number of unpaired electrons in the complex. This calculation will yield the spin-only value, which neglects any orbital contribution to the moment. High spin  $d^5$  systems have no orbital angular momentum, therefore no modification of the equation is required. High spin  $d^4$  systems however, do have orbital momentum, and the effect is to lower the moment slightly from the spin only value. A Mn(II) complex is expected to have five unpaired electrons, therefore a value of  $5.92 \mu_B$  is expected. Mn(III) should be high spin  $d^4$ , and a moment slightly below  $4.90 \mu_B$  is expected. Deviations from these values may be caused

Table IV. Physical Properties of Complexes

Complex	$\mu_{\text{eff}}, \mu\text{B}$	$\lambda_{\text{m}}, \text{m}\mu\text{o}\cdot\text{cm}^2\cdot\text{mol}^{-1} (a)$
<u>Mn(II)</u>		
Mn(SAL-PMA) <sub>2</sub>	5.94	NM
Mn(SAL-4-BrANL) <sub>2</sub>	5.88	NM
Mn(SALAEF) <sub>2</sub> ·2H <sub>2</sub> O	6.11	NM
Mn(SALAMP) <sub>2</sub> ·C <sub>3</sub> H <sub>7</sub> OH	(b)	NM
Mn(5-CISALAMP) <sub>2</sub> ·H <sub>2</sub> O	6.1	NM
Mn(5-NO <sub>2</sub> SALAEF) <sub>2</sub>	5.96	4.0
Mn(6-MePYAMP) <sub>2</sub> (NCS) <sub>2</sub>	6.11	77.5
Mn(PYAEF)(NCS) <sub>2</sub>	5.83	73.0
Mn(6-MePYAEF)(NCS) <sub>2</sub>	5.95	70.7
<u>Mn(III)</u>		
Mn(5-CISALAMP) <sub>2</sub> (NCS)	4.91	32.5
Mn(5-MeOSALAEF) <sub>2</sub> (NCS)	5.40	33.5
Mn(5-CISALAEF) <sub>2</sub> (NCS)	4.95	34.3

(a) In DMSO,  $\lambda_{\text{m}}(\text{C}_2\text{H}_5)_4\text{NClO}_4 = 35.0$ ,  $\lambda_{\text{m}} \text{Ni}(\text{ClO}_4)_2 \cdot 6\text{H}_2\text{O} = 74.2$ , at 0.001M.

(b) Unable to measure due to rapid oxidation.

NM - not measured

by interactions between individual complex molecules due to spin-spin coupling of the individual moments.  $\text{Mn}(5\text{-MeOSALAEP})_2(\text{NCS})$  had a rather high moment, which could be due to the presence of a strongly paramagnetic impurity, or, more likely, incorporation of a small amount of a manganese oxide. The very low molecular weight of such a species could increase the apparent  $\mu$  value of the complex without affecting its analytical results significantly.

### Oxygen Reactivity

#### 1. Solid State

##### a) Bidentate Ligands:

Only one of the two bidentate complexes isolated proved to be  $\text{O}_2$ -sensitive in the solid state. Exposing  $\text{Mn}(\text{SAL-4-BrANL})_2$  to the atmosphere for 24 hours caused the formerly red-orange complex to turn a dark brown color. Accompanying this visible change was the appearance in the IR spectrum of the complex of a new peak at  $\sim 630 \text{ cm}^{-1}$ . Absorption in this area has been assigned to Mn-O stretching frequencies in previous complexes.<sup>53</sup> There was no new peak near  $3600 \text{ cm}^{-1}$ , therefore the product could not be a hydroxy-complex, which would exhibit an O-H stretch at this frequency. Further characterization of this product was not performed, but based on solution uptake data for both bidentate and tridentate complexes, and formation of a similar solid tridentate compound (vide infra), we believe this complex is a  $\mu$ -peroxo-Mn(III) dimer. The reason for the insensitivity of  $\text{Mn}(\text{SALPMA})_2$  to  $\text{O}_2$  is not obvious, since it contains a more activating substituent (benzyl vs. 4-bromophenyl), but the difference may be due to different

crystal structures, as was the case with the Cl-substituted tetradentate complexes.<sup>53</sup>

#### b) Tridentate Ligands

Again, only one of the isolable complexes,  $\text{Mn}(\text{SALAMP})_2$ , with these ligands was solid state  $\text{O}_2$ -sensitive. The non-reactivity of the PY-based complexes was expected because of the inactivity of earlier reported complexes of this type, and this was also true for  $\text{Mn}(\text{5-NO}_2\text{SALAEP})_2$ , containing the deactivating  $\text{NO}_2$ -group. The inactivity of  $\text{Mn}(\text{SALAEP})_2$ , however, is surprising, since the ligand differs from SALAMP by the addition of a second methylene group between the imine nitrogen and the pyridine ring. A difference caused by different chain lengths was seen earlier in the  $\text{SALC}_n$  complexes between  $n = 5$  and  $6$ , with the longer chain complexes being reactive, but the shorter unreactive.<sup>53</sup> This case is the reverse, i.e. the longer chain HSALAEP ligand forms an unreactive complex. Unlike the explanation advanced for the  $\text{SALC}_n$  complexes, it is believed that pseudo-octahedral coordination is found for both tridentate complexes. The second  $-\text{CH}_2-$  group in the HSALAEP ligand probably allows freer coordination of the pyridine ring, and prevents  $\text{O}_2$  from attacking at that site. This theory is supported by the results of the solution kinetic study (vide infra) where the activation energy for reaction with  $\text{O}_2$  was found to be  $\sim 3x$  larger for  $\text{Mn}(\text{SALAEP})_2$  than  $\text{Mn}(\text{SALAMP})_2$ . The effect of the Cl-substituent on HSALAMP may be, as with the tetradentates, a combination of electronic and crystal packing factors. Finally, the Mn(III) complexes are inert to  $\text{O}_2$  in the solid state.

$\text{Mn}(\text{SALAMP})_2 \cdot \text{C}_3\text{H}_7\text{OH}$ , on exposure to air, rapidly darkens and becomes dark black after 12 hours. Comparison of initial and final IR spectra showed two changes. First, an increase in the intensity of the broad absorption from 3200 to 2700  $\text{cm}^{-1}$  appears, and second, the appearance of a new doublet at 630  $\text{cm}^{-1}$  is observed. The first change may be attributed to absorption of moisture by the complex as lattice water from the humid laboratory air. The second change, however, is more important because we attribute it to the formation of a Mn-O bond in the product. Elemental analysis of the oxygenated complex shows an increase in %H, due to absorption of moisture, but the ratio of carbon to nitrogen is 7.0, unchanged from the original complex. This implies that there was no gain or loss of either element during the reaction, or, less likely, that there was a simultaneous change in the content of both. With the preconceived idea that the product is a  $\mu$ -peroxo-Mn(III) dimer, a calculation of the magnetic moment from susceptibility measurements yields a value of 4.8  $\mu_B$  per Mn, close to the spin-only value of 4.90  $\mu_B$  for high spin  $d^4$ . This close agreement justifies the choice of the dimer as the actual compound, since an incorrect choice would likely result in an ambiguous result for the magnetic moment. A monomeric  $\text{Mn}^{\text{III}}\text{-O}_2^-$  complex would give the same result, but this type of complex has not been previously reported in the solid state for Schiff base complexes. Formation of such a complex is also indicated by the solution uptake results (vide infra).

It is interesting that  $\text{Mn}(\text{SAL-4-BrANL})_2$  did not seem to pick up moisture, at least from IR evidence, but  $\text{Mn}(\text{SALAMP})_2$  does. As explained

later (vide infra) both types of complexes prefer 6-coordination in the Mn(III) state in solution. Mn(SALAMP)<sub>2</sub> has the pyridine ligand available for coordination in the solid state to stabilize Mn(III), but seems to absorb water anyway, although as lattice water. Mn(SAL-4-BrANL)<sub>2</sub>, limited to four donor atoms from the ligands, does not. One would expect that H<sub>2</sub>O could coordinate trans to the O<sub>2</sub> to stabilize the higher oxidation state in [Mn(SAL-4-BrANL)<sub>2</sub>]O<sub>2</sub>. The reason for this not occurring is unclear, but may again be due to crystal structure.

## 2. Solution Oxygenation

### a) Bidentate Complexes

In solution, unlike the solid state, both of the isolated Mn(II) complexes are sensitive towards O<sub>2</sub>. When dissolved in organic solvents (DMSO, pyridine, methyl alcohol) and exposed to air, the yellow-orange solutions immediately darken to a brown or black color. In some cases, the reaction goes so far as to precipitate a dark brown or black solid. Uptake curves for the bidentate complexes are shown in Figures 18 and 19. The uptake curves have been corrected for a small amount of O<sub>2</sub> absorbed by the solvent alone. The plot of the uptake can be seen to resemble those of the penta- and hexadentate complexes in that there are two different sections. These are a fast initial reaction, which we have attributed to oxidation of Mn(II) to Mn(III), and a second, slower section attributed to oxidation of the ligand. There are, however, two major differences between these complexes and the previous ones. The first is that the break between the first and second sections is more pronounced with the bidentate complexes, i.e. the rate of ligand

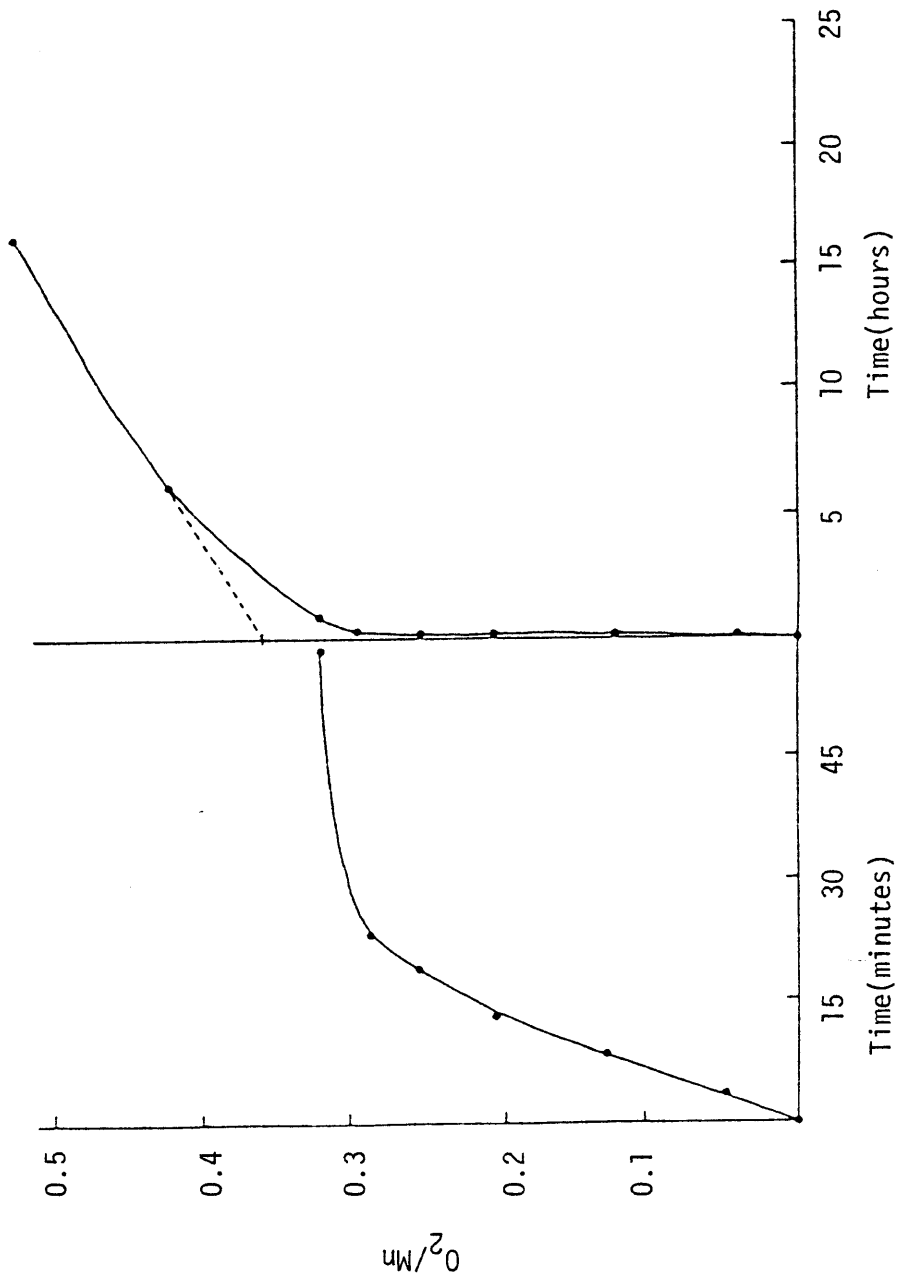


Figure 18: Oxygen Uptake of  $Mn(SALPMA)_2$  in DMSO.

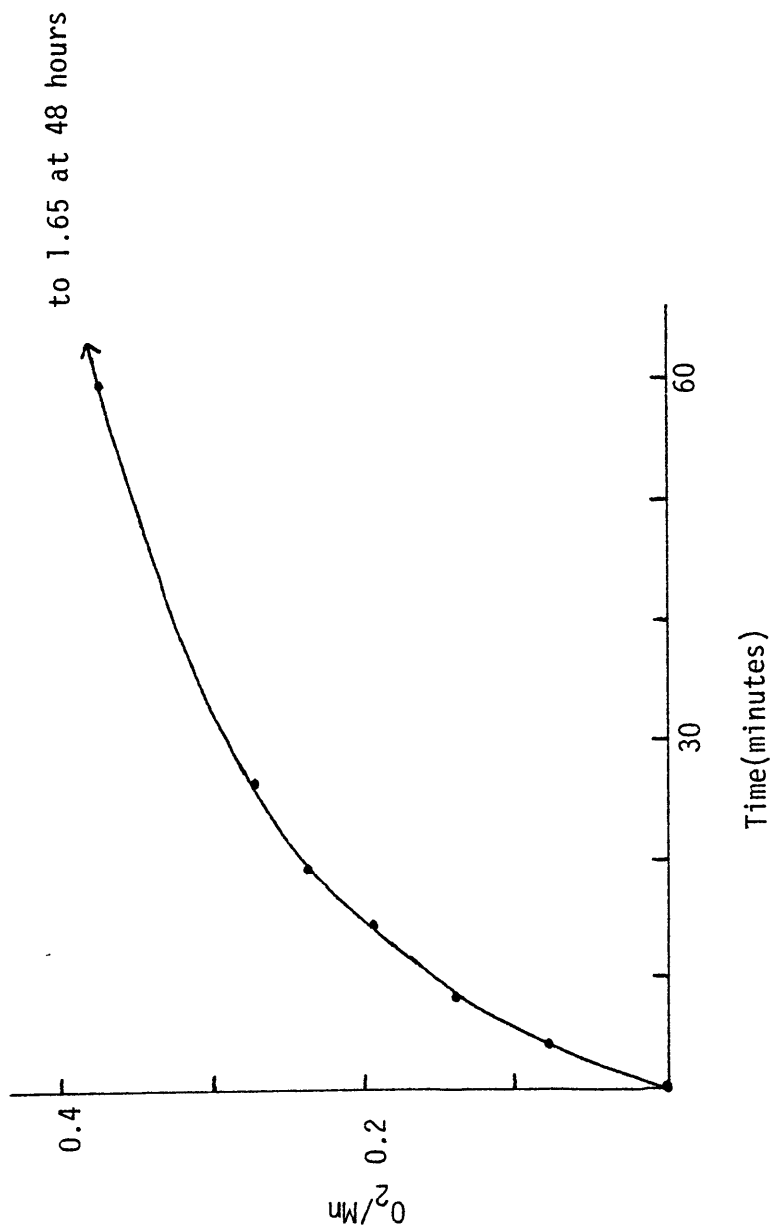


Figure 19. Oxygen Uptake of  $Mn(SAL-4-BRANL)_2$  in Pyridine.

oxidation is much slower for bidentate ligands. The second difference is that the first section seems to end at a non-stoichiometric ratio for the bidentates. A value of 1.0  $O_2/Mn$  would be expected if the product had a superoxo-Mn(III) structure, although this type of complex has not previously been reported. A value of 0.5 would be found if the final product had a  $\mu$ -peroxo-Mn(III), hydroxy-Mn(III) or di- $\mu$ -oxo-Mn(IV) type structure. If the product was of the  $\mu$ -oxo-Mn(III) type, the ratio would be 0.25. However, the value found is  $\sim 0.33 O_2/Mn$ , which has not previously been seen in these types of reactions. Characterization of the reaction products would undoubtedly give some clue as to the reaction mechanism, but, as was the case with the other two sets of ligands, the products, at least of simple oxygenations, were not characterizable. IR spectra of the products from DMSO solution bore some resemblance to those of the starting materials, but many peaks were missing after oxidation. In some cases, new peaks appeared between 600 and 700  $cm^{-1}$ , which could be assigned to Mn-O bonds, but the extreme changes in other areas of the spectra indicate that a substantial amount of other reaction besides Mn-O bond formation was occurring. If the oxygenations were performed in alcohol and  $H_2O/NH_4NCS$  was added in an attempt to produce a  $MnL_2NCS$  compound, similar effects occurred, but with a new peak occurring at  $\sim 2050 cm^{-1}$  due to  $NCS^-$ , often along with some formation of a Mn-O peak, probably due to formation of a mixture of products. This is unlike the penta- and hexadentate complexes, whose  $MnL^+$  ions could be precipitated with  $NCS^-$  without formation of any oxygen-containing species.

Rationalizing the above facts is rather difficult, especially the non-isolable character of the "MnL<sub>2</sub><sup>+</sup>" ion. One would gather from the IR data that severe degradation of the ligand had occurred during oxidation. However, if this were the case, one would not expect the penta- and hexadentate MnL<sup>+</sup> ions to be simple to isolate, since the second section of their uptake is much faster than that of the bidentates. One possible reason may lie in the method of attempted preparation of the thiocyanate salt. Performing the ligand and Mn(II) complex in situ, and then oxidizing the complex with O<sub>2</sub> may work fine for the penta- and hexadentate complexes since the Mn(II) complex is formed quite readily. However, as previously stated, the Mn(II) bidentate complexes are extremely difficult to synthesize, and the failure to prepare the Mn(III) complex may be due to initial formation of an impure Mn(II) complex.

The unusual ratio of 0.33 O<sub>2</sub>/Mn found in the uptake may be rationalized by a reaction mechanism which somehow recycles some of the oxygen. One possible scheme is:

- 1)  $\text{Mn}^{\text{II}}\text{L}_2 + \text{O}_2 \rightarrow \text{L}_2\text{Mn}^{\text{III}} - \text{O}_2^-$
- 2)  $\text{L}_2\text{Mn}^{\text{III}} - \text{O}_2^- + \text{Mn}^{\text{II}}\text{L}_2 \rightarrow \text{L}_2\text{Mn}^{\text{III}} - \text{O}_2^{2-} - \text{Mn}^{\text{III}}\text{L}_2$
- 3)  $\text{L}_2\text{Mn}^{\text{III}} - \text{O}_2^{2-} - \text{Mn}^{\text{III}} + \text{XH} \rightarrow 2 \text{Mn}^{\text{III}}\text{L}_2^+ + \text{HO}_2^- + \text{X}^-$
- 4)  $2\text{HO}_2^- \rightarrow \text{O}_2 + 2\text{OH}^-$
- 5)  $\text{Mn}^{\text{III}}\text{L}_2^+ + \text{O}_2 \rightarrow \text{Mn}^{\text{III}}\text{L}_2^{'+}$

As already noted, if the reaction stopped at 2), as it apparently does in the solid state, or 3) the ratio found would be 0.5 O<sub>2</sub>/Mn. If recycling is complete, i.e. no side reaction of HO<sub>2</sub><sup>-</sup> occurs, then the

ratio would be 0.25. Therefore, a plausible explanation assumes that some of the peroxy-species are removed before disproportionating back to  $O_2$ . Precedence for the individual reactions in the scheme is well established. The  $\mu$ -peroxy-dimer was isolated for  $Mn(5-NO_2SALDPT)$ ; further, this species could be cleaved by a proton source ( $H_2O$ ) in THF, although the reaction did involve reduction of Mn(III) back to Mn(II) and produced  $O_2$ . However, hydrolyses of other  $\mu$ -peroxy-complexes of other metals to give simple oxidized complexes is well established. Further reactions of the biperoxide ion (or  $H_2O_2$ ), including disproportionation in the presence of metal ions<sup>92</sup>, or even in pure DMSO<sup>93</sup>, and oxidation of organic compounds<sup>43</sup>, including DMSO and pyridine, are well known. Reaction 5) is that of the Mn(III) cation with  $O_2$  to give a complex with an oxidized ligand, a reaction which is also indicated by the repetitive spectrophotometric scans in the kinetic study.

### c) Tridentate Complexes

Mn(II) complexes containing PY-based tridentate ligands are  $O_2$ -insensitive in solution, as is  $Mn(5-NO_2SALAEP)_2$ . The  $O_2$  sensitivity of the Mn(III) complexes was not studied directly, but the continuing uptake of  $O_2$  by the Mn(II) complexes and the slow second step in the kinetics spectrophotometric study (vide infra) indicate possible reactivity, although it would very likely be oxidation of the ligand and not the Mn center. All Mn(II) SAL-based complexes, except  $Mn(5-NO_2SALAEP)_2$ , are  $O_2$  sensitive in solution. Exposure of a solution of the complex to  $O_2$  results in an immediate darkening of the color from

yellow to brown. Continued exposure produces a dark precipitate in some cases. Typical uptake curves are shown in Figures 20 and 21. The curves roughly resemble those of complexes with bi-, penta-, and hexadentate ligands but with some differences. The slope of the second part of the curves are the least of all complexes, indicating that the tridentate ligands are the least susceptible to oxidation while attached to Mn. Also, the breaks in the curves are at about the same ratio as for the bidentates, i.e.  $\sim 0.37 \text{ O}_2/\text{Mn}$ . These similarities in the uptake curves lead us to believe that the mechanisms of oxygenation are the same for the bi- and tridentate complexes, i.e. formation of a  $\mu$ -peroxo-Mn(III) dimer, which is subsequently cleaved to produce  $\text{HO}_2^-$ , which further reacts (disproportionates) to give some recycled  $\text{O}_2$ . As was the case with the bidentates, no characterizable product could be isolated after the oxygenation. However, unlike them, preparation of  $\text{MnL}_2\text{NCS}$  from an alcoholic solution was possible. This may reflect both the higher stability of the tridentate ligand in the complex as well as a greater tendency for formation of the initial Mn(II) complex.

Because of the greater ease of preparation of the tridentate complexes as compared to the bidentates, a number of experiments were performed besides  $\text{O}_2$  uptake studies on the complexes. One of these was a comparison of the spectrum of an authentic Mn(III) complex,  $\text{Mn}(5\text{-C1SALAMP})_2(\text{NCS})$ , with that of an oxygenated solution of  $\text{Mn}(5\text{-C1SALAMP})_2$ . Figure 22 shows that the spectra are similar. The Mn(II) complex was oxygenated in DMSO for  $\sim 12$  hours, which may not have been time for complete oxidation to occur, considering the deactivating

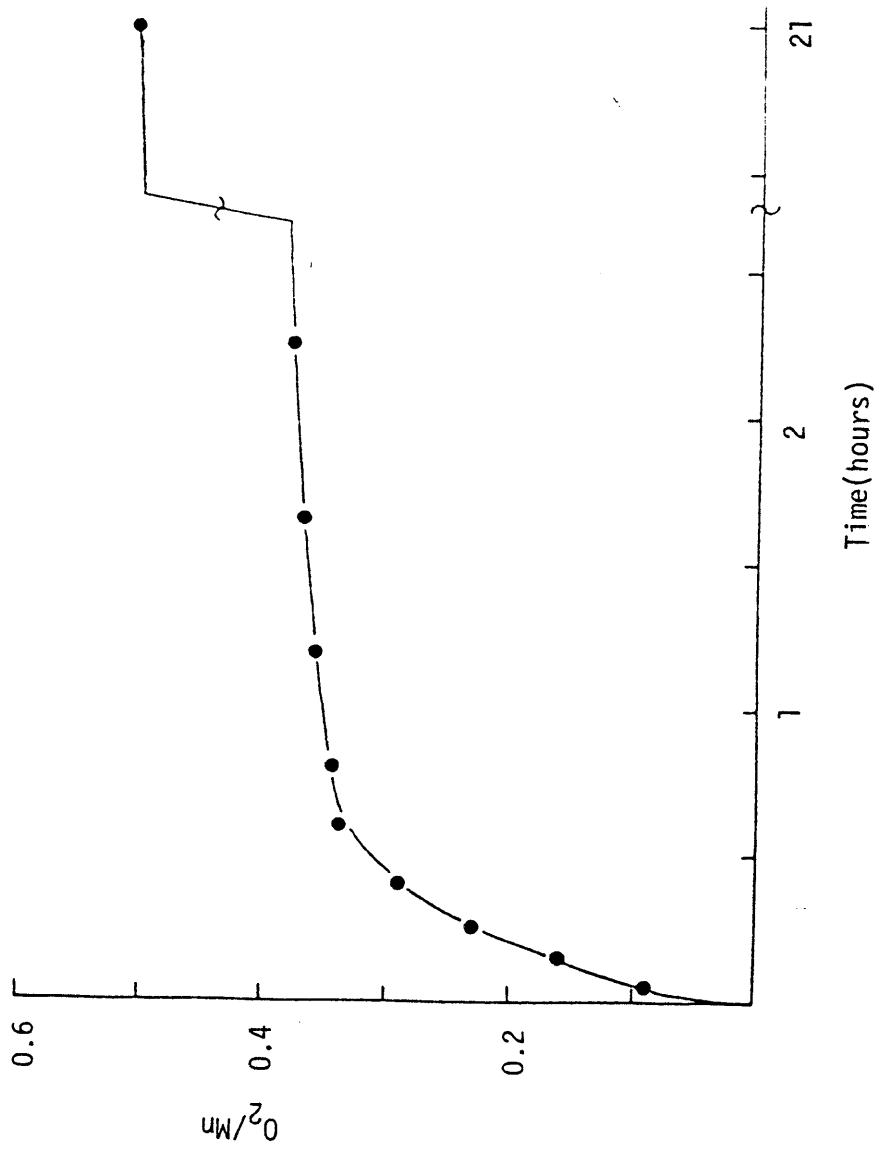


Figure 20: Oxygen Uptake of Mn(SALAEPP)<sub>2</sub> in DMSO.

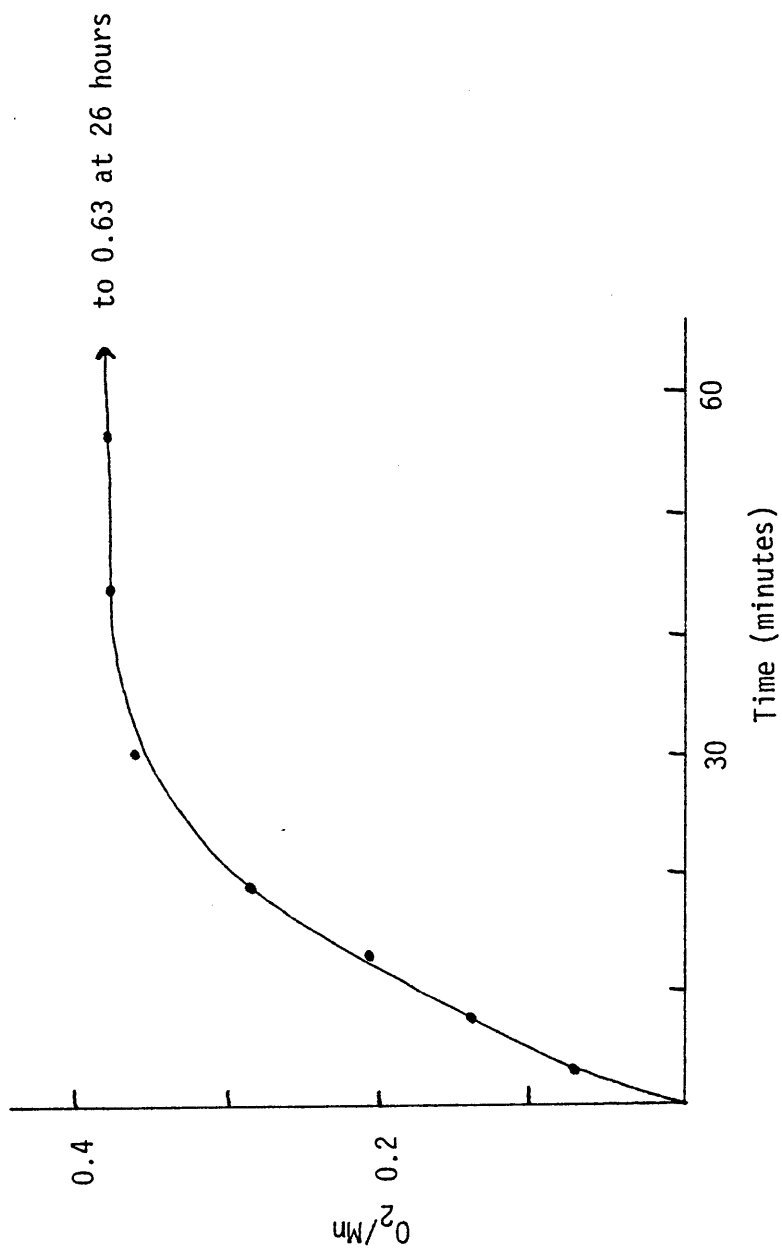


Figure 21. Oxygen Uptake of  $Mn(SALAMP)_2$  in Pyridine.

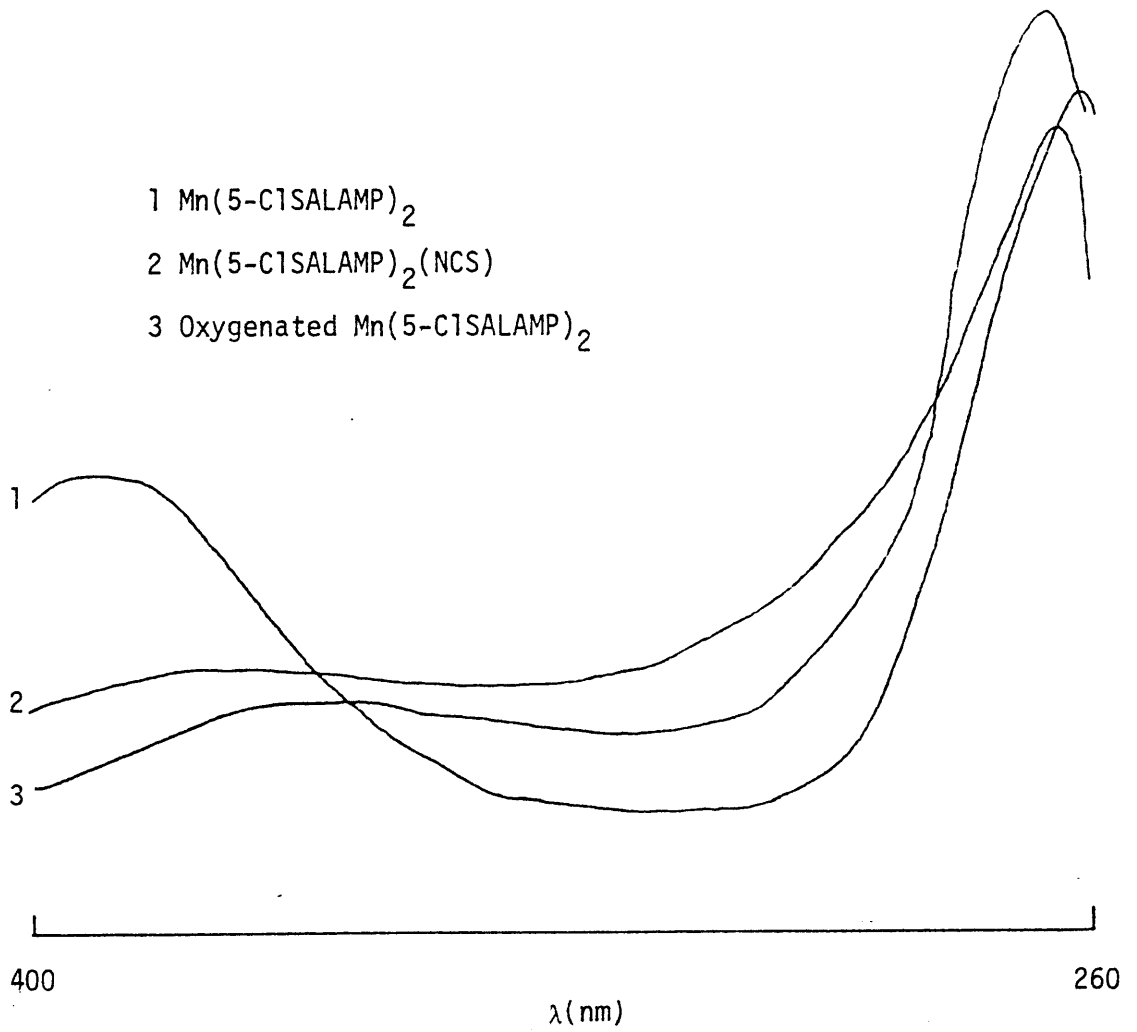


Figure 22:  $\text{MnL}_2^+$  and Oxygenated  $\text{MnL}_2$  Spectra in DMSO.

power of the Cl-substituent, but comparison with the original Mn(II) spectrum indicates substantial reaction. Also, there may be some complex present with oxidized ligand, which would interfere with comparison of the two Mn(III) spectra. However, this is good evidence that the complex is oxidized to the  $MnL_2^+$  ion, and not to a Mn(II) species containing coordinated oxygen. This point was substantiated by a study using Mn(SALEN). This complex may be chemically or electrochemically oxidized to  $Mn(SALEN)^{+94}$ , or oxygenated to give  $[Mn(SALEN)]_2O$ . The spectra of the chemically and electrochemically produced  $MnL^+$  species are not identical, but each is greatly different from that of the  $(MnL)_2O$  product.

Another study which was performed was the oxygen uptake of HSALAEP. Figure 23 shows the uptake curve for an equimolar DMSO solution of HSALAEP and KOH. A solution of the ligand alone in DMSO undergoes little or no reaction over a period of two hours. However, addition of an equimolar amount of KOH causes a fast, extensive reaction to occur. The reaction is much faster than the second step in the  $O_2$  uptake for  $Mn(SALAEP)_2$ . Therefore, it seems that the metal in the complex activates the ligand, but not to the same extent as complete deprotonation. Since the postulated mechanism for oxygenation of the tridentate complexes involves ligand oxidation in the second step, the results are not surprising. An oxidation should be facilitated by increasing the negative charge on the reactant, since electrons are formally removed in the process. The order of reactivity of HSALAEP in its various forms should therefore be: neutral ligand < complexed <

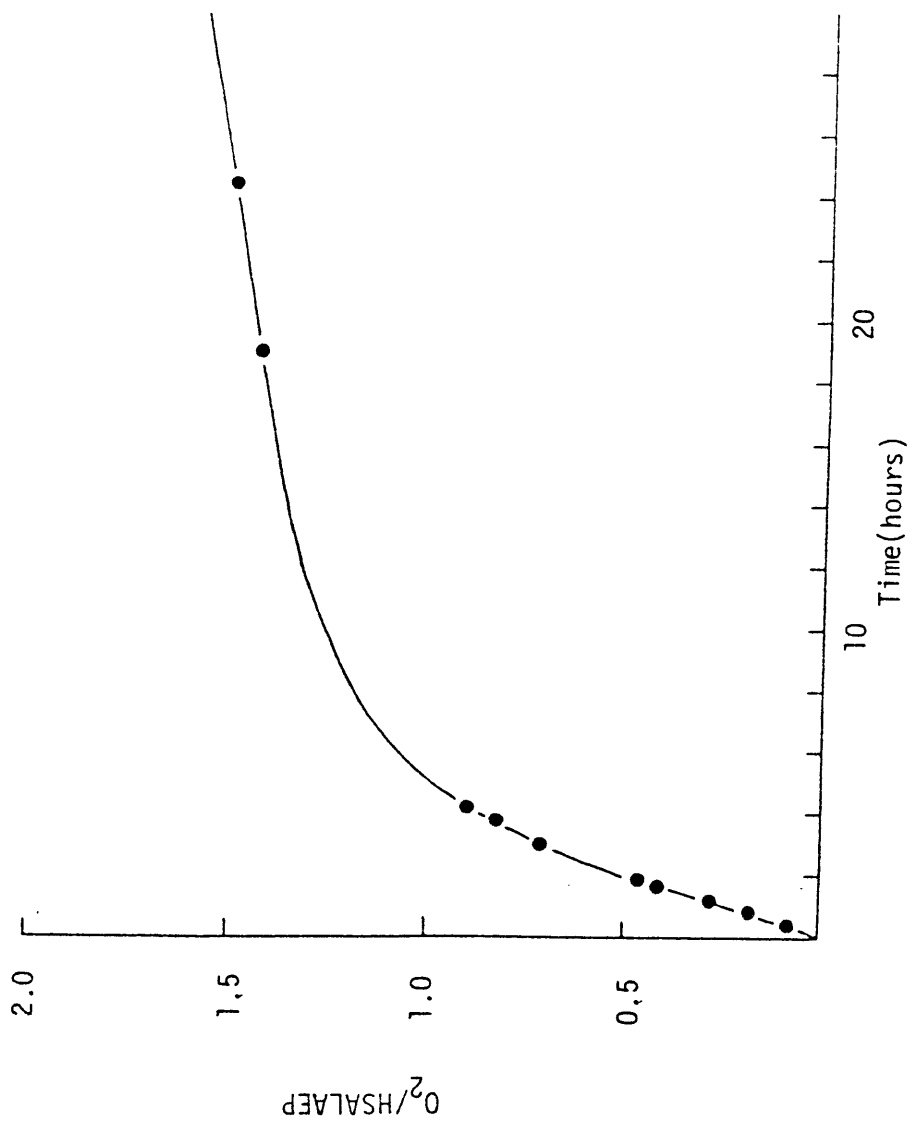


Figure 23: Oxygen Uptake of Deprotonated HSALAEP in DMSO

deprotonated. Surprisingly, DMSO with added KOH also absorbs  $O_2$  (a continuous uptake of  $\sim 1$  mL/hour). This is not due to simple dissolution of the  $O_2$ , since a run without KOH absorbs  $\sim 0.3$  mL of  $O_2$  in 25 mL of DMSO in under an hour and then stops. One would not expect addition of an innocuous salt to magnify the solubility of a gas to such a large extent, therefore the  $OH^-$  must be initiating a reaction with  $O_2$ . However, no attempt to characterize the products of the reaction was made.

This uptake due to  $OH^-$  is particularly interesting in view of the fact that  $OH^-$  is postulated to be the final reduction product of  $O_2$ . The continued slow uptake of  $O_2$  for both bi- and tridentate complexes may therefore be due to both ligand oxidation and the reaction caused by  $OH^-$ . The reaction mechanism for the oxygenation may therefore be more complex than the one presented.

### Electrochemistry

As stated in the Introduction, one of the goals of this research was to quantitatively correlate standard reduction potentials of these complexes with kinetic parameters of their reactions with  $O_2$ , since both processes involve oxidation of Mn. Electrochemical studies of previously prepared penta- and hexadentate complexes have been quite extensive, therefore data from these earlier papers could be used for these complexes. Sparse data, however, was available on tetradentate complexes of the type used in this work, and no studies had been performed on the new bi- and tridentate complexes, therefore a study of their cyclic voltammetric and coulometric behavior was undertaken.

### 1. Bidentate Complexes

The electrochemistry of the bidentate complexes is dependent on the solvent used. In pyridine, cyclic voltammograms exhibit an oxidation peak on the initial anodic scan, and a corresponding reduction peak on reversing the sweep (Figure 24). The peak separation is markedly greater than 59 mV, and increases with increasing scan rate (Table V). The ratio of anodic to cathodic current is greater than unity, and increases with increasing scan rate. The peak oxidation current was also roughly proportional to the square root of the scan rate, i.e.  $i_{ox}/v^{1/2}$  was constant. In general, these properties are the same as those of the majority of the aforementioned pentadentate Mn(II) complexes, and are therefore assignable to a quasireversible Mn(III)/Mn(II) couple. On closer examination, however, there are a number of significant differences which suggest some complexity in the system. The peaks are much wider than those for the pentadentate complexes, and the peak separation is greater than 59 mV even at the lowest scan rate of 1 mV/sec. Peak currents are a factor of 2 or 3 lower than in earlier studies with reversible Mn Schiff base systems, and the increase in the  $i_{ox}/i_{red}$  ratio with increasing scan rate is greater, with values up to 5.0 at 100 mV/sec, compared to ~1.2 for previous studies.

These effects may be due to a number of factors, most of which can be eliminated by a few simple experiments. Irreversibility due to electrode geometry, solution resistance, and dirty electrodes is often a problem in non-aqueous systems. However, reversible voltammograms ( $\Delta E_p <$

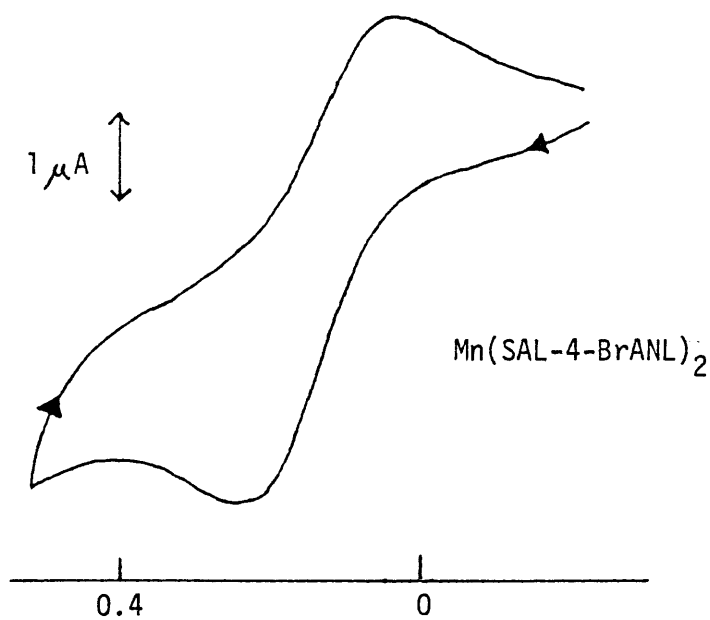
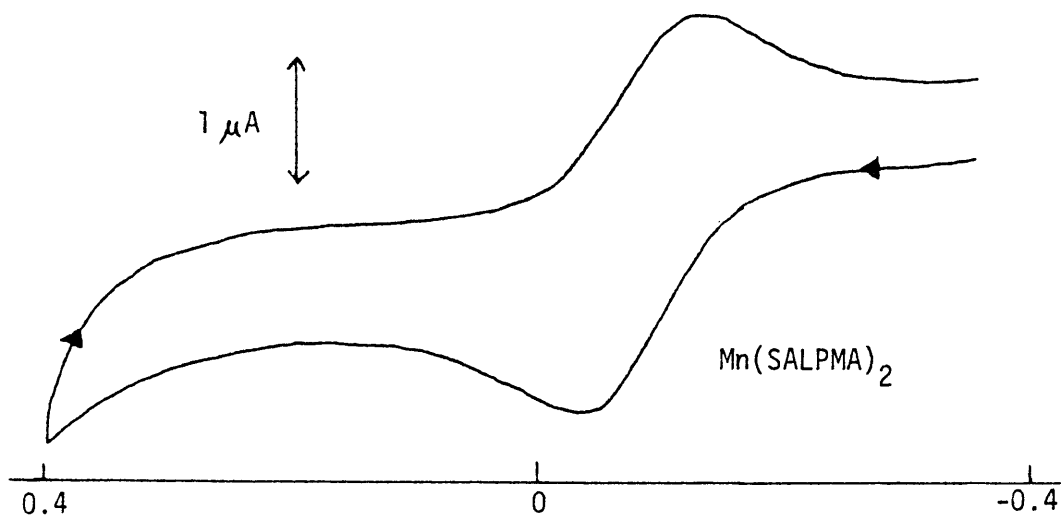


Figure 24. Cyclic Voltammograms of Bidentate Complexes in Pyridine (10 mV/sec).

Table V. Peak Potentials for Bidentate Complexes (V vs. SCE)

<u>Complex</u>	<u>Scan Rate (mV/sec)</u>	<u>E<sub>R1</sub></u>	<u>E<sub>R2</sub></u>	<u>E<sub>0</sub></u>	<u>E<sub>red</sub></u>	<u>E<sub>ox</sub></u>
Mn(SAL-4-Br-AML) <sub>2</sub>	1	(a)	-0.21	+0.01	+0.06	+0.20
	10	0.00(a)	-0.27	+0.03	+0.05	+0.24
	100	-0.03	-0.45	+0.08	-0.02	+0.35
Mn(SALPMA) <sub>2</sub>	1	-0.21(b)	-0.48(b)	-0.09(b)	-0.12	0.00
	10	-0.20	-0.59	-0.13	-0.12	-0.03
	100	-0.20	-0.67	-0.10	-0.12	+0.04

E<sub>R1</sub>, E<sub>R2</sub>, E<sub>0</sub> - in DMSOE<sub>ox</sub>, E<sub>red</sub> - in pyridine

(a) - shoulder

(b) - plateau

65 mV) of known reversible systems (ferrocene,  $O_2/O_2^-$ , and the first reduction of methyl viologen) could be obtained with the electrochemical cell and positive feedback iR compensation, therefore the effects could not be due to instrumental problems. The low peak currents could be due to impure complexes, i.e. containing a large amount of electroinactive material, but the characterization of the complexes leads us to believe that they are reasonably pure. Another reason for the low currents could be low diffusion coefficients caused by the apparent size of the complex in solution being larger than expected due to dimerization or oligimerization. There is, however, no reason to believe that the complexes are associated in solution, since the solid state properties suggest no dimerization, and association is much more probable for a solid. The magnetic moments, especially, suggest a monomeric solid state structure. The values (5.94 and 5.88  $\mu_B$ ) are near the spin-only value, suggesting no intermolecular interaction. Mn(SALEN) is dimeric, and has a lower moment of 5.24  $\mu_B$ , due to spin-spin coupling. The best explanation for the extreme quasireversible behavior of the systems is a very slow electron transfer rate between the redox couple and the electrode, which can produce very quasireversible behavior, although not usually as marked as in this case.

The slow electron transfer rate may be explained by geometrical differences between the stable Mn(II) and (III) species which would have to be accommodated during electron transfer. If reorganization of the complex is slow enough to inhibit electron transfer, it will produce the effects exhibited here.<sup>95</sup> The exact geometrical differences cannot be

elucidated from work in pyridine alone, but the study in DMSO suggests that a better description of the couple is distorted octahedral Mn(III)/tetrahedral Mn(II) (vide infra).

The peak positions are seen to be more negative for Mn(SALPMA)<sub>2</sub> than for Mn(SAL-4-BrANL)<sub>2</sub>. As in earlier studies, this may be explained by the relative electron-donating ability of the substituent on the imine nitrogen. The benzyl group is more strongly donating than the p-bromophenyl group, and produces a more basic nitrogen. This in turn stabilizes the relatively electron-deficient Mn(III) state and facilitates oxidation/inhibits reduction.

Voltammograms in DMSO are quite different from those in pyridine. An initial anodic scan produces one oxidation peak, but the reverse cathodic sweep produces two reduction peaks, R1 and R2, with R2 being more cathodic (Figure 25). The peaks are similar to those in pyridine in that they are very wide, having a separation that increases with increasing scan rate; they also have small anodic and total cathodic currents. The anodic current is again smaller by a factor of 2 to 4 times, as compared to earlier, more reversible results, and is also proportional to  $v^{1/2}$ . Relative total cathodic current also increases with decreasing scan rate. Again, these properties are attributed to a geometrically limited rate of electron transfer. However, the presence of two reduction peaks and their scan rate dependent behavior suggests a possible mechanism for reactions in the two solvents. It was first thought that water in the solvent may have been causing the effect, but addition of one or two drops (far more than should have been there) had

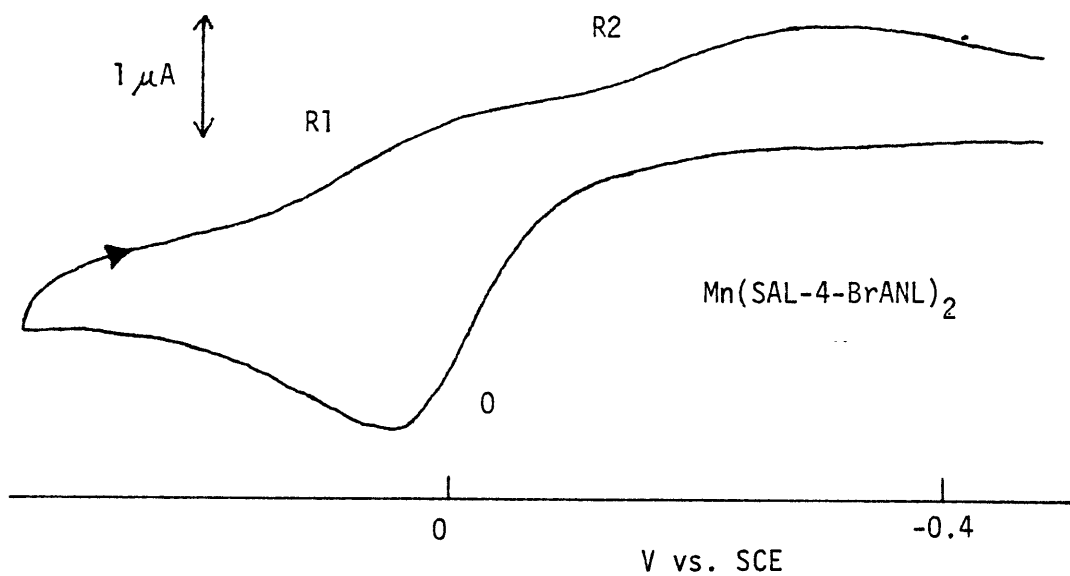
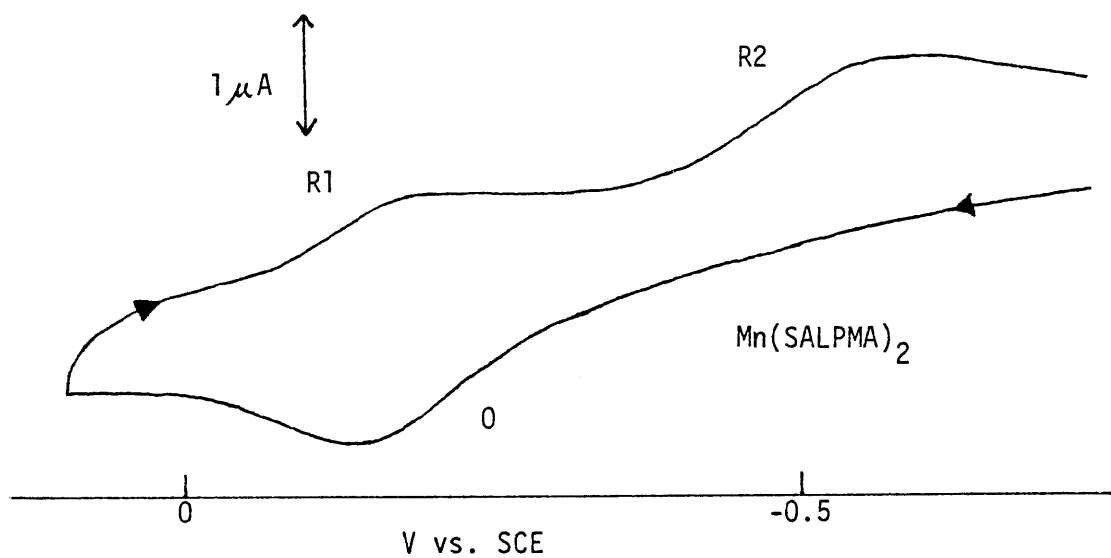


Figure 25. Cyclic Voltammograms of Bidentate Complexes in DMSO (10 mv/sec).

no apparent effect on the results. Water in DMSO may not have its expected effect in a number of instances because of the strong interaction of DMSO with  $H_2O$ <sup>96</sup>, which may decrease the activity of the water. At high scan rates, the ratio  $i_{R1}/i_{R2}$  is larger than at slow rates (Figure 26), implying that peak R1 is directly coupled to peak 0, i.e. that peak R1 is due to reduction of the immediate product of oxidation of the Mn(II) species. Peak R2 is due to reduction of a second oxidized species that slowly forms from the species that produces R1, and has little time to form at high scan rates. At low scan rates the reaction producing R2 would have more time to proceed, however, and the peak height should increase at the expense of peak R1, which indeed occurs. A similar effect was noted for one of the pentadentate complexes, Mn(5-NO<sub>2</sub>SALDIEN), in previous work.<sup>63</sup>

A plausible explanation for the changes in the reduction peak heights is conversion of an initially formed tetrahedral Mn(III) to octahedral Mn(III) by coordination of two solvent molecules. As summarized in Figure 27, the stable, and apparently only form of Mn(II) would be tetrahedral. The stability of this form is evidenced by the fact that no trace is seen of a second oxidation peak in any scans, even when a second scan is immediately performed after completion of a first. On oxidation to tetrahedral Mn(III), the slow attack of two solvent molecules would produce a preferred distorted octahedral species. The reactions at the electrode are therefore believed to follow the scheme shown on the next page.

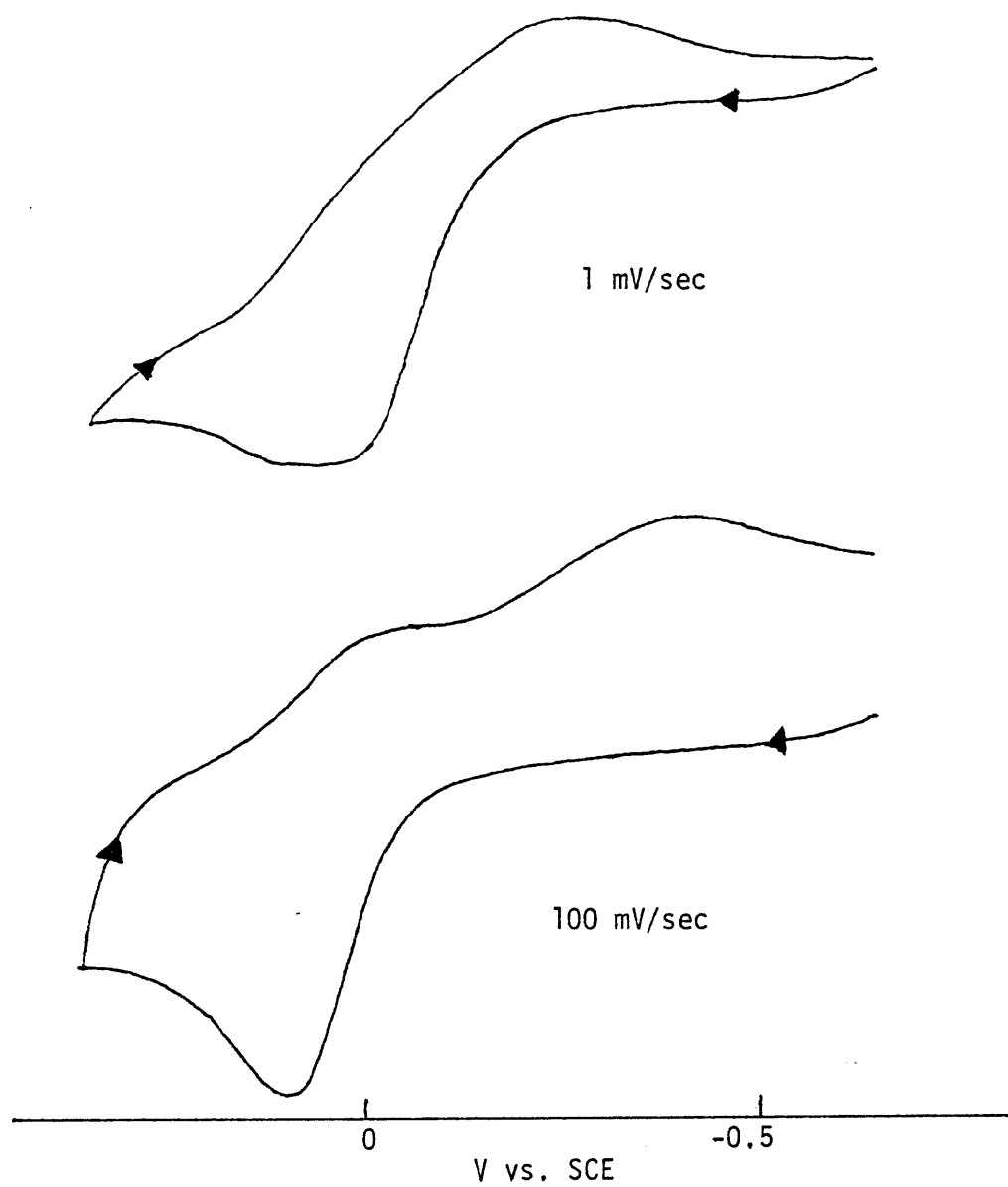
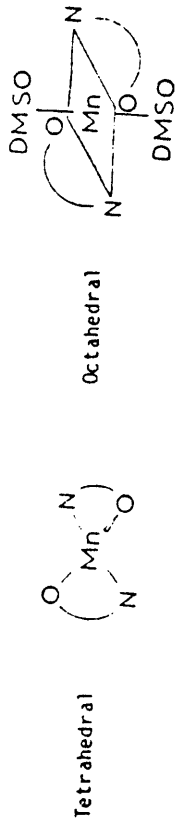


Figure 26. Cyclic Voltammograms of  $\text{Mn}(\text{SAL-4-BrANL})_2$  in DMSO.



Crystal Field  
Contribution

Favored by  $\Delta S$ ; 2 free  
DMSO molecules

Favored by  $\Delta H$ ; 2 more  
bonds to Mn

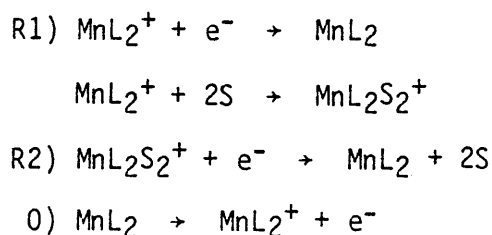
Mn(II)

Tetrahedral form favored; contribution of CFSE to  $\Delta H$  is zero for high spin  $d^5$ ;  $\Delta S_{\text{coordination}}$  for 2 DMSO molecules is substantial.

Mn(III)

Octahedral form favored; contribution of CFSE to  $\Delta H$  substantial for high spin  $d^4$ , apparently outweighs  $\Delta S$  due to DMSO coordination.

Figure 27: CFSE Stabilization of Bidentate Complexes



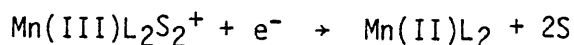
The more negative potential of peak R2 is compatible with this theory, since a more stable Mn(III) should be more difficult to reduce. Loss of solvent must be immediate on reduction of the octahedral form since, as previously stated, no second oxidation peak is ever seen. The fact that only two peaks are seen in pyridine, in conjunction with the fact that pyridine is a better ligand than DMSO for Mn(III), implies that attack of pyridine on Mn(III) is instantaneous (on the CV time scale). Since the couples for the two peaks in pyridine are therefore not the same, this unfortunately means that an  $E^\circ$  value cannot be extracted from the voltammograms in pyridine. A similar variable coordination theory was advanced for voltammograms of Mn(5-NO<sub>2</sub>SALDIEN) in DMSO but it involved coordination and decoordination of the central secondary nitrogen in the ligand to and from the coordination sphere of the metal as Mn was oxidized and reduced, respectively.

Changing the imine N substituent has two effects on the voltammograms. First, the expected shift in peak potentials due to electron-donating ability occurs, with Mn(SALPMA)<sub>2</sub> again being easier to oxidize than Mn(SAL-4-BrANL)<sub>2</sub>. Second there is a variation in the rate of increase of R2 with respect to R1. The ratio  $i_{R2}/i_{R1}$  is smaller for Mn(SALPMA)<sub>2</sub> at a given scan rate, (Figure 28) which, in terms of the

variable solvation theory would mean that attack of solvent is slower with the more electron donating substituent. This may be rationalized by the ligand partly stabilizing Mn(III) in the tetrahedral form, an effect which would produce slower solvation with a better donor ligand.

A voltammetric study in a mixed solvent system varied from pure DMSO to 20% DMSO/80% pyridine showed that peak R1 in DMSO shrank as the pyridine concentration increased, with peak R2 becoming larger (Figure 29). This was accompanied by a shift of all three peaks toward more positive potentials. These results indicate that the implications of the work in DMSO, i.e. that attack of pyridine on a tetrahedral Mn(III) species is very fast, and formation of the octahedral form is complete in the time scale of the scan, are true.

On comparing results in the two solvents, one sees that peak potentials are generally more negative in DMSO than pyridine. Initially, it was thought that this may have been due to junction potential differences between the two solvents, but a study using ferrocene as a pilot ion<sup>97</sup> in both solvents showed that  $\Delta E_{1j}$  is only 30 mV, in agreement with the literature value.<sup>98</sup> A direct comparison of peak R2 in DMSO and the reduction peak in pyridine, is, however, the only valid one which can be made, since both should involve the reaction:



Peak 0 and the oxidation peak in pyridine differ, according to the model, in that the product,  $\text{Mn(III)L}_2^+$ , is immediately solvated in

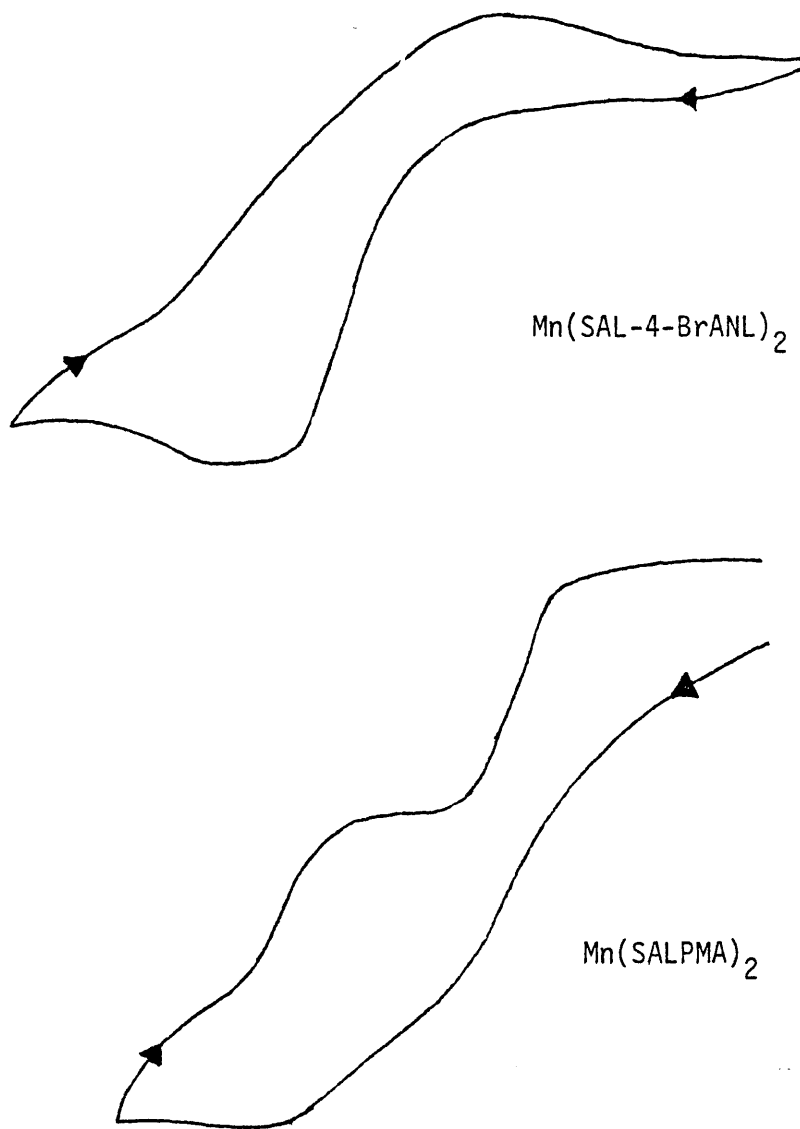


Figure 28. Effect of Substituent on Voltammetric Peak Heights  
(Scan Rate 1 mV/sec)

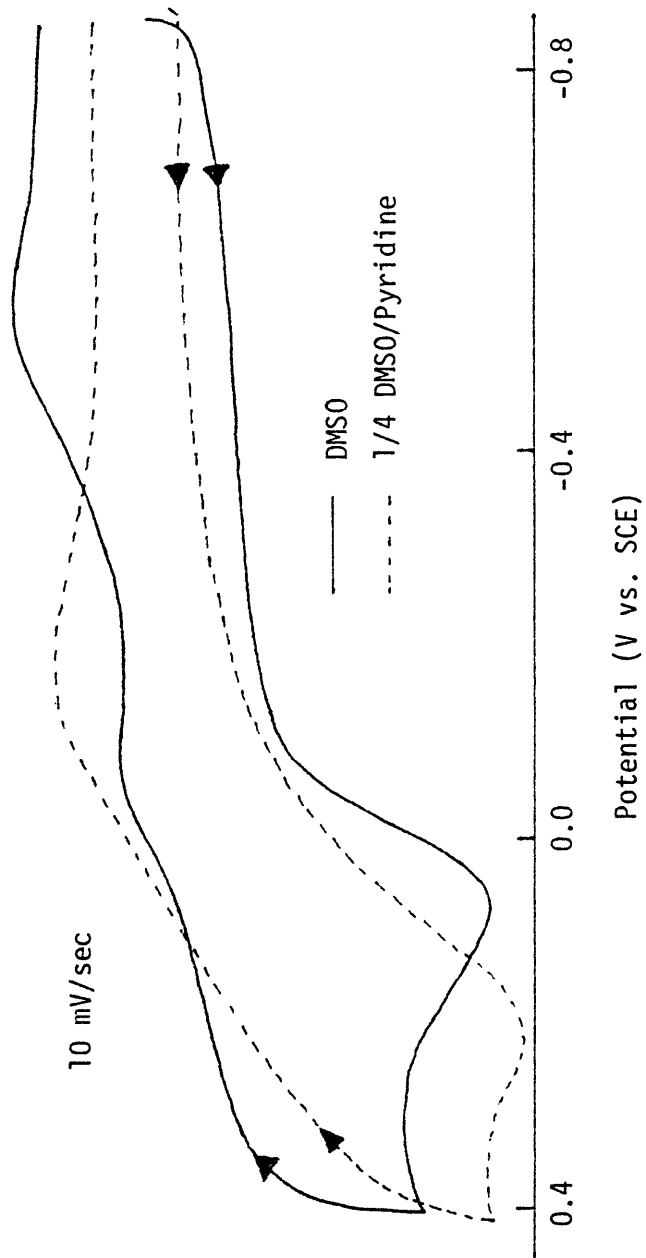


Figure 29: Cyclic Voltammograms of  $\text{Mn}(\text{SAL-4-BrANL})_2$  in DMSO and 1/4 DMSO/Pyridine.

pyridine but not in DMSO. Peak R1 in DMSO has NO counterpart in pyridine. The simplest, and possibly best explanation for the cathodic peak shifts on going from pyridine to DMSO is probably that of different dielectric constants of the two solvents (12 for pyridine, 45 for dimethylsulfoxide).<sup>99</sup> DMSO should stabilize the higher charge on the Mn(III) better than pyridine by electrostatic effects even when not involved in actual coordination.

Although the results of this electrochemical study did not produce valid  $E^\circ$  values for correlation with rate constants in the kinetic study, the interesting results found in DMSO made the study worthwhile, especially in view of similar unexpected results with the tri- and tetradentate complexes.

## 2. Tridentate Complexes

The electrochemistry of the tridentates exhibits similarities to, and differences from, that of the bidentates. In pyridine, initial cathodic scans produce a single reduction peak, with a corresponding oxidation peak on the reverse sweep, for the Mn(III) complexes. The same features appear with an initial anodic scan for the Mn(II) complex (Figure 30). Also, if the electrode potential is held a few hundred millivolts cathodic of the reduction peak for a Mn(III) solution, or anodic of the oxidation peak for a Mn(II) solution, and the current allowed to die away, i.e. the original oxidation state is totally depleted in the vicinity of the electrode, initiating the scan in the opposite direction (i.e. anodic for Mn(III), cathodic for Mn(II)) produces a voltammogram similar to that obtained in the normal manner.

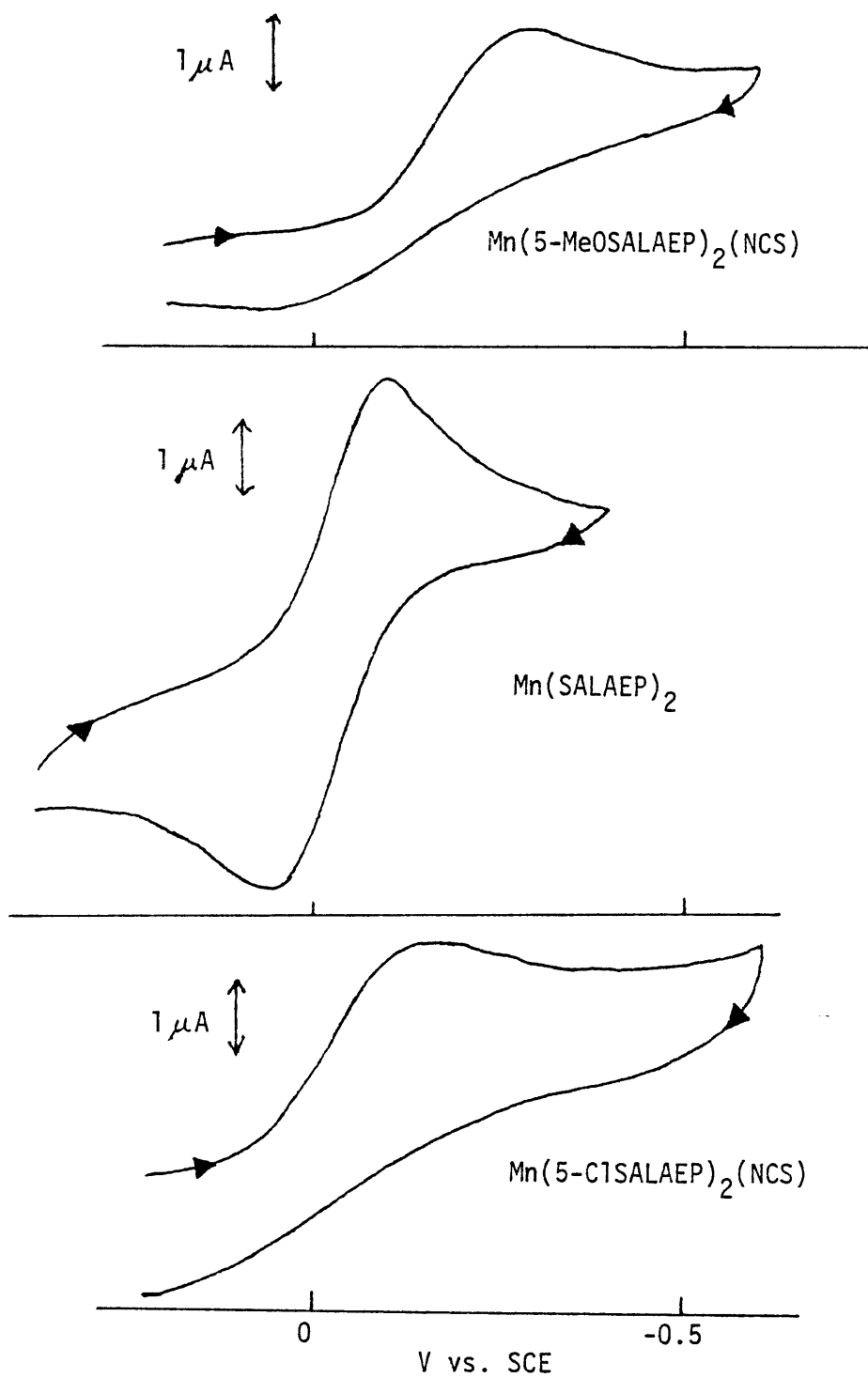


Figure 30. Cyclic Voltammograms of Tridentate Complexes in Pyridine (10 mV/sec).

This is convincing evidence that the couple producing the peaks is Mn(III)/Mn(II), especially when taken with the fact that the peak potentials for the unsubstituted Mn(II) complex fall between those of MeO- and Cl-substituted Mn(III) complexes (vide infra) (Table VI). The peaks themselves are similar to those of the bidentate complexes, i.e. they are fairly wide and short, with peak separation greater than 59 mV and increasing with increasing scan rate. For Mn(SALAEP)<sub>2</sub>, when run in the normal manner, the ratio of cathodic to anodic current is less than unity and decreases with increasing scan rate. The same is true for the anodic to cathodic ratio for the Mn(III) complexes. The anodic peak heights for Mn(SALAEP)<sub>2</sub> and the cathodic ones for the Mn(III) complexes are proportional to  $v^{1/2}$ .

Again, all of these factors can be attributed to a quasireversible Mn(III)/Mn(II) couple, with a low electron transfer rate constant. As was the case with the bidentate complexes, the exact nature of the solution species cannot be determined from the study in pyridine alone, but in conjunction with the results in DMSO (vide infra), the oxidized form of the couple is probably octahedral Mn(III) coordinated by the six donor atoms of two ligands. The reduced form is also octahedral Mn(II), but the 5th and/or 6th coordination positions may contain solvent molecules which have replaced the pyridine functionalities of two ligands. This unfortunately means that  $E^\circ$  values cannot be extracted from the voltammograms because the oxidized and reduced forms may not be the same complex.

Variation of substituents in the ligands has some dramatic effects.

Table VI. Peak Potentials for Tridentate Complexes (V vs. SCE)

Complex	Scan Rate (mV/sec)	$E_{O1}$	$E_{O2}$	$E_{O3}$	$E_R$	$E_{Ox}$	$E_{red}$
Mn(5-MeOSALAEp) <sub>2</sub> (NCS)	1	(a)	+0.21(a)	+0.32(a)	-0.17	(b)	(b)
	10	(a)	+0.21(a)	+0.34	-0.21	+0.08	-0.29
	100	(a)	(a)	+0.37	-0.29	(a)	-0.39
Mn(SALAEp) <sub>2</sub>	1	-0.03(a)	+0.19(a)	+0.33(a)	-0.15	(b)	-0.08
	10	(a)	+0.21	+0.33	-0.17	+0.06	-0.09
	100	(a)	+0.21(a)	+0.36	-0.21	+0.15	-0.16
Mn(5-CISALAMP) <sub>2</sub> (NCS)	1	+0.16	(a)	(a)	0.00	(b)	(b)
	10	+0.12(a)	+0.31(a)	+0.43	-0.04	(a)	-0.15
	100	(a)	(a)	+0.47	-0.10	(a)	-0.21

$E_{O1}$ ,  $E_{O2}$ ,  $E_{O3}$ ,  $E_R$  - in DMSO

$E_{Ox}$ ,  $E_{red}$  - in pyridine

(a) - shoulder

(b) - plateau

The most surprising of these occurs when one of the methylene linkages connecting the pyridine rings is removed, i.e. changing from a SALAEP- to a SALAMP- type ligand. This results in a total loss of electroactivity. Models have shown that the shorter chain ligand is capable of complete coordination so non-coordination by the pyridine groups is not a plausible explanation for the effect. Even total steric impedance, i.e.  $\text{Mn}(\text{SALAMP})_2$  being 4-coordinate in solution, should produce an electroactive species, since SALAMP is SALPMA with an N replacing a phenyl CH (Figure 31), and  $\text{Mn}(\text{SALPMA})_2$  is electroactive. This effect may be due to the strong electron-withdrawing effect of the pyridyl group, but one would expect that this drastic an effect on the electrochemistry would manifest itself in the oxygenation studies. However,  $\text{Mn}(\text{SALAMP})_2$  is quite easily oxidized (vide infra), although its  $E_a$  values are higher than those for  $\text{Mn}(\text{SAL-4-BrANL})_2$ , whose ligand is between SALAMP and SALPMA in electron-donating ability.

A less dramatic effect, one requiring some explanation, involves the complex  $\text{Mn}(\text{5-NO}_2\text{SALAEP})_2$ . This complex exhibits no redox peaks assignable to a  $\text{Mn}(\text{III})/\text{Mn}(\text{II})$  couple, but only a single irreversible reduction peak at  $\sim -1.4$  V, assignable to reduction of the  $\text{NO}_2$ -group. The electron-withdrawing effect of the  $\text{NO}_2$ -substituent has apparently shifted the potential for oxidation outside the accessible solvent range. This shift to more positive potentials by the nitro-group has been seen in a number of studies, but not to such a great extent. Changing the SAL-group to a PY-group also inhibits oxidation to  $\text{Mn}(\text{III})$ , but this effect has been previously reported. Finally, the by now

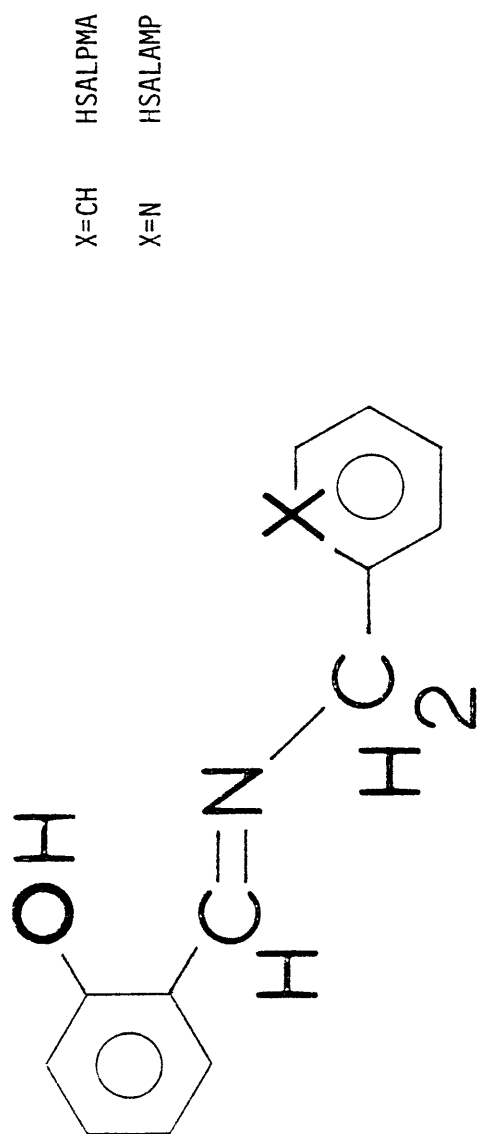


Figure 31: Comparison of HSALPMA and HSALAMP.

familiar effect of electron-donating ability can be seen from the peak potentials in Table VI. In general, the relative ease of oxidation of the complexes lies in the order  $Cl < H < MeO$ , paralleling the increasing electron-donating ability of the substituents.

In DMSO, the voltammograms are radically different. As with the bidentates in DMSO, there are multiple peaks present, but they are now found on the anodic part of the scans, and will be referred to as O1, O2, and O3, moving anodically (Figure 32). The peaks are again broad and short, they separate with increasing scan rate, and their current ratios are scan rate dependent. For both Mn(II) and Mn(III) complexes, run in normal directions, the total current on the reverse scan is lower than on the forward scan. Cathodic peak heights for the Mn(III) complexes are again proportional to  $v^{1/2}$ .

All of these features are once more explainable by a quasi-reversible set of reactions with a coupled chemical reaction. The different species responsible for the redox peaks may be, as with the bidentates, due to different degrees of solvent coordination to the metal (Figure 33). Again, this was shown not to be due to the presence of  $H_2O$ . A fast scan initiated with a Mn(III) solution produces primarily peak O3 on the reverse sweep, therefore peaks O3 and R are due to a single couple. As the scan rate is decreased, peaks O2 and O1 begin to grow in at the expense of peak O3 (Figure 34), i.e. the immediate product of R undergoes a slow reaction to produce species responsible for O2 and then O1. Using the theory of different solvated forms, this would be due to either gain or loss of first one, then a

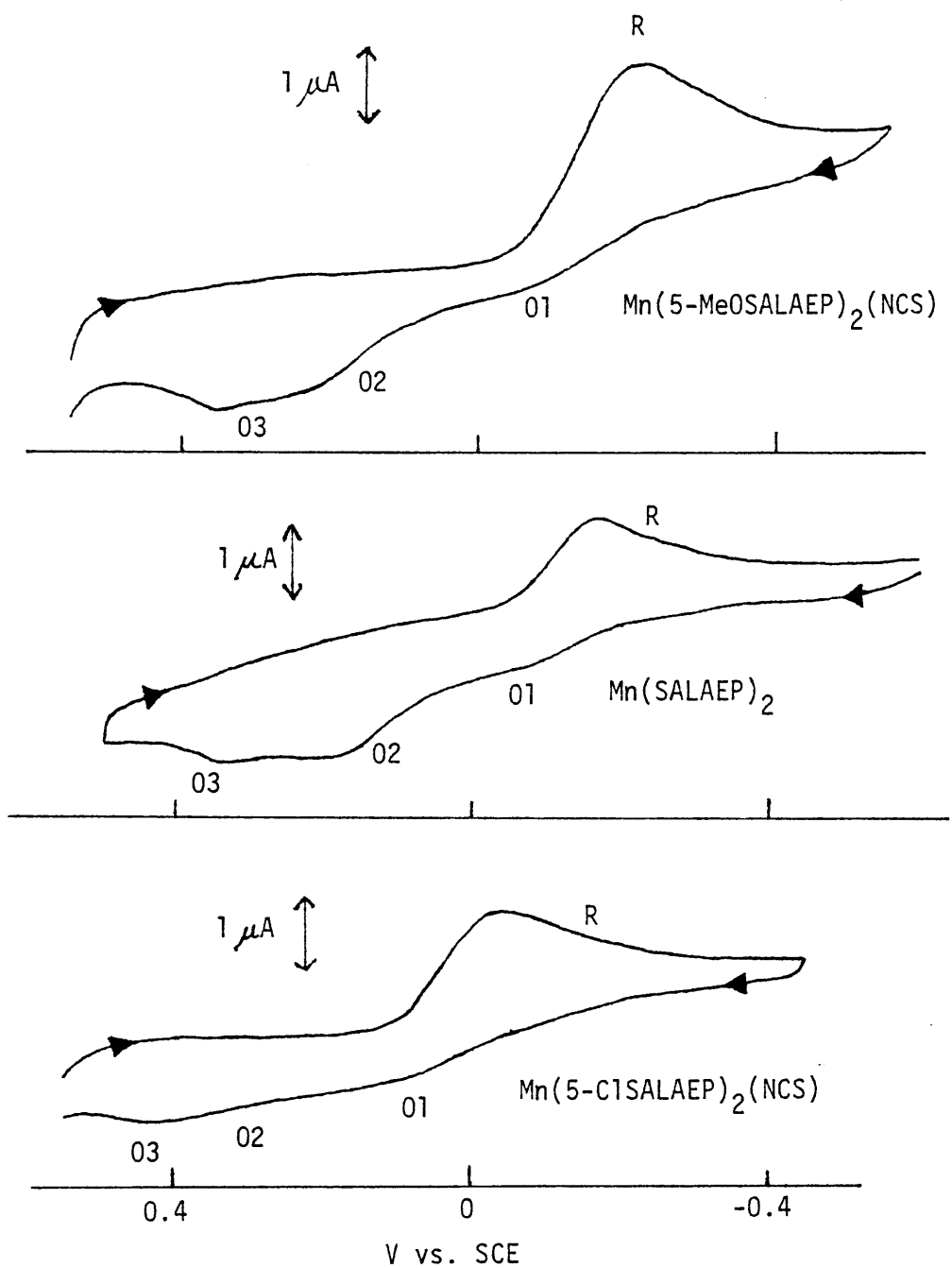
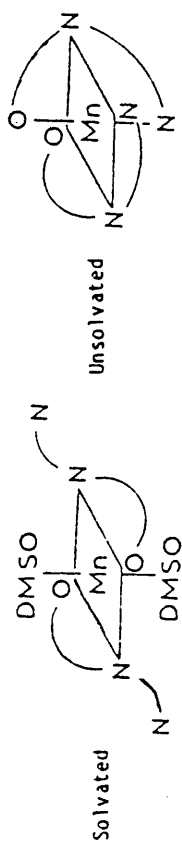


Figure 32. Cyclic Voltammograms of Tridentate Complexes in DMSO (10 mV/sec).



Unsolvated form favored by  $\Delta H$  and  $\Delta S$ , but to a lesser extent than with the bidentates:  
 $\Delta H$  more favorable because pyridine ring is a better donor than DMSO,  $\Delta S$  because two free  
 solvent molecules are available, but pyridines lose some flexibility on coordination.

- Mn(II) Even though unsolvated is favored, Keg includes the solvent, and the vast excess of solvent  
 ( $\sim 10^4 \times$  solute) forces DMSO into coordination sites.
- Mn(III) Effect of  $\Delta H$  much more substantial than for Mn(II) and pulls pyridines into coordination  
 sites, outweighing solvent effects.

Figure 33: Solvation Model for Tridentate Complexes.

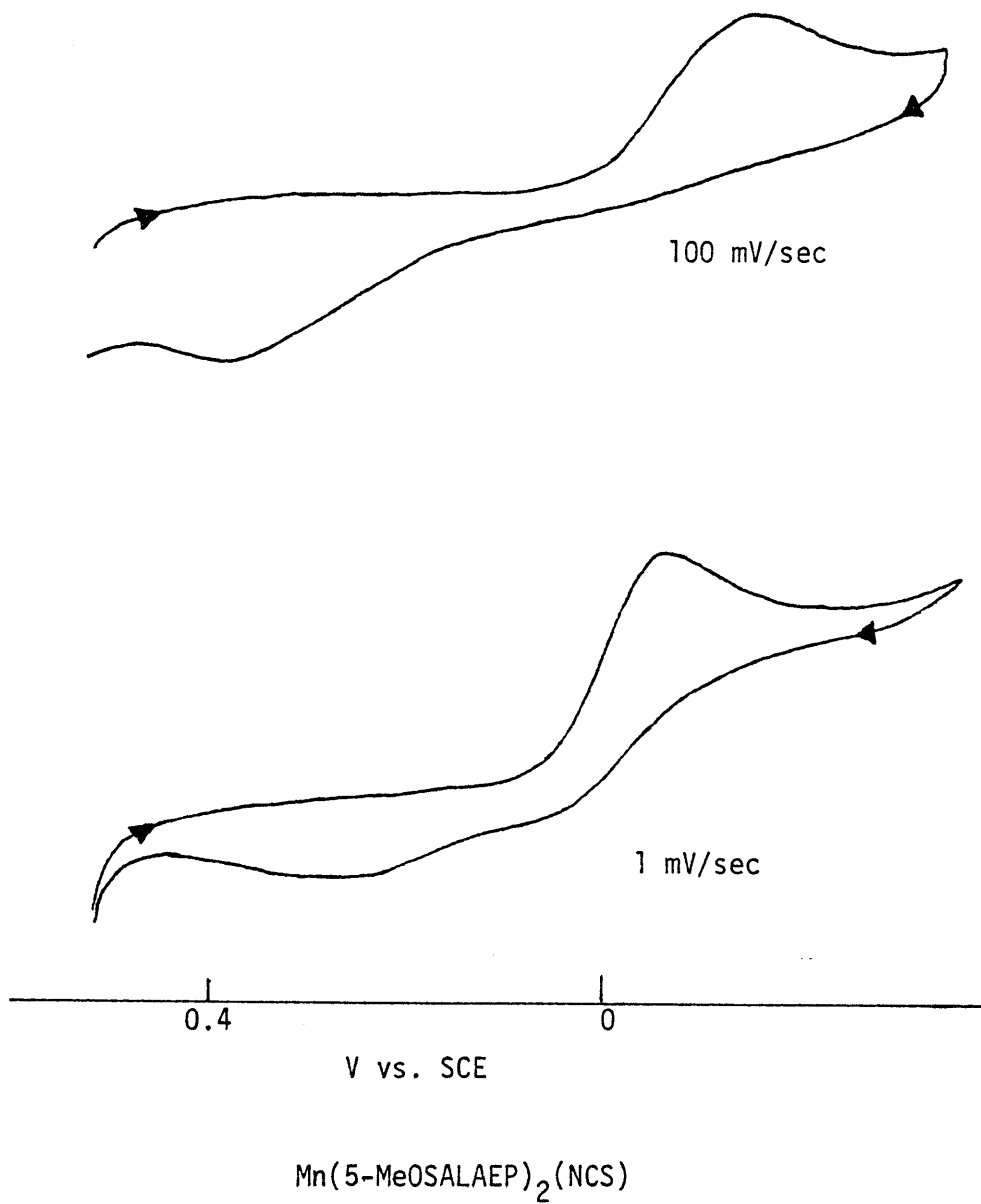


Figure 34. Effect of Scan Rate on Voltammetric Peak Heights.

second molecule of solvent, accompanied by production of, or coordination by two "dangling" pyridine groups in the ligands as they are forced out of or move into the coordination sites.

Sacconi et al.<sup>100</sup> demonstrated the existence of three forms (octahedral, square pyramidal, and square planar) for a similar ONN type ligand in a Ni(II) complex. Chakravorty et al.<sup>101</sup> found octahedral, pyramidal, and tetrahedral forms of an ONO type complex, where the O was in an ether linkage. A major difference between these two papers and the present work was that no solvent coordination was postulated, even in pyridine, where the six-coordinate species was assumed to be the fully closed complex. An even more dramatic change in coordination was shown by the potentially 7-coordinate ligand prepared by Drew et al.<sup>102</sup> which tautomerized to a 6-coordinate ligand in the presence of Ni(II), an effect attributed to the preference of Ni(II) for octahedral coordination (Figure 35).

A number of factors make the gain of solvent a more logical alternative. First, as explained in Figure 33, the enthalpy and entropy differences between solvated and unsolvated forms should favor an unsolvated form of the Mn(III) species. Second, as DMSO replaces a pyridine substituent as a ligand, one would expect a shift in the peak potential towards more negative values.<sup>103</sup> Third, in the study of oxygenation kinetics (vide infra), a solvent molecule is postulated to be at the site of attack of O<sub>2</sub>. The kinetic study should exhibit results for the most easily oxygenated species in solution, and a correspondence between ease of oxygenation and ease of electro-oxidation.

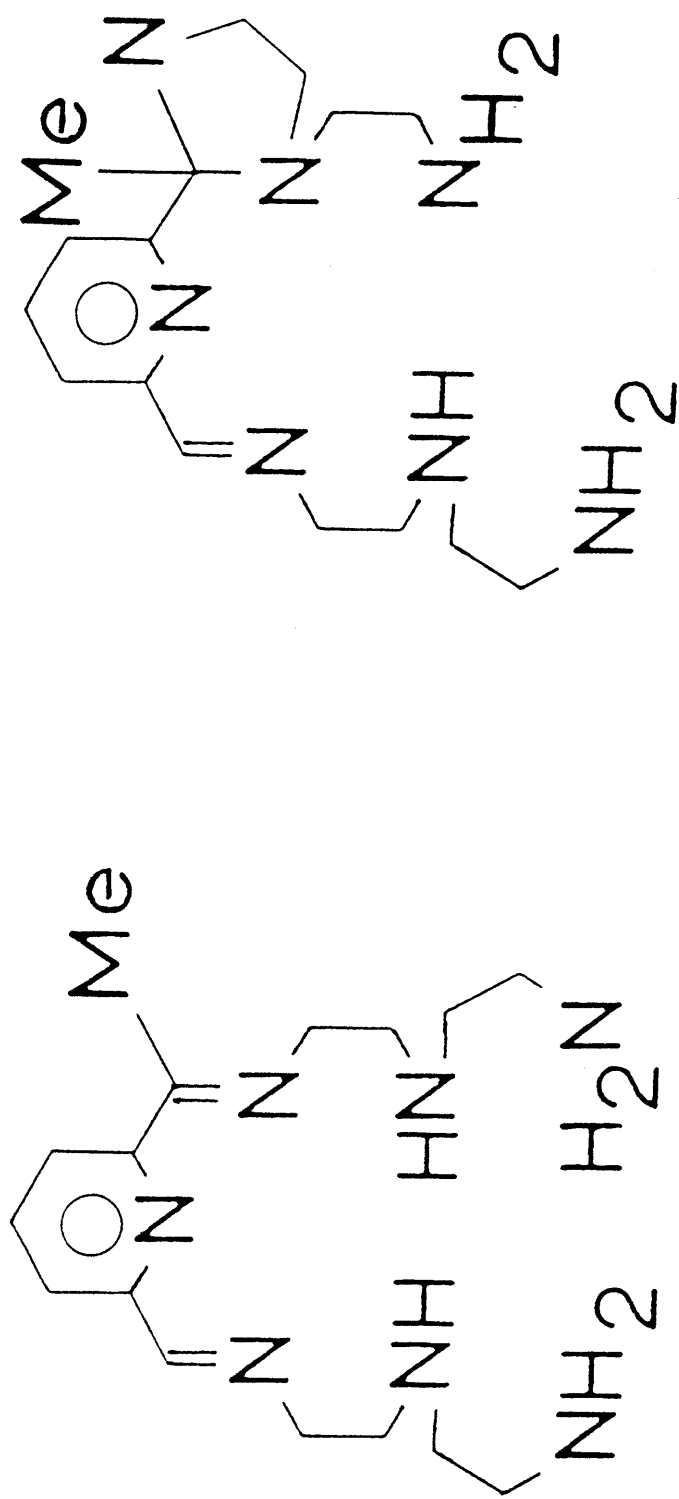
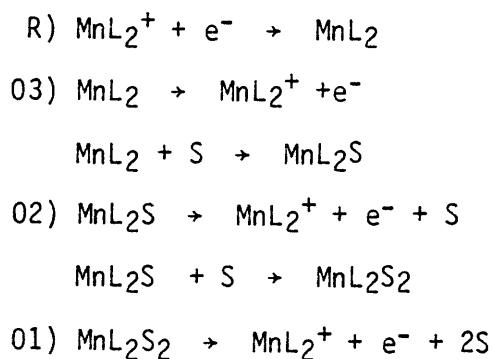


Figure 35: Tautomerization of N<sub>7</sub> Ligand.

has been demonstrated by the bidentates, and also the higher denticity complexes (vide infra), making assignment of peak 01 to a disolvated complex quite reasonable. The fact that the tridentate complexes exhibit three Mn(II) species in solution is due to the dangling pyridine linkages' ability to keep the metal 6-coordinate regardless of the number of coordinated solvent molecules. The bidentate complexes, on the other hand, only exhibited two Mn(III) species because a mono-solvated complex would have been a non-preferred 5-coordinate complex.

The reduction of an unsolvated  $MnL_2^+$  ion should therefore be followed by solvent attack, resulting in a mixture of  $MnL_2$ ,  $MnL_2S$ , and  $MnL_2S_2$ . On oxidation, the solvated forms of Mn(II) must immediately lose solvent since only one reduction peak is seen even at high scan rates. The electrode reaction scheme therefore is:



Attempts to isolate the disolvated species were unsuccessful. The methods attempted were both initiated by dissolving the Mn(II) complex in DMSO, and then either vacuum evaporating the solvent, or adding ether in an attempt to saturate the solution. Neither resulted in the formation of any precipitate after a reasonable loss of solvent or

addition of ether.

Substituent effects in DMSO are similar to those found in pyridine. Compounds with the AMP-, PY-, and 5-NO<sub>2</sub>-groups are inactive in DMSO. The effect of the other SAL substituents follows the order in pyridine, i.e. MeO- facilitates oxidation the most, and Cl- the least. However, there is a second effect of these substituents on the relative heights of peaks O1, O2 and O3. At a given scan rate, the Cl-substituted complex produces relatively the largest O1 peak, and the MeO-complex the smallest (Figure 36). This may be due to same effect as was the case of the bidentates, i.e. solvent attack would be slowest for electron-donating substituents. The case here is different, however, in that the solvated form is not thermodynamically favored. However, this effect can be rationalized if one considers that the substituent changes only affect the purely electronic part of the binding to Mn. The pyridyl groups on the ligands remain better overall donors than solvent DMSO groups, but DMSO is a better donor on electronic grounds.<sup>104</sup> A decrease in electron density on the metal, i.e. changing to a Cl- from a MeO-substituent, should therefore shift the solvation equilibrium towards coordination by DMSO, and apparently also increases the rate of solvation.

A mixed solvent study was again performed in mixtures from pure DMSO to 20% DMSO/80% pyridine. As the pyridine concentration increased, the peaks shifted cathodically, and peaks O1 and O2 disappeared as peak O3 grew in (Figure 37). If the solvation model is correct, one would expect that pyridine, being a better coordinating solvent for Mn(II)

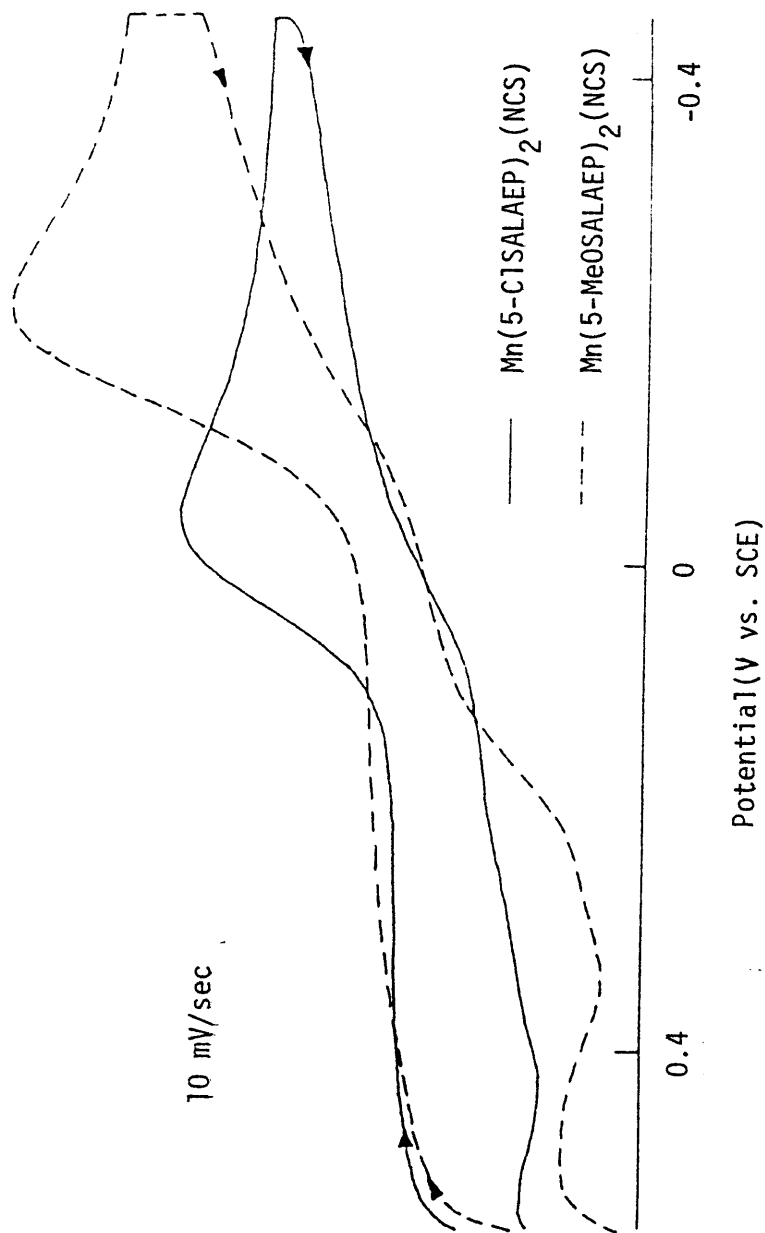


Figure 36: Cyclic Voltammograms of  $\text{Mn}(5\text{-ClSALAEP})_2(\text{NCS})$  and  $\text{Mn}(5\text{-MeOSALAEP})_2(\text{NCS})$ .

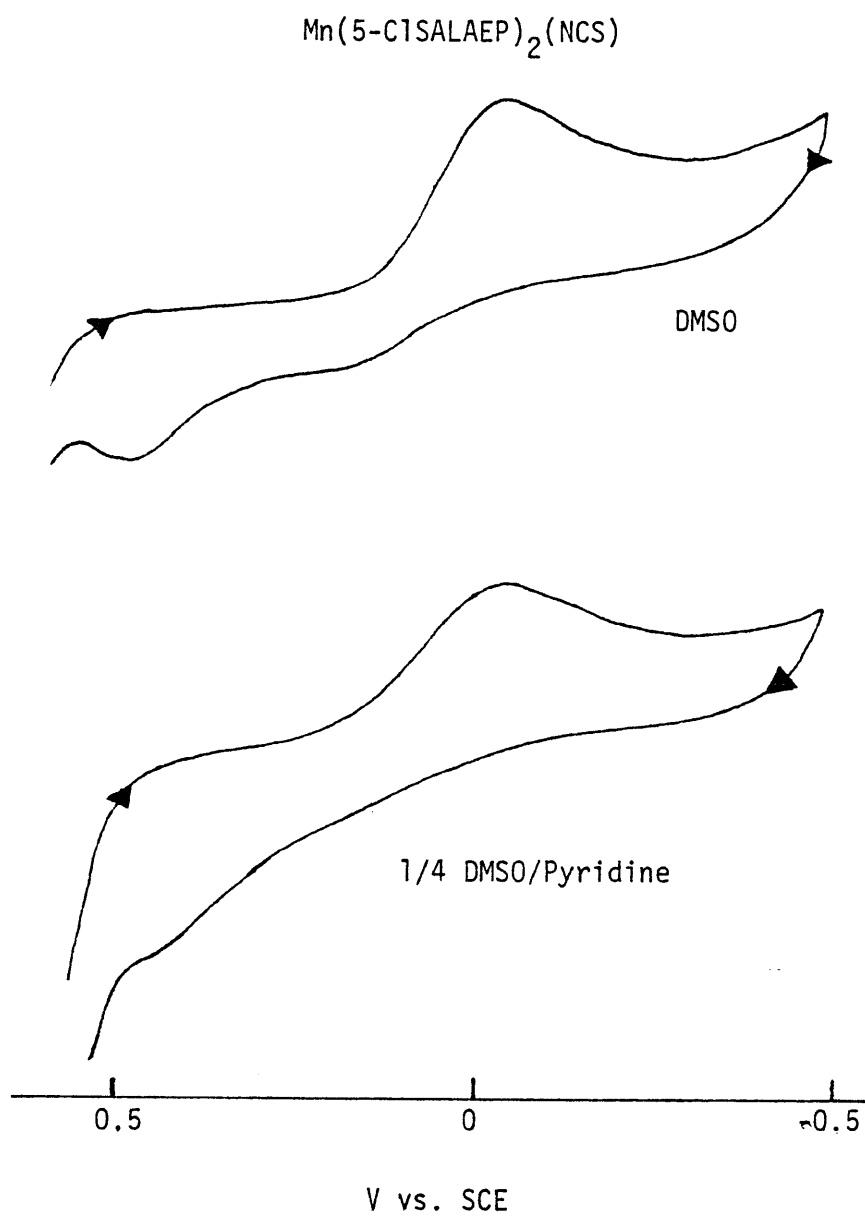
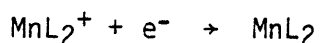


Figure 37. Effect of Solvent on Cyclic Voltammograms of Tridentate Complexes (10 mV/sec).

than DMSO, would cause peak 01 to grow at the expense of 02 and 03. However, if one realizes that a solvent pyridine and the ligand pyridine are virtually identical as far as determining the complexes' electrochemical properties, peak 01 may be growing with increasing pyridine content, but its potential, and that of peak 02, are shifted to coincide with that of 03. Peak 03, therefore, even in pure pyridine, may be a composite peak due to oxidation of  $MnL_2$ ,  $MnL_2S$ , and  $MnL_2S_2$ .

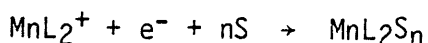
A coulometric study was attempted in DMSO using the Mn(III) complexes. The  $n$  values for reduction were found to be irreproducible but were generally  $0.8 \pm 0.1$ . The electrolyses took much longer than normal (~30 min), with times of up to 6 hours being required for the current to decay to 1% of its initial value. These results are compatible with the slow electron transfer postulated from the voltammograms. The solutions after electrolysis had a yellow color characteristic of a Mn(II) complex, but comparison of spectra with authentic spectra of the Mn(II) species was not possible because of the inability to synthesize both oxidation states with the same ligand set.

Comparison of the electrochemistry in the two solvents again reveals properties similar to the bidentates. Peak potentials are more negative in DMSO than in pyridine, i.e. DMSO facilitates the Mn(II) to Mn(III) oxidation. Direct comparison of the peaks may, however, still be questionable. The reduction peak may be the only one which is the same for both solvents, i.e. involves the reaction:



In pyridine, the immediate attack of solvent, however, may also be

involved, i.e.:



As previously stated, the oxidation peak in pyridine may correspond to one, two or all three oxidation peaks in DMSO. Thus simple dielectric effects remain the simplest explanation for the shifts.

### 3) Tetradentate Ligands

The electrochemical properties of the tetradentate complexes are as complex, in their own way, as those of the previously discussed bi- and tridentate complexes. Instead of changing radically from solvent to solvent, however, the difference is a function of the polymethylene chain length. The complexes thus divide themselves into two types, Mn(XSALEN), and the longer chain complexes.

The voltammograms of the XSALEN complexes are similar to those previously reported for SALOPHEN tetradentate complexes.<sup>58</sup> The peak potentials reported in an earlier paper for Mn(SALEN)Cl in DMSO are in agreement ( $\pm 30$  mV) with those found here for Mn(SALEN) (Table VII). In both DMSO (Figure 38) and pyridine (Figure 39) the complexes exhibit a single pair of coupled peaks. The initial anodic current is slightly larger than the cathodic current on the reverse sweep (Table VIII) and  $i_{ox}/v^{1/2}$  is constant (Figures 40 and 41). The peak separation is greater than 59 mV, and increases with increasing scan rate (Table IX), however, at low scan rates the separation is closer to 60 mV than for the bi- and tridentates. There is no evidence of a major loss of reduction current with increasing scan rate, nor are the peak currents lower than those reported for earlier quasireversible systems.

Table VII. Peak Potentials for XSALEN Complexes (V vs. SCE)

<u>Complex</u>	<u>Scan Rate (mV/sec)</u>	<u>E<sub>ox</sub>(a)</u>	<u>E<sub>red</sub>(a)</u>	<u>E<sub>ox</sub>(b)</u>	<u>E<sub>red</sub>(b)</u>
Mn(3-MeOSALEN)	1	-0.18	-0.29	-0.13	-0.22
	10	-0.20	-0.27	-0.12	-0.22
	100	-0.19	-0.28	-0.05	-0.24
Mn(SALEN)	1	-0.22	-0.36	-0.10	-0.28
	10	-0.25	-0.33	-0.06	-0.23
	100	-0.24	-0.33	+0.06	-0.31
Mn(5-ClSALEN)	1	-0.15	-0.21	0.00	-0.12
	10	-0.14	-0.21	+0.04	-0.13
	100	-0.13	-0.23	+0.15	-0.18

(a) - in DMSO

(b) - in Pyridine

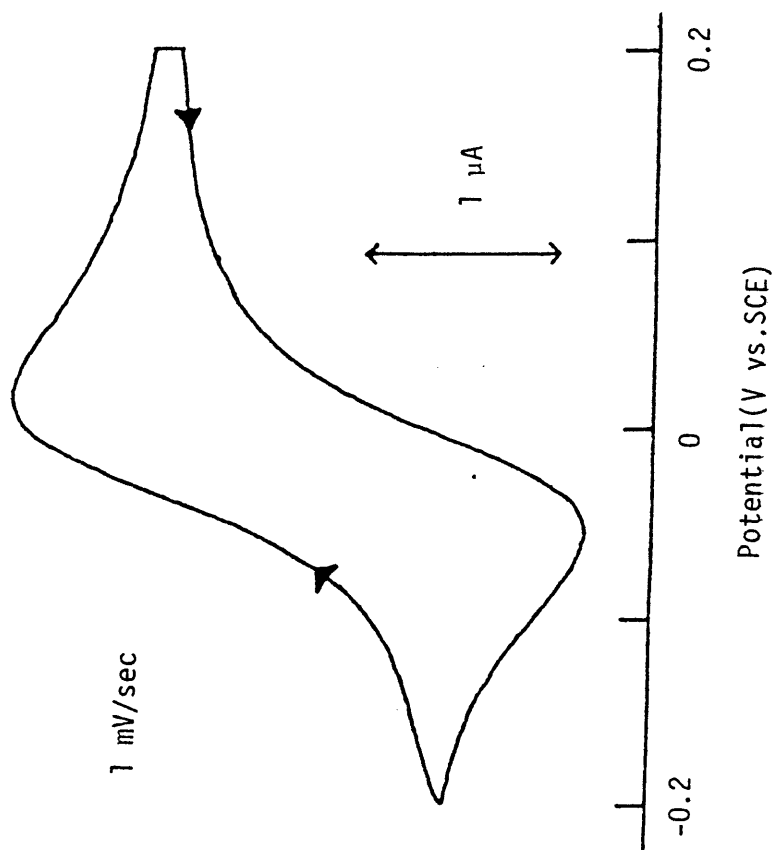


Figure 38: Cyclic Voltammogram of Mn(5-ClSALEN) in DMSO.

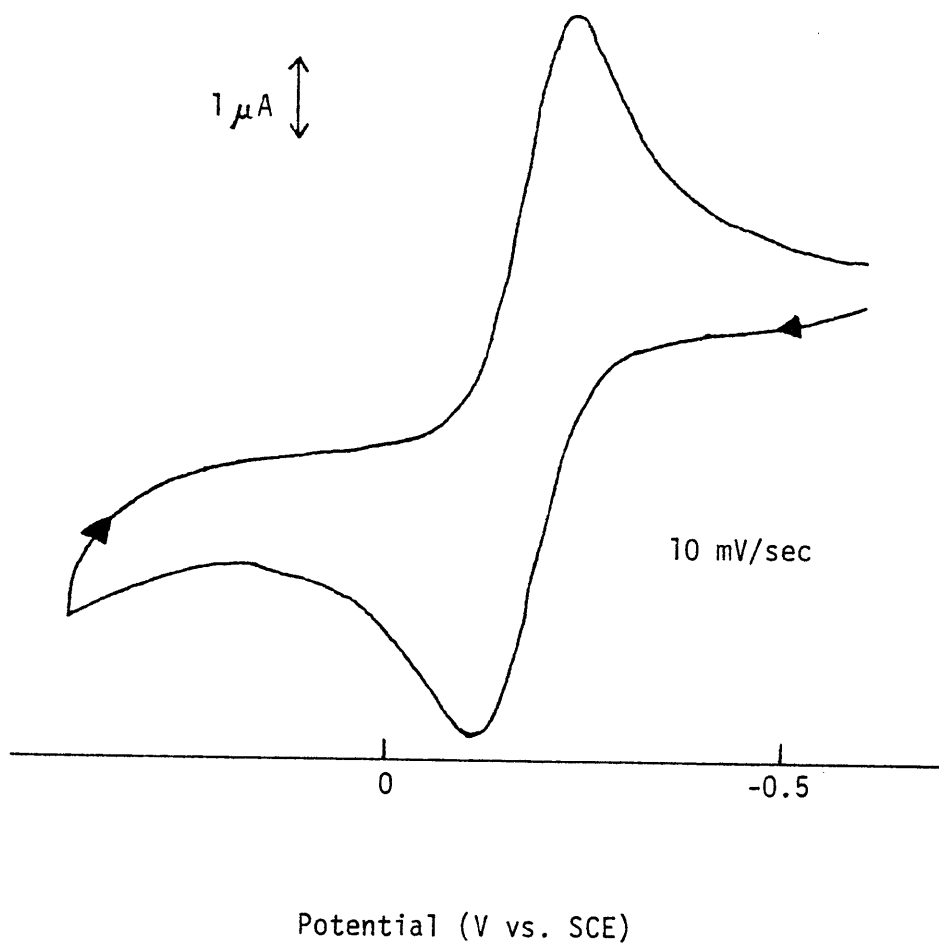


Figure 39. Cyclic Voltammogram of Mn(3-MeOSALEN) in Pyridine.

Table VIII. Peak Current Ratios for XSALEN Complexes

Complex	Scan Rate (mV/sec)	$i_{red}/i_{ox}(DMSO)(a)$	$i_{red}/i_{ox}(PY)(a)$
Mn(5-C1SALEN)	1	0.82	1.2
	10	0.73	0.99
	100	0.72	0.72
Mn(SALEN)	1	1.1	1.2
	10	0.94	1.3
	100	0.89	3.0(b)
Mn(3-MeOSALEN)	1	2.1(b)	0.93
	10	1.1	1.1
	100	0.78	0.93

(a) - normalized to  $i_{ox} = 1$ 

(b) - noisy baseline; visual inspection indicates ratio near 1.0

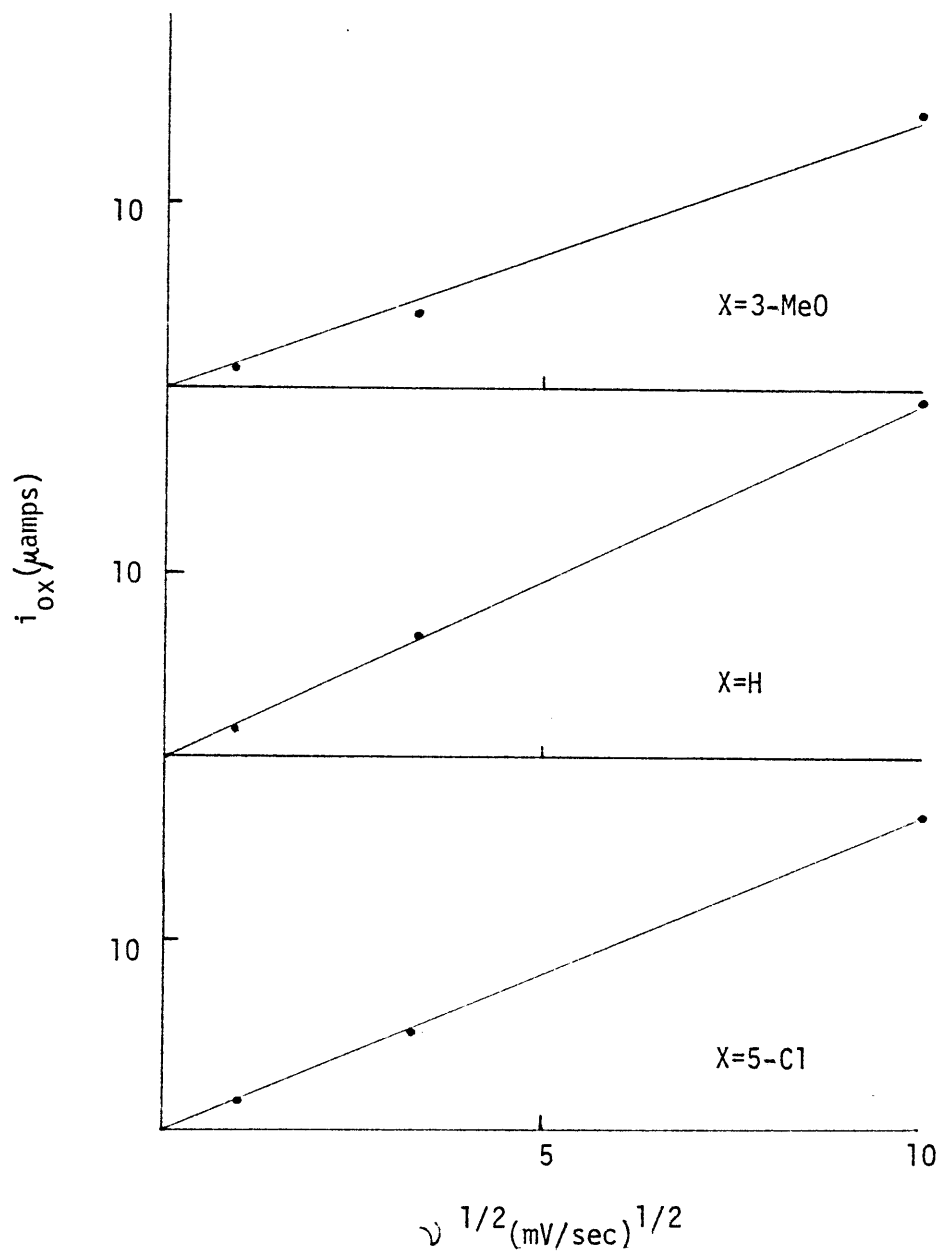


Figure 40: Anodic Peak Current vs. Square Root of Scan Rate for Mn(XSALEN) in DMSO.

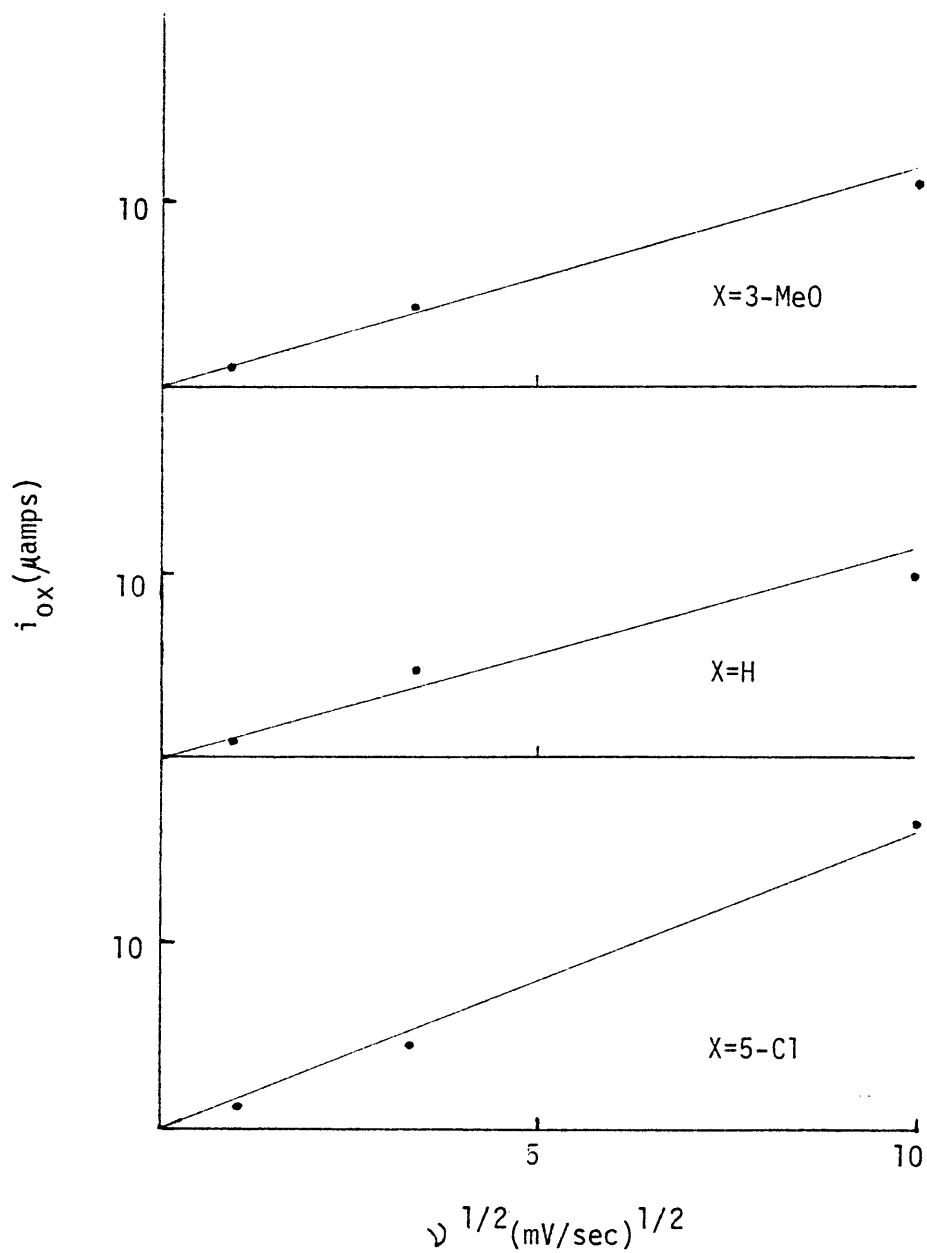


Figure 41: Anodic Peak Current vs. Square Root of Scan Rate for Mn(XSALEN) in Pyridine.

Table IX. Peak Separations(V) and  $E^*$ (V vs. SCE) for XSALEN Complexes

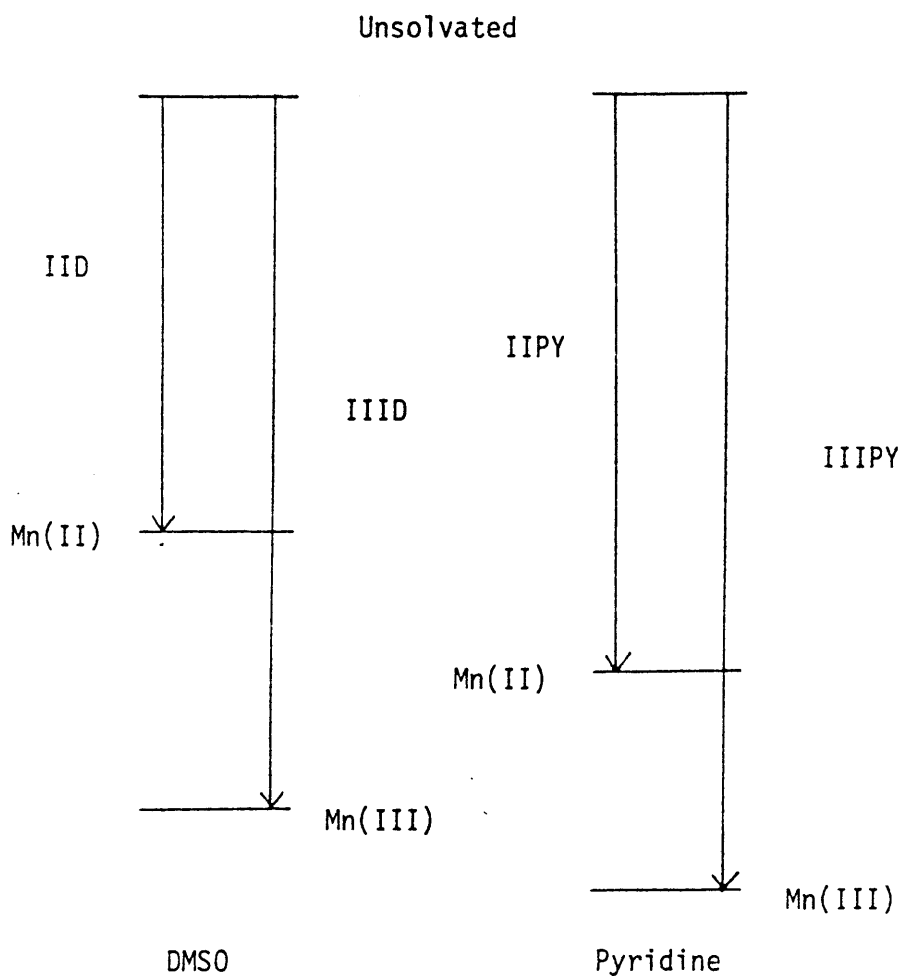
Complex	Scan Rate (mV/sec)	$\Delta E_p^{(a)}$	$E^*(a)$	$\Delta E_p^{(b)}$	$E^*(b)$
Mn(3-MeOSALEN)	1	0.11	-0.24	0.09	-0.18
	10	0.07	-0.24	0.10	-0.17
	100	0.09	-0.24	0.19	-0.14
Mn(SALEN)	1	0.14	-0.29	0.18	-0.19
	10	0.08	-0.29	0.17	-0.14
	100	0.09	-0.29	0.37	-0.12
Mn(5-ClSALEN)	1	0.06	-0.18	0.12	-0.06
	10	0.07	-0.18	0.17	-0.04
	100	0.10	-0.18	0.33	-0.02

(a) - in DMSO

(b) - in Pyridine

Therefore, the peaks are due to a quasireversible couple, presumably Mn(III)/Mn(II), with electron transfer faster than for the bidentates and tridentates. The effect of solvent on the peak potentials is, as expected, a shift toward more cathodic potential in pyridine. However, the solution geometry of both oxidation states is undoubtedly octahedral, with a planar ligand and trans solvent molecules, so an explanation besides simple dielectric effects may be advanced here as an explanation for the shifts. The more negative reduction potential for a solvated square planar species in DMSO is compatible with earlier work on phthalocyanine<sup>105</sup> and tetraphenylporphyrin<sup>106</sup> complexes. This may seem to be the reverse of the expected change. Since pyridine is a better donor solvent, and should therefore better stabilize the higher oxidation state, one would expect that oxidation would be more facile in pyridine. Lever and Minor<sup>103</sup> have advanced a simple theory to explain this effect for macrocyclic complexes of Fe, Co, Cr, and Mn, and this theory may also apply here. Pyridine may indeed stabilize Mn(III) more than DMSO, but it also stabilizes Mn(II) more. This is due to a soft acid-soft base interaction between the large Mn(II) ion and the pyridine N, which is softer than the DMSO oxygen. The relative stabilization of the two states is what determines the redox potential and apparently the effect favors Mn(II) more in pyridine than DMSO (Figure 42).

It is interesting to compare the order of potentials in the two solvents for the III/II couples of similar Fe and Co complexes.<sup>103</sup> Iron complexes shift potentials on changing the solvent in the same direction as manganese, but cobalt reverses the shift. Iron(II) is an even more



IIIPY is greater than IIID but IIPY is greater than IID  
 therefore IIPY/IIIPY is greater than IID/IIID, i.e. Mn(II)  
 is more stable in pyridine than in DMSO.

Figure 42. Coordinated Solvent Effect on Macrocyclic Complex Redox Potentials.

covalently binding ion than Mn(II), therefore the soft-soft interactions are similar and Fe(II) is stabilized by pyridine to a greater extent than DMSO. Cobalt(II) is a harder ion, and the control of the potential apparently shifts to the electronic donor properties of the solvent, allowing pyridine to stabilize Co(III) better than DMSO.

Substituent effects are generally those predicted from electron-donating effects, i.e. more negative potentials on going from Cl<sup>-</sup> to H<sup>-</sup> to MeO<sup>-</sup>. There is a break in this order in DMSO, however, where the MeO complex peaks are anodic to those of the unsubstituted complex. A similar discrepancy was seen for the 3-MeOSALOPHEN-complex, where molecular models showed steric hindrance between the MeO-groups in the cis configuration. This apparently prevented full coordination by the ligand and the effect of the substituent was minimized.<sup>58</sup> The 5-MeOSALOPHEN-complex had no steric hindrance and its peaks were cathodic to those of of the unsubstituted complex. The same effect may be occurring with 3-MeOSALEN<sup>2-</sup>, but the reason why the discrepancy disappears in pyridine is not clear. Steric interactions between the coordinated pyridine molecules and the ligand may force the ligand into a more planar configuration and allow the substituent to exert its full electron-donating ability. The better bonding of pyridine than DMSO and its larger size are possible reasons for this difference.

The longer chain complexes have completely different electrochemical properties. No data could be gathered in DMSO because of their low solubility. Mn(SALBTDA) was also insoluble in pyridine, therefore a large gap exists between the two carbon SALEN complexes and

the six carbon SALHXDA complex. In pyridine, a typical voltammogram contains a large "hump" near or on the solvent oxidation wave on the initial anodic scan, and a smaller cathodic peak on the reverse sweep (Figure 43). The peaks are quasireversible in that the separation increases with increasing scan rate, but the separation is much greater than 59 mV even at 1 mV/sec. The effect of increasing the chain length is rather surprising. The anodic hump moves into the solvent wave but the cathodic peak moves in the opposite, cathodic direction. This is a very strong indication that the two peaks are not directly coupled, since a ligand change should cause both peaks to move in the same direction. The earlier report of a reduction peak for Mn(SALHTDA)(NCS) is in agreement with this work wherein an irreversible reduction was suggested.<sup>59</sup> The explanation advanced was that the Mn(III) species was monomeric, but the Mn(II) reduction product was polymeric. The likely form of the polymer would be one containing bridging ligands (Figure 44). This theory may also explain the unexpected shifts in peak potentials. If the degree of polymerization determines how far the hump is shifted anodically, one would expect that the longest chains would promote the most polymerization and the most stable Mn(II), i.e. the most anodic hump. The extreme width of the hump would be due to a number of geometrically different sites oxidizing at slightly different potentials. On oxidation, the Mn(III) polymer would begin to depolymerize, but at a sufficiently slow rate that only a fraction of it was available for reduction. Some of the oxidized form may also react with the solvent and/or electrolyte if its reduction potential is high

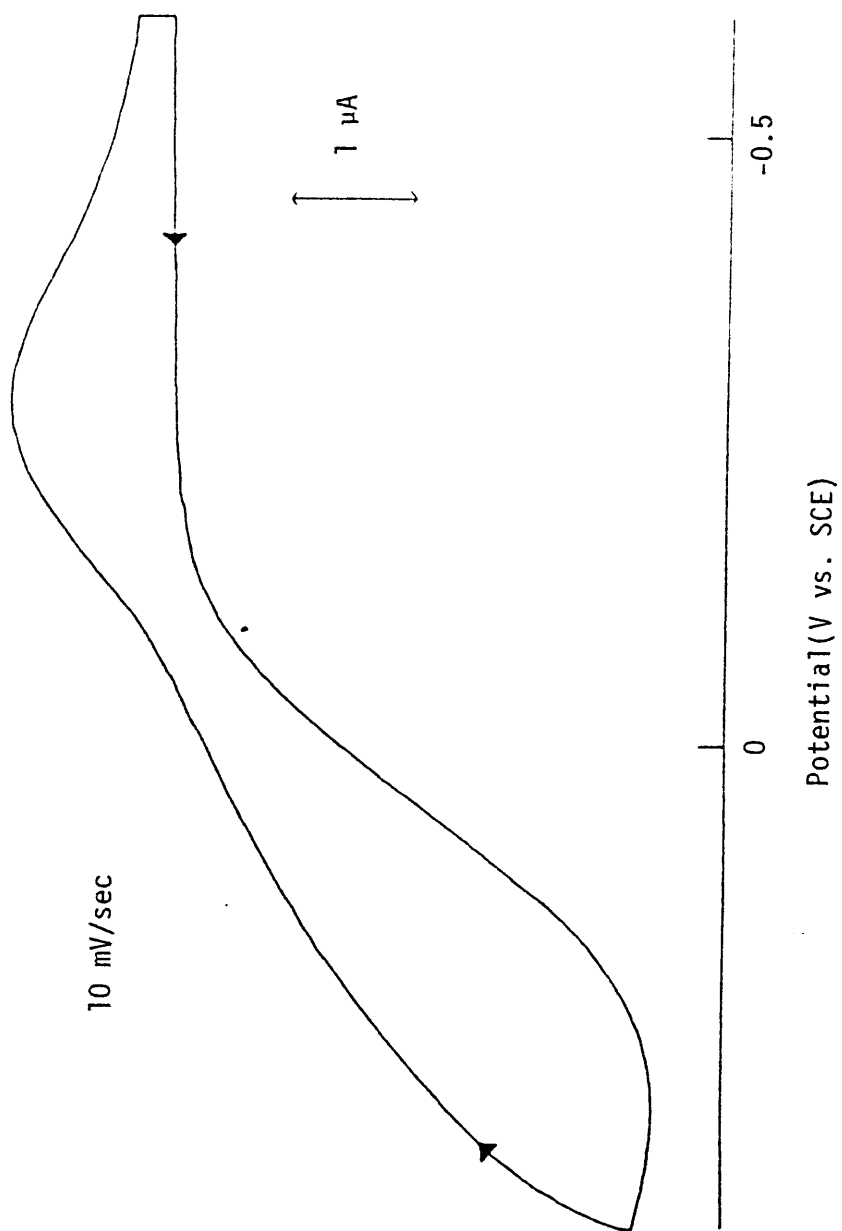


Figure 43: Cyclic Voltammogram of Mn(SALOTDA) in Pyridine.

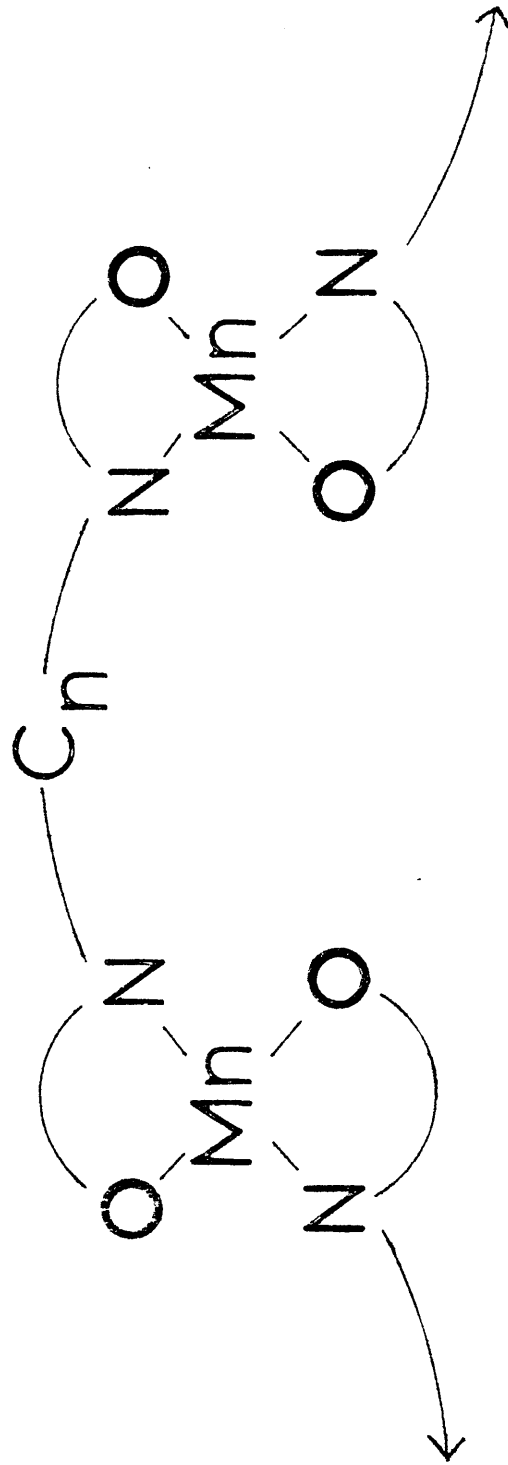


Figure 44: Possible Polymeric Structure of Mn(SALC<sub>n</sub>) Complexes.

enough. The monomeric Mn(III) also seems to be stabilized more in the longer chain compounds. This effect may be due to the increased flexibility of the ligand allowing better coordination, at the same time as it allows more polymerization of Mn(II).

Mn(SALDCDA) exhibits further irregularities in its voltammograms. At high scan rates, it resembles the other long chain complexes, but as the scan rate is decreased, a second reduction peak grows in at a potential cathodic to the first (Figure 45). If a model involving coordinated solvent is again postulated, these results can be explained by reaction of the species responsible for the original peak (tetrahedral Mn(III)) with the solvent to produce a new, more stable, electroactive species (octahedral Mn(III)). Mn(SALDCDA) will also be seen to differ from the other SALC<sub>n</sub> complexes in the kinetics section, where it is the only complex of this type to have a soluble  $\mu$ -oxo-Mn(III) oxygenation product. The conception of the original oxidation product as a tetrahedral species is feasible since it should resemble the Mn(II) starting material. This has been shown to possess "pseudo-tetrahedral" geometry in the solid state, and this property could carry over to a dissolved polymer. A second irregularity occurs when a second scan is performed immediately on completion of a very slow scan. A second oxidation peak is now found cathodic to the hump (Figure 46). This peak seems to be coupled to peak R2 and is therefore postulated to be due to oxidation of octahedral Mn(II). On a slow scan, sufficient octahedral Mn(III) would be built up such that its reduction (peak R2) would produce sizeable quantities of octahedral Mn(II). If

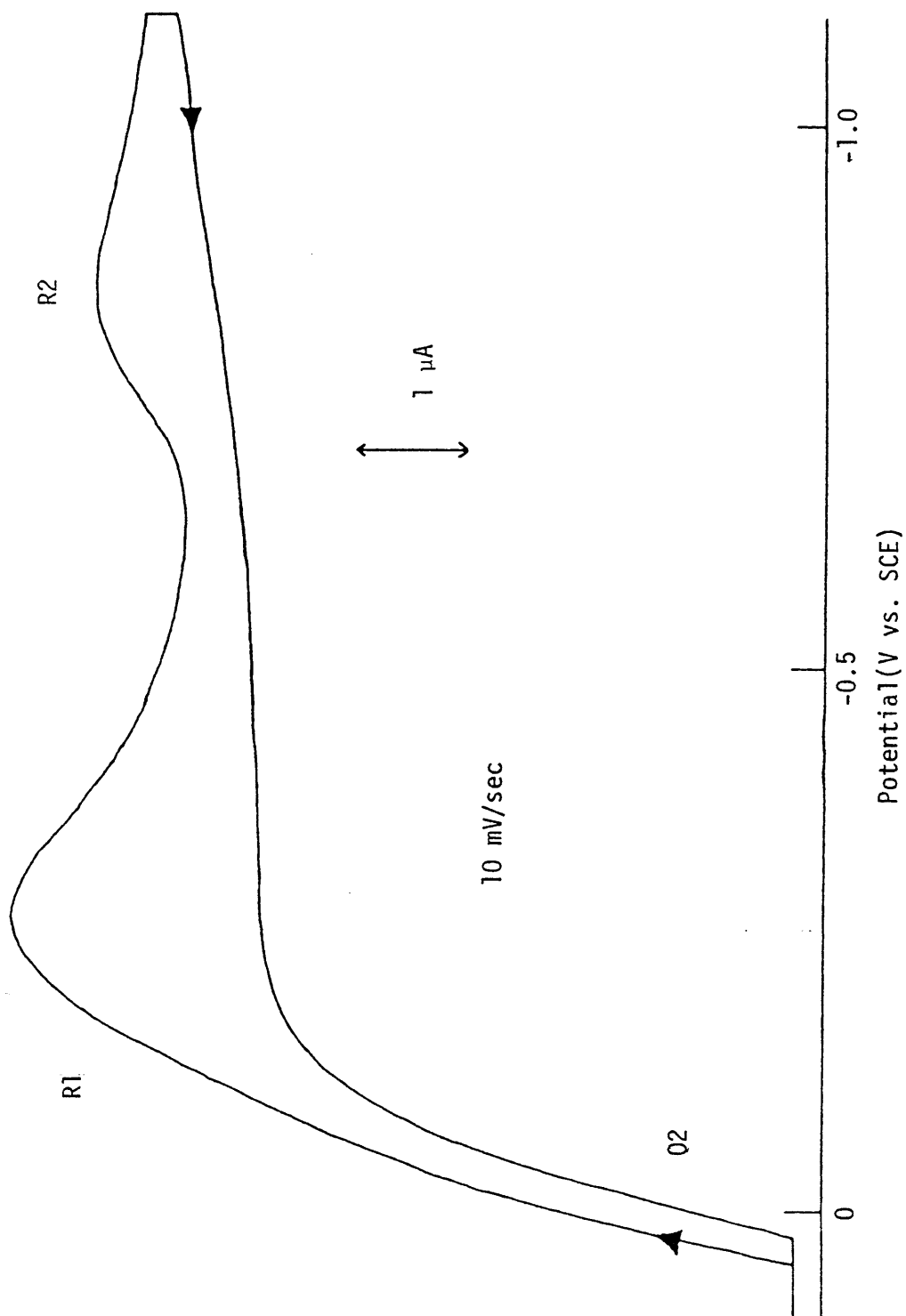


Figure 45: Cyclic Voltammogram of Mn(SALDCDA) in Pyridine.

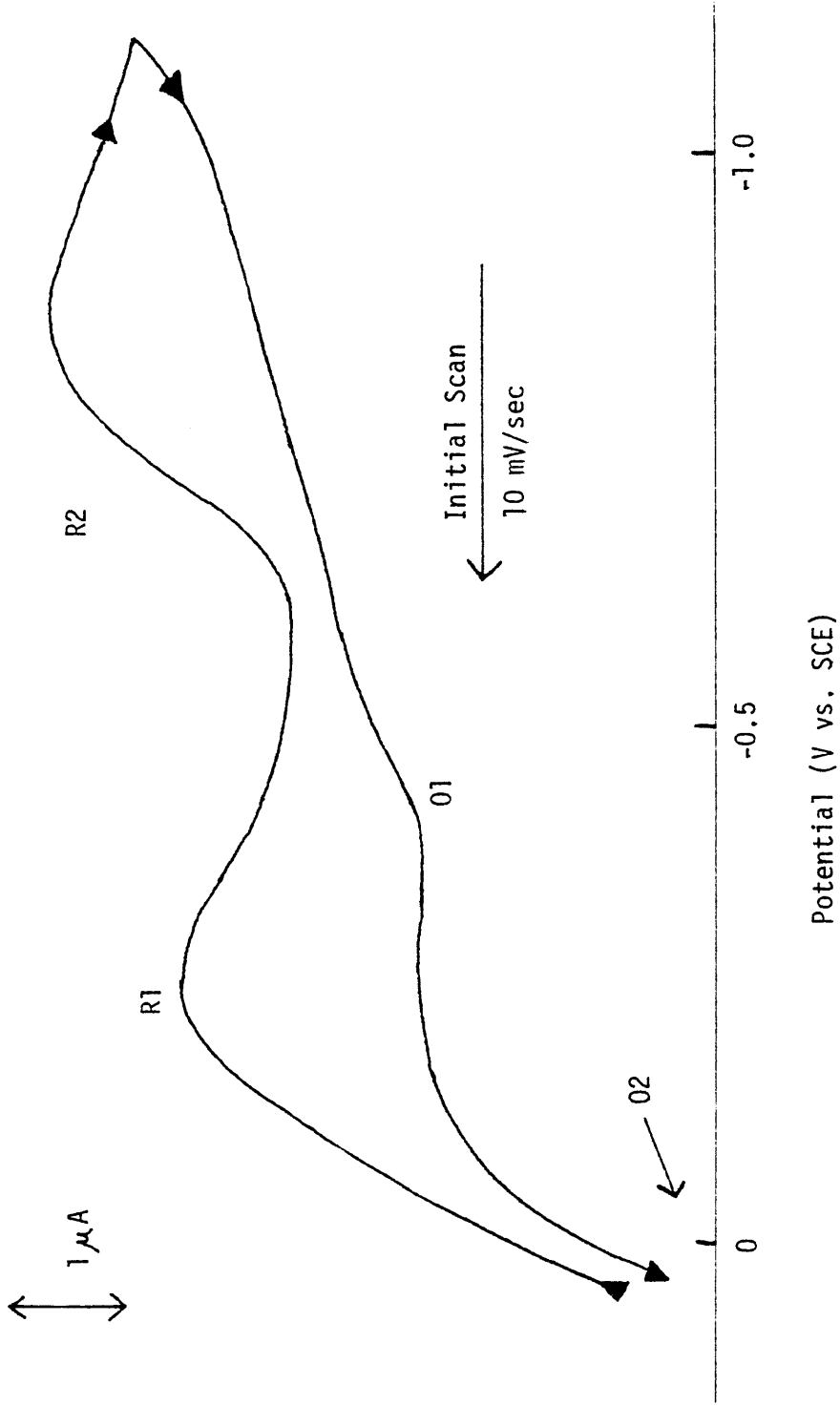


Figure 46. Second Oxidation Peak for Mn(SALDCDA).

loss of solvent and subsequent polymerization of this species is slow, it would appear in a scan initiated immediately after its formation.

An attempt was made to investigate the redox properties of the oxygenated  $[\text{Mn}(\text{SALC}_n)]_2\text{O}$  and  $[\text{Mn}(\text{SALC}_n)]_2\text{O}_2$  complexes, but they proved too insoluble for study in either solvent.

#### 4. Summary

Although this study of the electrochemistry of these complexes did not provide  $E^\circ$  values, in most cases, for comparison with kinetic parameters, the work did provide some interesting results. Extremely quasireversible reactions in pyridine were found for the bi- and tridentate complexes, which were difficult to interpret alone. However, coupled chemical reactions believed to be due to coordination of solvent were found to occur in DMSO, providing a basis for slow electron transfer in both solvents. The short chain XSALEN tetradentate complexes were unremarkable in demonstrating normal quasireversible behavior, but the long chain  $\text{SALC}_n$  complexes exhibited nearly irreversible behavior, believed to be due to polymerization effects, and a coupled chemical reaction, again possibly due to solvent coordination, for the longest chain ( $\text{C}_{10}$ ) complex.

### OXYGENATION KINETICS

#### 1. General Comments

A spectrophotometric kinetic study of reactions of manganese complexes with  $\text{O}_2$  is limited experimentally by a number of factors inherent to the system. The first of these is the low solubility of  $\text{O}_2$

in the various solvents employed. Unlike reactions such as ligand exchanges or hydrolyses, where the concentrations of reacting species can usually be pushed up into the molar range, here we have a maximum concentration of one of the reactants of  $\sim 10$  mM. To study the reaction under pseudo order conditions, i.e. at least a tenfold excess of  $O_2$ , the maximum concentration of complex allowable is 1 mM. This immediately rules out studying the reaction using d-d transitions because of their low intensity. The upper limit for observation is thus  $\sim 400$  nm, where the intensity of the charge-transfer or intraligand transitions becomes significant. Lower limits on the region of study are dictated by the solvent cutoff (260 nm for DMSO, 325 for pyridine, and 285 for toluene). Scans in pyridine were therefore always from 325 to 400 nm. In DMSO, normal limits were 275 and 350 nm, but on occasion, when a larger relative spectral change was occurring at a longer wavelength, the range for pyridine was used. Toluene was only used for the study with  $Mn(5-NO_2SALDPT)$ , which has an intense peak at  $\sim 380$  nm, and the 325-400 nm range was used here. Instrumental limits also determined these ranges since the lower and upper cutoffs for the tungsten lamp with a UV filter were 325 and 400 nm, respectively, and the upper limit for the deuterium lamp was 350 nm. A 75 nm range was convenient for calibration of the recorder.

The scan rates used were determined arbitrarily to provide a large number of spectral points without having overlap of the pen traces. The entire range of scan rates (0.1-20 nm/sec) was employed due to the large differences in rates of reaction of the various complexes. The choice

of absorbance range was determined by both the wavelength range being used and the spectral characteristics of the complex (and its reaction product) in that range. In a number of cases, parts of the spectra with high absolute absorbances were pushed to flatlines on top of the chart paper to study an area with a high relative absorbance change.

Temperature limits were rather restricted but wide enough in most cases for activation parameters to be calculated. The lower limits were determined by either the solvent (DMSO) or the water bath freezing. Less common was the reaction slowing to such an extent that spectra overlapped at the slowest scan speed. The upper limits on temperature were determined by decomposition of the complex, for the least stable ones, or by the reaction becoming too fast to follow. Thermal decomposition of most complexes was usually very fast when it occurred, and could be recognized in most cases by a rapid decrease in absorbance across the entire spectrum.

The Clark cell ( $O_2$  electrode) work also had some experimental problems, but fewer than the spectral work. Decomposition did not seem to be a problem, i.e. clean kinetics were obtained in most cases. This was true even though most of the complex solutions darkened markedly before the aliquot of oxygenated solution was injected. This was obviously due to reaction with unpurged  $O_2$ , but apparently this reaction removed only a fraction of the complex, since a drastic loss would show up as curved kinetic plots, because of loss of pseudo-order conditions. The very low solubility of the  $Mn(SALC_n)$  complexes in DMSO prevented the determination of the order of the reaction with respect to  $O_2$  in DMSO,

since the concentration of  $O_2$  ( $<0.1x[\text{complex}]$ ) was too low to sense with reasonable precision. Non- pseudo-order conditions i.e., higher concentrations of  $O_2$ , could not be used because calculations on such data would require the complex concentration to be known.

A final note should be made on the precision and accuracy of the data from the spectrophotometric runs. The precision was estimated by simply performing duplicate runs. The difference between the two calculated pseudo-first order rate constants was usually less than 10%. The accuracy of the second-order rate constants is limited primarily by the values for  $O_2$  solubilities, which were found to vary by up to 50% in the literature.<sup>107</sup> Because  $O_2$  saturation conditions were the same for each run, however, this error would be constant. This would not affect  $E_a$  calculations, but would shift  $k$  and  $\Delta S^\ddagger$  values either consistently higher or lower than they actually are. However, if the  $O_2$  solubilities used are not in error by more than a factor of 2, then the  $\Delta S^\ddagger$  values will only be in error by 2 eu due to this factor. The rate constants, of course, will be in error to the same degree as the solubility value. The accuracy and precision of the  $E_a$  and  $\Delta S^\ddagger$  values are also affected by the temperature control. Measurements were taken using a calibrated thermocouple thermometer in the cell itself therefore temperatures were of  $\pm 0.1^\circ\text{C}$  accuracy, and were found not to vary more than  $0.2^\circ\text{C}$  over the course of a run. The results are also limited by the precision and accuracy of the absorbance and time measurements, but these were very reliable because of the spectrophotometer used in the study.

The only data to be extracted from the Clark electrode study was

the order of the reaction in  $O_2$ , therefore control of conditions was not as important. It should be noted, however, that the data collected was rather noisy, with fluctuations in current of  $\sim\pm 2nA$ . The high sensitivity of the electrode to outside sources of noise is due to the small currents being measured and the high impedance of the electrode.

## 2. Bidentate Complexes

Instability of the bidentate complexes at even room temperature severely limited the amount of data that could be gathered on their reactions with  $O_2$ . Data in DMSO is particularly sparse since the complexes decompose at  $\sim 23^\circ C$ , and DMSO freezes at  $18^\circ C$ . A number of important points, however, can be drawn. First, the reaction was found to be first order in  $O_2$ . The Clark data plotted as current vs. time, with a residual background current of  $\sim 5nA$  at zero concentration of  $O_2$  subtracted out, shows a decay with a constant half-life, (Figure 47) and replotting it in the form  $\ln i$  vs.  $t$  produces a relatively straight line (Figure 48). Second order plots of  $1/i$  vs.  $t$  are markedly curved. This is in agreement with the mechanism postulated for the uptake data since only one molecule of  $O_2$  is involved in the reaction. However, data on the order in complex is required before assignment of the slow step can be made.

The order in complex is the second useful piece of data from the study. A typical repetitive scan of an oxygenation is shown in Figure 49. It can be seen from the Figure that there are two steps in the uptake, an initial fast one which is over in  $\sim 1$  hour, and a slow second one which appears to continue for a much longer period of time. A plot

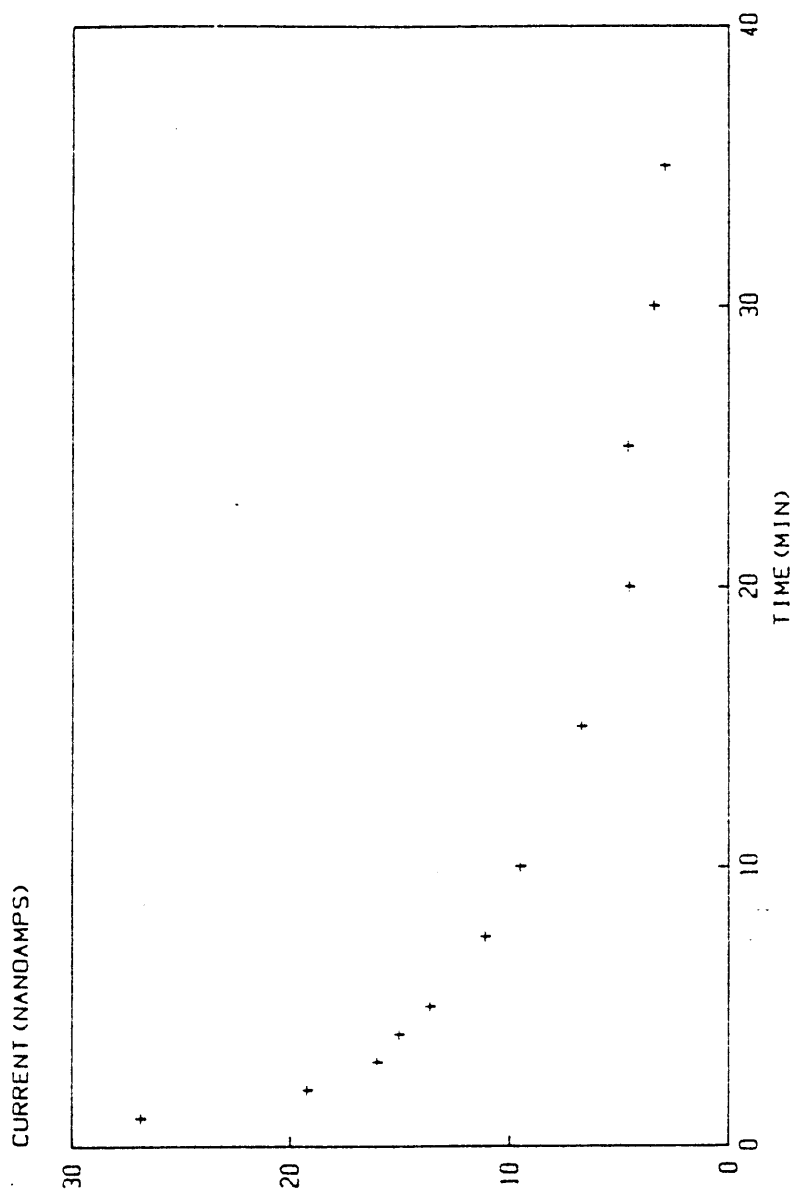


Figure 47: Clark Plot for Oxygenation of Mn(SALPMA)<sub>2</sub> in DMSO.

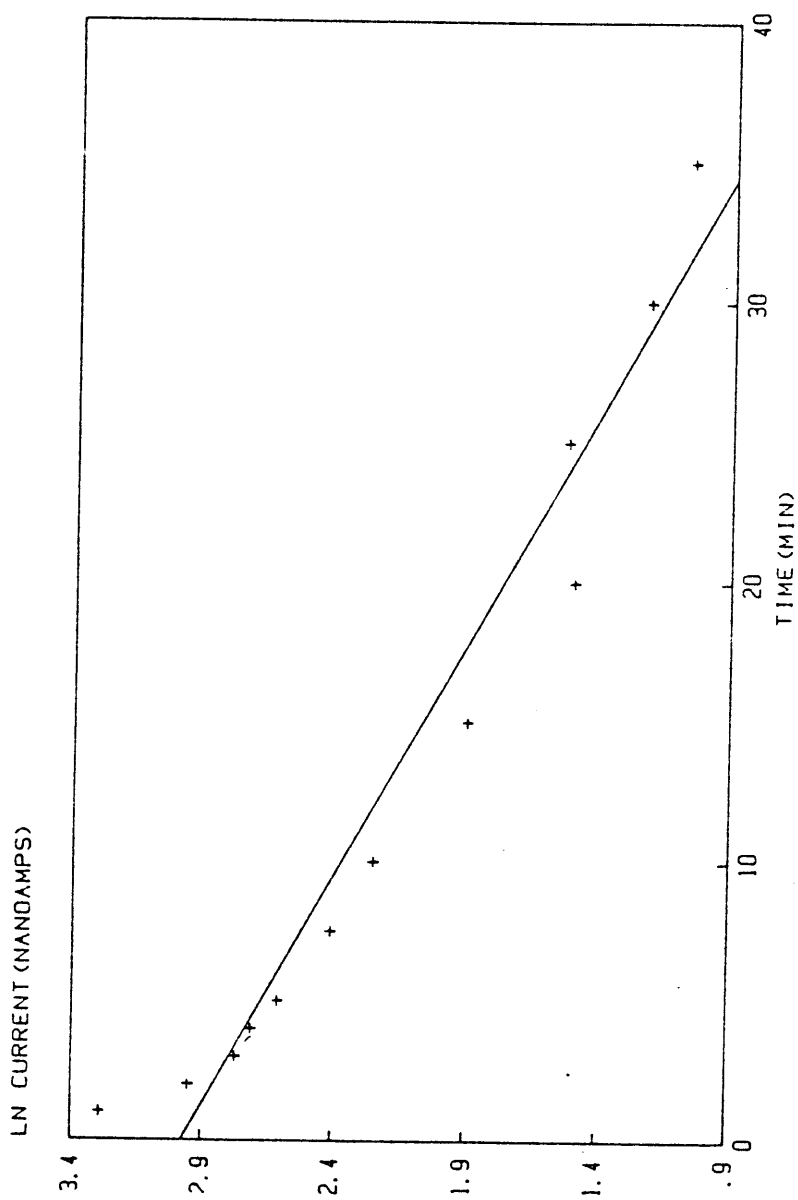


Figure 48: First Order Clark Plot for Oxygenation of  $\text{Mn}(\text{SALPMA})_2$  in  $\text{DMSO}$ .

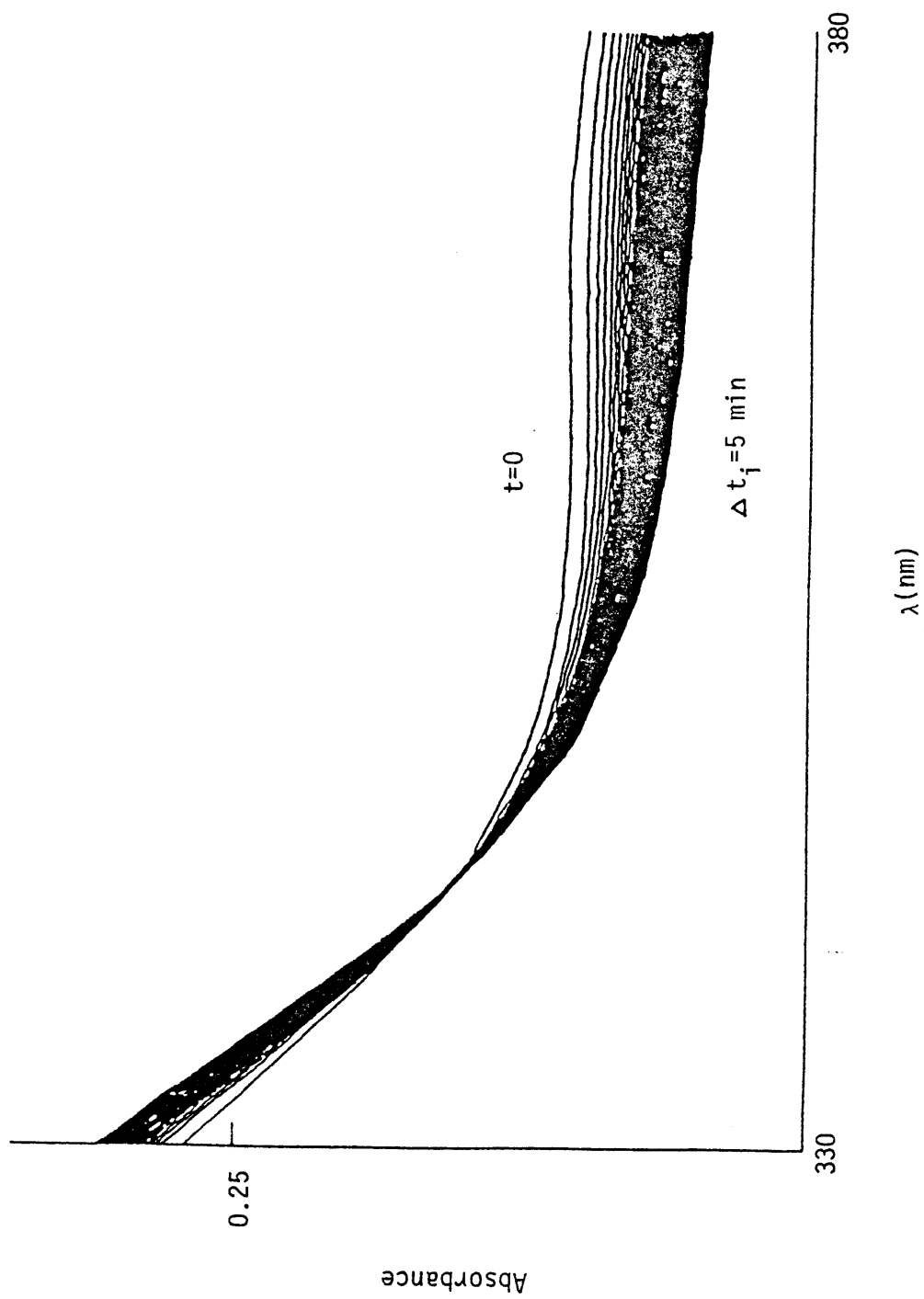
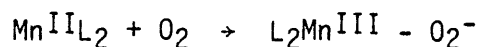


Figure 49: Repetitive Scan of Oxygenation of Mn(SALPMA)<sub>2</sub> in Pyridine.

of the absorbance change as a function of time should therefore resemble the oxygen uptake curve. It will differ slightly, however, since the uptake curve was a nonhomogeneous system, with solid-liquid and gas-liquid interfaces, as well as having a much higher concentration of complex. The slow second step causes some interference with calculations for the first. The choice of  $A_{t=\infty}$  is affected most, since the spectral changes never stop entirely. The choice of  $A_{t=\infty}$  was therefore a subjective "best guess", chosen at the approximate place where the first reaction seemed to end, and only the slow change due to the second step followed. Fortunately, the ratio of the rates (actually the rates of spectral change) is very different, so the relative error in  $A_{t=\infty}$  should not be great. There is also some error in the intermediate absorbances because the second reaction probably begins immediately after the first, but, again, this error should be minimal.

Plots of the various determinative functions give the best straight line for  $\ln|(A-A_{\infty})|$  vs. time (Figure 50). As with the Clark data, reasonably straight second order plots could only be obtained when values of  $A_{t=\infty}$  were chosen which were very questionable. The reaction is therefore first order in complex. Combining this result with the order in  $O_2$  (first) implies that the first step in the postulated reaction mechanism is the slow rate determining step:



and that the following steps are all relatively fast. The presence of one isobestic point in the runs provides evidence that only two species

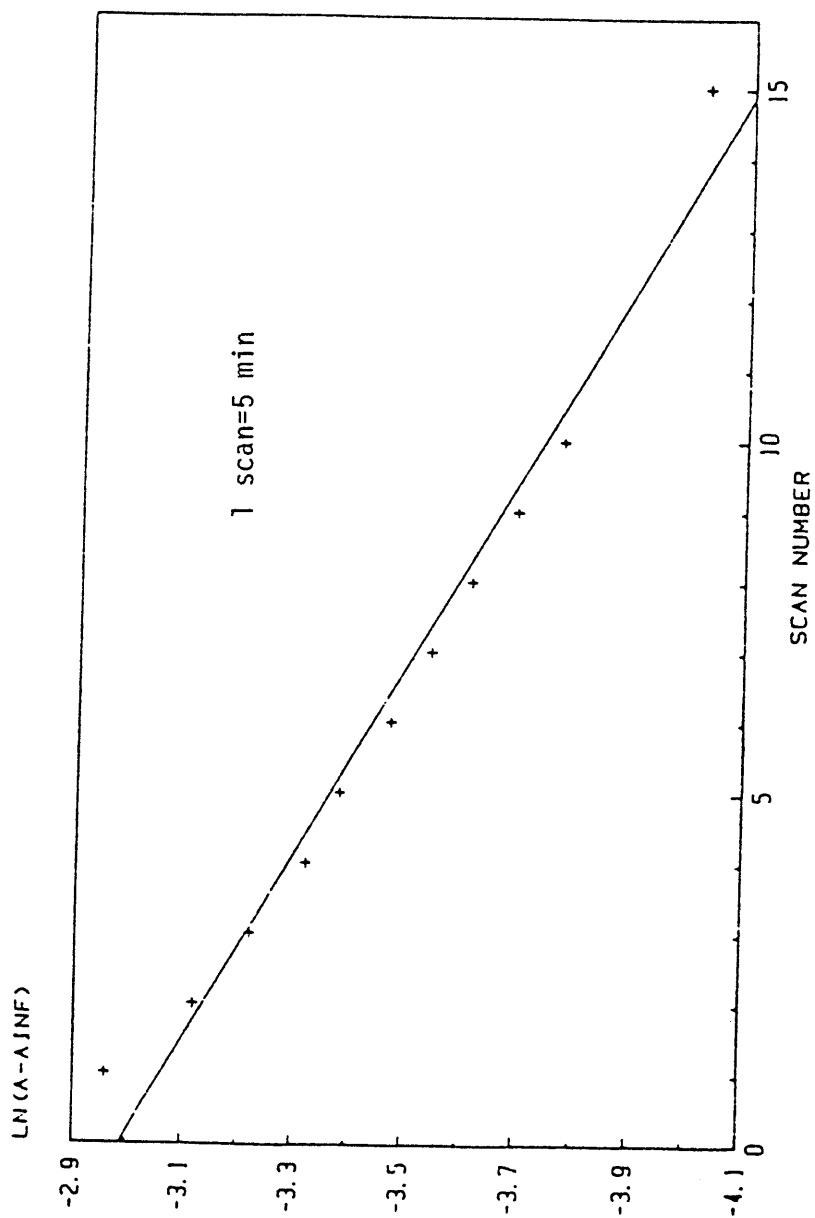


Figure 50: First Order Plot for Oxygenation of  $\text{Mn}(\text{SALPMA})_2$  in Pyridine.

are present in significant concentration at any time (or if more than two, all have identical  $\epsilon$ 's at that wavelength). This is usually taken to mean that no intermediates build up during the reaction, i.e. the two species are reactant and product.

Extending the study to other temperatures allows the calculation of activation parameters, at least in pyridine. In DMSO, the complexes decompose just above the freezing point of the solvent, and only one rate constant could be determined for each complex. Rate constants are determined from the slope of the  $\ln|(A-A_\infty)|$  plots via the simple relationship, slope =  $-k_{obs}$ . These pseudo-first order rate constants may be converted into actual second order rate constants by dividing by the "known" concentration of  $O_2$ , since the rate constant in the pseudo-order relationship, rate =  $k_{obs}[\text{complex}]^n$ , is actually  $k_{real} \times [O_2]$ . Activation parameters are calculated from the slope and intercept of an Arrhenius plot (Figure 51). The slope of the plot is  $-E_a/R$ , and the intercept is  $\ln k_0$ . The activation energy is therefore  $-\text{slope} \times R$ , and the activation entropy can be shown to be equal to  $2x(\ln k_0 - 30.4)$  if  $k_0$  is in  $M^{-1} \text{sec}^{-1}$ . Calculated second order rate constants and activation parameters are presented in Table X.

One point which should be noticed immediately is the large negative entropies of activation for both complexes. This means that the RDS involves a large increase in order. This is in perfect agreement with attack of a neutral  $O_2$  on a neutral tetrahedral molecule of complex to give a dipolar superoxo-complex. A decrease in entropy results from loss of freedom of motion of both reactants as well as solvent molecules

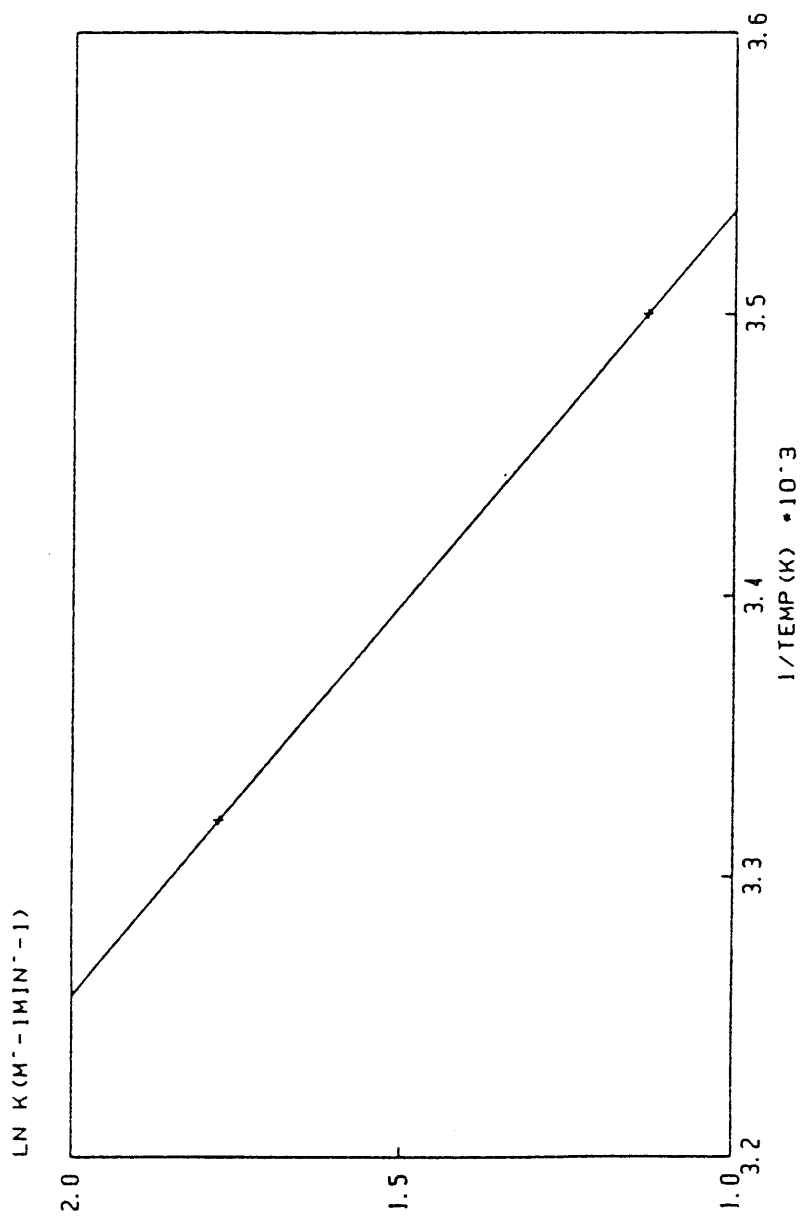


Figure 51: Arrhenius Plot for Oxygenation of  $\text{Mn}(\text{SALPMA})_2$  in Pyridine.

Table X. Kinetic Parameters for Oxygenation of Bidentate Complexes

<u>Complex</u>	<u>Solvent</u>	<u>T(°C.)</u>	<u>k(M<sup>-1</sup> min<sup>-1</sup>)</u>	<u>E<sub>a</sub> (kcal/mole)</u>	<u>ΔS<sup>‡</sup> (eu)</u>
Mn(SALPHA) <sub>2</sub>	Pyridine	13.0	3.1 (0.4)	7.1	-42
		27.7	5.9 (0.3)		
	DMSO	22.3	21 (2)		
Mn(SAL-4-Br-AML) <sub>2</sub>	Pyridine	10.1	11.3 (0.7)	8.8	-33
		24.7	24 (2)		
	DMSO	23.0	40 (4)		

[O<sub>2</sub>] = 4.8 × 10<sup>-3</sup> M(Pyridine), [O<sub>2</sub>] = 2.1 × 10<sup>-3</sup> M (DMSO)

The k values are averages with errors in parentheses.

which would be electrostricted by the dipolar product. If one considers the electrochemical data, which showed attack of solvent to give a stable  $\text{Mn}^{\text{III}}\text{L}_2\text{S}_2^+$  product of oxidation, it may be possible that a solvent molecule is pulled into the coordination sphere of the Mn in this step to stabilize the  $\text{Mn}^{\text{III}}$ . Although the attack of solvent was relatively slow after electrochemical oxidation, at least in DMSO, it may be sped up here since the superoxo-complex would be 5-coordinate, not a preferred coordination number for most metal ions in higher oxidation states. Attack of the remaining solvent molecule(s) in the following fast steps must occur, since the isobestic point implies that no intermediates build-up, and the "stable" final product is the disolvated species.

A second important conclusion may be drawn from the activation energies. If the kinetic results are to correlate with the electrochemical properties of the complexes, then  $\text{Mn}(\text{SALPMA})_2$  should oxygenate more easily than  $\text{Mn}(\text{SAL-4-BrANL})_2$  because its ligand is more electron-donating. This is indeed the case as seen in the  $E_a$  values, but we would also expect the absolute rate at a given temperature to be faster for  $\text{Mn}(\text{SALPMA})_2$ , which it is not. This would be true if the electron-donating ability of the substituent was the only effect it exerted on the reaction. This apparent anomaly can be explained by reexamination of the activation entropies. The value for  $\text{Mn}(\text{SALPMA})_2$  is seen to be 9 eu less favorable than that for  $\text{Mn}(\text{SAL-4-BrANL})_2$ . The only feasible reason for this would be the hindrance caused by the greater "apparent" steric bulk of the  $\phi\text{-CH}_2\text{-}$  group as compared to the  $\text{Br-}\phi\text{-}$

group. Free rotation about the methylene carbon would be hindered by the presence of the  $O_2^-$  ligand, leading to an extra source of loss of entropy in the RDS, and slowing the reaction down.

### 3. Tridentate Complexes

Although more tridentate complexes were prepared than bidentate ones, the number amenable to kinetic studies was still only two. Of the complexes that are solution  $O_2$ -sensitive, only  $Mn(SALAEF)_2$  and  $Mn(SALAMP)_2$  reacted quickly enough, whereas  $Mn(5-CISALAMP)_2$  was at least an order of magnitude slower, making repetitive spectral scans of its oxygenation, even at the instrument's slowest scan rate, overlapping traces useless for interpretation. The temperature range accessible to these two complexes was wider than that for the bidentates, so enough data was gathered for activation parameter calculations in both solvents.

The order in  $O_2$  was found to again be first (Figure 52). This was expected since the mechanism, at least in general, was postulated to be the same as for the bidentates, with only one molecule of  $O_2$  being involved. Other similarities were also found. First, a repetitive spectral scan (Figure 53) is again seen to contain two steps. However, with the tridentate complexes, the second step is so slow as to almost not interfere with the first. If similar reactions are occurring on the ligands, then relative uptake changes should be paralleled by relative spectral changes, which is seen here. Again, the  $A_{t=\infty}$  values chosen given good first order fits (Figure 54). This, of course, means that

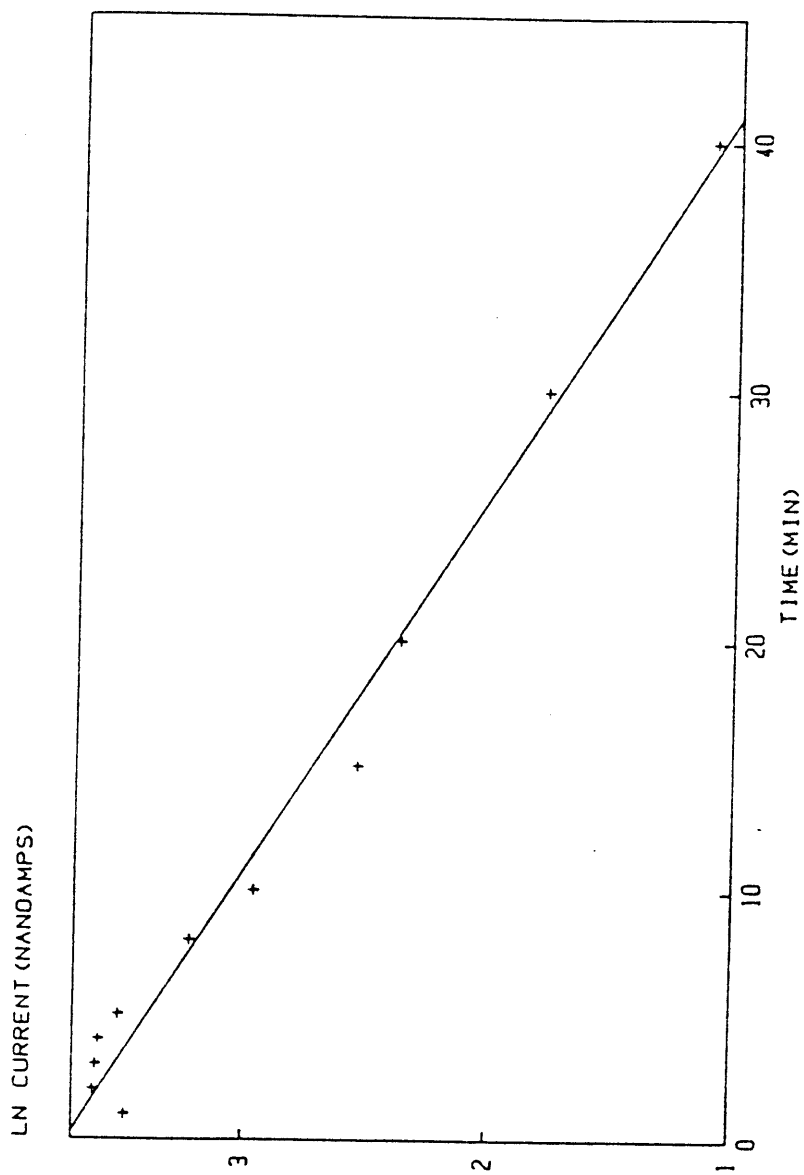


Figure 52: First Order Clark Plot for Oxygenation of  $\text{Mn}(\text{SALAEPP})_2$  in DMSO.

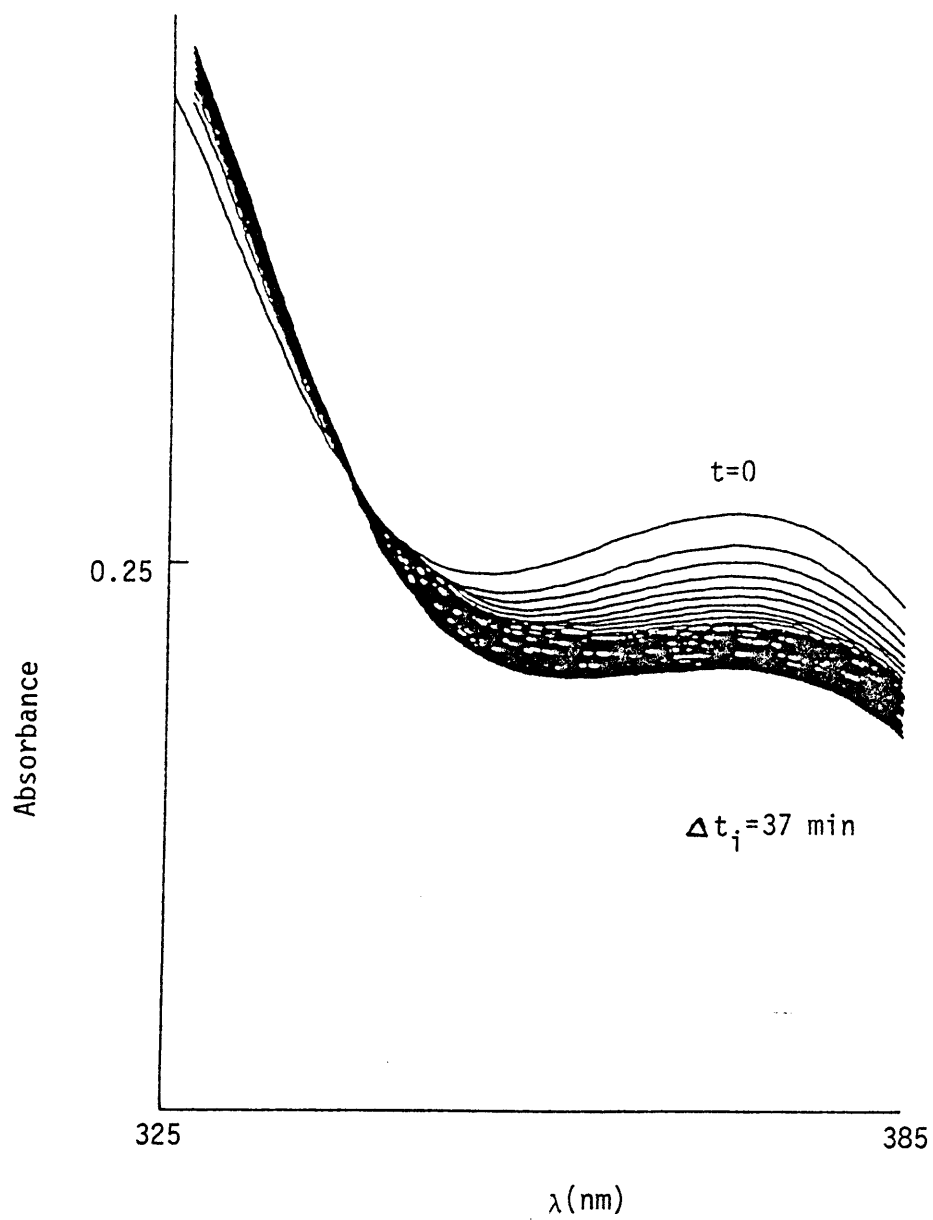


Figure 53: Repetitive Scan of Oxygenation of Mn(SALAMP)<sub>2</sub> in Pyridine.

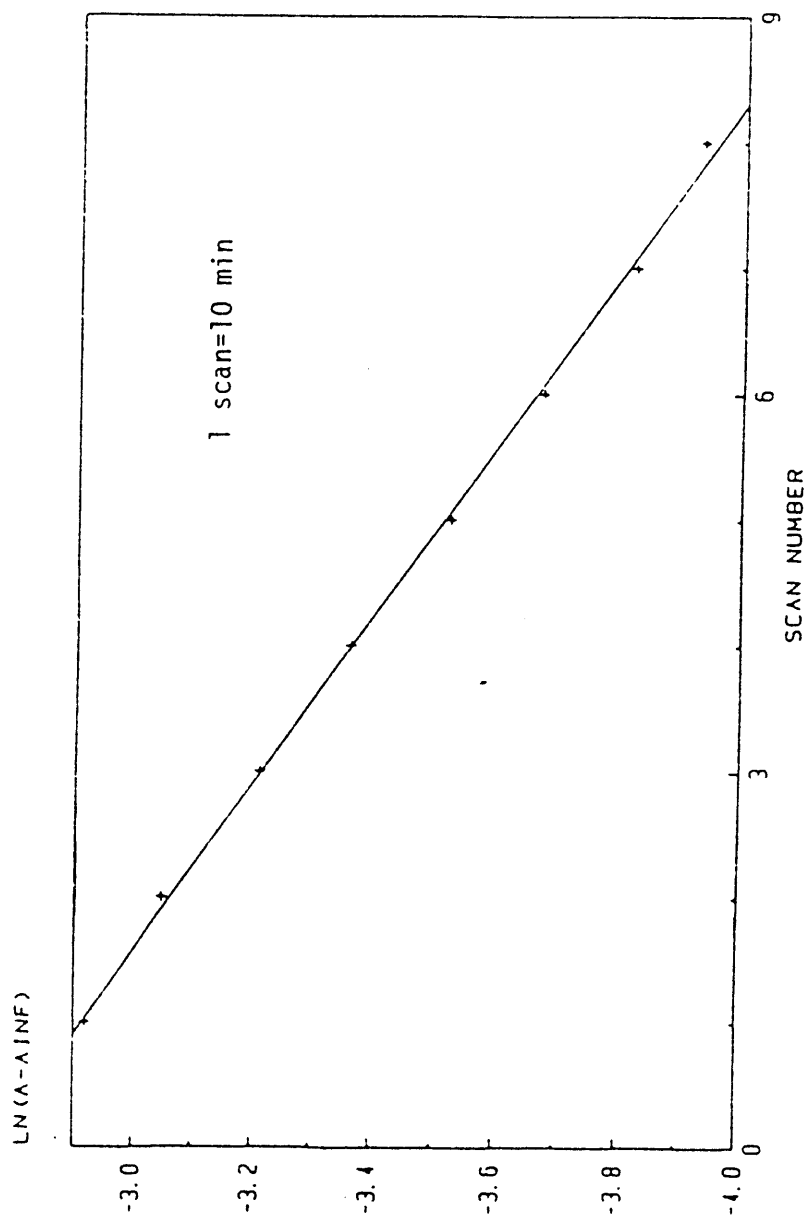
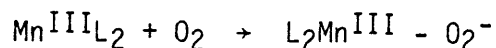


Figure 54: First Order Plot for Oxygenation of  $\text{Mn}(\text{SALAMP})_2$  in DMSO

the reaction is first order in complex and that the RDS is:



The presence of an isobestic point in the scans is again supportive evidence for this assignment. However, calculation of activation parameters leads us to the conclusion that the reaction is more complex.

As can be seen in Table XI, the  $E_a$  and  $\Delta S^\ddagger$  values for  $\text{Mn}(\text{SALAMP})_2$  are similar to those for the bidentate complexes in pyridine. The activation energy and  $k$  values may be compared to those of  $\text{Mn}(\text{SALPMA})_2$ , and are seen to be higher and lower, respectively. This would be expected if  $\text{SALAMP}^-$  acted only as a bidentate ligand, i.e. had a dangling pyridine group, and  $\text{Mn}(\text{SALAMP})_2$  was tetrahedral, since a pyridylmethyl-group is more electron-withdrawing than a benzyl group and has nearly the same steric effect. Also, the rate constants at 22°C in DMSO are in the correct order, i.e. lower for  $\text{Mn}(\text{SALAMP})_2$ . However, there are also an  $E_a$  and a  $\Delta S^\ddagger$  value in DMSO which should be explained. If the tetrahedral coordination theory is correct, then the lower  $E_a$  in pyridine is most easily explainable, as were some of the electrochemical results, by the higher dielectric constant of DMSO. A more polar solvent will stabilize the dipolar superoxo-complex, as it may have done for the simple  $\text{MnL}_2^+$  cation. The smaller loss of entropy in DMSO may be due to partial immobilization of the dangling pyridyl group by electrostatic interaction with DMSO before attack of  $\text{O}_2$ . In this case this would be due to the larger dipole moment of DMSO (4.0D vs. 2.2D for pyridine) interacting more strongly with the pyridyl dipole.

Table XI. Kinetic Parameters for Oxygenation of Tridentate Complexes

<u>Mn(SALAMP)<sub>2</sub></u>		
<u>Solvent</u>	<u>T(°C)</u>	<u>k(M<sup>-1</sup>min<sup>-1</sup>)</u>
Pyridine	17.5	0.40 (0.03)
	28.0	0.79 (0.07)
DMSO	22.2	9.4 (0.7)
	31.1	14.2 (1.3)

Activation Energy = 8.2 Kcal/mole (DMSO)  
11.3 Kcal/mole (Pyridine)

Activation Entropy = -36 eu (DMSO)  
-32 eu (Pyridine)

<u>Mn(SALAEF)<sub>2</sub></u>		
<u>Solvent</u>	<u>T(°C)</u>	<u>k(M<sup>-1</sup>min<sup>-1</sup>)</u>
DMSO	22.5	12.6 (1.5)
	28.2	34 (3)
	36.3	80 (4)
Pyridine	19.1	0.46 (0.04)
	23.1	0.80 (0.03)

Activation Energy = 24 Kcal/mole (DMSO)  
27 (Pyridine)

Activation Entropy = 18 eu (DMSO)  
24 eu (Pyridine)

The k values are averages with errors in parentheses.

$\text{Mn}(\text{SALAMP})_2$  seems to raise an unanswerable question; how can a compound be nonelectrooxidizable, yet  $\text{O}_2$ -sensitive even in the solid state? It may be possible that the redox potential has been pushed out past the solvent limit, but larger  $E_a$  values for oxygenation would then be expected if the complex was bidentate and large effects on electrochemical properties due to substituents are paralleled by changes in oxygenation kinetics. A pentadentate complex,  $\text{Mn}(5\text{-NO}_2\text{SALAEP})_2$  had its redox potential shifted outside the solvent oxidation limit, but it was also non-reactive towards  $\text{O}_2$ .

Unfortunately, the electrochemistry of the  $\text{Mn}(\text{XSALAEP})_2$  complexes suggested that two molecules of solvent were attached to the most easily oxidizable form of the complex (at least for the AEP-containing complexes). An alternative explanation must therefore be advanced for the situation where the initial complex is of the form  $\text{MnL}_2\text{S}_2$ , and no direct correlation can be made with the bidentate mechanism. The difference in  $E_a$ 's between solvents, if this theory is correct, may be attributable to loss of solvent before, or simultaneously with, attack of  $\text{O}_2$ , in addition to a simple dielectric effect, i.e. that favoring the reaction in DMSO. Pyridine is a better ligand than DMSO (higher in the spectrochemical series and forms more stable complexes) for  $\text{Mn}(\text{II})$  complexes. It should therefore be more difficult for  $\text{O}_2$  to displace it, i.e. the activation energy should be higher. The difference in  $\Delta S^\ddagger$  between the two solvents may be due to a number of factors. One is the aforementioned restriction of the pyridyl group by DMSO. Another is the relative degree of loss of coordinated solvent in the RDS. If, as the

O<sub>2</sub> attacks, both DMSO's are released to a greater extent than the pyridines, then the decrease in entropy due to formation of the dipolar bimolecular activated complex would be less. However, these two factors would have to be balanced with effects on  $\Delta S^\ddagger$  of solvent electrostriction, which is greater for DMSO, and also the inward motion of a dangling pyridine group on one ligand to replace the leaving solvent not replaced by O<sub>2</sub>.

Oxygenation of MnL<sub>2</sub>S<sub>2</sub> where L = SALAEP<sup>-</sup> has also been investigated. From Table XI, it may be seen that a number of significant differences exist between this reaction and that for Mn(SALAMP)<sub>2</sub>. First, although the reactions have similar rate constants at ambient temperatures, the activation energies are ~3x larger for Mn(SALAEP)<sub>2</sub> in both solvents. As mentioned in the O<sub>2</sub> uptake section, this may be due to the increased flexibility of the two carbon chain vs. the one carbon chain connecting the pyridyl group. The SALAEP<sup>-</sup> ligand may be geometrically able to coordinate the Mn much better than SALAMP<sup>-</sup>, therefore O<sub>2</sub> must compete with both solvent and ligand to attack the metal. The difference between E<sub>a</sub>'s in the two solvents for the reaction of Mn(SALAEP)<sub>2</sub> would again be due to the better coordinating power of pyridine making it more difficult to remove from the Mn.

The  $\Delta S^\ddagger$  values for Mn(SALAEP)<sub>2</sub> are also different. Instead of being large and negative, they are moderate and positive. A substantial amount of randomness must therefore be produced in the RDS. One good explanation for this would be complete loss of both coordinated solvent molecules as O<sub>2</sub> attacked. This would produce three free molecules from

two, and if the released molecules of solvent were involved in the solvent sheath, this would reduce the loss of entropy due to uncoordinated solvent mobility loss. Again, this would be partly counterbalanced by coordination of the dangling pyridines. Further increase in  $\Delta S^\ddagger$  may be contributed to by the change in stereochemistry in the reaction. The Mn(II) probably has trans solvent molecules (symmetrically favored) but the final product should have meridional ligand coordination because of the limited flexibility of the ligands. This change would require breaking, at least partially, some metal-ligand bonds, thus increasing  $\Delta S^\ddagger$ .

#### 4. Tetradentate Complexes

The kinetics of the reactions of Mn(XSALEN) complexes and Mn(SALC<sub>n</sub>) (n = 6, 7, 8, 10) complexes with O<sub>2</sub> are as different as their electrochemical properties. Mn(XSALEN) exhibits simple kinetic behavior, although the explanations of the activation parameters are not straightforward. Mn(SALC<sub>n</sub>), on the other hand, oxygenates in a manner that does not conform to any simple kinetic treatment, but an explanation for this behavior is simpler.

##### a) Mn(XSALEN)

A typical repetitive scan for Mn(XSALEN) (X = 3-MeO, H) in DMSO is illustrated in Figure 55. Mn(5-ClSALEN) oxidized too slowly for convenient study. Two differences are immediately apparent between this Figure and those of the corresponding bi- and tridentate complexes. First, there are no isobestic points present, as absorption increases

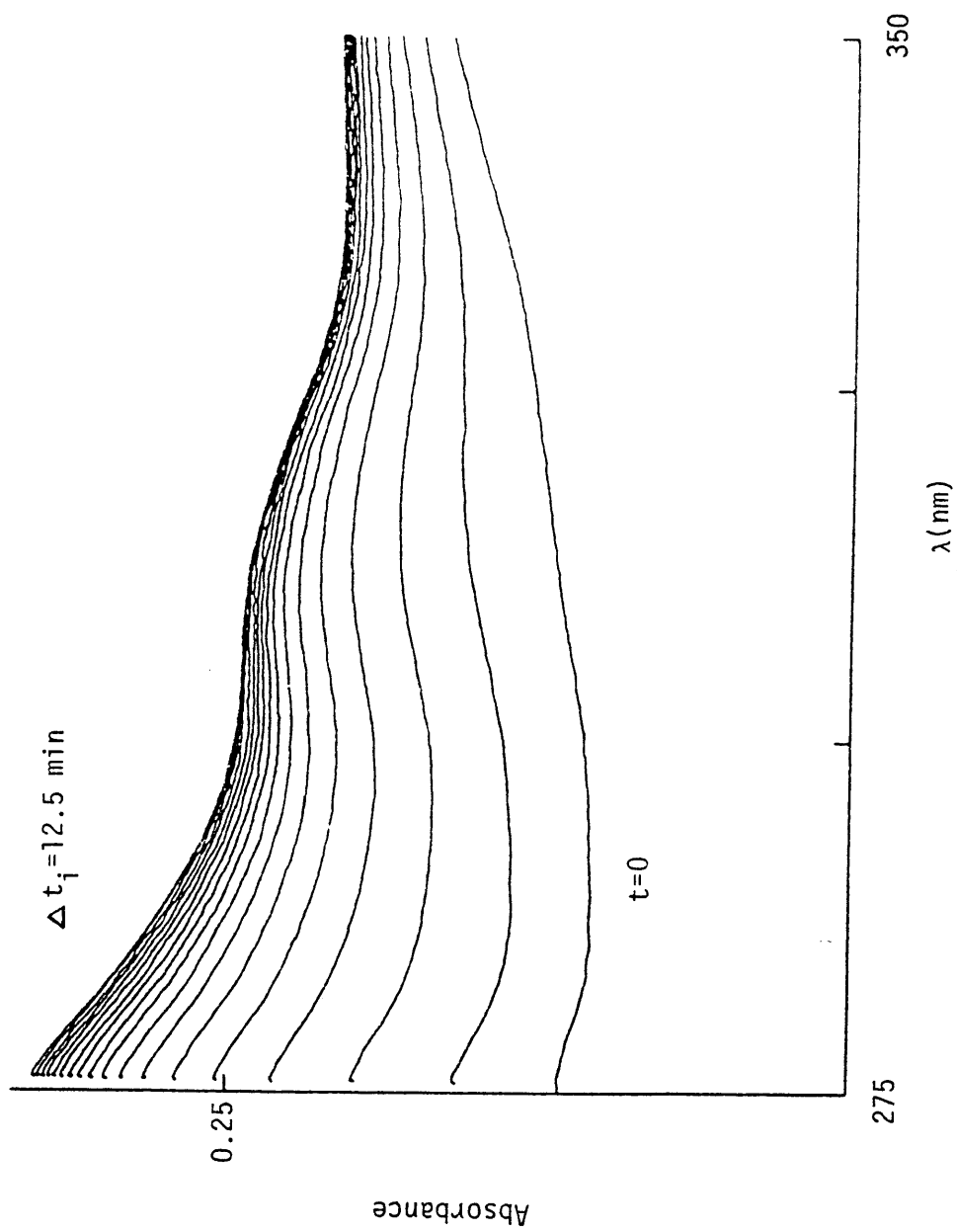


Figure 55: Repetitive Scan of Oxygenation of Mn(SALEN) in DMSO.

monotonically across the entire spectrum. This does not necessarily mean that there is any buildup of intermediates. This difference was earlier attributed to the fact that  $O_2$  is attached to Mn in the product for the tetradentates but not for the bi- and tridentates. The second thing is that there seems to be no slow second step in the reaction, at least not the type found for compounds of other denticities. From the uptake data, we know that there is a second step, but that it involves further oxidation of Mn, and there is an incubation period between the two. At higher temperatures the spectral changes due to the second step become visible, (Figure 56) an effect also seen in pyridine at lower temperatures (Figure 57). This effect occurs at lower temperatures for Mn(3-MeOSALEN) in either solvent. This is undoubtedly due to the strong electron-donating ability of the methoxy group. There are two isobestic points for this reaction. This is fortunate, since the spectral changes are of about the same extent as the first step's. If there were no isobestic points, it would be difficult to separate the two steps for rate constant calculations.

It is interesting to note that there is no incubation period apparent in Figure 56. This may be due to one of two causes which may be operating in conjunction. The increased temperature may have caused the second reaction to accelerate to such an extent that no incubation is required. This is plausible since the reactions at room temperature or lower come to a temporary stop after one step. A second explanation may involve the relative concentrations used in the two studies. The uptakes were performed at low temperature with concentrated solutions or

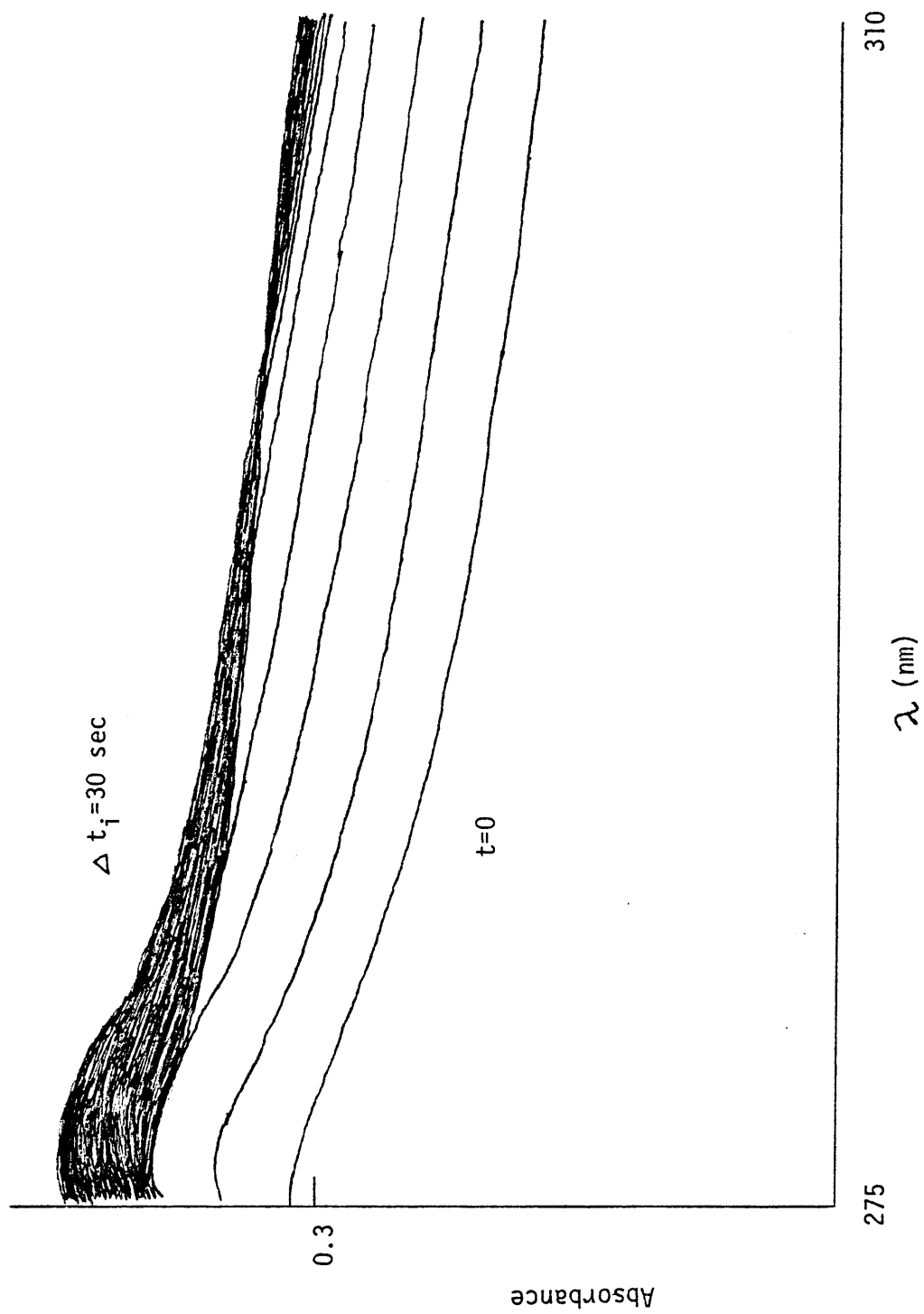


Figure 56. High Temperature Repetitive Scan of Oxygenation of Mn(SALEN) in DMSO.

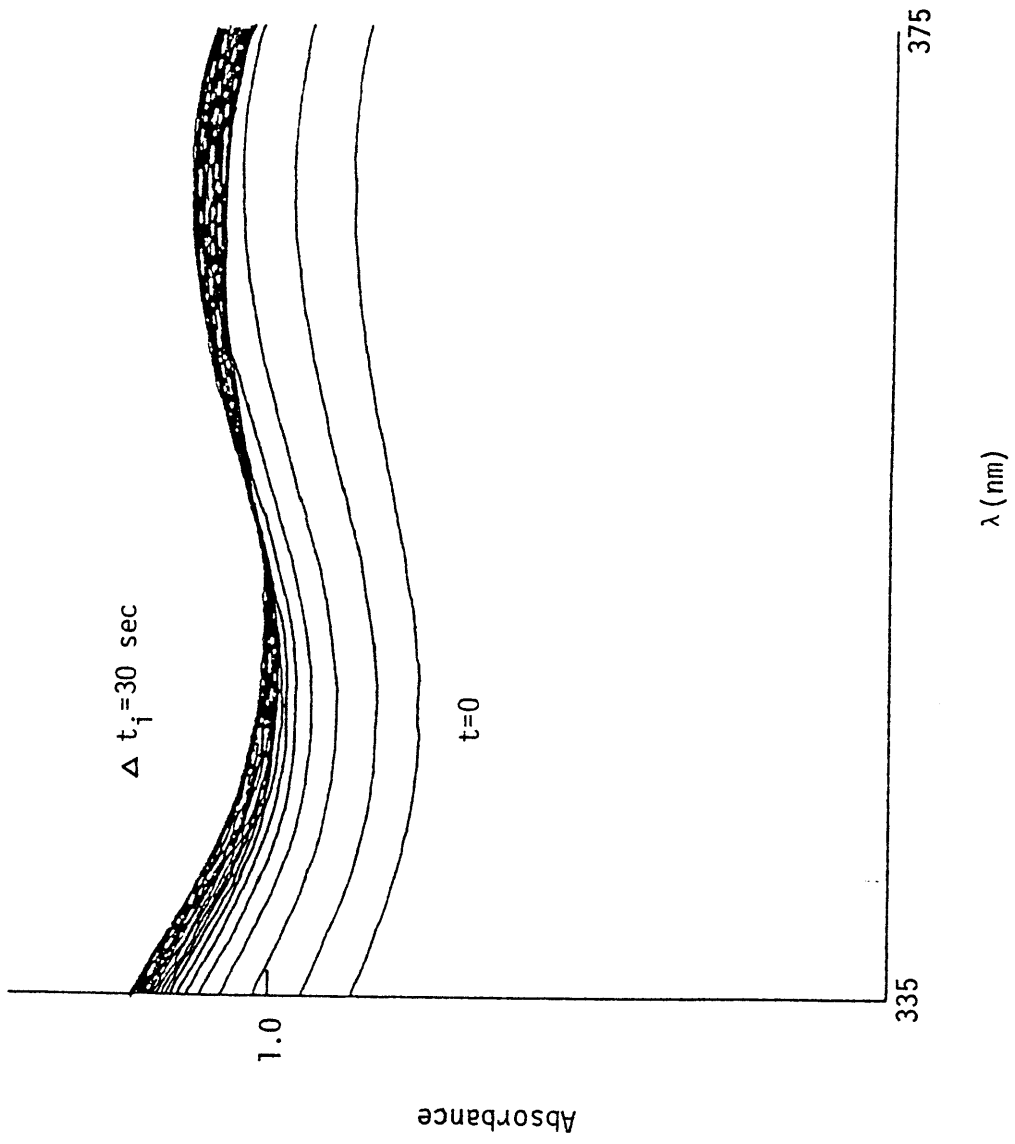
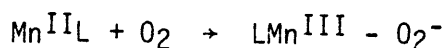


Figure 57: Repetitive Scan of Oxygenation of Mn(SALEN) in Pyridine.

suspensions where some degree of agglomeration may have occurred. The incubation period may have been due to time required for O<sub>2</sub> to penetrate the matrix of the first product. The kinetic studies, however, were performed at submillimolar concentrations, where primarily monomeric complex and product should be present in solution.

Another interesting fact to arise from the kinetic study was that the tetradentate ligands, or at least 3-MeOSALEN<sup>2-</sup>, are oxidizable in the complex. A very slow scan of the reaction of that complex shows a very fast initial step, a slower second step, and a still slower third step (Figure 58). Again, the electron-donating MeO group is activating the complex, in this case the ligand itself, towards oxidation. One difference between the results for this third step and the second step for complexes of different denticity is that the isobestic points are different between steps two and three. An explanation for this must wait, however, for isolation of the various oxidized-ligand complexes.

The Clark electrode data for the reactions of the XSALEN complexes with O<sub>2</sub> show that the first step is first order in O<sub>2</sub> (Figure 59). Again, this is not surprising because the postulated stoichiometry is 4 manganese to 1 O<sub>2</sub>. Numerical analysis of the spectral changes for the first step reveals that it is also first order in complex (Figure 60). No attempt was made to study the kinetics of the second step. The RDS for the first step must be the same as that for bi- and tridentates, i.e.:



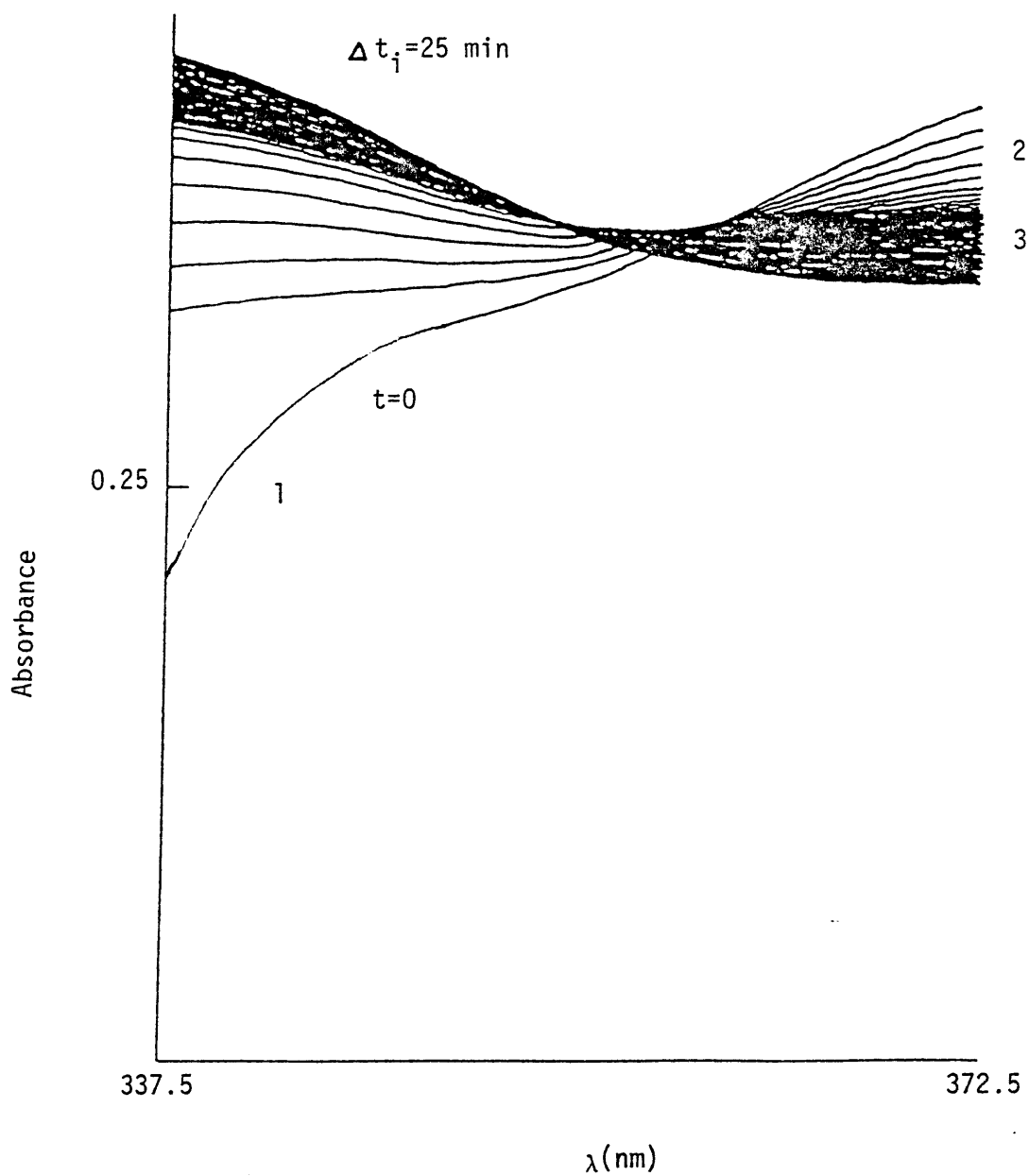


Figure 58: Slow Repetitive Scan of Oxygenation of Mn(3-MeOSALEN) in Pyridine.

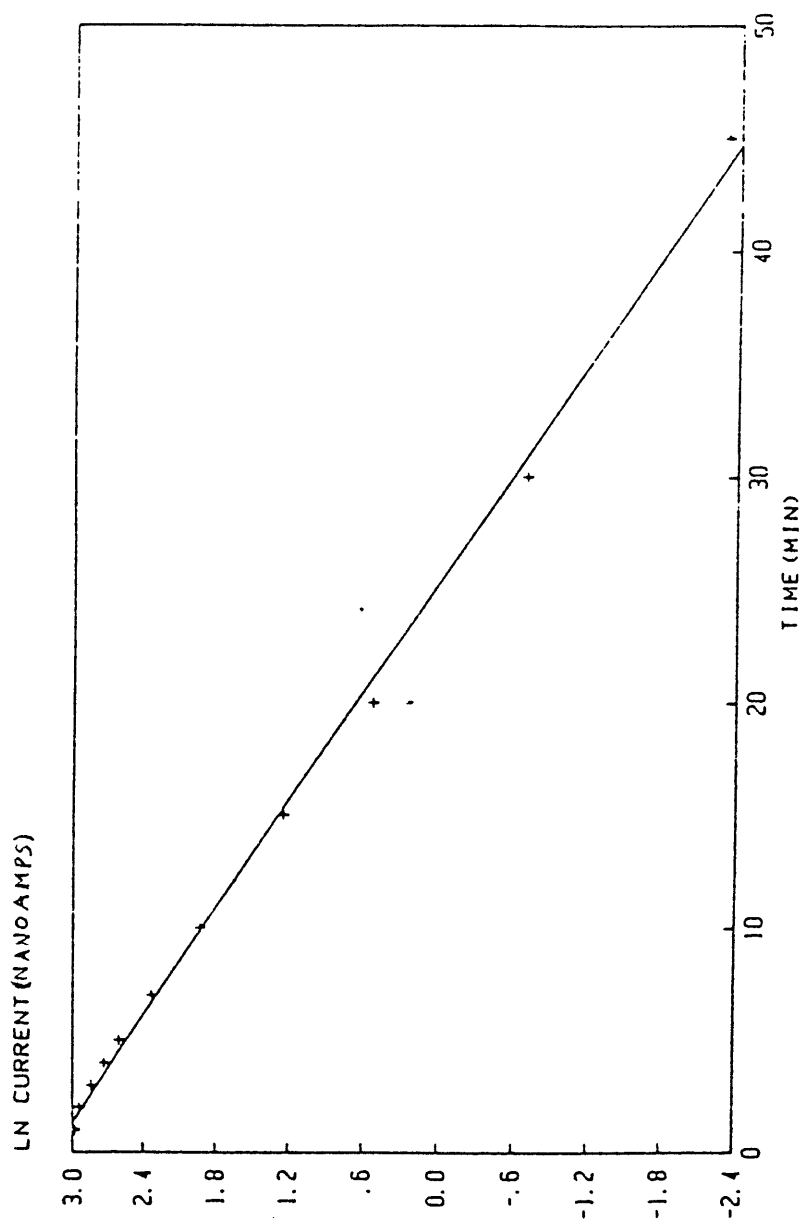


Figure 59: First Order Clark Plot for Oxygenation of Mn(SALEN) in DMSO.

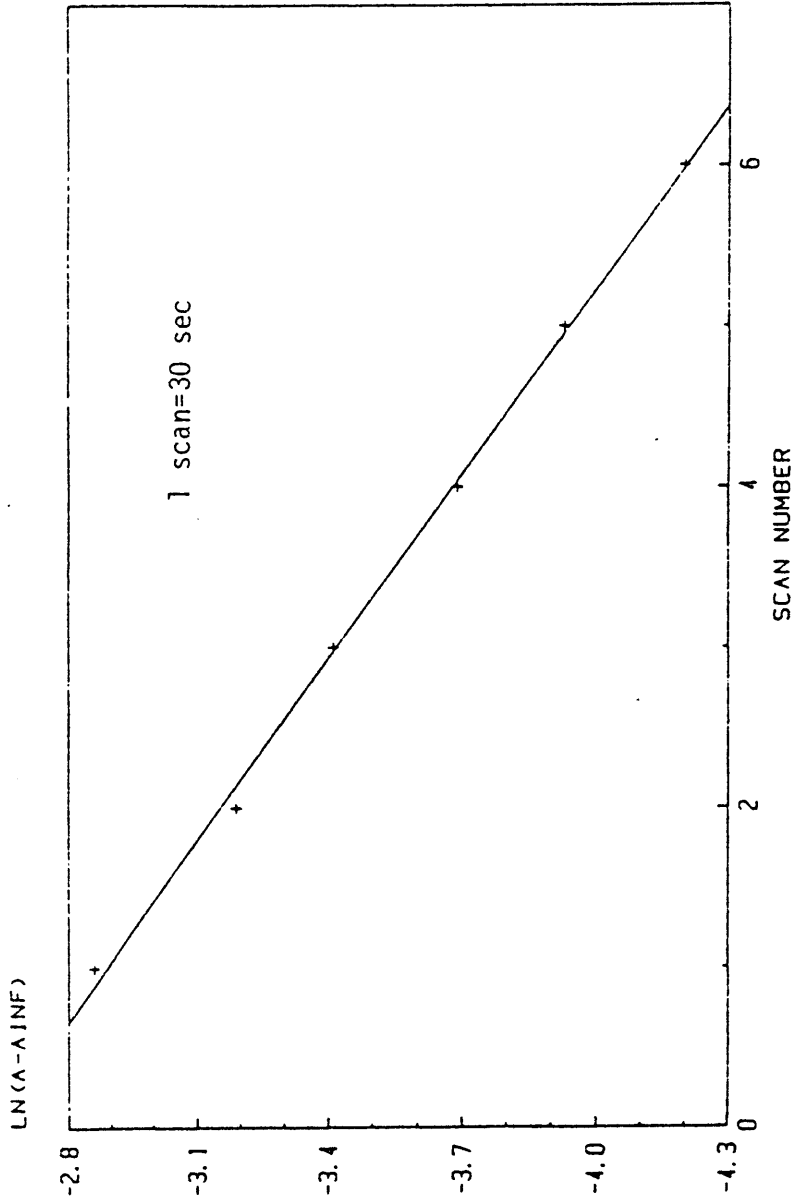


Figure 60: First Order Plot for Oxygenation of Mn(3-MeOSALEN) in Pyridine.

However, the rate constants and activation parameters (Table XII) again show some complexity in the system. The vastly greater rate constants for Mn(3-MeOSALEN) were expected because of the activating MeO group. Also, if the theory of solvent removal being involved in the RDS is correct, then the lower  $E_a$  values in DMSO are also no surprise, although the differences between solvents are substantially larger than for the tridentates. With these SALEN complexes, however, there is no potential donor besides the solvent for the trans coordination positions, and the difference may be magnified.

Explaining the activation entropies is again difficult. Two consistent shifts can be seen on changing solvent and substituent. Because the MeO-group is not completely sterically isolated in the ligand (vide supra the electrochemistry), it may be interacting with solvent and  $O_2$ . Regardless, its presence lowers  $\Delta S^\ddagger$  by  $\sim 10$  eu in both solvents. Conversely, on changing from DMSO to pyridine,  $\Delta S^\ddagger$  increases by  $\sim 40$  eu. The effect of the MeO-group on the degree of coordination of solvent is undoubtedly to lessen it, since it increases the ligand donor strength. Solvent release in the RDS, would therefore be more facile. Conversely, the degree of electron transfer to  $O_2$  would increase, as electron density increases on Mn, and the  $O_2^{\delta-}$  should be held tighter. Greater electron transfer would also induce more restriction in the solvent sheath.

The solvent effect on  $\Delta S^\ddagger$  is also due to a number of factors. Expulsion of a more tightly held pyridine will produce more randomness than a looser DMSO. Restriction of non-coordinated solvent will be

Table XII. Kinetic Parameters for Tetradentate Oxygenations

<u>Complex</u>	<u>Solvent</u>	<u>T(°C.)</u>	<u>k(M<sup>-1</sup> min<sup>-1</sup>)</u>	<u>E<sub>a</sub>(kcal/mol)</u>	<u>ΔS<sup>‡</sup>(eu)</u>
Mn(SALEN)	DMSO	21.8	12.4 (0.6)	11.4	-25
		35.1	29 (2)		
		47.9	58 (4)		
Mn(3-MeOSALEN)	DMSO	22.3	19.7 (1.3)	22	10
		35.8	123 (10)		
		47.9	320 (40)		
Mn(3-MeOSALEN)	DMSO	23.3	320 (20)	5.6	-38
		33.8	470 (20)		
		39.7	510 (30)		
Mn(3-MeOSALEN)	Pyridine	6.6	47 (5)	17.2	0
		16.0	110 (10)		
		23.7	300 (20)		

The k values are averages with errors in parentheses.

greater for DMSO, thereby lowering the entropy.

b) Mn(SALC<sub>n</sub>)

The longer chain compounds present peculiarities of their own. Mn(SALBTDA)(n=4) oxygenates so slowly that no data could be gathered on its reaction. The other four compounds' behavior is similar to that of the Mn(XSALEN) complexes in pyridine, i.e. the reaction produces an increase in absorbance across the entire spectrum (Figure 61). In DMSO, however, the absorbance decreases to a flat line raised above zero absorbance (Figure 62), at least for the first step in the reaction. The Mn(II) complexes are much more soluble in pyridine than in DMSO, and this difference apparently carries over to their  $\mu$ -oxo-Mn(III) products, but to an even greater degree. The flat baseline is typical of a suspension instead of a solution, i.e. the Mn(III) compounds precipitate out in DMSO. At first, this was thought to be decomposition, but continuing the scan reveals that a second step follows soon after completion of the first, which is undoubtedly due to further oxygenation to the di- $\mu$ -oxo-Mn(IV) complex. The second step produces an overall absorbance increase, indicative of redissolution, but the final spectrum is relatively featureless, as was the Mn(II) spectrum.

Mn(SALDCDA) differs from the other three complexes in that its Mn(III) product is soluble, with repetitive scans showing an isobestic point near 300 nm for the first step. The extra two methylene groups may impart enough organic nature to the complex to make its oxygenation products soluble at these low concentrations.

The reaction of all long chain complexes with O<sub>2</sub> was found to be

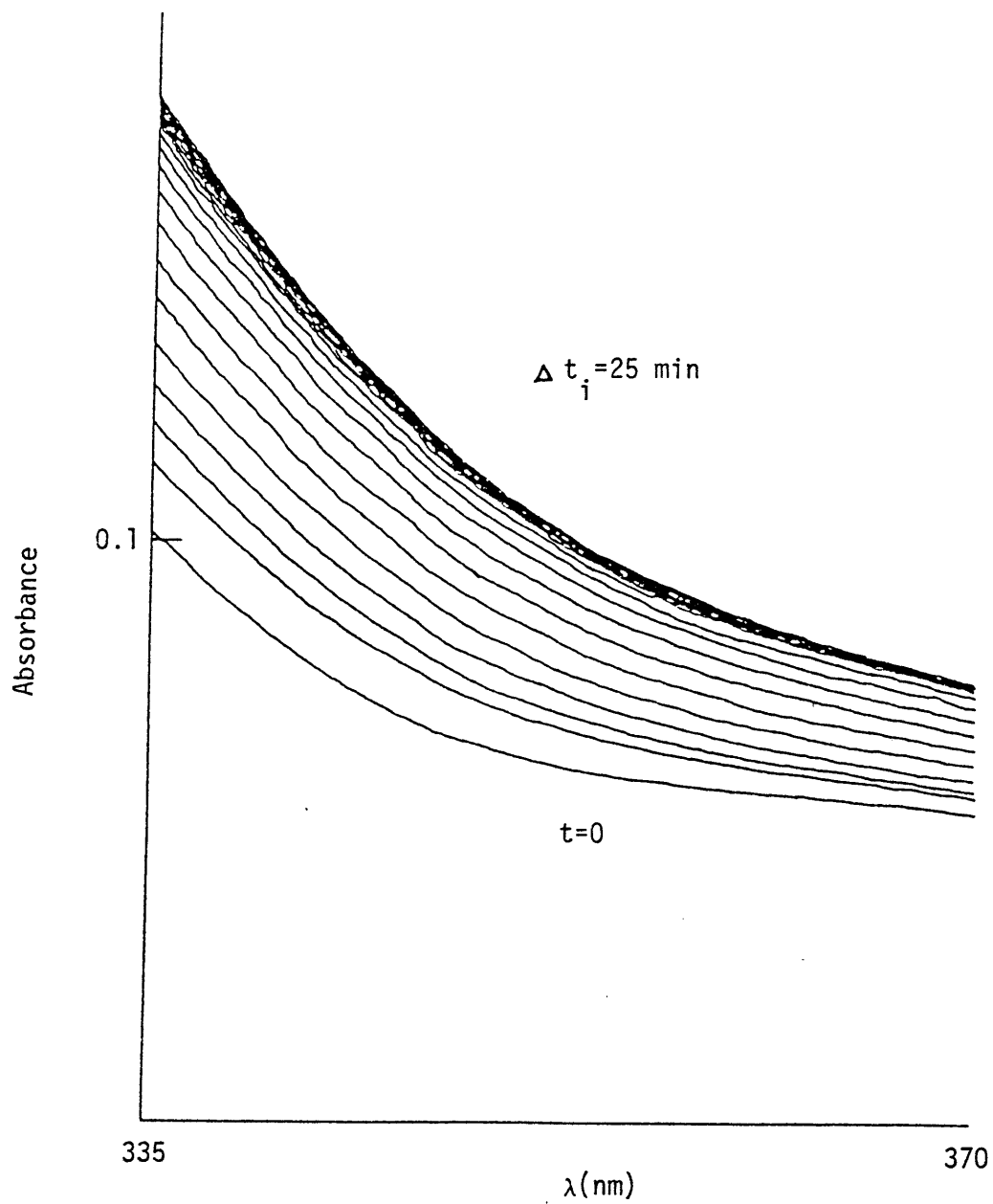


Figure 61: Repetitive Scan of Oxygenation of Mn(SALHXDA) in Pyridine.

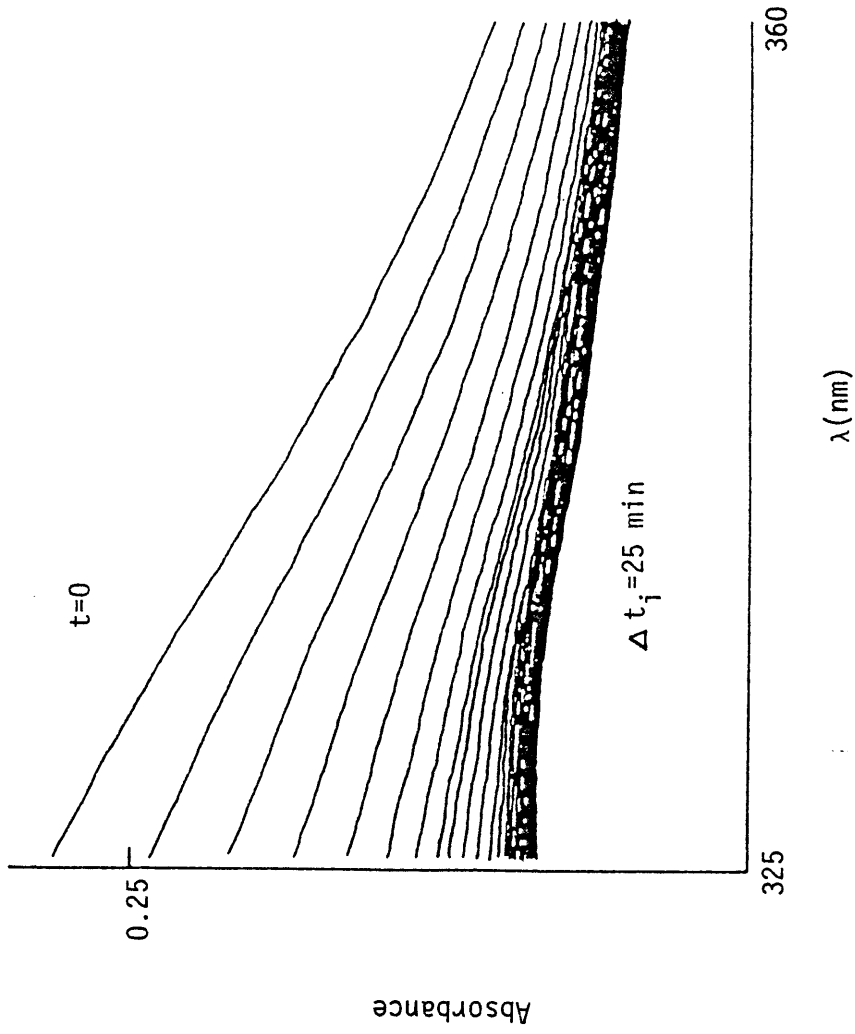
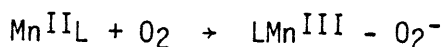
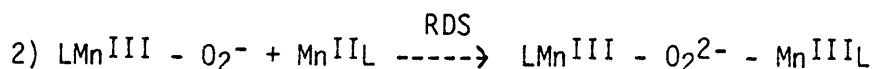
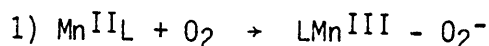


Figure 62: Repetitive Scan of Oxygenation of Mn(SALOTDA) in DMSO.

first order in  $O_2$  in pyridine (Figure 63). However, difficulties were encountered when an order with respect to complex was being determined. First order plots showed marked curvature (Figure 64). This excluded the reaction:



from being the RDS. The next step was to plot the data as a second order reaction, i.e.  $1/(A-A_\infty)$  vs.  $t$ . Second order plots were also curved (Figure 65), therefore mechanisms producing a second-order reaction were also discarded. Extreme steric hindrance would be expected to stop the reaction completely at the  $Mn^{III}-O_2^-$  stage, but a limited amount of steric hindrance may slow the second step until it becomes the RDS:



The long chain complexes are undoubtedly more hindered than the  $Mn(XSALEN)$ 's, so this theory is plausible, if the geometry of  $Mn(SALC_n)$  in solution was either square planar (with two coordinated solvent molecules) or tetrahedral, both possible for these ligands.<sup>108</sup> This type of reaction, however, would require that the first step be extremely fast, i.e. attain equilibrium almost instantaneously, and there is no reason to expect this step to be so much faster for the  $SALC_n$  complexes than for the other complexes. Another means by which second order kinetics could appear is if a dynamic monomer dimer equilibrium existed, and only the dimer was reactive. Dimers could have

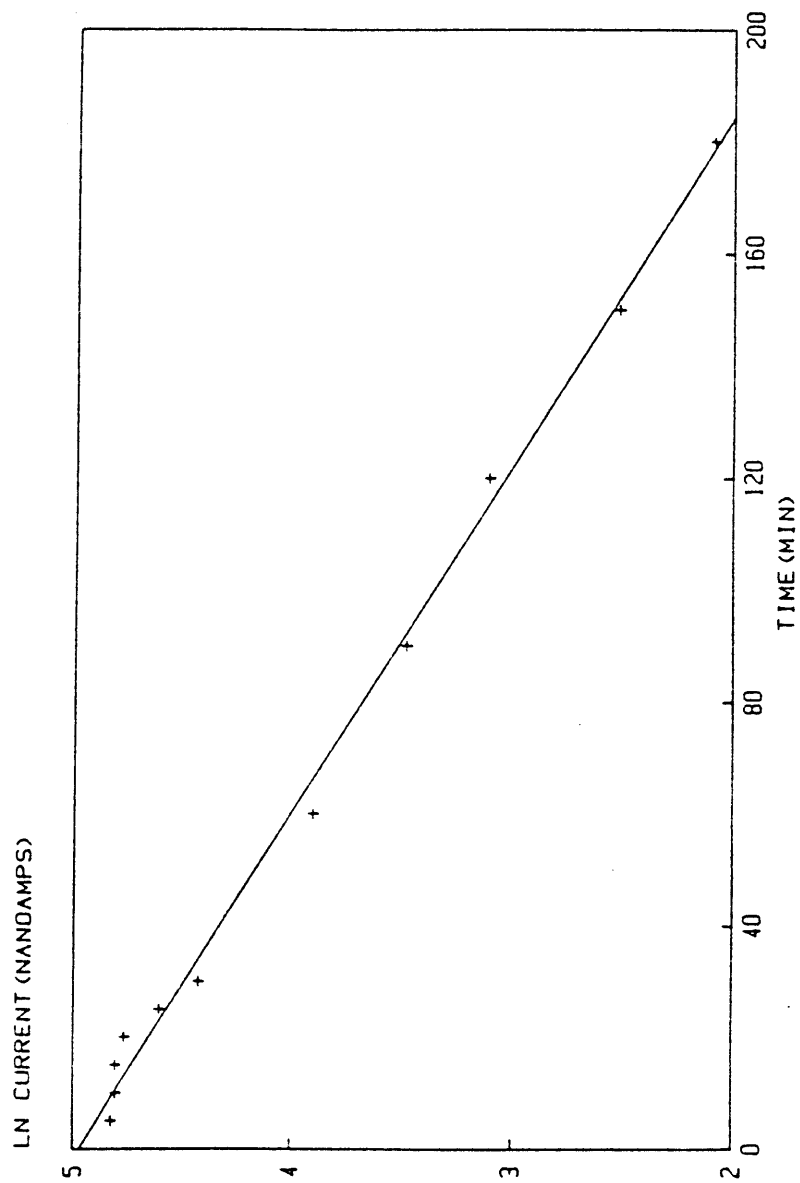


Figure 63: First Order Clark Plot for Oxygenation of Mn(SALHTDA) in Pyridine.

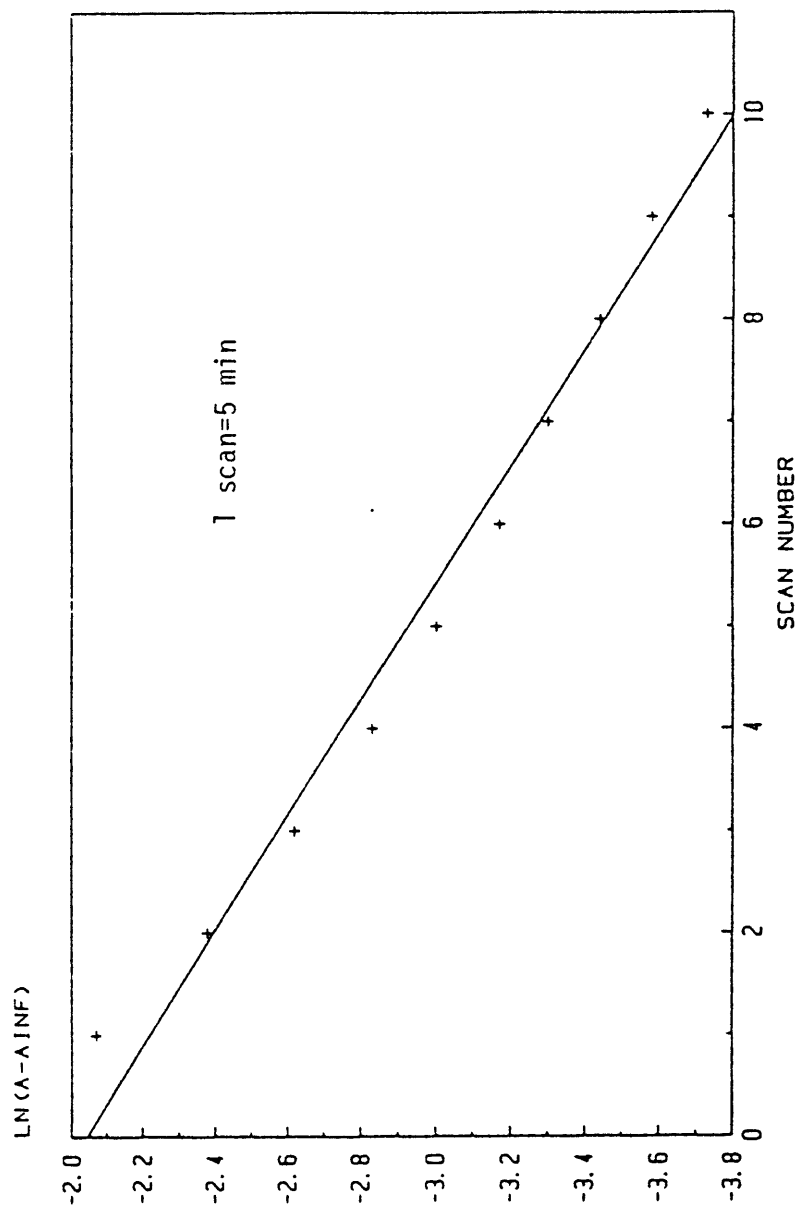


Figure 64: First Order Plot for Oxygenation of Mn(SALOTDA) in Pyridine.

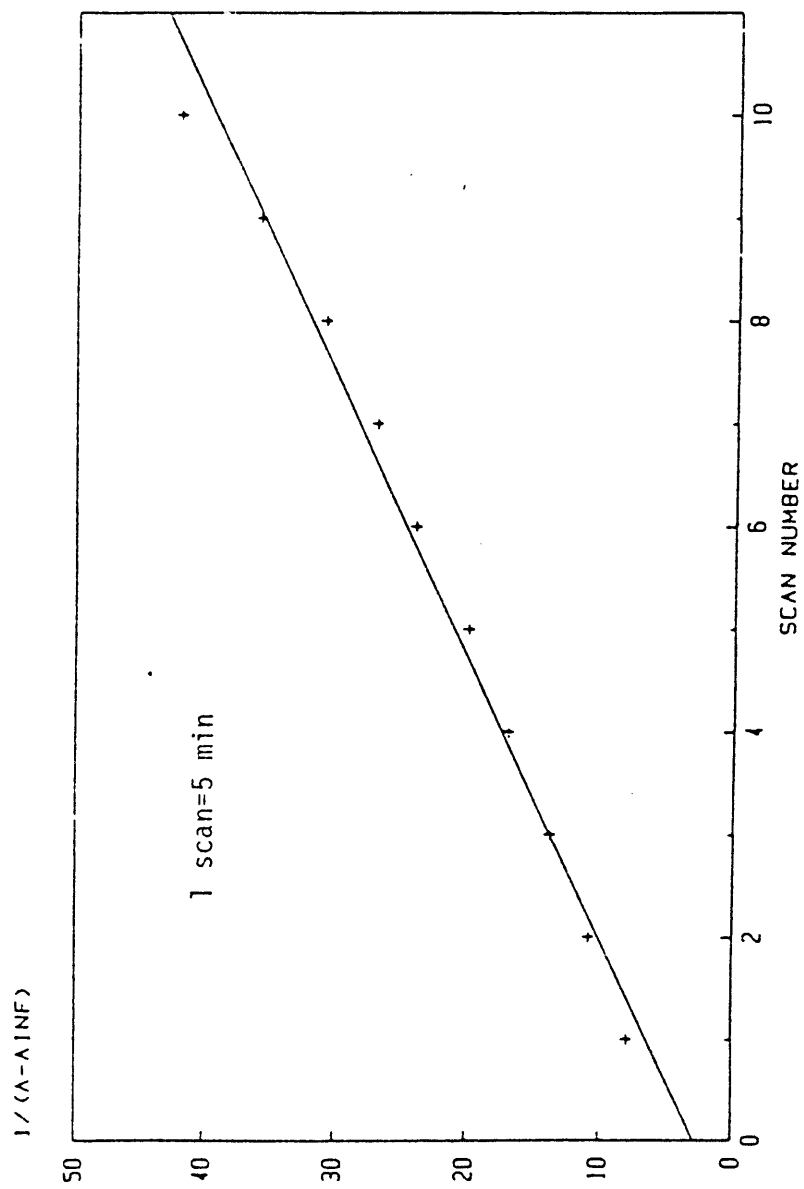
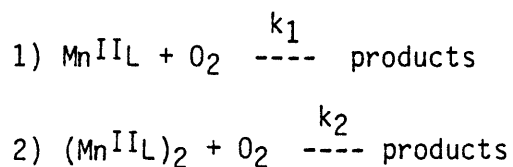


Figure 65: Second Order Plot for Oxygenation of Mn(SALOTDA) in Pyridine

bridging  $C_n$  linkages of the type shown in Figure 66.

To investigate the possibility of some dimerization in the solid state, mass spectra of the complexes were obtained. No evidence of such was seen, with the parent  $M^+$  peak being dominant, and only  $M+1$  and  $M+2$  peaks at higher mass. Of course, conditions in the spectrometer are very different from those in solution, and the possibility of some dimerization occurring in solution could not be entirely ruled out. Another test for dimerization was performed by recording spectra of the Mn(II) complexes at different concentrations. The spectra should have undergone perturbations in shape or  $\epsilon$  values if dimerization affected these properties, i.e. a change in the monomer/dimer ratio occurred at these concentrations and the two forms had different spectra. However, the absorbances at all wavelengths followed Beer's law, therefore a significant amount of dimerization is not believed to be occurring.

Two mechanisms involving mixed-order reactions were also investigated. If only partial dimerization were occurring, then one possible mechanism would involve mixed first and second order reactions:



Kelter and Carr<sup>109</sup> have developed a simple one-pass microcomputer compatible program for fitting such data. The ratio of the two rate constants ( $k_1/k_2$ ) may be from  $10^{10}$  to  $10^{-6}$ , and the two forms must be in rapid dynamic equilibrium, i.e.  $K_{dim}$ , the equilibrium constant for

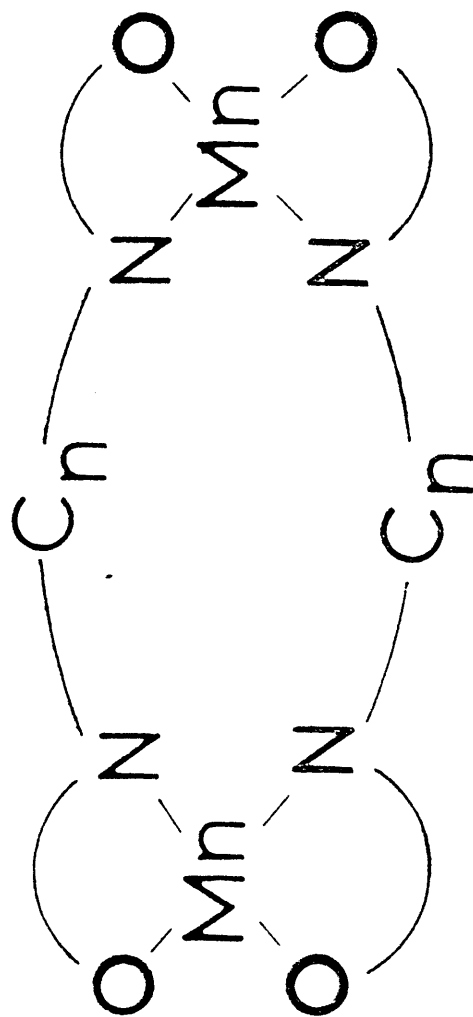
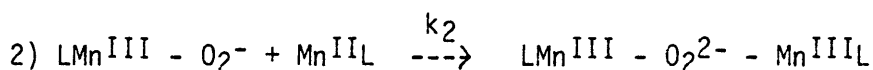
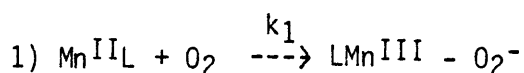


Figure 66: Potential Dimeric Structure of  $\text{Mn}(\text{SALC}_n)$  Complexes.

dimerization, must be obeyed at all times. If this was not the case, such improbable occurrences as a shift from 1st to 2nd order during the reaction could occur if the monomer were more reactive. This mechanism was also discarded when the calculations turned out such things as negative rate constants, negative activation energies, and generally poor fits to the experimental data. Most disconcerting were differences of up to 50% in the calculated rate constants for duplicate runs, far in excess of results for all other complexes. This did not eliminate a reaction with a non-dynamic equilibrium between the two forms, which remains a possibility.

A second mechanism involving mixed-order kinetics is similar to the first second-order mechanism postulated:



but where the rates are approximately equal, i.e.  $k_1[\text{MnL}][\text{O}_2] \approx k_2[\text{MnL-O}_2^-][\text{MnL}]$ . This could occur if the steric hindrance of the long chain inhibited the second step, but not enough to make it the RDS. A simple graphical or numerical test for this type of mechanism could not be found, so this must remain speculation.

One other mechanism was also plausible. It assumed that the dominant form of complex in solution is a dimer, but the monomer is the reactive form. This would lead to 1/2 order kinetics. A graphical test of this theory can be performed by plotting  $(\Delta A)^{-1/2}$  vs. time.

Unfortunately this plot showed a terrible linear fit, and eliminated

this possibility.

At this time, therefore, the kinetics of oxygenation of the  $\text{Mn}(\text{SALC}_n)$  complexes are still not known, but two simple possibilities remain after eliminating a number of others. These are: first, reactive monomeric and dimeric forms which are not in dynamic equilibrium; and second, a two step reaction producing superoxo- and  $\mu$ -peroxo-complexes with rates of the same order of magnitude for the two steps.

#### 5. Pentadentate Complexes

Of the four pentadentate complexes prepared, only  $\text{Mn}(5\text{-NO}_2\text{SALDPT})$  was amenable to kinetic study. Since it was known from the uptake experiments that ligand oxidation occurred at about the same rate as Mn oxidation for all complexes but the  $\text{NO}_2$ -substituted one, it was assumed that spectral overlap would make data abstraction difficult. For the  $\text{NO}_2$ -complex, however, the reaction with  $\text{O}_2$  only involves the Mn center, and is complete after  $\sim 1$  hr.

A typical repetitive scan in toluene is presented in Figure 67. The disappearance of the  $\text{NO}_2$ -peak with time and the final flat absorbance spectrum are reminiscent of the long chain tetradentates in DMSO, therefore precipitation or suspension of the product is probably occurring. The nature of the product is undoubtedly  $\text{Mn}(5\text{-NO}_2\text{SALDPT})\text{OH}$ , since no special care was taken to dry the solvent.<sup>62</sup> The spectra in DMSO and pyridine indicate product solubility, i.e. isobestic points during the reaction and peaks in the product spectra (Figure 68). However, they are much more polar than toluene and are also donor

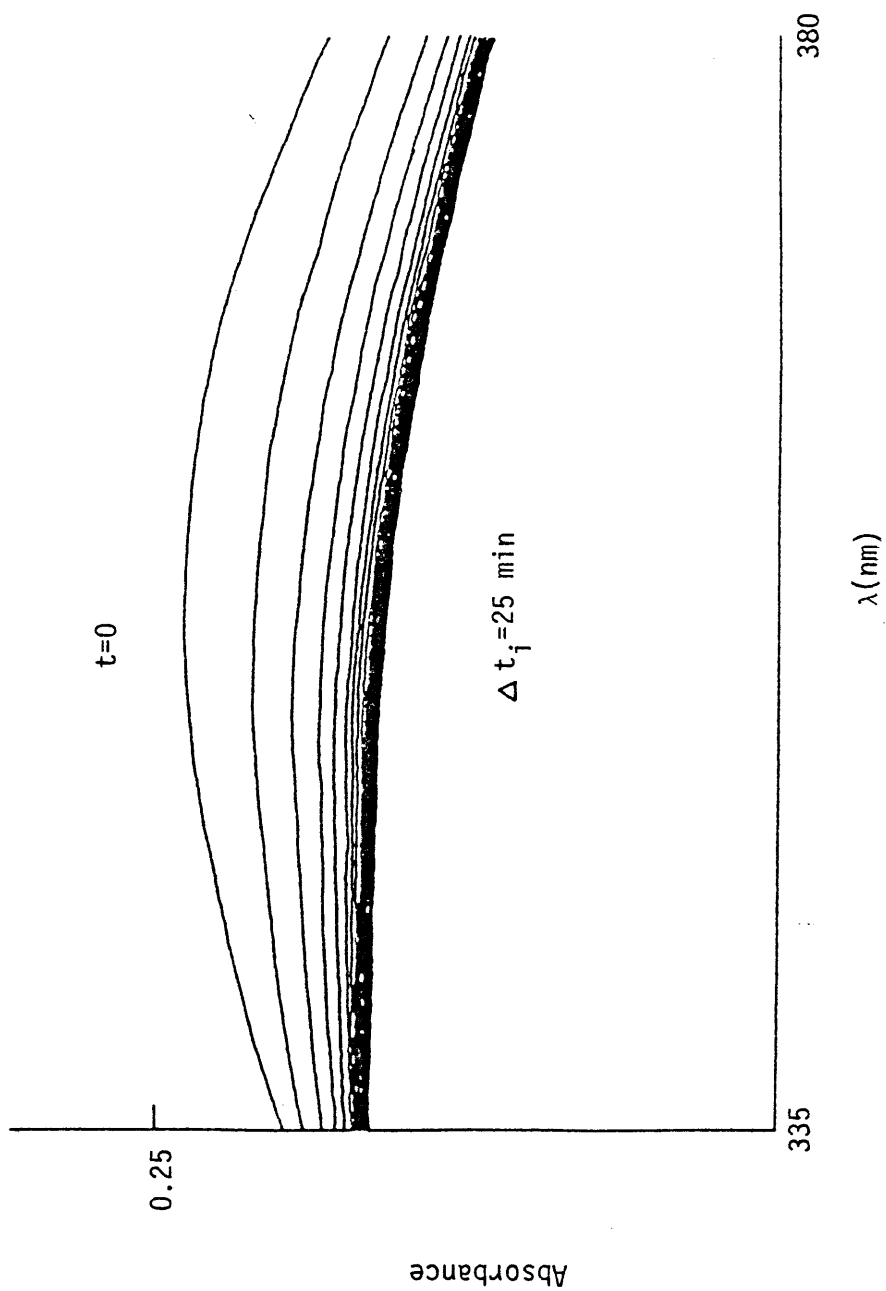


Figure 67: Repetitive Scan of Oxygenation of Mn(5-NO<sub>2</sub>)SALDPT) in Toluene.

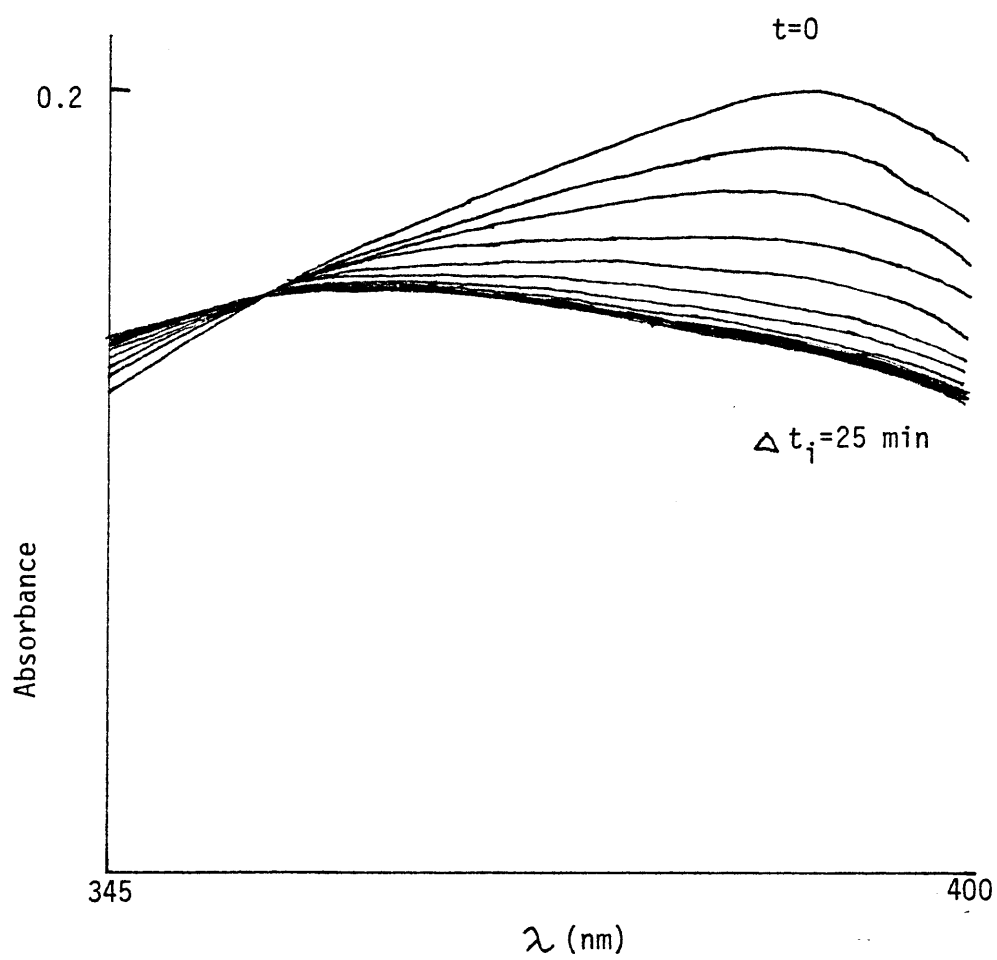
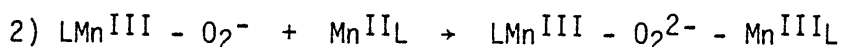
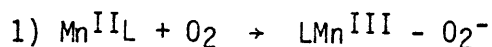


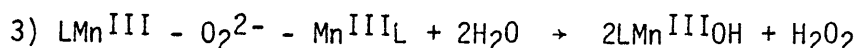
Figure 68. Repetitive Scan of Oxygenation of Mn(5-NO<sub>2</sub>SALDPT) in Pyridine.

solvents, and can apparently dissolve the hydroxy-complex.

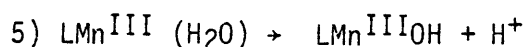
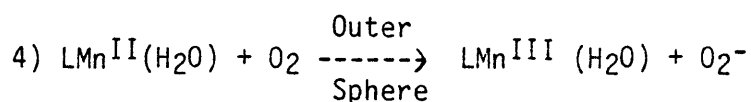
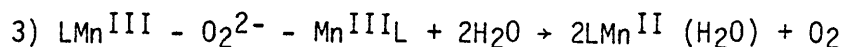
The postulated mechanism in dry toluene was as follows<sup>91</sup>:



The next step in the reaction, occurring in wet toluene, was first believed to be:



However, if the isolated  $\mu$ -peroxo dimer was suspended in THF and  $\text{H}_2\text{O}$  was added, the result was formation of the Mn(II) complex and  $\text{O}_2$ . The reaction was therefore changed to:



The final oxygen reduction product(s) from  $\text{O}_2^-$  were not identified.

A number of inconsistencies were unexplained, however. First, the  $\mu$ -peroxo dimer was never hydrolyzed in toluene. The difference in the solvents may have made the earlier mechanism correct in the aromatic solvent. A smaller change, moving the  $\text{NO}_2$ -group to the 3-position, caused hydrolysis to result in a "black tarry substance." Also, DMSO and pyridine are quite different from THF, and hydrolysis of the peroxo-bridge, rather than dismutation, may also occur in these solvents. Second, the  $\mu$ -peroxo-dimer did not hydrolyze when added to water, and it is difficult to see how THF as a reaction solvent would

facilitate a hydrolysis more than water. Finally, if outer sphere hydrolysis of a hydrated Mn(II) species is possible, why did the reaction not start at this point in wet toluene?

Before addressing these questions, the data from the kinetic study should be examined. The reaction was found to be first order in both O<sub>2</sub> (Figure 69) and complex (Figure 70). Calculated rate constants and activation parameters are shown in Table XIII. A number of points should be noted here. First, the highest E<sub>a</sub> is found in toluene, not a great surprise considering that the reaction involves significant charge transfer and toluene is relatively non-polar. Second, the E<sub>a</sub> is higher in DMSO than in pyridine, a first for these types of reactions. This implies that removal of solvent from a coordination site by O<sub>2</sub> is not significant in the reaction. Third, the reproducibility of the runs is the best of all complexes (~ ±2%). If water has such a great effect on the reaction, then it must not be involved in the RDS, because variable water concentrations in the solvents would have produced less reproducible rate constants, or alternatively, it was present at constant concentration (saturated?) in all runs. This is possible for toluene and DMSO where H<sub>2</sub>O has limited solubility but pyridine and water are infinitely miscible.<sup>99</sup>

Yet one more piece of data should be added before a discussion of the reaction is attempted. Cobalt(II) complexes with XSALDPT ligands have been shown to be 5-coordinate in pyridine, except for the NO<sub>2</sub>-complex, which exists as a mixture of 5- and 6-coordinate species, i.e. without and with a coordinated pyridine<sup>110</sup>. The other complexes

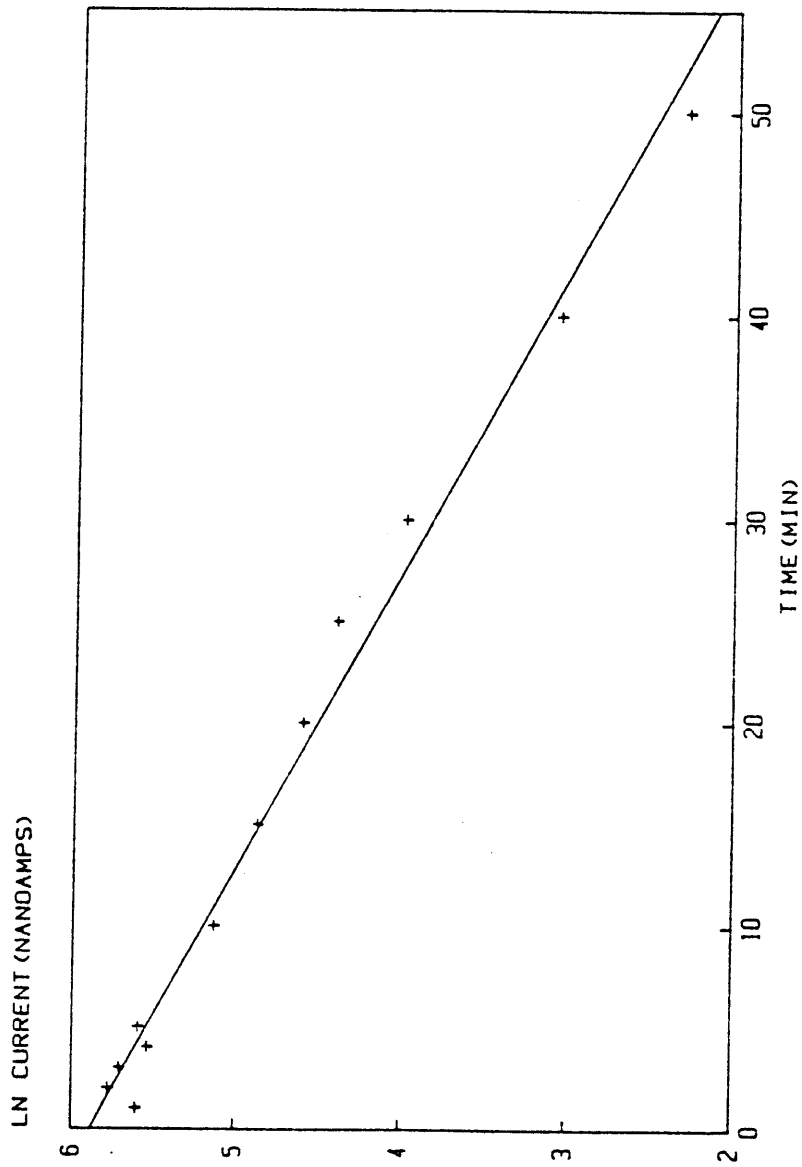


Figure 69: First Order Clark Plot for Oxygenation of Mn(5-NO<sub>2</sub>SALDPT) in Toluene.

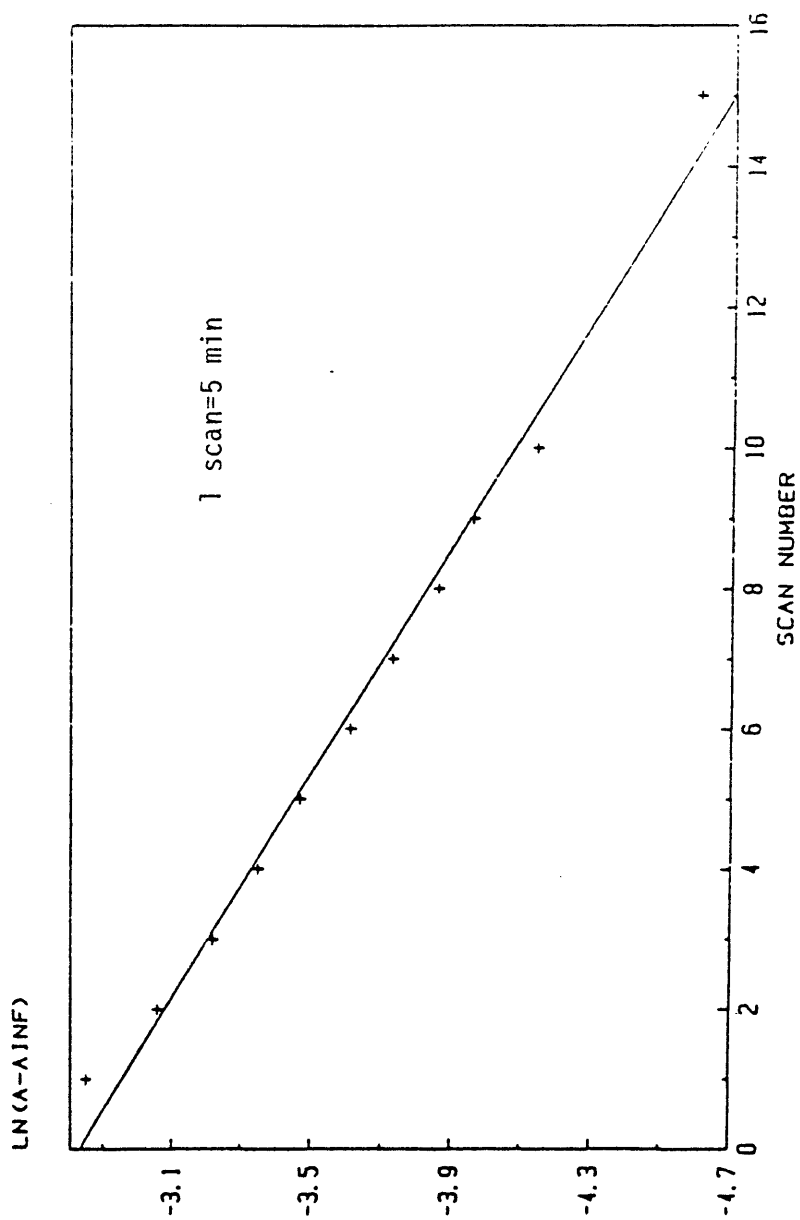


Figure 70: First Order Plot for Oxygenation of Mn(5-NO<sub>2</sub>)SALDPT) in Toluene.

Table XIII. Kinetic Parameters for Oxygenation of Pentadentate Complex

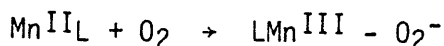
<u>Solvent</u>	<u>T(°C.)</u>	<u>k(M<sup>-1</sup> min<sup>-1</sup>)</u>	<u>E<sub>a</sub>(kcal/mol)</u>	<u>ΔS<sup>‡</sup>(eu)</u>
Toluene(a)	23.2	1.47 (0.02)	23	10
	28.3	2.9 (0.1)		
	35.7	7.5 (0.2)		
DMSO	25.6	3.4 (0.2)	18.1	-6
	33.3	7.7 (0.1)		
Pyridine	9.0	2.5 (0.1)	7.7	-40
	14.4	2.9 (0.3)		
	29.4	6.2 (0.2)		

(a)[O<sub>2</sub>] in Toluene = 8.5 x 10<sup>-3</sup>M

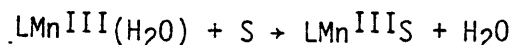
The k values are averages with errors in parentheses.

apparently provide enough electron density that a 6th donor is not necessary, but the NO<sub>2</sub>-group withdraws electron density, and the pyridine molecule is pulled in to overcome this effect.

Correlating all these pieces of information leads to a number of conclusions. First, the rate law states that the slow step has the general form:



Second, the lack of effect of H<sub>2</sub>O on the reaction indicates that it is probably not coordinated to the Mn(II) complex initially, i.e. the complex is 5-coordinate. This could have been surmised from the Co study where pyridine was shown to coordinate to Co(5-NO<sub>2</sub>SALDPT) in equilibrium with an unsolvated form, since Mn(II) has less driving force to become 6-coordinate, therefore coordination of an H<sub>2</sub>O molecule (or DMSO or pyridine) would not occur. Third, coordination of H<sub>2</sub>O to Mn(III) in the two polar solvents would be inhibited by the orders of magnitude greater concentration of donor solvent competing for the coordination site. This may force inclusion of a step in the reaction such as:



This would have to be reversible, however, so that deprotonation could produce the hydroxy product. Finally, another reaction which undoubtedly occurs is:



since the 6-coordinate species is unstable. A given Mn(II) species could therefore pass through a number of  $\mu$ -peroxo-cycles before an

outer-sphere oxidation occurred.

Rationalizing the activation parameters in toluene is not difficult. The high  $E_a$  has already been attributed to the low dielectric constant and dipole moment of the solvent.  $\Delta S^\ddagger$  would be much more negative in a polar solvent, where solvent reorganization would be extensive, but here this effect is negligible. Significant movement of the ligand may be occurring, however, which would add an additional positive increment to  $\Delta S^\ddagger$ . An explanation of the activation parameters in DMSO and pyridine, however, is not obvious. The  $E_a$  and  $\Delta S^\ddagger$  values in pyridine are appropriate for a reaction involving a simple bimolecular slow step with attendant charge-transfer and electrostriction, similar to the reaction of the bimolecular complexes with  $O_2$ . The activation parameters in DMSO should have about the same values as those in pyridine, assuming no initial solvent coordination, because of the similar solvent properties of DMSO and pyridine. The radically different values, with DMSO actually more closely resembling toluene than pyridine, are difficult to explain unless some sort of specific interaction between the complex and one of the solvents, but not the other, occurs in the reaction.

One possibility is that DMSO is bound to the Mn(II) center but pyridine is not. Earlier sections of this discussion have dwelled largely on the fact that pyridine is a better ligand for Mn(II) because of strong covalent interaction. The fact that DMSO is a better donor to Mn(II) on purely electronic grounds has been largely ignored. The  $C_B$  and  $E_B$  values given by Drago et al.<sup>104</sup>, indicating covalent and

electronic contributions to total base strength, are 2.85 and 1.34 for DMSO, and 6.40 and 1.17 for pyridine, i.e. DMSO is a better electronic donor than pyridine, and coordination may be affected more by the electronic effect with pentadentate ligands. Electronic donor control of coordination in Co compounds was previously mentioned in the electrochemistry section. Further contribution to electronic control of coordination may come from the higher dipole moment of DMSO (4.00 vs. 2.20), which could induce polarization in the metal-solvent bond, enhancing the electronic effect. Another factor which should be included is the smaller size of DMSO, which gives it freer access to the sixth coordination site. A possible steric effect was noted for Mn(3-MeOSALEN) and the pentadentates are undoubtedly more impeding than the tetradentates. Added to this should be the observation that coordination geometries of Mn(II) and (III) complexes of 5-NO<sub>2</sub>SALDPT are believed to be identical due to an earlier electrochemical study<sup>63</sup>.

Another possibility is interaction of DMSO with the ligand instead of the metal. MacGregor<sup>96</sup> has published a paper containing numerous examples of abnormally strong interactions of DMSO with substrates in organic reactions. If some type of interaction prevented free movement of the ligand from its initial coordination positions, a similar increase of  $E_a$  would be seen. The pentadentate ligands are unique in having a secondary amine as a donor, which has been stated to have interesting effects on the electrochemistry. Also, attack of O<sub>2</sub> has been postulated to occur cis to this nitrogen (Figure 71), therefore interaction of DMSO with the amine group could cause steric hindrance

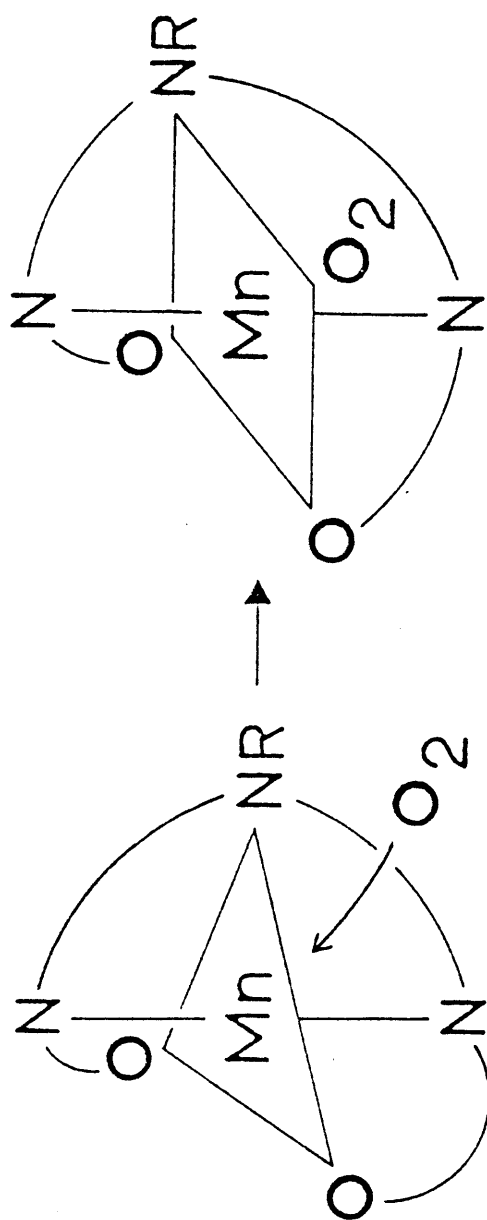


Figure 71:  $O_2$  Attack on Pentadentate Complexes.

towards  $O_2$ .

#### 6. Hexadentate Complexes

Only one hexadentate complex,  $Mn(SAL\ 1,5,8,12)$ , was investigated in this study. The regular repetitive scan study was not applicable because of spectral overlap of the two steps in the reaction (Figure 72). An interesting piece of information from this Figure is that, like  $Mn(3-MeOSALEN)$ , there seems to be a third step in the reaction. If it is indeed ligand oxidation that causes the second step, then the third step may be due to a different part of the ligand. It was previously postulated that the aliphatic chains in the ligand are dehydrogenated in this step, and a hexadentate ligand has two different types of chains. The ones nearest the imine nitrogens are probably more active than the central one, therefore it is this central chain which may be responsible for the third step. An alternative explanation may be oxidation of  $Mn(III)$  to  $Mn(IV)$ , as was the case with the tetradentates.

The inapplicability of the usual spectral study required that a different method be employed to obtain data on this system. The method of choice in this case was an initial rate study to avoid complexities introduced by the second (and third) step(s). Performing this with an air-sensitive compound required that some rather crude techniques be employed. Briefly, the method used was as follows: A stock solution of complex in deaerated solvent ( $\sim 10^{-4}M$ ) was prepared in the inert atmosphere box. Aliquots of the solution were then diluted to give samples with total complex concentrations in the ratios 1:2:3:4. Five mL of these solutions were then placed in four 20 mL glass ampoules,

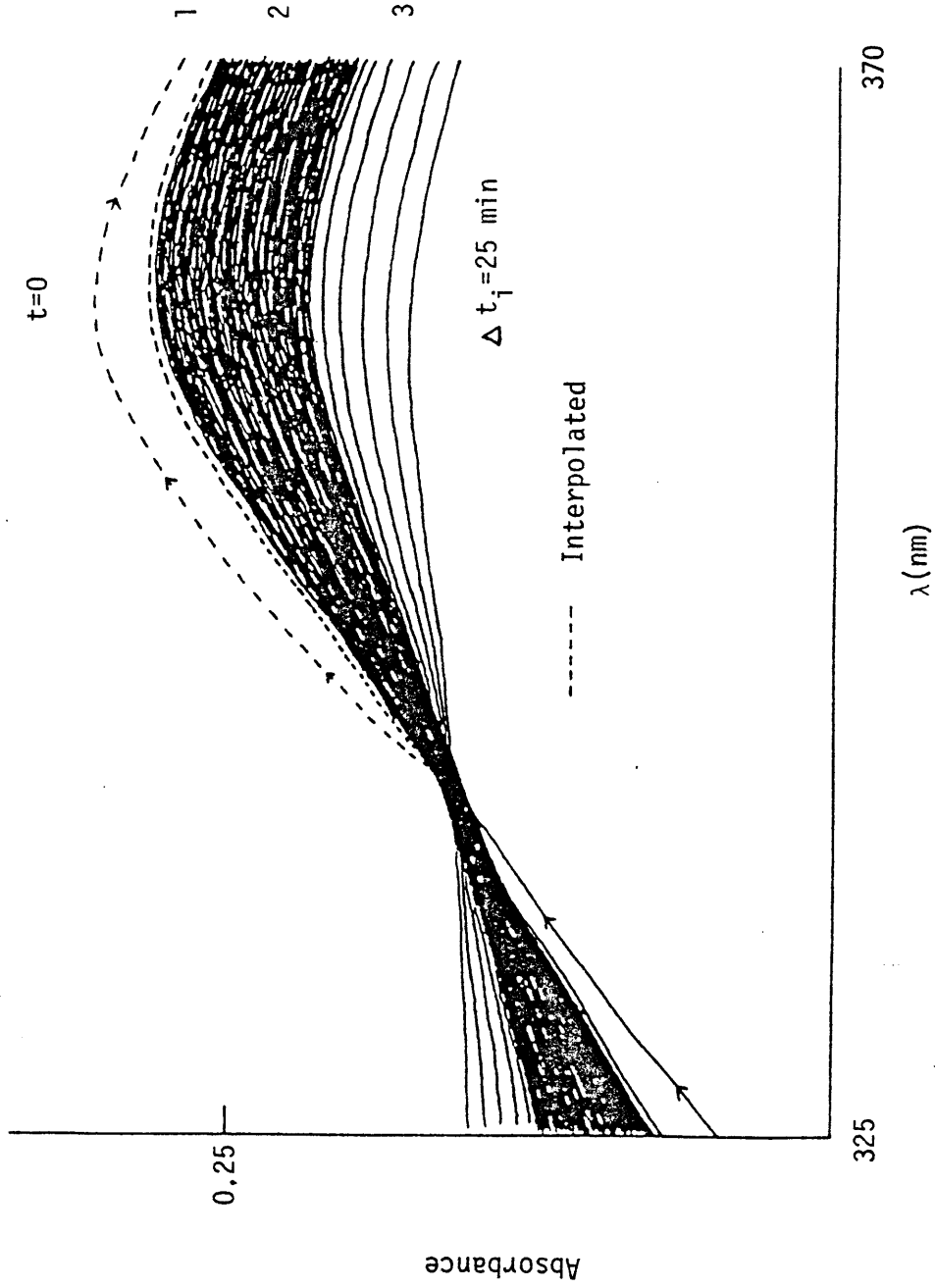
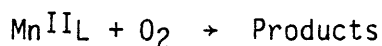


Figure 72: Repetitive Scan of Oxygenation of Mn(SAL 1,5,8,12) in Pyridine.

capped with rubber septa, and brought out of the box. To initiate the reaction, a 5 mL aliquot of oxygenated solvent was added with a hypodermic needle, the ampoule shaken to mix the solutions, and ~3 mL was then syringed into the spectrophotometer cell. The absorbance at a fixed wavelength was then followed for 10 minutes. Figure 73 is a plot of  $\Delta A$ , the change in absorbance over a ten minute period, vs. the relative concentration of the solution. The straight line represents the expected result for a first order reaction, where  $\Delta A$  should be proportional to the concentration, and the curved line the result for a second order reaction, where  $\Delta A$  is proportional to the square of the concentration, with both lines forced through the origin and the first data point. It can be seen that the fit is better for the first order plot, although it is still not a very good one, therefore the order in complex is tentatively assigned as one, at least over this concentration range. The ten minute period (~16% of reaction) was much longer than the time for 1 or 2% of the reaction to occur, which is preferred when using the initial rate method. However, the absorbance change is very small for this reaction, and the ten minutes was a compromise between a true initial rate and producing a measurable  $\Delta A$ .

Of course, no problems with side reactions were encountered with the Clark electrode, which give the order in  $O_2$  as also being one (Figure 74). The slow step is therefore the same as that of most of the other complexes, i.e.:



No attempt was made to calculate rate constants or activation

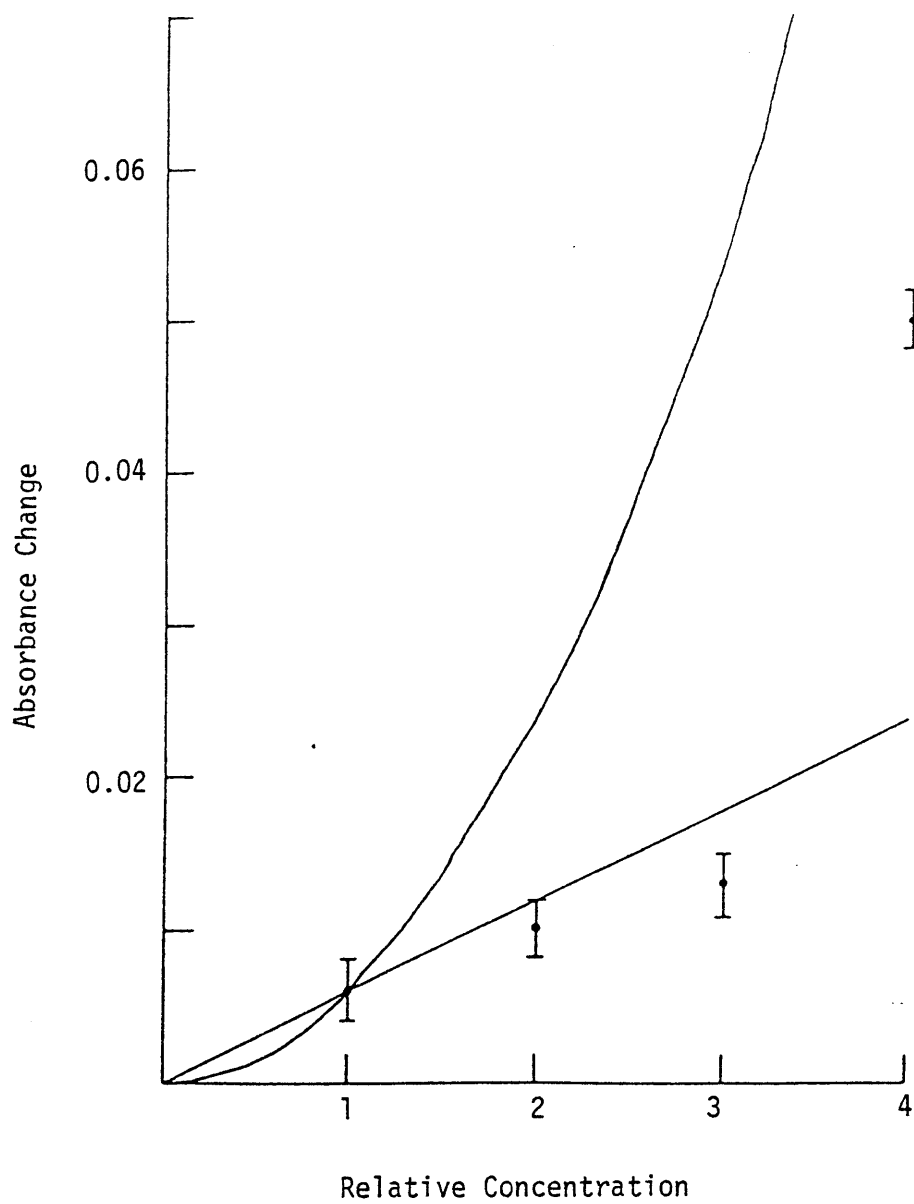


Figure 73: Initial Rate Plot for Oxygenation of Mn(SAL 1,5,8,12) in DMSO.

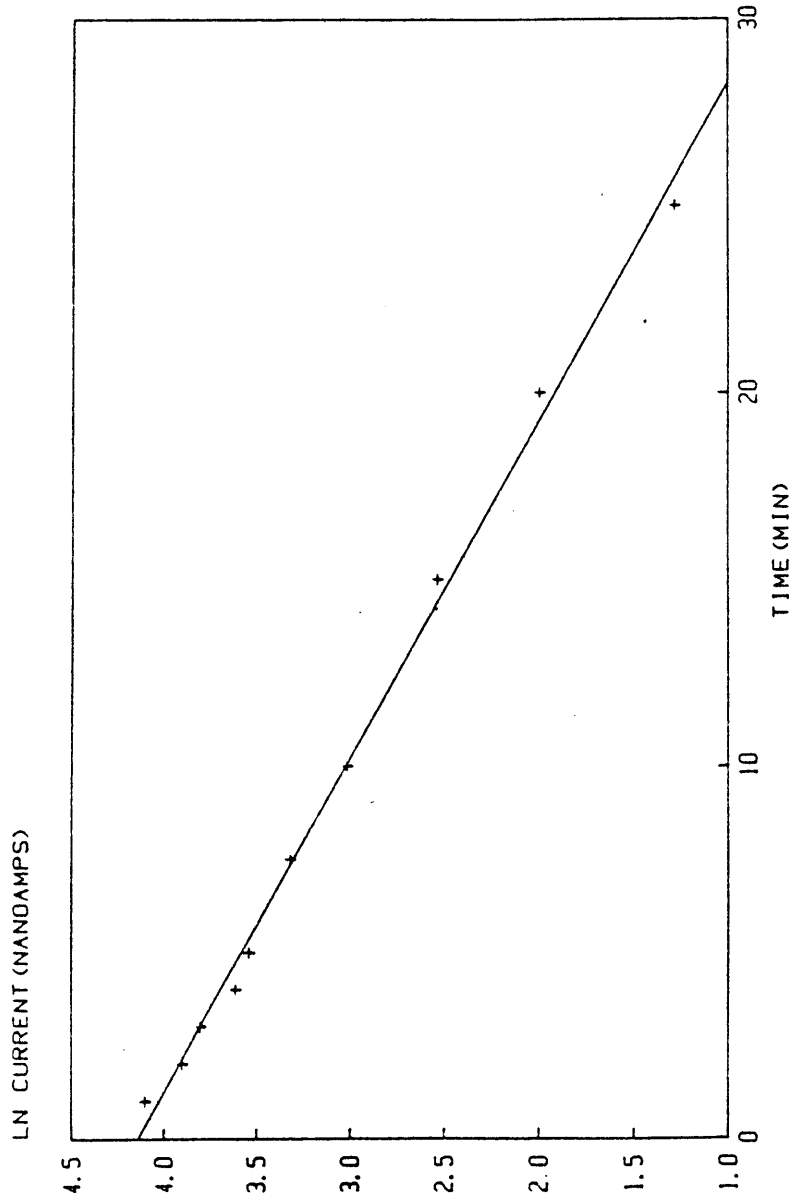


Figure 74: First Order Clark Plot for Oxygenation of Mn(SAL 1,5,8,12) in DMSO.

parameters for this reaction because application of even the initial rate method to this system gave results of insufficient accuracy and precision to warrant further calculations.

### Oxygenation Mechanisms Review

#### 1. Bidentate Complexes

Bidentate oxygenations very likely follow the pathway:

- 1)  $\text{Mn}^{\text{II}}\text{L}_2 + \text{O}_2 + \text{S} \xrightarrow{\text{RDS}} \text{SL}_2\text{Mn}^{\text{III}} - \text{O}_2^-$
- 2)  $\text{SL}_2\text{Mn}^{\text{III}} - \text{O}_2^- + \text{Mn}^{\text{II}}\text{L}_2 + \text{S} \rightarrow \text{SL}_2\text{Mn}^{\text{III}} - \text{O}_2^{2-} - \text{Mn}^{\text{III}}\text{L}_2\text{S}$
- 3)  $\text{SL}_2\text{Mn}^{\text{III}} - \text{O}_2^{2-} - \text{Mn}^{\text{III}}\text{L}_2\text{S} + \text{XH} \rightarrow 2 \text{Mn}^{\text{III}}\text{L}_2\text{S} + \text{X}^- + \text{HO}_2^-$
- 4)  $\text{Mn}^{\text{III}}\text{L}_2\text{S} + \text{S} \rightarrow \text{Mn}^{\text{III}}\text{L}_2\text{S}_2$
- 5)  $2\text{HO}_2^- \rightarrow \text{O}_2 + 2\text{OH}^-$
- 6)  $\text{Mn}^{\text{III}}\text{L}_2\text{S}_2 + \text{O}_2 \rightarrow \text{Mn}^{\text{III}}\text{L}'_2\text{S}_2$

The only two parts of the mechanism which are questionable are the exact sequence of solvent attack and the nature of L' in step 6.

#### 2. Tridentate Complexes

The reaction mechanism for the tridentate complexes is very similar to that of the bidentates, except for the involvement of solvent:

- 1)  $\text{Mn}^{\text{II}}\text{L}_2\text{S}_2 + \text{O}_2 \xrightarrow{\text{RDS}} \text{L}_2\text{Mn}^{\text{III}} - \text{O}_2^- + 2\text{S}$
- 2)  $\text{L}_2\text{Mn}^{\text{III}} - \text{O}_2^- + \text{Mn}^{\text{II}}\text{L}_2\text{S}_2 \rightarrow \text{L}_2\text{Mn}^{\text{III}} - \text{O}_2^{2-} - \text{Mn}^{\text{III}}\text{L}_2 + 2\text{S}$
- 3)  $\text{L}_2\text{Mn}^{\text{III}} - \text{O}_2^{2-} - \text{Mn}^{\text{III}}\text{L}_2 + \text{XH} \rightarrow 2\text{Mn}^{\text{III}}\text{L}_2 + \text{HO}_2^-$
- 4)  $2\text{HO}_2^- \rightarrow \text{O}_2 + 2\text{OH}^-$
- 5)  $\text{Mn}^{\text{III}}\text{L}_2 + \text{O}_2 \rightarrow \text{Mn}^{\text{III}}\text{L}'_2$

This is the pathway followed by the  $\text{Mn}(\text{XSALAEP})_2$  complexes, but

there is a chance that  $\text{Mn}(\text{XSALAMP})_2$  reacts in a manner intermediate between this and the bidentate scheme:

- 1)  $\text{Mn}^{\text{II}}\text{L}_2 + \text{O}_2 \xrightarrow{\text{RDS}} \text{L}_2\text{Mn}^{\text{III}} - \text{O}_2^-$
- 2)  $\text{L}_2\text{Mn}^{\text{III}} - \text{O}_2^- + \text{Mn}^{\text{II}}\text{L}_2 \rightarrow \text{L}_2\text{Mn}^{\text{III}} - \text{O}_2^{2-} - \text{Mn}^{\text{III}}\text{L}_2$
- 3)  $\text{L}_2\text{Mn}^{\text{III}} - \text{O}_2^{2-} - \text{Mn}^{\text{III}}\text{L}_2 + \text{XH} \rightarrow 2\text{Mn}^{\text{III}}\text{L}_2 + \text{HO}_2^-$
- 4)  $2\text{HO}_2^- \rightarrow \text{O}_2 + 2\text{OH}$
- 5)  $\text{Mn}^{\text{III}}\text{L}_2 + \text{O}_2 \rightarrow \text{Mn}^{\text{III}}\text{L}'_2$

Here, there is no solvent involvement because the stable Mn(II) species is tetrahedral with dangling pyridines; whereas the Mn(III) is closed octahedral.

### 3. Tetradentate Complexes

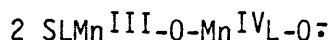
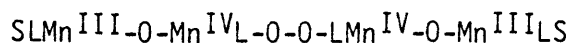
For Mn(XSALEN) complexes, the first step in the reaction probably follows:

- 1)  $\text{Mn}^{\text{II}}\text{LS}_2 + \text{O}_2 \xrightarrow{\text{RDS}} \text{SLMn}^{\text{III}} - \text{O}_2^- + \text{S}$
- 2)  $\text{SLMn}^{\text{III}} - \text{O}_2^- + \text{Mn}^{\text{II}}\text{LS}_2 \rightarrow \text{SLMn}^{\text{III}} - \text{O}_2^{2-} - \text{Mn}^{\text{III}}\text{LS} + \text{S}$
- 3)  $\text{SLMn}^{\text{III}} - \text{O}_2^{2-} - \text{Mn}^{\text{III}}\text{LS} \rightarrow 2\text{SLMn}^{\text{III}} - \text{O}^-$
- 4)  $\text{SLMn}^{\text{III}} - \text{O}^- + \text{Mn}^{\text{II}}\text{LS}_2 \rightarrow \text{SLMn}^{\text{III}} - \text{O}_2^- - \text{Mn}^{\text{III}}\text{LS} + \text{S}$

The second step was not studied.

For Mn(SALC<sub>n</sub>) (n = 6,7,8,10) complexes, the initial steps in the reaction are unknown, but the final steps are probably 3) and 4) above.

The second step in the reaction may also follow this mechanism, involving an intermediate step such as cleavage of the O-O bond as shown on the next page:



followed by internal closure and loss of S to form the  $\text{Mn}_2\text{O}_2$  ring. However, another possible mechanism for this reaction (Figure 75) involves a structure similar to that found for one of Werner's doubly bridged  $\text{Co}^{\text{III}}$  complexes<sup>111</sup> which could be formed by end-on attack of  $\text{O}_2$  on  $\text{Mn-O-Mn}$ . Reaction of this complex with a  $\mu$ -oxo- $\text{Mn}(\text{III})$  dimer would produce a complex with a bridging  $-\text{O}-\text{O}-$  which could cleave to give two di- $\mu$ -oxo- $\text{Mn}(\text{IV})$  dimers. One advantage of this route is the avoidance of the free radical in the linear species above which could lead to formation of a catena-oxo-species by attack on another  $\text{Mn}(\text{III})$  dimer.

#### 4. Pentadentate Complex

The best mechanism to explain the majority of the data is:

- 1)  $\text{Mn}^{\text{II}}\text{L} + \text{O}_2 \xrightarrow{\text{RDS}} \text{LMn}^{\text{III}} - \text{O}_2^-$
- 2)  $\text{LMn}^{\text{III}} - \text{O}_2^- + \text{Mn}^{\text{II}}\text{L} \rightarrow \text{LMn}^{\text{III}} - \text{O}_2^{2-} - \text{Mn}^{\text{II}}\text{L}$
- 3)  $\text{LMn}^{\text{III}} - \text{O}_2^{2-} - \text{Mn}^{\text{II}}\text{L} + 2\text{H}_2\text{O} \rightarrow 2\text{LMn}^{\text{II}}(\text{H}_2\text{O}) + \text{O}_2$
- 4)  $\text{LMn}^{\text{II}}(\text{H}_2\text{O}) + \text{O}_2 \rightarrow \text{LMn}^{\text{III}}(\text{H}_2\text{O}) + \text{O}_2^-$
- 4a)  $\text{LMn}^{\text{II}}(\text{H}_2\text{O}) \rightarrow \text{Mn}^{\text{II}}\text{L} + \text{H}_2\text{O}$
- 5)  $\text{LMn}^{\text{III}}(\text{H}_2\text{O}) \rightarrow \text{LMn}^{\text{III}}\text{OH} + \text{H}^+$
- 5a)  $\text{LMn}^{\text{III}}(\text{H}_2\text{O}) + \text{S} \rightarrow \text{LMn}^{\text{III}}\text{S} + \text{H}_2\text{O}$

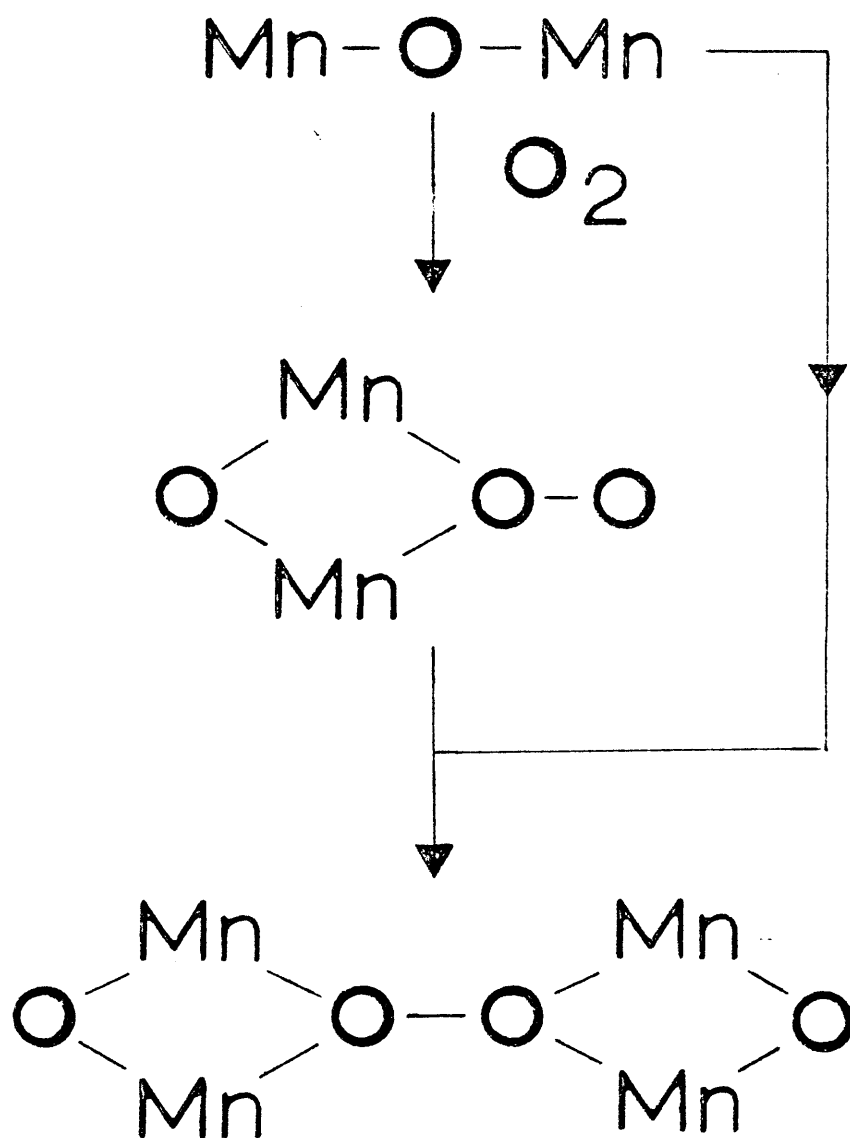
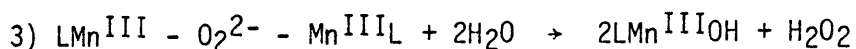


Figure 75: Possible Intermediates in Reaction of  $(\text{LMn})_2\text{O}$  with  $\text{O}_2$  (L=Tetradentate Ligand).

However, a simpler reaction scheme which is also plausible ends with:



### 5. Hexadentate Ligands

Little information was forthcoming on these complexes because of their extreme reactivity towards  $\text{O}_2$ , therefore a detailed mechanism is not possible. However, a number of points should be noted. In the solid state,  $\text{O}_2$  uptake produced a compound with an Mn-O bond, although ligand oxidation precluded its isolation.<sup>76</sup> Solution oxygenation reactions for some of the other studies seem to include the solid state mechanisms as their initial steps, therefore it seems plausible that an  $\text{LMn}^{\text{II}}\text{O}_2^-$  species is the product of the RDS. The geometry of the complex may be 6-coordinate, with one of the nitrogens displaced, as with the tridentates, or 7-coordinate, which has been found to exist for similar  $\text{N}_7$  ligands which have shown that heptacoordinate manganese is possible. Further similarities with the tridentate case, since both have  $\text{O}_2\text{N}_4$  donor sets and isolable  $\text{Mn}^{\text{III}}\text{L}_2^+$  ions, may suggest similar mechanisms after the RDS, i.e. formation of a  $\mu$ -peroxo-dimer followed by a complex with both oxidized metal and ligand, but no coordinated oxygen reduction products.

## CHAPTER V

### SUMMARY AND CONCLUSIONS

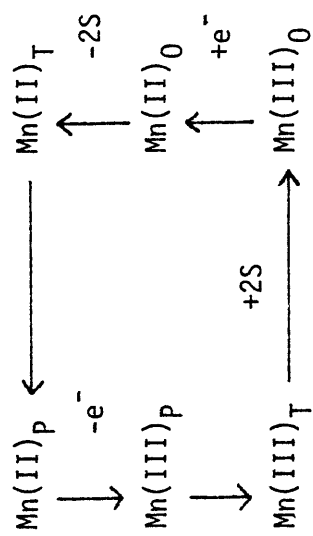
Manganese(II) and (III) complexes of potentially bidentate and tridentate Schiff base ligands with ON, ON<sub>2</sub>, and N<sub>3</sub> donor sets have been synthesized and characterized. The physical properties of the complexes (IR, UV-VIS, solution conductivities, and magnetic moments) are like those of similar previously reported complexes. Those complexes containing pyridine-based ligands with the general formula MnL(NCS)<sub>2</sub> (L = ZPYAEP) must have coordination geometries different from the others with both salicylaldehyde- and pyridine-based ligands, which have a MnL<sub>2</sub>(NCS)<sub>x</sub> (x = 0,1,2) formula (L = ZSALAMP<sup>-</sup>, ZSALAEP<sup>-</sup>, ZPYAMP). Oxygen sensitivities of the complexes are also similar; those containing PY- or NO<sub>2</sub>SAL-based ligands are O<sub>2</sub>-insensitive, while the others containing Mn(II) are all solution sensitive. Solid state oxygenation reactions occur for two complexes, Mn(SAL-4-BrANL)<sub>2</sub> and Mn(SALAMP)<sub>2</sub>, and are believed to produce a μ-peroxo-Mn(III) dimer. Solution products are uncharacterizable.

Oxygen uptakes of the bi- and tridentate complexes in solution superficially resemble previously reported pentadentate and hexadentate results, having an initial fast step (Mn(II) → Mn(III)) and a subsequent slow step (ligand oxidation). Previously reported uptakes of tetradentate complexes differed from all other results, in that they exhibited two distinct stoichiometric steps involving oxidation to first Mn(III) and then Mn(IV). The relative rates of the second steps for the bi- and tridentates are much lower than for the penta- and hexadentates

and the first step ends at a nonstoichiometric  $O_2:Mn$  ratio ( $\sim 0.35$ ). The reaction mechanism is therefore believed to involve cleavage of a  $\mu$ -peroxo-Mn(III) dimer to produce  $HO_2^-$ , which disproportionates to recycle some  $O_2$ .

The electrochemical properties of the complexes were found to be strongly solvent dependent. Cyclic voltammograms of the bidentates,  $Mn(SAL-4-BrANL)_2$  and  $Mn(SALPMA)_2$ , in DMSO produced one oxidation peak and two time-dependent reduction peaks. Three tridentate complexes,  $Mn(ZSALAEP)_2$  ( $Z = 5-MeO, 5-Cl, H$ ) gave one cathodic and three anodic peaks. The peaks in both cases were postulated to be caused by complexes with different numbers of coordinated solvent molecules. In pyridine, only one coupled set of peaks was seen, bidentate complexes undergoing (de)solvation faster than the CV time scale, and tridentates having interchange between electrochemically indistinguishable solvent and ligand pyridine moieties. The other tridentate complexes were all electrochemically inactive, even, strangely, the  $Mn(ZSALAMP)_2$  type. An exception was the tridentate 5- $NO_2$ -complex which exhibited no Mn(III)/(II) couple, but only irreversible reduction of the nitro-group.  $Mn(ZSALEN)$  ( $Z = 5-Cl, 3-MeO, H$ ) tetradentate complexes were also studied in both solvents and produced only one pair of peaks due to Mn(III)/(II).  $Mn(SALC_n)$  ( $n = 6, 7, 8, 10$ ), on the other hand, produced voltammograms indicative of a complex cycle involving slow conversions between polymeric and monomeric species with and without complexed solvent (Figure 76).

The kinetics of the reactions with  $O_2$  gave second-order rate laws



P=polymer

T=tetrahedral monomer

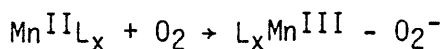
O=disolvated octahedral monomer

Figure 76: Reaction Scheme for Electrochemistry of  $\text{Mn}(\text{SALC}_n)$  Complexes.

of the type:

$$\text{Rate} = k[\text{O}_2][\text{complex}]$$

for nearly all complexes. The exception was the  $\text{Mn}(\text{SALC}_n)$  complexes, where a simple rate law could not be fitted. The slow step is believed to be:



except for  $\text{Mn}(\text{SALC}_n)$ , where attack on a second  $\text{Mn}^{\text{III}}\text{L}$  to give  $\text{LMn}^{\text{III}} - \text{O}_2^{2-} - \text{Mn}^{\text{III}}\text{L}$  may be partly rate-determining, or where both monomeric and dimeric forms of the complex are reactive. Activation parameters of all reactions except that of the pentadentate complex indicated that the RDS usually involved replacement of coordinated solvent by  $\text{O}_2$  and competition with potential ligand donor atoms. For  $\text{Mn}(5\text{-NO}_2\text{SALDPT})$ , the parameters were best explained by interaction of solvent DMSO, but not pyridine or toluene, either by coordination to Mn, or strong dipolar attraction to the secondary donor nitrogen, and  $\text{O}_2$  attack near that nitrogen. Numerous other factors such as loss of other coordinated solvent molecules, ligand rearrangement, and interaction of solvent molecules with uncoordinated ligand donor atoms had to be considered to satisfactorily explain the activation entropies.

From the results of this study, it can be seen that the denticity of ligands in manganese complexes has a substantial effect on the properties of the complexes. Because of this, it may no longer be acceptable to group complexes into classes by donor atom sets; for example, the bidentate and tetradentate complexes could be referred to

as  $(ON)_2$  and  $O_2N_2$  complexes, respectively, instead of both being simply  $O_2N_2$  types. Particular examples demonstrate this quite well. The bidentate complexes were shown to have very different electrochemical and oxygenation properties from the tetradentates. This was due to both different coordination geometries available to the ligands, and the presence of the polymethylene linkage in the tetradentates. Similar differences were found between the tridentate and hexadentate complexes, both with  $O_2N_4$  donor sets.

Another important finding was that stepwise changes in denticity do not always have predictable effects on the complexes. For example, the complexes  $Mn(SALPMA)_2$ ,  $Mn(SALAEP)_2$ , and  $Mn(SALEN)$  oxygenate in pyridine with  $E_a$  values of 7.1, 24, and 22 kcal/mole, respectively. If one substitutes  $Mn(SALAMP)_2$  for  $Mn(SALAEP)_2$  as the tridentate complex, a monotonic sequence of  $E_a$  values results; 7.1, 11.3, and 22 kcal/mole. However, an anomaly in the redox potentials of the complexes now appears.  $Mn(SALEN)$  has voltammetric peaks cathodic to those of  $Mn(SALPMA)_2$ , but  $Mn(SALAMP)_2$  is electrochemically inactive.  $Mn(SALAEP)_2$  is electroactive, but even it does not fall in place, having peaks anodic to those of  $Mn(SALPMA)_2$ .

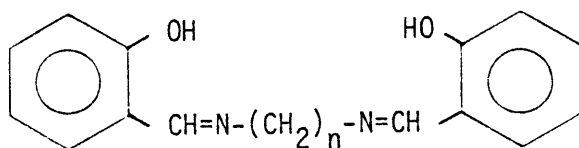
One of the aims of this work was to correlate electrochemical and oxygenation properties. Unfortunately, the convoluted electrochemistry of most complexes prevented extensive conclusions from being drawn. However, a quantitative correlation could be drawn for the first time for substituent effects within individual groups. In particular, bidentate and  $Mn(XSALEN)$  complexes exhibited a decrease in  $E_a$  values for

reaction with  $O_2$  with a corresponding cathodic shift in voltammetric peak potentials, even though the bidentates did exhibit multiple reduction peaks in one of the two solvents used.

The effect of ligand denticity on the properties of these complexes has therefore been shown to be quite significant, although the effects of solvent are also seen to be quite important. Denticity changes affect the reactivities of the complexes, as well as their stabilities, by a combination of both electronic and steric effects, and it seems that the two are intimately related. Although none of the reactions were found to mimic the natural  $O_2$  carriers, insight into the effects of ligands on reactions of metal ions with oxygen has been gained.

## APPENDIX I

### Structures of Previously Reported Ligands

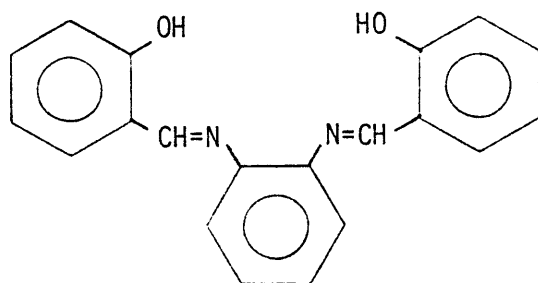


$n$	
—	
2	SALEN
4	SALBTDA
6	SALHXDA
7	SALHTDA
8	SALOTDA
10	SALDCDA

Ligands with  $n = 3$  and greater are normally referred to as  $\text{SALC}_n$ .

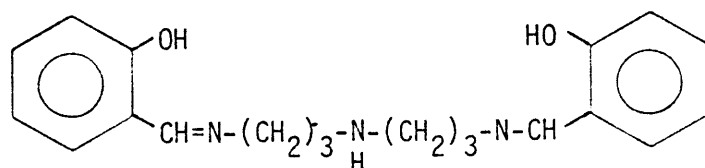
Substitution of pyridine-2-carboxaldehyde for salicylaldehyde produces PY- ligands.

Substituents may be placed on the salicylaldehyde ring,  
eg. 5-Cl-



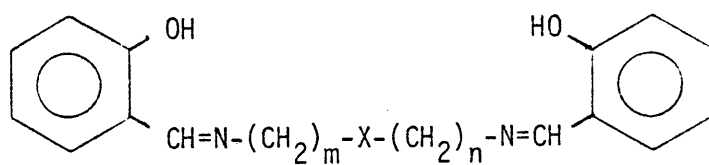
SALOPHEN

Substituents may be placed on the salicylaldehyde ring or on the bridging phenyl ring (SALROPHEN).

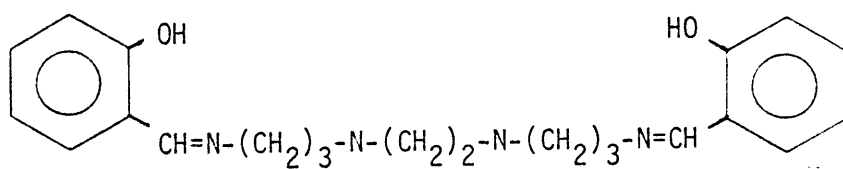


SALDPT

Substituents may be placed on the salicylaldehyde ring, on the imine carbon, or on the central nitrogen (SALRDPT). Substitution of 2-hydroxy-3-naphthaldehyde for salicylaldehyde produces NAPDPT. Substitution of a phenyl ring on the imine carbon produces SALHBDPT.



$m$	$n$	$X$	
3	3	P-Ph	SALPhDAPP
3	3	O	SALDAPE
3	4	NH	SALBPT
2	3	NH	SALEPT
2	2	NH	SALDIEN
2	2	S	SALDAES



SAL 1,5,8,12

## REFERENCES

1. Werner, A., and A. Myelius, *Z. Anorg. Chem.*, 16, 245 (1898).
2. Ochiai, E.-I., *Inorg. Nucl. Chem. Lett.*, 10, 453 (1974).
3. McAuliffe, C. A., H. Al-Khateeb, M. H. Jones, W. Levason, K. Mintern, and F. P. McCullough, *J. Chem. Soc., Chem. Commun.*, 736 (1979).
4. Bull, C., R. G. Fisher, and B. M. Hoffman, *Biochem. Biophys. Res. Commun.*, 59, 140 (1974).
5. Boggess, R. K., J. R. Absher, S. Morelen, L. T. Taylor, and J. W. Hughes, *Inorg. Chem.*, 22, 1273 (1983).
6. Richens, D. T., C. G. Smith, and D. T. Sawyer, *Inorg. Chem.*, 18, 706 (1979).
7. Bodini, M. E., and D. T. Sawyer, *J. Amer. Chem. Soc.*, 98, 8366 (1976).
8. Walling, C., *Acc. Chem. Res.*, 8, 125 (1975).
9. Magers, K. D., C. G. Smith, and D. T. Sawyer, *Inorg. Chem.*, 19, 492 (1980).
10. Chin, D.-H., and D. T. Sawyer, *Inorg. Chem.*, 21, 4317 (1982).
11. Wilshire, J. P., and D. T. Sawyer, *J. Amer. Chem. Soc.*, 100, 3972 (1978).
12. Cooper, S. R., Y. B. Koh, and K. N. Raymond, *J. Amer. Chem. Soc.*, 104, 5092 (1982).
13. Cooper, S. R., and J. R. Hartman, *Inorg. Chem.*, 21, 4315 (1982).
14. Allcock, H. R., P. P. Greigger, J. E. Gardner, and J. L. Schmutz, *J. Amer. Chem. Soc.*, 101, 606 (1979).
15. Boyer, E., and G. Holzbach, *Angew. Chemie Int. Ed. Eng.*, 16, 117 (1977).
16. Fieldhouse, S. A., B. W. Fullam, C. W. Nielson, and M. C. R. Symons, *J. Chem. Soc., Dalton Trans.*, 567 (1974).
17. Nyholm, R. S., and A. Turco, *Chem. Ind. (London)*, 74 (1960).
18. Cooper, S. R., and M. Calvin, *J. Amer. Chem. Soc.*, 99, 6623 (1977).

19. Otsuji, Y., K. Sawada, J. Morishita, Y. Taniguchi, and K. Mizuno, *Chem. Lett.*, 983 (1977).
20. Mizuno, K., J. Ogawa, and Y. Otsuji, *Chem. Lett.*, 945 (1979).
21. Elvidge, J. A., and A. B. P. Lever, *Proc. Chem. Soc., London*, 195 (1959).
22. Canham, G. W. R., and A. B. P. Lever, *Inorg. Nucl. Chem. Lett.*, 9, 513 (1973).
23. Vogt, L. H., A. Zalkin, and D. H. Templeton, *Inorg. Chem.*, 6, 1725 (1967).
24. Yamamoto, A., L. K. Philips, and M. Calvin, *Inorg. Chem.*, 7, 847 (1968).
25. Lever, A. B. P., J. P. Wilshire, and S. K. Quan, *Inorg. Chem.*, 20, 761 (1981).
26. Lever, A. B. P., J. P. Wilshire, and S. K. Quan, *Inorg. Chem.*, 101, 3668 (1979).
27. Jones, R. D., D. A. Summerville, and F. Basolo, *J. Amer. Chem. Soc.*, 100, 4416 (1978).
28. Moxon, N. T., P. E. Fielding, and A. K. Gregson, *J. Chem. Soc., Chem. Commun.*, 98 (1981).
29. Fee, J. A., and J. S. Valentine, Superoxide and Superoxide Dismutases, Academic Press, New York, 1977.
30. Fleischer, E. B., and T. S. Srivastava, *J. Amer. Chem. Soc.*, 91, 2403 (1969).
31. Kelly, S. L., and K. M. Kadish, *Inorg. Chem.*, 21, 3631 (1982).
32. Carnieri, N., A. Harriman, and G. Porter, *J. Chem. Soc., Dalton Trans.*, 931 (1982).
33. Schardt, B. C., F. J. Hollander, and C. L. Hill, *J. Chem. Soc., Chem. Commun.*, 765 (1981).
34. Groves, J. T., W. J. Kruper, and R. C. Haushalter, *J. Amer. Chem. Soc.*, 102, 6375 (1980).
35. Willner, J., J. O. Orvos, and M. Calvin, *J. Chem. Soc., Chem. Commun.*, 964 (1980).

36. Urban, M. W., K. Nakamoto, and F. Basolo, *Inorg. Chem.*, 21, 3406 (1982).
37. Hanson, L. K., and B. M. Hoffman, *J. Amer. Chem. Soc.*, 102, 4603 (1980).
38. Perée-Fauvet, M., and A. Gaudemer, *J. Chem. Soc., Chem. Commun.*, 874 (1981).
39. Tabushi, I., and N. Koga, *J. Amer. Chem. Soc.*, 101, 6456 (1979).
40. Schardt, B. C., F. J. Hollander, and C. L. Hill, *J. Amer. Chem. Soc.*, 104, 3964 (1982).
41. Naves, D. R., and J. G. Dabrowiak, *Inorg. Chem.*, 15, 129 (1976).
42. Burness, J. H., J. G. Dillard, and L. T. Taylor, *Syn. React. Inorg. Metal-Org. Chem.*, 6, 165 (1976).
43. *Preparative Organic Chemistry*, G. Hilgetag and A. Martini, Ed., John Wiley and Sons, Fourth Ed., New York, 1972.
44. Pfeiffer, P., E. Breith, E. Lubbe, and T. Tomaki, *Annalen*, 503 84 (1933).
45. Coleman, W. M., and L. T. Taylor, *Coord. Chem. Rev.*, 32, 1 (1980).
46. Lewis, J., F. E. Mabbs, and H. Weigold, *J. Chem. Soc. A*, 1699 (1968).
47. Matsushita, T., and T. Shono, *Bull. Chem. Soc. Jpn.*, 51, 631 (1981).
48. Matsushita, T., M. Fujiwara, and T. Shono, *Chem. Lett.*, 631, (1981).
49. Butler, K. D., K. S. Murray, and B. O. West, *Aust. J. Chem.*, 24, 2249 (1971).
50. Dey, K., and K. G. Ray, *J. Indian Chem. Soc.*, 50, 66 (1973).
51. Chiswell, B., and K. D. Lee, *Inorg. Chim. Acta*, 6, 567 (1972).
52. Van Den Bergen, A., K. S. Murray, M. J. O'Connor, and B. O. West, *Aust. J. Chem.*, 22, 39 (1969).
53. Titus, S. J. E., W. M. Barr, and L. T. Taylor, *Inorg. Chim. Acta*, 32, 103 (1979).

54. Earnshaw, A., E. King, and L. Larkworth, *J. Chem. Soc. A*, 1048 (1968).
55. Matsushita, T., T. Yorino, I. Masuda, T. Shono, and K. Shima, *Bull. Chem. Soc. Jpn.*, 46, 1712 (1973).
56. Miller, J. D., and F. D. Oliver, *J. Inorg. Nucl. Chem.*, 34, 1873 (1972).
57. Potter, W. G., and L. T. Taylor, *Inorg. Chem.*, 15, 1329 (1976).
58. Boggess, R. K., J. W. Hughes, W. M. Coleman, and L. T. Taylor, *Inorg. Chim. Acta*, 38, 183 (1980).
59. Coleman, W. M., R. K. Boggess, J. W. Hughes, and L. T. Taylor, *Inorg. Chem.*, 20, 1253 (1981).
60. Coleman, W. M., and L. T. Taylor, *J. Inorg. Nucl. Chem.*, 41, 95 (1979).
61. Coleman, W. M., III, *Inorg. Chim. Acta*, 49, 205 (1981).
62. Coleman, W. M., and L. T. Taylor, *Inorg. Chem.*, 16, 1114 (1977).
63. Coleman, W. M., R. K. Boggess, J. W. Hughes, and L. T. Taylor, *Inorg. Chem.*, 20, 700 (1981).
64. Coleman, W. M., R. R. Goehring, L. T. Taylor, J. G. Mason, and R. K. Boggess, *J. Amer. Chem. Soc.*, 101, 2311 (1979).
65. Constantini, M., A. Dromard, M. Jouffret, B. Brossard, and J. Varagnat, *J. Mol. Cat.*, 7, 89 (1980).
66. Lewis, J., T. D. O'Donoghue, and P. R. Raithby, *J. C. S. Dalton*, 1383 (1980).
67. Drew, G. B., J. Nelson, and S. M. Nelson, *J. C. S. Dalton*, 1685 (1981).
68. Cinquantini, A., R. Seeber, and R. Cini, *Transition Met. Chem.*, 7, 271 (1982).
69. Matsushita, T., M. Nishino, and T. Shono, *Bull. Chem. Soc. Jpn.*, 55, 2663 (1982).
70. Coleman, W.M., III, and L.T. Taylor, *Inorg. Chim. Acta*, 61, 13 (1982)
71. Boucher, L. J., and C. G. Coe. *Inorg. Chem.*, 14, 1289 (1975).

72. Boucher, L. J., and C. G. Coe, *Inorg. Chem.*, 15, 1334 (1976).
73. Bryan, P. S., and C. K. Stone, *Inorg. Nucl. Chem. Lett.*, 13, 581 (1977).
74. Coleman, W. M., R. R. Goehring, and L. T. Taylor, *Syn. React. Inorg. Metal-Org. Chem.*, 7, 333 (1977).
75. Matsushita, T., H. Kono, and T. Shono, *Bull. Chem. Jpn.*, 54, 2646 (1981).
76. Coleman, W. M., and L. T. Taylor, *J. Inorg. Nucl. Chem.*, 42, 683 (1980).
77. Wilkins, R. G., The Study of Kinetics and Mechanism of Reactions of Transition Metal Complexes, Allyn and Bacon, Boston, 1974.
78. Moore, J. W., and R. G. Pearson, Kinetics and Mechanism, John Wiley and Sons, New York, Third Ed., 1981.
79. Laidler, K. J., Chemical Kinetics, McGraw-Hill, New York, Second Ed., 1965.
80. Ebbs, S. J., M. S. Thesis (Chemistry), Virginia Polytechnic Institute and State University, June 1975.
81. Nakamoto, K., Infrared and Raman Spectra of Inorganic and Coordination Compounds, John Wiley and Sons, New York, Third Ed., 1978.
82. Barr, M., M. S. Thesis, Virginia Polytechnic Institute and State University, June 1976.
83. Vogel, A., Textbook of Practical Organic Chemistry, Longman Group, London, Fourth Ed., 1978.
84. Harharian, M., and F. Urbach, *Inorg. Chem.*, 8, 556 (1969).
85. Holm, R. H., *J. Amer. Chem. Soc.* 82 5632 (1960).
86. Zelentsov, V. V., Yu. V. Rakitin, J. K. Somova, and T. B. Nikolaeva, *Koord. Khim.*, 8, 1099 (1982).
87. Taylor, L. T., and W. M. Coleman, III, *Inorg. Chim. Acta*, 63, 183 (1982).
88. Lever, A. B. P., Inorganic Electronic Spectroscopy, Elsevier Publishing, Amsterdam, 1968.

89. Angelici, R. J., Synthesis and Technique in Inorganic Chemistry, W. B. Saunders, Philadelphia, 1969.
90. Drago, R. S., Physical Methods in Chemistry, W. B. Saunders, Philadelphia, 1977.
91. Coleman, W. M., and L. T. Taylor, *Inorg. Chim. Acta*, 30, L291 (1978).
92. Cotton, F. A., and G. Wilkinson, Advanced Inorganic Chemistry, John Wiley and Sons, New York, Fourth Ed., 1980.
93. Goolsby, A. D., and D. T. Sawyer, *Anal. Chem.*, 40, 83(1968).
94. Boggess, R. K., private communication.
95. Bard, A. J., and L. R. Faulkner, Electrochemical Methods, John Wiley and Sons, New York, 1980.
96. MacGregor, W. S., *Quart. Rep. on Sulfur Chem.*, 3, 149 (1968).
97. Gagne, R. R., C. A. Koval, and G. C. Lisensky, *Inorg. Chem.*, 19, 2854 (1980).
98. Lever, A. B. P., and J. P. Wilshire, *Inorg. Chem.*, 17, 1145 (1978).
100. Sacconi, L., P. Nannelli, N. Nardi, and U. Campigli, *Inorg. Chem.*, 4, 26 (1965).
101. Charkravorty, A., J. P. Fennessey, and R. H. Holm, *Inorg. Chem.*, 4, 26 (1965).
102. Drew, M. G. B., J. Nelson, and S. M. Nelson, *J. Chem. Soc., Dalton Trans.*, 1691 (1981).
103. Lever, A. B. P., and P. G. Minor, *Adv. Mol. Relaxation Interact. Processes*, 18, 115 (1980).
104. Drago, R. S., G. C. Vogel, and T. E. Needham, *J. Amer. Chem. Soc.*, 93, 6014 (1971).
105. Lever, A. B. P., P. C. Minor, and J. P. Wilshire, *Inorg. Chem.*, 20, 2250 (1981).
106. IUPAC Solubility Data Series, Volume 7, Oxygen and Ozone, R. Battino, Ed., Pergamon Press, Great Britain, 1981.
107. Weigold, H., and B. O. West, *J. Chem. Soc. A*, 1310 (1967).

108. Kelter, P. B., and J. D. Carr, *Anal. Chem.*, 51, 1828 (1979).
109. Niswander, R. H., Ph. D. Dissertation, Virginia Polytechnic Institute and State University, March, 1976.
110. Thewalt, U., and R. Marsh, *J. Amer. Chem. Soc.*, 89, 6364 (1967).

## VITA

Fred Charles Frederick was born in Regina, Saskatchewan on January 9, 1956. He received his formal secondary education at Campion High School in Regina, receiving his diploma in June, 1972.

From September, 1972 to June, 1977, he attended the University of Regina, receiving the degree of Bachelor of Science (Honors) in Chemistry in October, 1977. He entered the graduate school at the University of Regina in September, 1977. He left this institute in December, 1979, and received the degree of Master of Science in Chemistry in May, 1980.

He entered the graduate school at Virginia Polytechnic Institute and State University in Blacksburg, Virginia in January, 1980. He was awarded the degree of Doctor of Philosophy in Chemistry in December, 1983.

*Fred Frederick*